

INVESTIGATIONS INTO THE MECHANOCHEMICAL SYNTHESIS OF
STERICALLY BULKY ALLYL COMPLEXES

By

Nicholas Rowe Rightmire

Dissertation

Submitted to the Faculty of the
Graduate School of Vanderbilt University
in partial fulfillment of the requirements
for the degree of

DOCTOR OF PHILOSOPHY

in

Chemistry

December 2015

Nashville, Tennessee

Approved

Timothy P. Hanusa, Ph.D.

Charles M. Lukehart, Ph.D.

David W. Wright, Ph.D.

James E. Wittig, Ph.D.

*In loving memory of Sadie,
I could not have asked for a better friend, supporter, and
four-legged companion for my time at Vanderbilt.
My couch will always have room for the pillow with legs.*

Acknowledgements

There are numerous people who have helped shape my education that deserve my gratitude. I would like to first thank my parents, Pete Rightmire and Nannette Bernales, for all you have done for me. I am extremely grateful for the opportunities, in both life and education, that you have provided. To my brother Zacko, thank you for your support, confidence, and sense of humor. I would also like to thank Dr. Patrick Holt, Dr. Wendy Burns Foulis, and Bob Bernauer for shaping a majority of my chemistry career during my time at Bellarmine and Vanderbilt.

None of the work here would have been possible without the strong support of Tim Hanusa. I could not have asked for a better mentor for my research. Thank you for your constant support, knowledge, advice, and confidence in me throughout my time in your lab. I am not sure many other PI's would have provided the freedom and intrigue you have during my first forays into mechanochemistry. Both your excitement and interest in my research provides the best motivation I could ask for.

A special thank you is required for David Bruns, without whom my projects would not be where they are today. It was a great pleasure to work with you during your junior and senior years at Vanderbilt. You exhibited a remarkable competency and confidence in research that made my role as a mentor enjoyable and our time in research extremely productive. Without your help, we would have only a fraction of the organometallic mechanochemistry foundation we now have. I wish you the best of luck with your research and educational endeavors.

I would like to extend a special thank you to Tara Todd for all you have done to shape me into a better teacher. I am extremely thankful for the freedom you have allowed and the faith you placed in me during my teaching career at Vanderbilt. The degree to which you have valued my opinions has been a tremendous boost in my confidence as teacher. It has been a pleasure to teach with you these past several years.

To the members of my committee, Dr. Lukehart, Dr. Wright, and Dr. Wittig, thank you all for the support and direction you have provided. Thank you for pushing the limits of my knowledge during our meetings and examinations. While I would rather not repeat many of those, I am grateful for your input and critical analysis of my ideas and work.

To group members both past and present, my fellow classmates, and friends within the department, thank you for sharing this journey with me. The sense of camaraderie, the generosity of ideas, and the friendship have been invaluable components of my graduate school experience. Thank you to Ryan Meier and Eric Bierschenk for showing me the ropes of the

Hanusa lab and your friendship. To Nicholas Boyde, thank you for your friendship and I wish you the best of luck in your time at Vanderbilt.

I would like to acknowledge the financial support for research provided by the National Science Foundation (CHE-1112181), the Petroleum Research Fund, administered by the American Chemical Society, and a Discovery Grant from Vanderbilt University. Most importantly, I want like to thank Vanderbilt University for the opportunity to pursue this research and the financial support throughout my time in the program.

Most importantly, to Kelly: thank you for your unending friendship, support, advice, and love throughout these past few years at Vanderbilt, without which I would not have made it this far. I cannot express how grateful I am for all you have done and continue to do. I am unbelievably lucky to have someone as amazing as you are in my life.

Table of Contents

	Page
ACKNOWLEDGEMENTS	iii
LIST OF FIGURES	vii
LIST OF TABLES	ix
COMMON ABBREVIATIONS AND SYMBOLS	x
Chapter	Page
1. The ‘M-Chem Way’: Advances in Mechanochemical Organometallic Synthesis	1
Introduction.....	1
Equipment for Mechanochemical Synthesis.....	5
Removing Solvent from Organometallic Synthesis.....	8
Challenges and Opportunities.....	11
Conclusions.....	14
2. Mechanochemical Synthesis and Investigations as a Potential Allyl Transfer Agent of the Base-Free Tris(allyl)aluminum Complex [Al(1,3-(SiMe₃)₂C₃H₃)₃]	16
Introduction.....	16
Experimental.....	17
Results and Discussion.....	25
Conclusion.....	37
3. Mechanochemical Influence on Stereoisomer Formation in the Syntheses of Group 15 Bis(1,3-trimethylsilyl)allyl Complexes (As–Bi)	38
Introduction.....	38
Experimental.....	39
Results and Discussion.....	44
Conclusion.....	51
4. Organometallic Mechanochemistry of s-Block Metal Complexes	52
Introduction.....	52
Experimental.....	53
Results and Discussion.....	59
Conclusion.....	73

	Page
5. Mechanochemical Investigations of d-Block and p-Block Metal Centers	74
Introduction	74
Experimental	75
Results and Discussion	80
Conclusion	86
6. Balancing Adduct Formation and Ligand Coupling with the Bulky Allyl Complexes $M[1,3-(SiMe_3)_2C_3H_3]_2$ (M = Fe, Co, Ni)	88
Introduction	88
Experimental	90
Results and Discussion	91
Conclusion	102
 Appendices	
A. Selected Spectra	103
B. Crystallographic Data	125
C. Computational Details	146
REFERENCES	197

List of Figures

Figure	Page
1. A sampling of organometallic species produced through mechanochemical methods.....	3
2. Mechanochemical synthesis of <i>fac</i> -(TMEDA)ReCO ₃ F from Re ₂ (CO) ₁₀	13
3. Mechanochemically induced Ru-catalyzed olefin metathesis reactions.....	13
4. Thermal ellipsoid plot of [AlA'₃].....	26
5. Optimized geometries of Al(C ₃ H ₅) ₃	28
6. Calculated reaction product of benzophenone with the parent [Al(C ₃ H ₅) ₃].....	29
7. Calculated reaction product of benzophenone with the solvated [Al(C ₃ H ₅) ₃ (thf)] complex.....	29
8. Plot of the non-hydrogen atoms of [ScA'₃].....	30
9. Selected portions of the ¹ H NMR spectrum from the [SnA'ₓ] oil.....	32
10. Selected portions of the ¹ H NMR spectrum from the [SnA'ₓ] oil.....	33
11. Selected portions of the ¹ H NMR spectrum from the [SnA'ₓ] solid.....	33
12. Selected portions of the ¹ H NMR spectrum from the [SnA'ₓ] mill.....	34
13. Structure and bonding configuration of selected A' complexes.....	39
14. Proton labeling of π- and σ- bonded A' ligand.....	39
15. ¹ H NMR of the H _(ω) region of [AsA'₃] and [SbA'₃].....	46
16. Thermal ellipsoid plot of [AsA'₃].....	48
17. Basic structural types considered for geometry optimization of [EA'₃] complexes.....	49
18. Relative energies of the [EA'₃] diastereomers.....	50
19. Thermal ellipsoid plot of K[BeA'₃].....	60
20. Thermal ellipsoid plot of [BeA'₂(Et₂O)].....	61
21. Structure of [K(tol)(μ-A')K(tol)][(A')Mg(μ-A')₂].....	63

Figure	Page
22. Calculated structure of $K[MgA'_3]$	64
23. Selected portions of the 1H NMR spectrum of $[CaA'_2]$	66
24. Selected portions of the 1H NMR spectrum of $K[CaA'_3]$	66
25. Thermal ellipsoid plot of selected portion of $[K[(\mu-A')CaA'_2]]_\infty$	68
26. Calculated structures of $K[CaA'_3]$	69
27. Packing diagram of $Cs_{0.5}K_{0.5}[A']$	72
28. Selected portions of the 1H NMR spectrum of $[YA'_3]$	81
29. Labeling of <i>syn</i> , <i>anti</i> and <i>syn, syn</i> arrangements of $SiMe_3$ groups of the A' ligand.....	92
30. Calculate structures of $[M(R_2C_3H_3)_x(CO)_y]$ Complexes.....	99
A1-41 Complete 1H NMR and FT-IR spectra of selected complexes.....	103
B1 Thermal ellipsoid plot of $[SbA'_3]$	133

List of Tables

Table	Page
1. Relative amounts of the C_1 and C_3 -symmetric isomers of $[EA'_3]$	47
2. Selected calculated structural parameters and $\nu(\text{CO})$ values.....	100
3. Crystal data and summary of $[AlA'_3]$ and $[ScA'_3]$	126
4. Atomic coordinates for $[AlA'_3]$	127
5. Atomic coordinates for $[ScA'_3]$	128
6. Crystal data and summary of $[AsA'_3]$ and $[SbA'_3]$	131
7. Atomic coordinates for $[AsA'_3]$	132
8. Atomic coordinates for $[SbA'_3]$	135
9. Crystal data and summary of $K[BeA'_3]$	138
10. Atomic coordinates for $K[BeA'_3]$	139
11. Crystal data and summary of $K[CaA'_3]$	141
12. Atomic coordinates for $K[CaA'_3]$	142
13. Crystal data and summary for $[K_{0.5}Cs_{0.5}A']$	144
14. Atomic coordinates for $[K_{0.5}Cs_{0.5}A']$	145
15. Coordinates of optimized structures (\AA).....	147
16. Average energy differences in EA'_3 conformations.....	150
17. Coordinates of optimized structures (\AA).....	151
18. Coordinates of optimized structures (\AA).....	186
19. Cartesian coordinates of optimized structures (\AA).....	190

Common Abbreviations and Symbols

$\xrightarrow{\infty}$	Mechanochemical processing (grinding or milling)
A'	$[1,3-(\text{SiMe}_3)_2\text{C}_3\text{H}_3]^-$
KA'	$\text{K}[1,3-(\text{SiMe}_3)_2\text{C}_3\text{H}_3]$
HA'	$1,3-(\text{SiMe}_3)_2\text{C}_3\text{H}_4$
A' ₂	1,3,4,6-tetrakis(trimethylsilyl)-1,5-hexadiene ($[1,3-(\text{SiMe}_3)_2\text{C}_3\text{H}_3]_2$)
Ae	Alkaline-earth Metal
COSY	Correlation Spectroscopy
Et ₂ O	Diethyl Ether
ICP-OES	Inductively Coupled Plasma Optical Emission Spectrometry
LAG	Liquid assisted Grinding
THF	Tetrahydrofuran
tol	Toluene

Chapter 1

The ‘M-Chem Way’: Advances in Mechanochemical Organometallic Synthesis

Introduction

Those of us involved with chemistry are reminded—perhaps not often enough—to “question our assumptions” about concepts and conventions that seem too well-established or reasonable to doubt.¹ It is prudent advice, as the failure to reconsider long-held beliefs has repeatedly stalled advances in multiple areas of the science, including synthetic studies. Entire chemical families, such as molecular complexes containing ‘inaccessible’ divalent lanthanides (e.g., those with Pr^{II}, Gd^{II}, Ho^{II}, and others²⁻³), or compounds of the ‘unreactive’ noble gases,^{4,5} were at one time thought to be unisolable, for seemingly impeccable scientific reasons. Yet an assumption far older and more pervasive than those associated with these examples is still infrequently questioned: namely, that a solvent is needed when conducting reactions. The roots of this supposition go back centuries, if not millennia; the obvious dependence of biological processes on liquid water perhaps helped promote the idea that solvents are required for nearly all chemical transformations. In recognition of the solvent/reaction relationship, the alchemists even had a Latin phrase for it: “*corpora non agunt nisi soluta*” (bodies do not react unless dissolved).⁶

It would be wrong to characterize the use of solvents as purely reflexive, however; as solvent-based reactions remain the overwhelming norm in synthetic chemistry, and for empirically sound reasons. Solvents promote the interaction of reagents, affect the rates of reactions, often change the distribution of products, and disperse heat in exothermic reactions. There are significant issues to contend with when solvents are *not* used: many reactions are simply not amenable to a solvent-free approach, particularly on a large scale, where efficient mixing can be problematic. Solvents are still often required for the extraction, separation and purification of products.⁷ Thus ‘solvent-free’ (or often more accurately, ‘reduced solvent’) chemistry is not necessarily a completely green approach to synthesis.⁸⁻⁹

Despite such limitations, reactions conducted through grinding or milling, rather than solvent mediation, hold great promise for synthetic chemists.¹⁰ This has already been extensively demonstrated in organic chemistry¹¹⁻¹⁴ and, to a lesser but growing extent, in inorganic and coordination chemistry,¹⁵⁻¹⁸ especially in the area of metal organic frameworks (MOFs).^{9,19-20} In contrast, the area of mechanochemical *organometallic* synthesis is markedly underdeveloped. As noted below, the first papers on the subject appeared scarcely a quarter century

ago, and only in the present decade have such solid-state syntheses become more widely appreciated, even if not broadly practiced. A goal of this chapter, and overall thesis, is to describe recent developments and investigations in the area. This is a rapidly evolving field, and the various consequences—some advantageous, others perhaps less so—that can arise when solvents are removed from an organometallic system are only partially known. There are multiple entry points into the field, several quite inexpensive and well worth examining. It is perhaps not too much to suggest that more chemists consider mechanochemical approaches when designing strategies for preparing new organometallic molecules and studying their reactions.¹⁴

A brief history of mechanochemical synthesis

It should be stressed that, despite the alchemical adage mentioned above, the grinding or milling of chemical compounds to initiate reactions is not a new practice. Recognition of the distinctive activation processes involved in grinding was slow in coming, however. A detailed history of this area can be found elsewhere;²¹ only a few points are summarized here. Among the earliest recorded reactions that could be considered mechanochemical is one mentioned by Theophrastus of Eresos (4th century BC), who noted that the grinding of cinnabar (HgS) with vinegar in a copper vessel (what would today be considered ‘liquid assisted grinding’, LAG) results in the formation of elemental mercury (i.e., $\text{HgS} + \text{Cu} \rightarrow \text{Hg} + \text{CuS}$).²² Grinding has also long been known to facilitate displacement reactions between a metal oxide and a more reactive metal (e.g., $4 \text{CuO} + 3 \text{Fe} \rightarrow 4 \text{Cu} + \text{Fe}_3\text{O}_4$). In 1820, Michael Faraday published his research on the reduction of AgCl with various active metals (Zn, Sn, Fe, Cu) by grinding in a mortar, in a procedure he called ‘the dry way’.²³ Even though not all his results can be cleanly replicated today,²⁴ his marked one of the first systematic studies of mechanochemical processes. The problem with interpreting the nature of these reactions is that they can be initiated with either grinding or heat (note that the HgS/Cu, CuO/Fe, and AgCl/Zn reactions above are also thermodynamically spontaneous, $\Delta G^\circ_{\text{rxn}} < 0$). A reasonable assumption (that word again!) made when discussing these systems was that the only direct result of grinding was the generation of heat through friction, and that any chemical changes were due to secondary thermochemical processes. Not surprisingly, in a discussion of this topic in a well-regarded chemistry textbook from the 1880s, it was categorically stated: “One cannot assume that chemical changes come about through mechanical action itself”.²⁵

Within a decade, this view was about to change, as at the end of the 19th century the American chemist M. Carey Lea (1823–1897) began to distinguish systematically the results of grinding from thermochemical effects. He identified chemical systems that behaved

differently depending on how they were activated. Among these were the silver halides, which form elemental silver on grinding, but melt without decomposition when simply heated.²⁶⁻²⁷ Lea's work was important in the recognition of mechanochemistry (as it was termed by Wilhelm Ostwald in 1919²⁸) as a distinct subdiscipline of chemistry.²⁹

The potential for transformative results in organometallic chemistry through mechanochemical means would seem to be as great as in organic and coordination chemistry. In fact, reactions of organometallic compounds in the solid state have been known for at least half a century.³⁰ Many of these, however, including thermally induced ligand isomerizations and reactions at surfaces, do not involve the application of mechanical energy, and are not properly considered mechanochemical.³¹ The range of organometallic complexes synthesized through truly mechanochemical methods is actually quite substantial, and is only partially indicated by the examples in Figure 1.³²⁻³⁹ Combined thermal and mechanochemical synthesis is also known, such as with the solid-state desolvation of the dimeric alkoxide [$\{t\text{BuZn}(\mu\text{-O}(t\text{-Bu}))(\text{thf})\}_2$], which produces the trimeric [$\{(t\text{-Bu})\text{ZnO}(t\text{-Bu})\}_3$]; grinding of the latter generates the tetrameric cubane [$\{(t\text{-Bu})\text{ZnO}(t\text{-Bu})\}_4$].⁴⁰

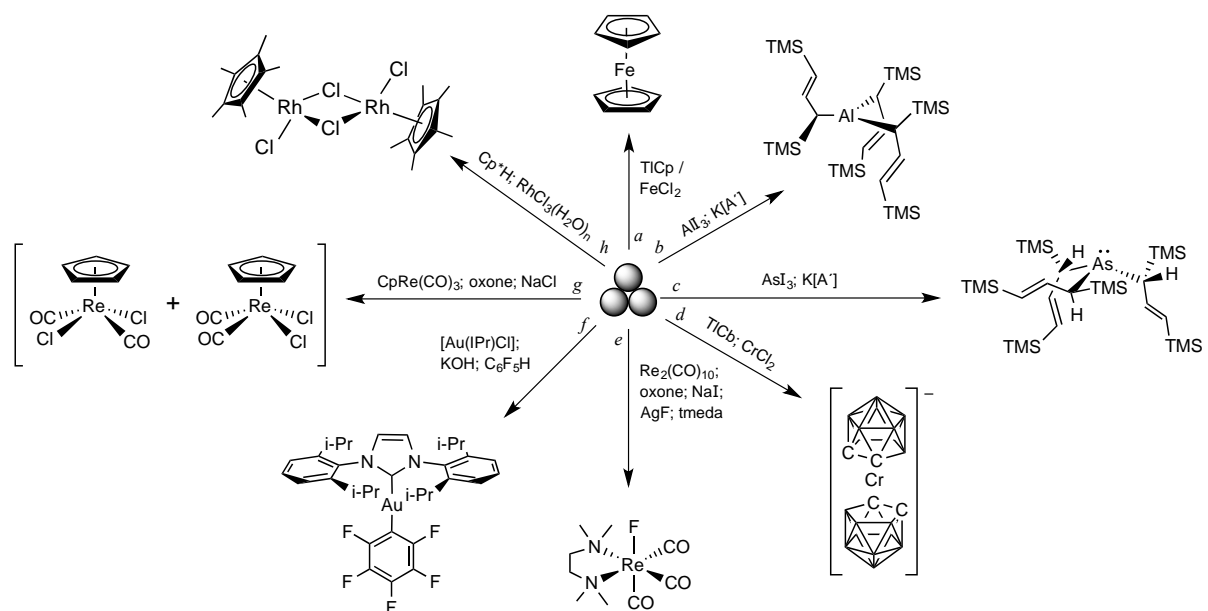


Figure 1. A sampling of organometallic species produced through mechanochemical methods: **a**) ferrocene;³⁶ **b**) $\text{Al}[1,3\text{-(SiMe}_3)_2\text{C}_3\text{H}_3]_3$;³⁸ **c**) one of two diastereomers of $\text{As}[1,3\text{-(SiMe}_3)_2\text{C}_3\text{H}_3]_3$;³⁷ **d**) the metallocarborane $[\text{Me}_4\text{N}][\text{Cr}(\text{C}_2\text{B}_9\text{H}_{11})_2]$;³² **e**) *fac*-(TMEDA) ReCO_3F ;³⁹ **f**) $[\text{Au}(\text{IPr})(\text{C}_6\text{H}_5)]$ (IPr = 1,3-bis(2,6-diisopropylphenyl)imidazol-2-ylidene);³³ **g**) *diag*- $\text{CpRe}(\text{CO})_2\text{Cl}_2$ and *lat*- $\text{CpRe}(\text{CO})_2\text{Cl}_2$;³⁵ **h**) $[(\text{C}_5\text{Me}_5)\text{RhCl}_2]_2$ ³⁴

The first reports of these organometallic reactions appeared in the early 1990s, and included the preparation of various cyclopentadienyl, indenyl, and metallocarborane complexes.^{32, 41-42} Despite the novelty of the solvent-free approach and a steady accumulation of synthesis reports on various metal complexes over the next decade,⁴³⁻⁴⁶ interest in the technique remained low, at least if judged by paper citation counts. Part of the reason for this may have been that many of the compounds made in the initial years were already known from conventional solution routes, so any special advantages (apart from reduced solvent use) of the mechanochemical alternatives were not apparent. In addition, it was not always clear what role grinding or milling actually played in the processes. The products were typically removed from reaction mixtures by sublimation (with heating) or solvent extraction, and the possibility that most or all of a reaction occurred during workup could not be excluded. This was explicitly shown to be true in the formation of Cr(acac)₃ from the reaction of CrCl₃ and Na[acac]; grinding was said to have ‘activated’ the mixture, but no product was actually detected until external heat was subsequently applied.⁴⁷ This was also demonstrated during the formation of various monocyclopentadienyl complexes, whose reagents, although ground, had to be heated to form products.⁴⁸⁻⁴⁹

One of the first reports to clarify this issue involved a detailed investigation with IR and powder X-ray diffraction of ground reaction mixtures of FeCl₂ and TiCp; ferrocene formation was shown to increase as a function of milling time.³⁶ Later, solid state NMR was added to the list of techniques used for characterizing reaction mixtures, confirming that reactions to form *cis*-(Ph₃P)₂PtCl₂ and *cis*-(Ph₃P)₂PtCO₃ from PtCl₂ and the other ligands occurred before any workup procedures.⁵⁰ It is now well established that organometallic syntheses can occur in a truly mechanochemical fashion, without the assistance of auxiliary heating or solvents, thus vindicating (with a nod to Faraday, and to the informal abbreviations of physical chemistry as ‘P-chem’ and electrochemistry as ‘E-chem’) ‘the M-chem way’.

The Mechanochemical Regime

IUPAC has formalized the definition of a mechanochemical process as: “a chemical reaction that is induced by the direct absorption of mechanical energy”.⁵¹ Although this leaves many specifics undefined, it does help distinguish mechanochemical reactions from purely thermal ones.

Heat may be involved, but it is not the major driving force of a mechanochemical transformation. Several processes are understood to be active during grinding and milling, including mass transfer and the generation and relaxation of mechanical stress; the latter is associated with the disruption of crystalline lattices.⁸ The cracking of crystals, for example,

has been estimated to involve the energy equivalent of 1000–5000 K, crack propagation near velocity of sound (10^5 cm s^{-1}), and bond excitation lifetimes of $\sim 100 \text{ fsec}$.⁸ In this regard, there are parallels to the processes associated with ultrasonic cavitation in solution, where during bubble collapse temperatures over 1000 K for a time period of 10^{-4} – 10^{-3} sec and pressures of several tens of kilobars may be involved.⁵² A considerable amount of energy can be added to the system with a negligible increase in macroscopic temperature. Furthermore, the magnitude of the electric field near the tip of a mobile crack has been estimated at $\sim 10^8 \text{ V m}^{-1}$,⁵³ and high defect density introduced in crystals by grinding may also contribute as a driving force.⁵⁴ Such energies can fracture bonds and create radicals in ways that do not occur in solution. Not surprisingly, the outcome of mechanochemical reactions need not be the same as in solution, or when externally heated.

A fundamental difficulty in studying the mechanism of mechanochemical reactions is monitoring their progress. In some cases, grinding can be stopped after different intervals of time and the reaction mixture analyzed. In other cases, mechanochemical activation is required only to initiate a reaction, which will proceed without continuous grinding. In these instances, powder X-ray diffraction⁵⁵ or solid-state NMR⁵⁰ have been used to monitor the appearance of products and disappearance of reagents. A particularly elegant demonstration of real-time monitoring of reaction progress during grinding has been provided with synchrotron diffraction through the work of Frišćić and coworkers.⁵⁶ Such instrumental investigation, as valuable as it is, is not widely available, and some mechanochemical reactions can be completed on relatively short time scales (30–60 sec)³⁷, providing little time for conventional data acquisition. Most reactions mechanisms are generally inferred from an analysis of the product mixtures. Real-time monitoring of mechanochemical reactions is an area that will likely see considerable development in the coming years.

Equipment for Mechanochemical Synthesis

Mechanochemical reactions can be conducted under a range of conditions with equipment ranging from nearly free to tens of thousands of dollars. More expensive equipment can conveniently and consistently process larger amounts of reagents and decrease reaction time, but is certainly not required for exploratory work or proof-of-concept investigations. Several mechanochemical techniques ranging from low to high cost are listed here. The inventory is not exhaustive. There are, for example, commercially available motorized mortar and pestles, but these have not found extensive use in small-scale organometallic synthesis.

Mortar and Pestle

As the most time-honored and one of the least expensive tools for mechanochemistry, mortar and pestles are routinely employed for size reduction. Depending on the system of interest, these may also be used to promote mechanochemical reactivity. Many chemists have inadvertently done so when preparing pellets for IR spectra by grinding KBr with an organic compound, and discovering bromine incorporation into the sample. This has been done with coordination polymers to deliberately promote anion exchange.⁵⁷ Although widely available, mortar and pestle grinding suffers significant limitations in regards to defined reaction conditions.¹³ Factors ranging from atmospheric conditions (if performed on a benchtop), grinding frequency, strength of the grinder, and mixing of reagents can all play an important role during milling reactions.⁵⁸ Despite these limitations, the venerable mortar and pestle combination offers an inexpensive entry point for examining proof-of-concept organometallic mechanochemistry.

Glass flask milling

In a round bottom flask partially filled with ball bearings, reagents can be gently milled when the flask is swirled by hand or attached to a rotary evaporator. The latter allows for greater control of reaction conditions. An advantage of this method is the ability to visually monitor reactions; furthermore, reaction size in principle is limited only by flask volume. In practice, however, small ball bearings (ca. ≤ 6 mm dia) and slow rotational speeds must be used in order to avoid glass breakage. This consequently limits the mechanical energy that can be transferred to the reagents, which has the effect of reducing yields and extending reaction times.⁵⁹ Nevertheless, this method has been found to be useful for initial studies and screenings. The tri(allyl) complexes $[MA'_{3}]$ ($A' = 1,3-(SiMe_{3})_{2}C_{3}H_{3}$); $M = Al, Sc$) were first produced by glass flask milling; the aluminum compound was isolated in ca. 30% yield after a 2 h milling.³⁸ This will be discussed in more detail in Chapter 2.

An alternative to the rotary evaporator milling is to use a magnetic stir bar as an agitator for ball bearings, similar to the arrangement that will be discussed for the tube disperser. In place of solvent, several small ball bearings can be added to a flask containing solid reagents and long stir bar. Spinning of the stir bar provides enough agitation of ball bearings to grind reagents successfully. This method may provide another accessible low-end technique.

Wig-L-Bug™ and Tube Dispenser Milling

Several ‘mid-level’ milling techniques are available that use commercially available, easily portable equipment, such as the Wig-L-Bug™ (Dentsply Rinn.), tube dispersers (e.g., the Ultra-Turrax® Tube Drive, IKA) and lapidary grinders. These provide higher energy, greater adaptability, and increased control for moderate cost (~USD 1000). It should be noted that although such equipment is designed for grinding and mixing samples, their use in mechanochemical synthesis could tax their efficiency. The Wig-L-Bug™, tube dispersers and similar homogenizers employ different motions for the grinding of samples, so it is possible that one will be better suited to a given application than another. Typically, such units require little space and can easily be used in glove boxes. However, as these are not designed for bulk grinding, reaction scale-up is limited.

A tube disperser, which uses a spinning agitator to move ball bearings, is easily adaptable to air-sensitive chemistry. Reactions can be taken to completion in as little as 10-15 min, visually monitored, and the products easily extracted. There are limits to the system, as efficient motion of the agitator and ball bearings are needed for grinding. A practical maximum of ca. 0.5 g total reagents can be used at one time and soft or malleable solid reagents must be avoided.

Mixer and Planetary Mills

Specialized ball mills such as mixer mills and planetary mills occupy the high end of the ball-milling spectrum, and serve as gold standards for mechanochemical synthesis. Both mill types are designed for high-energy milling and size reduction of a wide range of materials over long periods, and are ideally suited for controlled, consistent mechanochemical synthesis. As with the mid-level techniques, mixer and planetary mills differ in how grinding is accomplished. Planetary mills utilize a spinning jar on an oppositely spinning ‘sunwheel’ to impart high centrifugal and frictional forces on materials through the motion of ball bearings.⁶⁰ In contrast, mixer mills utilize cylindrical jars oscillating horizontally to impart high impact forces between the ball bearing and the curved ends of the jar. Mixer mills in general provide overall higher energy impacts than planetary mills. Planetary mills tend to have a wider distribution of mechanical energy and generally offer larger reaction volumes. Despite these differences, both mixer and planetary mills have been used to synthesize a variety of inorganic and organometallic complexes.⁶¹ As a measure of the energy imparted by these mills, the preparation of $[AlA_3]$ that required 2 h of glass flask milling (see above) was completed in 20 min in a tube disperser (80% yield) and in 88% yield after 5 min grinding at 600 rpm in a planetary ball mill (details in Chapter 2).³⁸

The energy input into a mechanochemical reaction can be varied not only by the design of the mill itself but also by the use of ball bearings of different materials or size, and by the frequency of grinding. Balls for grinding are available in a variety of materials, including Teflon[®] (2.3 g cm⁻³), alumina (Al₂O₃, 4.0 g cm⁻³), zirconia (ZrO₂, 5.7 g cm⁻³), stainless steel (ca. 8.0 g cm⁻³) and tungsten carbide (WC, 15.6 g cm⁻³), with the denser materials providing more kinetic energy during impact. Grinding chambers themselves can be made of various materials, and their combination with various ball bearings can change the mechanochemical outcome, such as initiating redox chemistry.⁶²

Removing Solvent from Organometallic Synthesis

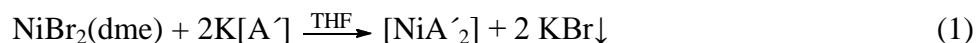
Just as “solventless” and “mechanochemical” are not interchangeable terms when describing reactions, the absence of a solvent during a mechanochemical synthesis can have varied consequences. For simplicity, one can anticipate three different outcomes: 1) solid-state and solution syntheses give the same or closely related products; 2) solution synthesis gives the desired product, whereas solid state does not; and 3) solid-state synthesis gives the desired product, but solution does not. Which of these is the most likely is not yet readily predictable. Whether the first case is obtained certainly depends on the stability of the product and the saturation of the metal coordination sphere. If the compound is commonly isolated with coordinated solvent, then its absence leaves open the possibility that other reactions may occur.

Solvent removal does not change the product

Coordinationally saturated metal complexes may be among the most predictably synthesized with mechanochemical methods. This is typified by ferrocene, prepared from FeCl₂ and TiCp,³⁶ or bis(indenyl)nickel, from NiBr₂(dme) and Na[Ind].⁶³ The same is true with sterically congested homoleptic allyl complexes. [ScA₃] can be made from ScCl₃ and K[A] in THF in approximately 60% yield,³⁸ and mechanochemically in 15, 25, and 42% yield by glass flask, disperser, and planetary ball milling, respectively (discussed in Chapter 2).³⁸ The same is true of [HoA₃], [ErA₃], [YA₃], and [GaA₃], which can be made equally well in solution⁶⁴⁻⁶⁷ or by ball milling.⁶⁸ Some multimetallic clusters are also in this category; the 1:2 reactions of [Au(C≡CPh)PPh₃] with [Ag(OTf)] or [Ag(OTf)(tht)] (tht = tetrahydrothiophene) lead to the high nuclearity species [Ag₁₂Au₁₀(C≡CPh)₁₇(OTf)₅(PPh₃)₃] and [Ag₂₆Au₂₀(C≡CPh)₃₄(OTf)₁₂(PPh₃)₆(tht)₁₂], respectively. The same products are produced whether the reactions are conducted in acetone or with ball milling.⁶⁹

Solvent removal is detrimental

Solvent removal may not always be benign in an organometallic reaction. In such cases, it may be possible to distinguish the effects of the removal of solvent during a mechanochemical reaction from the direct consequences of the addition of mechanical energy. This situation was encountered during the synthesis of the trimethylsilylated bis(allyl)metal nickel complex $[\text{NiA}'_2]$ from the combination of $\text{NiBr}_2(\text{dme})$ and the substituted potassium allyl $\text{K}[\text{A}']$,⁷⁰ both of which are highly soluble in THF (eq 1).



Under solvent-free ball milling conditions, however, the reaction yields the dimerized ligand (1,3,4,6-tetrakis(trimethylsilyl)-1,5-hexadiene) ($[\text{A}'_2]$) instead (eq 2).⁶⁸



Although it might seem as if grinding has changed the primary mechanism from halide metathesis to a redox reaction, use of the (THF-insoluble) NiCl_2 in place of $\text{NiBr}_2(\text{dme})$ in the magnetically stirred THF-based reaction also results in allyl coupling.⁷⁰ Based on the known ability of nickel centers to couple allyl ligands,⁷¹ it was reasonable to propose that oxidative coupling of the allyl anions occurred at the surface of the insoluble NiCl_2 in THF. By extension, the same process is likely occurring under ball milling conditions with the solid $\text{NiBr}_2(\text{dme})$. Clearly, dissolution of the metal reagent is critical to avoid unwanted coupling reactions. It is the absence of solubilized metal ions, rather than specifically the grinding, which promotes the coupling. Allyl coupling reactions have also been found to occur during the preparation of other first-row allyl complexes $[\text{MA}'_2]$ ($\text{M} = \text{Cr}-\text{Co}$)⁷²⁻⁷⁵ from the metal halides MX_2 and $\text{K}[\text{A}']$ under solvent-free milling conditions, even though all the reactions are successful in THF (discussed in Chapter 5).⁶⁸

Solvent removal is advantageous

The synthesis of $[\text{AlA}'_3]$ provides an excellent instance of the power of organometallic mechanochemistry to circumvent otherwise intractable synthetic difficulties; it will be discussed in significant depth in Chapter 2. A tri(allyl)aluminum complex was an especially inviting target, as unsuccessful attempts to generate the base-free parent species, $\text{Al}(\text{C}_3\text{H}_5)_3$, date from the 1920s.⁷⁶ Okuda has prepared several complexed derivatives ($\text{L}:\text{Al}(\text{C}_3\text{H}_5)_3$; $\text{L} = \text{THF}$, OPPh_3 , pyridine), however,⁷⁷ and the related gallium complex $[\text{GaA}'_3]$ had been previously

synthesized from GaCl_3 and $\text{K}[\text{A}^-]$ in THF,⁶⁷ so the synthesis of the aluminum complex was not expected to be especially problematic.

Nevertheless, solution-based techniques do not allow isolation of $[\text{AlA}'_3]$. Attempted salt metathesis between AlX_3 and $\text{K}[\text{A}^-]$ in ethereal solvents (Et_2O , THF) give complex, unidentifiable mixtures, and in a hydrocarbon solvent (hexanes) no reactivity is observed.

By grinding $\text{K}[\text{A}^-]$ and AlX_3 ($\text{X} = \text{Cl}, \text{Br}, \text{I}$), however, $[\text{AlA}'_3]$ can be isolated as large yellow crystals in high yield on a multigram scale.³⁸ A single crystal X-ray study indicates $[\text{AlA}'_3]$ is a three-coordinate metal complex, and is found to be highly fluxional in solution. If dissolved in an ethereal solvent, $[\text{AlA}'_3]$ cannot be recovered, but instead, forms an unidentifiable solid.

Despite the bulk of the A' ligands, they do not appear to interfere with the reactivity of the metal center. In a test with benzophenone, $[\text{AlA}'_3]$ reacts immediately to yield the insertion product $[\text{Al}(\text{COPh}_2\text{A}')_3]$ in quantitative yield.³⁸ In contrast, treatment of the $[\text{Al}(\text{C}_3\text{H}_5)_3(\text{thf})]$ complex with benzophenone to form the equivalent compound $[\text{Al}(\text{COPh}_2\text{C}_3\text{H}_5)_3(\text{THF})]$ is much slower.⁷⁸ Preliminary calculations (discussed in Chapter 2) suggest the three-coordinate metal center of $[\text{AlA}'_3]$ plays a vital role in its high reactivity.

Despite such behavior, $[\text{AlA}'_3]$ is less reducing than the more ionic alkali metal salts of $[\text{A}^-]$, and can be used with BiI_3 to form $[\text{BiA}'_3]$. In contrast, the same reaction with $\text{K}[\text{A}^-]$ produces bismuth metal and the coupled ligand $[\text{A}^-]_2$.³⁷ Use of $[\text{AlA}'_3]$ offers a chance to investigate synthesis of metal allyl complexes of the more reducible metals of the d-block and p-block.

Solvent removal or reduction can be beneficial to synthesis even when the product obtained is ultimately the same. This was demonstrated in the synthesis of the CVD precursor $[\text{SrCp}'_2(\text{OEt}_2)]$ ($\text{Cp}' = \text{C}_5\text{Me}_4(n\text{-Pr})$) on a 0.5 kg scale.⁷⁹ Although the compound can be produced in small amounts through conventional metathesis in diethyl ether (i.e., $\text{SrI}_2 + 2 \text{K}[\text{Cp}^-]$), the reaction does not scale. Owing partially to the density of SrI_2 (5.46 g mol^{-1}), and the fact that the reagents are poorly soluble in Et_2O , magnetic or mechanical stirring, sufficient for gram-scale reactions, is inadequate with larger amounts of reagents. With the aid of ball milling and the use of a small amount of Et_2O to create a LAG environment, however, the solvated metallocene is produced in 88% yield. The ether can be subsequently removed through distillation.

Challenges and Opportunities

Degradation of products

A particular issue that must be addressed during mechanochemical synthesis is that, even if macroscopic temperatures do not rise significantly during grinding, a continual input of energy is involved. At the minimum, this can cause degradation of the product and place a cap on product yield. The production of ferrocene from FeCl_2 and TICp was found to reach a maximum after 60 min of milling; decomposition of ferrocene was responsible for the subsequent decrease in yield as milling continued.³⁶ This was established in two ways; one was by grinding ferrocene itself in a ball mill; the compound degraded detectably after 75 min, with release of cyclopentadiene. A second, more interesting test was the grinding of ferrocene with TICl ; in addition to the decomposition of ferrocene, some TICp could be detected in the mixture (eq 3).



This reaction is of course the reverse of the one that formed ferrocene, and touches on the question of the extent to which equilibrium is established in mechanochemical reactions.⁸⁰ The reaction in eq. 3 also hints at another potential problem with a mechanochemical reaction; namely, unwanted by-products of a reaction are usually in the same phase as the reactants and products, and can react with them. This may require a redesign of the reaction to avoid the formation of such by-products; this of course is beneficial when pursuing 'green' synthesis.

Stoichiometric and Stereochemical Variations

The concentrations of reagents in a solid-state reaction are high, if measured on a purely reagent/volume ratio. Yet this does not necessarily translate into the speed of mass transport of reagents, which is dependent on the grinding agent (e.g., milling balls). Although mechanochemical synthesis can increase control over reaction stoichiometries,⁸¹⁻⁸³ this may not always be the case. The consequences of this have been encountered in the context of alkaline earth metal allyl chemistry, discussed in detail in Chapter 4.

The reaction of BeCl_2 with $\text{K}[\text{A}^-]$ in Et_2O produces the solvated $[(\text{Et}_2\text{O})\text{BeA}'_2]$ (eq. 4).⁸⁴ Attempts to desolvate the complex leads to its decomposition. As an alternative route to a base-free bis(allyl) compound, the two solid reagents were ball milled, and the reaction mixture extracted with hexanes. Crystals of a beryllium allyl were readily isolated from the hexanes mixture, but they were found to be of the beryllate $\text{K}[\text{BeA}'_3]$. The structure of this

complex is of a type found before in solution syntheses where the tri-coordinate metal is Sn(II)⁸⁵ or Zn(II).⁸⁶ The fact that this forms only in the solid state, despite the non-optimum ratio of reagents (i.e., the reaction is effectively $\text{BeCl}_2 + 3 \text{K}[\text{A}'] \rightarrow \text{K}[\text{BeA}'_3] + 2 \text{KCl}$), indicates that without solvent the coordination sphere of beryllium is able to accept a third σ -bonded allyl ligand.



A more subtle consequence of solvent removal can be found in shifts of stereoisomer ratios. Although this is well documented in organic chemistry⁸⁷⁻⁸⁸, organometallic examples are rare. The Group 15 $[\text{MA}'_3]$ ($\text{M} = \text{As}, \text{Sb}, \text{Bi}$) complexes can be readily formed through both solution and mechanochemical synthesis methods, and are found as pairs of diastereomers (Chapter. 3)³⁷. One form has apparent C_3 -symmetry with all of the $[\text{A}']$ groups pointing in one direction, similar to the structure of $\text{M}[\text{M}'\text{A}'_3]$ complexes. The other has only C_1 symmetry, confirmed with X-ray crystallography. These complexes are strictly σ -bound and cannot be interconverted between C_1 and C_3 diastereomers.³⁷

An unpredictable element of reactivity manifests itself through the ratio of the stereoisomers produced in the mechanochemical and solution-based methods. The ratio of C_1 to C_3 is dependent upon the method of synthesis and identity of the metal center, with variations of reagents, reaction temperature, and length having no effect.³⁷ Ball milling promotes the formation of the C_1 isomer, evidently the kinetic product, sometimes substantially increasing the relative ratio between C_1 and C_3 (up to 10:1 for the arsenic derivative).

Despite the uncertainties in mechanism that can accompany mechanochemical reactions, it has been gratifying to see the advances that have been made in multistep organometallic synthesis. Multistep mechanochemical coordination chemistry has been demonstrated before,⁸⁹ but even more complex transformations, involving both redox chemistry and covalent bond transformations, have been demonstrated with metal carbonyls. Perhaps the most elaborate to date is illustrated in Figure 2, in which $\text{Re}_2(\text{CO})_{10}$ is converted to *fac*-(TMEDA) $\text{Re}(\text{CO})_3\text{F}$ through the agency of NaI, $\text{K}[\text{HSO}_5]$ (oxone), AgF and *N,N,N',N'*-tetramethylethylenediamine (TMEDA).

The individual steps of the reaction, which can be conducted separately, comprise oxidative addition of a zero-valent metal carbonyl, halogen exchange, and addition of a chelating ligand. Most impressively, however, they can be conducted in a one-pot five-reagent process, generating the final rhenium tricarbonyl complex in 45% yield, an elegant example of orthogonal synthesis.³⁹ The potential for expanding such multicomponent reactions to other systems is large.

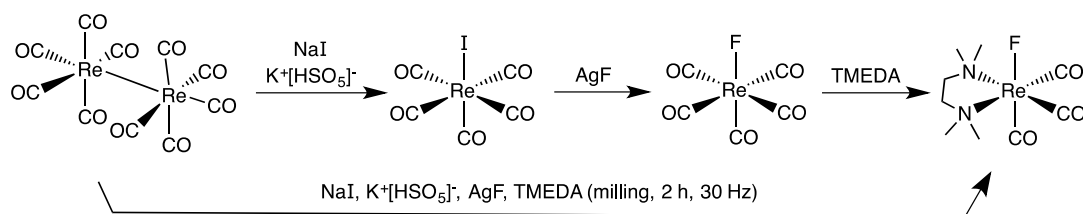


Figure 2. Mechanochemical synthesis of *fac*-(TMEDA)ReCO₃F from Re₂(CO)₁₀. The steps can be performed separately, but a one-pot multicomponent synthesis works also.

Catalyzed reactivity

Heterogeneous catalysis is another frontier in organometallic mechanochemistry that has much room for growth. Both condensation⁹⁰⁻⁹¹ and coupling reactions have been examined;⁹²⁻⁹⁶ developments in this area have been reviewed.¹³ Recently Ru-catalyzed olefin metathesis, including cross-metathesis and ring-closing metathesis, has been demonstrated with commercially available catalysts, including first and second-generation Grubbs catalysts, and the second-generation Hoveyda–Grubbs catalyst (Figure 3).⁹⁷

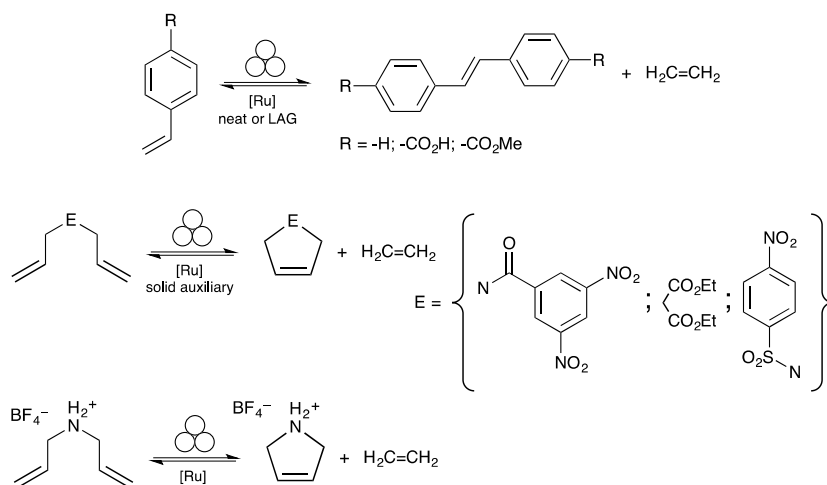
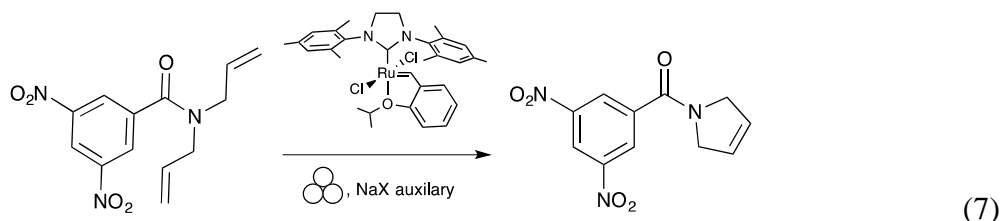


Figure 3. Mechanochemically induced Ru-catalyzed olefin metathesis reactions, including cross-metathesis and ring-closing metathesis.

Steel-based equipment had to be avoided with neat liquids, owing to irreducible behavior, and in some cases, an inert abrasive auxiliary (e.g., NaCl, K₂SO₄) had to be added to prevent the balls from being coated with reaction mixtures, limiting the product yields. In many cases, high yields were obtained, with minimal solvent use required in workup. Especially notable was the higher conversion (90+ %) observed with ball milling compared to

reactions conducted under other conditions, such as with the ring-closing metathesis of *N,N*-diallyl-3,5-dinitrobenzamide to 1-(3,5-dinitrobenzoyl)-2,5-dihydro-1H-pyrrole (eq 7); a static solid state reaction (reagents ground, but subsequently left undisturbed) produced the pyrrole in only ca. 3% yield after one day.⁹⁸ The scalability and solvent efficiency of mechanochemically driven catalysis promises many avenues for future exploration.



Conclusions

In this chapter, it has been shown that mechanochemistry, and specifically ball milling, offers the organometallic chemist a powerful synthetic tool that complements standard solution-based methodologies. The ‘M-chem way’ brings its own challenges and sets of rules to synthesis, and many of the latter are not yet fully understood. Mechanism(s) of reactions in the solid state are by no means required to follow those of their solution-based counterparts. Manipulating solid materials introduces different issues of mass transport, and can reduce the effects of steric hindrance to reactivity.⁸² These changes can contribute to (yet) unpredictable patterns of reactivity, whether they involve the promotion of undesired decomposition routes, the formation of nonstoichiometric products, or the generation of products previously believed to be unattainable. The last of these is of course a part of the great allure of mechanochemistry, especially if solvent-free species have considerably higher reactivity than do comparable solvated complexes. This has implications for the design of more active reagents and catalytic initiators.

What can be said with certainty even at this point, however, is that mechanochemistry offers a route to circumvent solvent effects, and can be practiced with readily available or inexpensively purchased equipment. As more data is gathered that compares the outcomes of mechanochemical and solution-based reactions, the potential of solid-state synthesis to challenge prevailing assumptions about the role of solvents should become more apparent. Too often, chemists still ask “what solvent is needed?” when planning a reaction, when perhaps the better question is “do I really need a solvent at all?”

Discussed in the following chapters are the efforts towards the adaptation of ball milling to bulky allyl metal chemistry paired with the results of the removal of solvents, previously assumed essential. A detailed discussion of these topics (i.e., aluminum, group 15, and group 2) can be found in the subsequent chapters (Chapters 2-4, respectively). Additionally, forays into other areas of the periodic table and how these investigations impact our knowledge of organometallic mechanochemistry will be discussed as well (Chapter 5). Work conducted on carbonyl derivatives of allyl complexes, completed prior to the initiation of the mechanochemical studies, is described in Chapter 6.

Chapter 2

Mechanochemical Synthesis and Investigations as a Potential Allyl Transfer Agent of the Base-Free Tris(allyl)aluminum Complex [Al(1,3-(SiMe₃)₂C₃H₃)₃]

Introduction

Solvent-free organometallic reactions, although far less common than solvent-mediated versions, can encompass a variety of transformations, including isomerization, ligand rearrangement and replacement, and oxidative addition/reductive elimination.^{12, 31, 33, 99-101} Solid-state reactions provide the opportunity to investigate compounds not attainable when a solvent is present, either because useable solvents interfere with the interaction of the reagents, or because solvent molecules bind strongly to the product, and change its structure and reactivity. Described here is a mechanochemical synthesis of an aluminum allyl not available via conventional solvent-based routes, which displays reactivity different from a related solvated version, and has been utilized as an allyl transfer reagent for metal allyl complexes of easily reduced metals. Later, extensions of this method to allyl complexes of other metals will be described.

Among organoaluminum compounds, the tri(allyl) complex [Al(C₃H₅)₃] is a surprisingly elusive species; it has never been isolated in pure form, although attempts to generate it date from the time of Grignard.⁷⁶ Compounds known or believed to be allyl chloro “-ate” or [Al₂(C₃H₅)₃Br₃] species have been prepared *in situ* and used in organic synthesis.¹⁰²⁻¹⁰⁸ More recently, Okuda and coworkers have synthesized the THF adduct of tri(allyl)aluminum, [Al(C₃H₅)₃(thf)], as a yellow oil from the halide metathesis reaction of AlBr₃ and K[C₃H₅].⁷⁸ The THF can be replaced with the stronger base OPPh₃ to form the solid [Al(η¹-C₃H₅)₃(OPPh₃)], or with pyridine to form the yellow oil [Al(C₃H₅)₃(py)].⁷⁷ The THF adduct has been transformed into the bis(allyl)aluminum cations [Al(η¹-C₃H₅)₂(THF)_{3-n}]⁺ [BPh₄]⁻·(n+1)THF (n = 0, 1), and the tetrakis(allyl) aluminate K⁺[Al(η¹-C₃H₅)₄]⁻.⁷⁸ Reactions of the allyl complexes with benzophenone, allyl halides, halogens and pyridines have also been explored.⁷⁷⁻⁷⁸

Our interest in metal complexes of trimethylsilylated allyl ligands stems from the considerable kinetic stability and high hydrocarbon solubility they exhibit, particularly when compared to unsubstituted versions, which may be unknown or substantially less stable.¹⁰⁹⁻¹¹⁰ The 1,3-(SiMe₃)₂C₃H₃⁻ (A[∧]) ligand has previously been used to generate the group 13 complex [GaA[∧]₃] with halide metathesis,⁶⁷ and it was thought that preparation of the aluminum homologue would be straightforward.

This proved not to be the case; for example, treatment of AlX_3 ($\text{X} = \text{Cl}, \text{I}$) with $\text{K}[\text{A}']$ in either THF or diethyl ether, followed by removal of the solvent yields thick orange oils containing unidentifiable mixtures of products. Variation in the temperature (room temp, -78°C) does not change the outcome. A typical oil from the reaction of AlI_3 with $\text{K}[\text{A}']$ in THF displays at least 8 resonances in its ^1H NMR spectrum in the SiMe_3 region (δ 0.0–0.4), plus another 8 multiplets in the olefinic region (δ 5.0–7.0), indicative of a complex mixture. Similar results are obtained under the same conditions when AlX_3 ($\text{X} = \text{Cl}, \text{I}$) is treated with the less bulky $\text{K}[1-(\text{SiMe}_3)\text{C}_3\text{H}_4]$, which suggests that the mixture of products is not a result of the high steric demand of the $[\text{A}']$ ligand.

In an attempt to avoid the issues experienced through a salt metathesis synthetic route, attempts were made to deprotonate HA' with an alkylaluminum. However, treatment of $[\text{AlR}_3]$ ($\text{R} = \text{Me}, \text{Et}$) with HA' in diethyl ether results only in the isolation of starting material. Evidently HA' is not a sufficiently acidic substrate for such proton transfer reactions. Treatment of $1-(\text{SiMe}_3)_2\text{C}_3\text{H}_5$ in place of HA' is similarly unsuccessful. Combined with the inability to produce identifiable products, the lack of deprotonation reactivity suggests $[\text{AlA}'_3]$ is not available using standard solvent-based synthetic approaches.

Experimental

General Considerations. All syntheses were conducted under rigorous exclusion of air and moisture using Schlenk line and glovebox techniques. Proton (^1H), carbon (^{13}C), and COSY spectra were obtained on an Advance AV-400 MHz spectrometer. Proton and carbon were referenced to residual resonances of C_6D_6 (δ 7.15 and δ 128). Variable temperature ^1H NMR was obtained on a Bruker DRX-500 and referenced to residual resonances of $\text{tol-}d_8$. Metal analysis was obtained with ICP-OES on a Perkin Elmer Optima 7000 DV. Combustion analysis was performed by ALS Environmental, Tucson, AZ.

Materials. Aluminum halides (anhydrous) and alkyls, and ScCl_3 were purchased from Strem Chemicals and used as received. All other anhydrous metal salts were previously purchased from Strem and Sigma-Aldrich, stored under an N_2 atmosphere and used as received. Anhydrous inhibitor-free tetrahydrofuran (THF) was used as obtained from Aldrich. Other commercially available reagents were used without additional purification. Toluene, hexanes, and diethyl ether were distilled under nitrogen from potassium benzophenone ketyl.¹¹¹ Deuterated benzene (C_6D_6) was distilled from Na/K (22/78) alloy prior to use. Deuterated toluene ($\text{tol-}d_8$) was purchased from Cambridge Isotopes and dried over molecular sieves prior to use. The HA' and $\text{K}[\text{A}']$ ($\text{A}' = 1,3-(\text{SiMe}_3)_2\text{C}_3\text{H}_3$) reagents were synthesized as previously described.¹¹² Stainless steel (440 grade) ball bearings (6 mm, 3/8 in, and 1/2 in dia) were thoroughly cleaned with hexanes and acetone prior to use. Disperser milling was performed with

an Ultra-Turrax Tube Drive and BMT-20-S tubes, both purchased from IKA. Planetary milling was performed with a Retsch model PM100 mill, 50 mL stainless steel grinding jar type C, and safety clamp for air-sensitive grinding. ^1H NMR spectra of HA', K[A'], and [A'₂] available in Appendix A, Figures A1, A2, and A3, respectively.

Syntheses and reactivity of [AlA'₃]

Attempted synthesis of [AlA'₃] from AlX₃ (X = Cl, I). The preparation of [AlA'₃] was attempted from the treatment of AlX₃ (X = Cl, I) with K[A'] in Et₂O at 25 °C. In a typical procedure, AlI₃ (0.173 g, 0.43 mmol) was dissolved in Et₂O in a 125 mL Erlenmeyer flask equipped with magnetic stir bar. K[A'] (0.293 g, 1.31 mmol) was dissolved in a 20 mL vial in Et₂O. The K[A'] solution was added dropwise to the 125 mL flask and the mixture was stirred for 12 h. Work up yielded a mixture of unidentifiable products (^1H NMR). Attempts to involve varying reaction temperature (−78 °C), solvent (THF, hexanes), and halide (AlCl₃) were similarly unsuccessful.

Attempted synthesis of [AlA'₃] from AlR₃. A 125 mL Erlenmeyer flask was filled with hexanes (40 mL) and sealed with a septum. AlEt₃ in hexanes (4.4 mL, 4.4 mmol) and HA' (2.46 g, 13.2 mmol) were added to the flask by syringe. The mixture was stirred for 24 h at room temperature. Removal of the volatiles under vacuum yielded a turbid white oil. Analysis of product by ^1H NMR showed only the presence of HA' and residual solvent. The attempted reaction was repeated with AlMe₃ with the same result.

Synthesis of [AlA'₃] by disperser milling. A 20 mL dispersing tube (IKA BMT-20) was charged with AlI₃ (0.11 g, 0.27 mmol), K[A'] (0.20 g, 0.88 mmol), and stainless steel ball bearings (6 mm diameter, 20 count) under a nitrogen atmosphere and tightly sealed. The tube was connected to the dispersing unit and milled for 15 min at a high rate. The mixture was extracted with minimal hexanes (< 50 mL) and filtered through a medium porosity ground glass frit, providing a pale yellow filtrate. Removal of hexanes under vacuum gave a pale yellow solid, mp 40–44 °C (0.13 g, 80% yield); comparable yields (up to 85%) have been obtained in other runs. Crystals suitable for X-ray diffraction were obtained from a hexanes solution dried under vacuum. Exposure to air results in the production of white smoke within a minute, leaving a dark yellow oil. Anal. Calcd (%) for C₂₇H₆₃AlSi₆: C, 55.6; H, 10.9, Al, 4.63. Found: C, 54.6; H, 11.2; Al, 4.67. ^1H NMR (400 MHz, 298 K, C₆D₆): δ 0.19 (s, 54H, SiMe₃); δ 3.66 (d, 6H, J = 15 Hz, C_(1,3)-H); δ 6.38 (t, 3H, J = 15 Hz, C₍₂₎-H). ^1H NMR (500 MHz, 233K, tol-d₈): δ 0.22 (s, 54H, SiMe₃); δ 3.67 (d, 6H, J = 15 Hz, C_(1,3)-H); δ 6.40 (t, 3H, J = 15 Hz, C₍₂₎-H) ^{13}C NMR (100 MHz, 298 K, C₆D₆): δ 0.01 (SiMe₃); δ 114.07 (C_(1,3)); δ 163.45

(C₂). Comparable results were obtained using AlCl₃ or AlBr₃ in place of AlI₃. Full ¹H NMR spectra at 25 °C and -70 °C available in Appendix A, Figures A4 and A6, respectively)

Synthesis of [AlA'₃] by planetary ball milling. Solid AlBr₃ (0.68 g, 2.54 mmol) and K[A'] (1.76 g, 7.78 mmol) were added to a 50 mL stainless steel grinding jar (type C). The jar was charged with stainless steel ball bearings (6 mm diameter, 50 count) and closed tightly with the appropriate safety closer device under an N₂ atmosphere. The reagents were milled for 5 min. at 600 rpm, resulting in a light brown solid. The product was extracted with minimal hexanes (< 100 mL) and filtered through a medium porosity ground glass frit, providing a pale yellow filtrate. Drying under vacuum initially yielded bright yellow oil (1.31 g, 88% yield), which formed transparent pale yellow crystals overnight. The product was identified as A'₃Al of high purity from its characteristic ¹H NMR spectrum.

Synthesis of [Al(A'Ph₂CO)₃]. A 50 mL Schlenk flask equipped with a magnetic stir bar was charged with A'₃Al (0.19 g, 0.32 mmol) dissolved in hexanes. A 125 mL Schlenk flask with magnetic stir bar was charged with Ph₂CO (0.17 g, 0.95 mmol) dissolved in hexanes. The [AlA'₃] solution was cannulated into the Ph₂CO at -78 °C, resulting in an immediate color change to red at the point of addition. When all [AlA'₃] had been added, the solution had become light pink. Removal of hexanes under vacuum yielded a thick orange-red paste, containing [Al(A'Ph₂CO)₃] in quantitative yield (0.37 g). Anal. Calcd (%) for C₆₆H₉₃AlO₃Si₆: C, 70.16; H, 8.30, Al, 2.39. Found: C, 68.94; H, 8.31; Al, 2.41. ¹H NMR (400 MHz, 298 K, C₆D₆): δ -0.04 (s, 27H, SiMe₃); δ 0.01 (s, 27H, SiMe₃); δ 3.01 (d, 3H, *J* = 10 Hz C₍₃₎-H); δ 5.60 (d, 3H, *J* = 19 Hz, C₍₁₎-H); δ 6.04 (dd, 3H, *J* = 19 Hz, *J* = 10 Hz, C₍₂₎-H); δ 7.01 (m, *o*-Ph); δ 7.69 (dd, 18H, *J* = 8 Hz, *J* = 1.5 Hz, *m,p*-Ph). ¹³C NMR (100 MHz, 298 K, C₆D₆): δ -1.10 (SiMe₃); δ -0.43 (SiMe₃); δ 50.38 (C₍₁₎); δ 80.54 (CO[Al]); δ 125.80, δ 126.53 (C₍₃₎); δ 128.34 (*m*-Ph); δ 130.23 (*o*-Ph); δ 132.18 (*p*-Ph); δ 138.12 (*ipso*-Ph); δ 148.35, δ 148.68 (C₍₂₎). Full ¹H NMR spectrum available in Appendix A, Figure A5.

Reaction of [AlA'₃] with HOCPh₃: [AlA'₃] Al (0.16 g, 0.28 mmol) was dissolved in toluene in a 50 mL Erlenmeyer flask equipped with magnetic stir bar to form a clear pale yellow solution. HOCPh₃ (68 mg, 0.26 mmol) was dissolved in toluene in a 20 mL vial. The Ph₃COH solution was added to the Erlenmeyer flask dropwise and stirred at room temperature for 12 hr. Removal of toluene by vacuum resulted in the isolation of starting material. Attempts made using a 3 HOCPh₃ : 1 [AlA'₃] ratio resulted in the isolation of starting material, although there was some evidence (¹H NMR) for the formation of unidentified side products. Reactions performed in hexanes showed a similar lack of reactivity.

Synthesis of [ScA'₃] by disperser milling: A 20 mL dispersing tube (IKA BMT-20) was charged with ScCl₃ (60.6 mg, 0.40 mmol), K[A'] (0.271 g, 1.21 mmol), and stainless steel ball bearings (6 mm diameter, 20 count) in an N₂ atmosphere and tightly sealed. The tube was connected to the dispersing unit and milled for 15 min at a high rate. Product was extracted with minimal hexanes (< 50 mL) and filtered through a medium porosity ground glass frit, providing a pale yellow filtrate. Removal of hexanes under vacuum gave yellow crystals (65.3 mg, 25%). Crystals melt and decompose around 140 °C. Anal. Calcd for C₂₇H₆₃ScSi₆: C, 53.94; H, 10.56. Found: C, 50.95; H, 9.49; the low values may reflect the high air-sensitivity of the compound. ¹H NMR (400 MHz, 298 K, C₆D₆): δ 0.23 (s, 54H, Si(CH₃)₃); δ 3.83 (d, 6H, C_(1,3)-H, *J* = 16 Hz); δ 7.60 (t, 3H, C₂-H, *J* = 16 Hz). ¹³C NMR (100 MHz, 298 K, C₆D₆): δ 0.84 (SiMe₃); δ 100.3 (C_(1,3)); δ 164.5 (C₍₂₎). Full ¹H NMR spectrum available in Appendix A: Figure A7

Synthesis of [ScA'₃] by planetary ball mill. Solid ScCl₃ (0.214 g, 1.41 mmol) and K[A'] (0.990 g, 4.41 mmol) were added to a 50 mL stainless steel grinding jar (type C). The jar was charged with stainless steel ball bearings (6 mm diameter, 50 count) and closed tightly with the appropriate safety closer device under an N₂ atmosphere. The reagents were milled for 10 min. at 600 rpm, resulting in a lime green powder. The product was extracted with minimal hexanes (< 100 mL) and filtered through a medium porosity ground glass frit, providing a dark orange filtrate. Removal of hexanes under vacuum yielded [ScA'₃] as a yellow-orange solid in moderate yield (0.41 g, 48%). NMR spectra (¹H and ¹³C) were identical to the product prepared with the disperser mill.

Using [AlA'₃] as an [A'] transfer agent.

Attempted synthesis of [ScA'₃]. Solid ScCl₃ (0.136 g, 0.90 mmol) and crystalline [AlA'₃] (0.477 g, 0.82 mmol) were placed in a 50 mL grinding jar (Type C). The jar was charged with stainless steel ball bearings (6 mm, 50 count) and closed tightly with the appropriate safety closer device under an N₂ atmosphere. The reagents were milled for 10 min. at 600 rpm, resulting in a light yellow-brown solid. Extraction with hexanes and drying under vacuum resulted in the isolation of the starting material [AlA'₃]. No chemical shifts corresponding to [ScA'₃] were visible in the ¹H NMR spectra.

Synthesis of [SnA'ₓ] complex in hexanes. SnI₄ (0.134 g, 0.214 mmol) was partially dissolved in hexanes in a 50 mL Erlenmeyer flask, with magnetic stir bar, to create a clear yellow solution over orange crystalline solid. [AlA'₃] (0.161 g, 0.275 mmol) was dissolved in hexanes in a 10 mL vial to create a pale yellow solution. The [AlA'₃] solution was added to the 5 mL flask dropwise with stirring, resulting in a cloudy yellow solution with a faint green

tint. After 15 min no solid SnI_4 remained in solution. The solution was stirred overnight at room temperature yielding a slightly turbid yellow solution. Filtering through a medium porosity ground glass frit yielded a bright yellow filtrate and an off white solid being retained in the frit. Removal of hexanes under vacuum yielded a viscous yellow oil and a yellow solid on the sides of the flask (0.326 g total). The yellow oil was highly soluble in hexanes, whereas the solid was only sparingly so. The ^1H NMR spectra of the solid and oil were largely different, with the oil containing at least six distinct $[\text{A}']$ ligands and a coupled set of quartets and triplets (labeled as $[\text{q/t}]$), identified with COSY. The ^{13}C NMR spectra was highly complex due to the large number of signals, many of which overlap with similar shifts and those of residual solvents, preventing an accurate assignment and identification. Separation of the oil components is needed for assignment of the ^{13}C NMR chemical shifts. The NMR of the solid contained resonances almost solely for two distinct A' ligands referred to as “doubled” (Appendix A, Figure A9), relatively close to one set of resonances observed with the oil, but with no indication of the other ligands or the quartets and triplet. The solid seems to suggest the presence of two very similar A' ligands, as two resonances are observed for each proton, not just those adjacent to the tin metal center. This suggests that the “doubling” of the peaks are different A' ligands and not the result of splitting from tin isotopes. Neither the oil nor the solid crystallized. There was insufficient solid product for a high signal to noise ^{13}C NMR spectrum to be obtained. **$[\text{SnA}'_x]$ oil product***: ^1H NMR (400 MHz, C_6D_6 , 298K): $[\text{A}'_{\text{A}}]$: δ 0.1082 (s, 9H, SiMe_3); δ 0.3597 (s, 9H, SiMe_3); δ 1.4328 (d, 1H, $J = 11.88$ Hz, $\text{H}_{(\alpha)}$); δ 5.2695 (d, 1H, $J = 18.12$ Hz, $\text{H}_{(\gamma)}$); δ 6.3541 (dd, 1H, $J_1 = 18.16$ Hz, $J_2 = 11.96$ Hz, $\text{H}_{(\beta)}$). $[\text{A}'_{\text{B}}]$: δ 0.1372 (s, 9H, SiMe_3); δ 0.2055 (s, 9H, SiMe_3); δ 2.6605 (d, 1H, $J = 11.4$ Hz, $\text{H}_{(\alpha)}$); δ 5.7074 (d, 1H, $J = 18.28$ Hz, $\text{H}_{(\gamma)}$); δ 6.1282 (dd, 1H, $J_1 = 18.08$ Hz, $J_2 = 11.4$ Hz, $\text{H}_{(\beta)}$). $[\text{A}'_{\text{C to F}}]$: δ 0.1627 (s, 9H, SiMe_3); δ 0.1662 (s, 9H, SiMe_3); δ 0.1710 (s, 9H, SiMe_3); δ 0.1806 (s, 9H, SiMe_3); δ 0.2244 (s, 9H, SiMe_3); δ 0.2399 (s, 9H, SiMe_3); δ 0.2602 (s, 18H, SiMe_3). $[\text{A}'_{\text{C}}]$: δ 2.4990 (d, 1H, $J = 11.68$ Hz, $\text{H}_{(\alpha)}$); δ 5.6627 (d, 1H, $J = 17.44$ Hz, $\text{H}_{(\gamma)}$); δ 6.3202 (dd, 1H, $J_1 = 18.28$ Hz, $J_2 = 11.68$ Hz, $\text{H}_{(\beta)}$). $[\text{A}'_{\text{D}}]$: δ 2.5713 (d, 1H, $J = 11.8$ Hz, $\text{H}_{(\alpha)}$); δ 5.6190 (d, 1H, $J = 17.52$ Hz, $\text{H}_{(\gamma)}$); δ 6.2150 (dd, 1H, $J_1 = 18.00$ Hz, $J_2 = 11.76$ Hz, $\text{H}_{(\beta)}$). $[\text{A}'_{\text{E}}]$: δ 2.4566 (d, 1H, $J = 11.88$ Hz, $\text{H}_{(\alpha)}$); δ 5.6297 (d, 1H, $J = 17.92$ Hz, $\text{H}_{(\gamma)}$); δ 6.2743 (dd, 1H, $J_1 = 18.40$ Hz, $J_2 = 11.84$ Hz, $\text{H}_{(\beta)}$). $[\text{A}'_{\text{F}}]$: δ 2.4174 (d, 1H, $J = 11.52$ Hz, $\text{H}_{(\alpha)}$); δ 5.5938 (d, 1H, $J = 18.00$ Hz, $\text{H}_{(\gamma)}$); δ 6.1816 (dd, 1H, $J_1 = 18.00$ Hz, $J_2 = 11.52$ Hz, $\text{H}_{(\beta)}$). **$[\text{q/t}]^{**}$** : δ 0.7560 (t, $J = 7.04$ Hz); δ 3.6137 (q, $J = 7.04$ Hz); δ 3.6453 (q, $J = 7.04$ Hz); δ 3.7296 (q, $J = 7.04$ Hz); δ 3.7610 (q, $J = 7.04$ Hz). **$[\text{SnA}'_x]$ solid product**: ^1H NMR (400 MHz, C_6D_6 , 298K): $[\text{A}'_{\text{A}}]$: δ 0.1492 (s, 9H, SiMe_3); δ 0.2162 (s, 9H, SiMe_3); δ 2.6845 (d, 1H, $J = 11.4$ Hz, $\text{H}_{(\alpha)}$); δ 5.7321 (d, 1H, $J = 18.08$, $\text{H}_{(\gamma)}$); δ 6.1605 (dd, 1H, $J_1 = 18.04$ Hz, $J_2 = 11.4$ Hz, $\text{H}_{(\beta)}$). $[\text{A}'_{\text{B}}]$: δ 0.1597 (s, 9H, SiMe_3); δ 0.2162 (s, 9H, SiMe_3); δ 2.6242 (d, 1H, $J = 11.48$ Hz, $\text{H}_{(\alpha)}$); δ 5.7261 (d, 1H,

$J = 17.92$, $H_{(\gamma)}$; δ 6.1699 (dd, 1H, $J_1 = 18.1$ Hz, $J_2 = 11.28$ Hz, $H_{(\beta)}$). *Labels [$A'_{(A)}$], [$A'_{(B)}$], [$A'_{(C)}$], [$A'_{(D)}$], [$A'_{(E)}$], and [$A'_{(F)}$] (oil product) and [$A'_{(A')}$], and [$A'_{(B')}$], (solid product) indicate H assignments to specific [A'] ligands. ** Label [q/t] signifies the quartets and triplets that split each other, identified by COSY, but were unassignable to [A'] complexes.) Full ^1H NMR spectra of the [SnA'_x] oil and [SnA'_x] solid available in Appendix A, Figures A8 and A9, respectively.

Synthesis of an [SnA'_x] complex by milling. SnI_4 (0.162 g, 0.258 mmol) and [AlA'_3] (0.194 g, 0.333 mmol) were added to a 50 mL stainless steel grinding jar (type C). The jar was charged with stainless steel ball bearings (1/2 in dia, 3 count) and closed tightly with the appropriate safety closer device under an N_2 atmosphere. The reagents were milled for 15 min at 600 rpm, resulting in bright yellow oil with no sign of solid reagents. The product was extracted with minimal hexanes (< 100 mL) and filtered through a medium porosity ground glass frit, providing a yellow filtrate. Removal of hexanes under vacuum yielded a yellow oil and a yellow solid along the flask sides (0.264g total). The solid was not crystalline and once out of solution was sparingly soluble in hexanes. The ^1H NMR spectra displayed signals for three distinct A' ligands closely matching [A'_A], [$A'_{A'}$], and [$A'_{B'}$] from reactions conducted in hexanes. Signals corresponding to [q/t] set were also present. Identical results were obtained for 48 h reactions conducted in hexanes. ^1H NMR (400 MHz, C_6D_6 , 298K): [A'_A]: δ 0.100 (s, 9H, SiMe_3); δ 0.337 (s, 9H, SiMe_3); δ 1.421 (d, 1H, $J = 11.9$ Hz, $H_{(\alpha)}$); δ 5.267 (d, 1H, $J = 18.2$ Hz, $H_{(\gamma)}$); δ 6.329 (dd, 1H, $J_1 = 18.2$ Hz, $J_2 = 11.9$ Hz, $H_{(\beta)}$). [$A'_{A'}$]: δ 0.137 (s, 9H, SiMe_3); δ 0.199 (s, 9H, SiMe_3); δ 2.590 (d, 1H, $J = 11.4$ Hz, $H_{(\alpha)}$); δ 5.689 (d, 1H, $J = 18.1$ Hz, $H_{(\gamma)}$); δ 6.115 (dd, 1H, $J_1 = 18.1$ Hz, $J_2 = 11.4$ Hz, $H_{(\beta)}$). [$A'_{B'}$]: δ 0.137 (s, 9H, SiMe_3); δ 0.199 (s, 9H, SiMe_3); δ 2.648 (d, 1H, $J = 11.4$ Hz, $H_{(\alpha)}$); δ 5.694 (d, 1H, $J = 18.1$ Hz, $H_{(\gamma)}$); δ 6.107 (dd, 1H, $J_1 = 18.1$ Hz, $J_2 = 11.4$ Hz, $H_{(\beta)}$). [q/t]: δ 0.791 (t, $J = 7.04$ Hz); δ 0.875 (t, $J = 7.04$ Hz); δ 3.645 (q, $J = 7.04$ Hz); δ 3.676 (q, $J = 7.04$ Hz); δ 3.756 (q, $J = 7.04$ Hz); δ 3.787 (q, $J = 7.04$ Hz). Full ^1H NMR spectra available in Appendix A, Figures A10 and A11.

Attempted preparation of a [PtA'_x] complex using [AlA'_3]. PtCl_2 (0.112 g, 0.420 mmol) was partially suspended in hexanes, in a 50 mL Erlenmeyer flask equipped with magnetic stir bar, resulting in a muddy brown solution. [AlA'_3] (0.159 g, 271 μmol) was dissolved in hexanes in a 20 mL vial, producing a pale yellow solution. The [AlA'_3] solution was added dropwise to the 50 mL Erlenmeyer flask with no immediate visible change. Within 10 min. the solution became noticeably darker and after 24 h a brown-black solution was present. Filtration through a medium porosity ground glass frit gave a brown filtrate with a particulate brown solid. Drying under vacuum gave a thick viscous brown oil-solid mixture (0.177 g). Attempts to grow crystals through the slow evaporation of hexanes were unsuccessful. The ^1H NMR spectra showed the product to be a complex mixture of [A'_2] and a possible product; no

[AlA'₃] was observed. The spectrum appears consistent with the presence of several σ -bound [A'] ligands, as indicated by the chemical shift ranges,³⁷ not unlike the ¹H NMR spectra of possible [SnA'_x] and [PdA'_x] complexes also synthesized from [AlA'₃]. The similarities with [SnA'_x] and [PdA'_x] products included the presence of apparent quartet (δ 3.5-4.0) and triplet (δ 0.6-0.8) resonances that do not correspond with known A' splitting. Full ¹H NMR spectrum available in Appendix A, Figure: A12

Attempted preparation of a [PdA'_x] complex using [AlA'₃]. PdCl₂ (0.102 g, 0.577 mmol) and [AlA'₃] (0.222 g, 0.381 mmol) were added to a 50 mL stainless steel grinding jar (type C). The jar was charged with stainless steel ball bearings (6 mm dia, 50 count) and closed tightly with the appropriate safety closer device under an N₂ atmosphere. The reagents were milled for 10 min at 600 rpm, resulting in viscous black oil. The product was extracted with minimal hexanes (< 100 mL) and filtered through a medium porosity ground glass frit, providing a yellow-brown filtrate. Removal of hexanes under vacuum yielded viscous brown oil that did not solidify. The ¹H NMR spectra suggested a complex mixture with only [A'₂] as an identifiable component; however, [AlA'₃] was not present. Several other peaks could be seen that did not correspond to known complexes, including the quartets (δ 3.5-4.0) and triplet (δ 0.6-0.8).

Attempted preparation of a [TeA'_x] complex. TeI₄ (0.130 g, 0.204 mmol) and [AlA'₃] (0.1177 g, 0.201 mmol) were added to a 50 mL stainless steel grinding jar (type C). The jar was charged with stainless steel ball bearings (6 mm dia, 50 count) and closed tightly with the appropriate safety closer device under an N₂ atmosphere. The reagents were milled for 10 min at 600 rpm, resulting in a yellow solid. The product was extracted with minimal hexanes (< 100 mL) and filtered through a medium porosity ground glass frit, providing a yellow filtrate. Removal of hexanes under vacuum yielded a yellow residue (0.058 g), tentatively identified as [TeA'₄]. Due to the low yield, the entire sample was used for ¹H NMR analysis, but was of insufficient concentration for conclusive ¹³C NMR, and no attempts at crystallization were made. The ¹H NMR spectra are consistent with the presence of two σ -bound [A'] ligands, one of significantly greater intensity than the other. The presence of [A'₂] was confirmed along with several other unidentifiable signals. Additionally several overlapping quartets (δ 3.5-4.0) and two triplets (δ 0.6-0.8) were present. Major [A'] complex, [TeA'₄]: ¹H NMR (400 MHz, C₆D₆, 298K): δ 0.130 (s, 36H, SiMe₃); δ 0.136 (s, 36H, SiMe₃); δ 3.403 (d, 4H J= 11.0 Hz, H_(α)); δ 5.478 (d, 4 H, J = 18.0 Hz, H_(γ)); δ 6.268 (dd, 4H, J₁ = 18.0 Hz, J₂ = 11.0 Hz, H_(β)). Minor [A'] complex: ¹H NMR (400 MHz, C₆D₆, 298K): δ 0.117 (s, 9H, SiMe₃); δ 0.142 (s, 9H, SiMe₃); δ 3.241 (d, 1H J= 10.4 Hz, H_(α)); δ 5.283 (d, 1H, J = 18.1 Hz, H_(γ)); δ 6.093 (dd, 4H, J₁ = 18.0 Hz, J₂ = 10.1 Hz, H_(β)). Quartet and Triplet: ¹H NMR (400 MHz, C₆D₆, 298K): δ 0.654 (t, ~2H, J = 7.0 Hz); δ 0.746 (t, ~2H, J = 7.0 Hz); δ 3.62 (m,

~4H); δ 3.726 (q, ~1H, $J = 7.0$ Hz); δ 3.757 (q, ~1H, $J = 7.0$ Hz). Full ^1H NMR spectrum available in Appendix A, Figure A13.

Attempted mechanochemical synthesis of $[\text{NiA}'_2]$ from $\text{NiBr}_2(\text{dme})$. $\text{NiBr}_2(\text{dme})$ (0.126 g, 0.409 mmol) and $[\text{AlA}'_3]$ (0.1630 g, 0.280 mmol) were added to a 50 mL stainless steel grinding jar (type C). The jar was charged with stainless steel ball bearings (6 mm dia, 50 count) and closed tightly with the appropriate safety closer device under an N_2 atmosphere. The reagents were milled for 10 min at 600 rpm, resulting in yellow-brown solid. The product was extracted with minimal hexanes (< 100 mL) and filtered through a medium porosity ground glass frit, providing an orange filtrate. Drying under vacuum yielded a small amount of viscous yellow-orange oil. Unlike $[\text{NiA}'_2]$, the oil did not solidify or crystallize after several days.¹¹³ From ^1H NMR spectra, the oil appeared to be a complex mixture of products and reagents, among which was $[\text{AlA}'_3]$. The presence of several unidentified peaks, the color changes, and the presence of starting material suggest that a partial reaction likely occurred and not just the decomposition observed with $\text{NiBr}_2(\text{dme})$ and $\text{K}[\text{A}']$.

Attempted mechanochemical synthesis of $[\text{NiA}'_2]$ from NiCl_2 . NiCl_2 (0.056 g, 0.171 mmol) and $[\text{AlA}'_3]$ (0.163 g, 0.279 mmol) were added to a 50 mL stainless steel grinding jar (type C). The jar was charged with stainless steel ball bearings (6 mm dia, 50 count) and closed tightly with the appropriate safety closer device under an N_2 atmosphere. The reagents were milled for 10 min at 600 rpm, resulting in dark yellow-brown oil. The product was extracted with minimal hexanes (< 100 mL) and initially took on a green tint. Filtration through a medium porosity ground glass frit resulted in the collection of a brown-green solid and a yellow-brown filtrate. Drying under vacuum yielded a small amount of viscous yellow-brown oil. Unlike $[\text{NiA}'_2]$ the oil did not solidify or crystallize after several days.¹¹³ Over the period of several days, the oil began to deposit a gray-black solid, suggesting the presence of a thermally unstable compound. The ^1H NMR spectrum of the oil was inconclusive owing to an extreme broadening of all peaks, likely from the decomposition to nickel metal during the experiment. The isolation of the yellow-brown oil indicates the presence of some reactivity and not just the decomposition observed with NiCl_2 and $\text{K}[\text{A}']$.

Reaction of $\text{U}_4(\text{dioxane})$ with $[\text{AlA}'_3]$. Treatment of $\text{U}_4(\text{dioxane})$ with $[\text{AlA}'_3]$, under both mechanochemical (dispenser milling) conditions and in hexane solutions, appeared to involve a reaction, although the products could not be identified. Milling for 15 min in the dispenser followed by an extraction with hexanes yielded dark brown oil that only partially solidified over a period of days. The ^1H NMR spectra suggested that a highly complex mixture of several products was present, including a minor amount of $[\text{A}'_2]$, but no $[\text{AlA}'_3]$ was identifiable. When performed in hexanes, an immediate color change to red-orange was observed on the addition of $[\text{AlA}'_3]$, and stirring for 72 h at room temperature yielded an orange

brown solution. Extraction with hexanes yielded a brown oil in low yield. The ^1H NMR spectra suggested that a highly complex mixture was present, and also that starting material was completely consumed. A full ^1H NMR spectrum is available in Appendix A, Figure A14.

Attempts towards the preparation of $[\text{TiA}'_4]$. Treatment of TiBr_4 with stoichiometric amounts of $[\text{AlA}'_3]$ in solutions of hexanes did not yield a $[\text{TiA}'_4]$ complex. The addition of $[\text{AlA}'_3]$ resulted in immediate color change, yielding a deep red to purple solution from the initial yellow. Within 60 min of stirring, a nearly black solution was present, though a closely held light confirmed the solution was in fact very deep red. Filtration through a medium porosity ground glass frit and drying under vacuum yielded a mixture of brown and gray solids. The only product in ^1H NMR spectra was $[\text{A}'_2]$. The presence of the initial deep red solution may indicate a rapidly forming and decomposing product or intermediate. Alterations of the synthesis conditions and isolation procedure may allow for the isolation of this complex.

Attempts towards the preparation of $[\text{TlA}']$ complexes. Treatment of TlCl with $[\text{AlA}'_3]$ yielded a dark gray solid, consistent with Tl metal, from which only $[\text{A}'_2]$ could be isolated and identified with ^1H NMR. Reactions conducted by ball milling and in hexane solutions rapidly resulted in the reduction and decomposition products associated with the $[\text{A}']$ ligand. It appears that Tl^+ is too easily reduced in the presence of $[\text{A}']$ regardless of whether it is from $\text{K}[\text{A}']$ or $[\text{AlA}'_3]$.

Results and Discussion

A procedure used for the production of magnesium borohydrides¹¹⁴ was adopted for the solid state synthesis of the aluminum allyl. AlX_3 ($\text{X} = \text{Cl}, \text{Br}, \text{or I}$) and $\text{K}[\text{A}']$ were combined in a 50 mL round bottom flask containing stainless steel ball bearings (6 mm) and turned on a rotary evaporator for 1–2 hours, producing an off-white to yellow powder. Extraction with hexanes gives the solid product $[\text{AlA}'_3]$ (**1**) in approximately 30% yield. No reaction occurred if the reagents were simply magnetically stirred in hexanes without grinding, confirming that mechanochemical activation was responsible for the production of **1**, and did not occur during the extraction procedure.

Although the flask reactor is inexpensive and sufficient for test reactions, significantly shorter reaction times (15 min) and higher yields (up to 85%) were obtained with the use of a tube disperser,¹¹⁵ which provides more energetic impact of the ball bearings. Even shorter reaction times (5 min, 600 rpm) and equivalent yields (up to 88%) on a multigram scale were obtained with the use of a planetary ball mill. Compound **1** is a low-melting crystalline solid (40–44 °C), soluble in both aromatic and aliphatic hydrocarbons, and stable indefinitely under

an inert atmosphere at room temperature. It can survive only 30–60 sec exposure to air before decomposition occurs with the production of white smoke. In THF, **1** readily dissolves to form a pale yellow solution. Removal of the THF leaves yellow oil that does not solidify over a period of days; ^1H NMR spectra contain multiple broad resonances that suggest a mixture of products is present.

The ^1H NMR spectrum of **1** at room temperature gives the appearance of a structure with symmetrically bound (“ π -type”) allyl ligands; e.g., in benzene- d_6 , the resonance for all six SiMe_3 groups appears as a sharp singlet (δ 0.19). The central hydrogen atom on the allyl ligands appears as a triplet (δ 6.38); the terminal hydrogens are represented by a doublet (δ 3.66). At room temperature in toluene- d_8 , the terminal hydrogens appear as a broad resonance ($w_{1/2} \approx 125$ Hz) that sharpens at -20 °C into a doublet ($J = 15$ Hz). Further cooling to -70 °C produces no additional major changes in the spectrum. In particular, the SiMe_3 resonance broadens slightly but remains unsplit. This behavior is reminiscent of the fluxional $[\text{GaA}'_3]$ complex, which also displays “ π -type” allyl ligands in solution, and whose resonance for SiMe_3 remains unresolved at -75 °C.

A single-crystal X-ray diffraction study of **1** reveals that it crystallizes from hexanes as a monomer with the aluminum atom σ -bound to the bis(trimethylsilyl)allyl ligands in a trigonal planar manner (Figure 4). All three ligands are roughly perpendicular to the AlC_3 plane, with one antiparallel to the other two. The complex is isostructural with the gallium analogue.⁶⁷

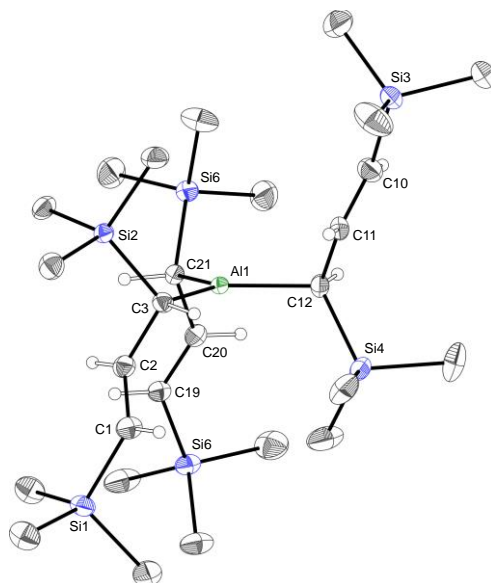


Figure 4. Thermal ellipsoid plot of **1**; ellipsoids are drawn at the 50% level, and hydrogen atoms on the trimethylsilyl groups have been omitted for clarity. Bond angles and distances available in Appendix B: Section B1.

The average Al–C distance of 1.964(3) Å is typical for aluminum-carbon single bonds; cf. those of the mononuclear trimesitylaluminum (1.951(1) Å),¹¹⁶ [Al(*t*-Bu)₃] (2.006(7) Å),¹¹⁷ and [Al(PhCH₂)₃] (1.99(1) Å).¹¹⁸ The nearly perfect planarity of the central AlC₃ unit in **1** is indicated by the sum of the C–Al–C' angles of 359.8°; the Al atom is only 0.046 Å from the C₃ plane. The planarity reflects the isolation of the metal center from neighboring molecules; in contrast, close intermolecular Al···C contacts in the solid state structures of [Al(*t*-Bu)₃] and [Al(PhCH₂)₃] lead to puckering of the AlC₃ units, with the metal center lifted 0.25 Å¹¹⁷ and 0.475 Å,¹¹⁸ respectively, from the C₃ planes. The fully localized carbon-carbon bonding in the allyl ligands in **1** is indicated by the average C=C and C–C bond distances of 1.334(5) and 1.503(5) Å, respectively.

The bulkiness of the Al ligands not only shields the Al center in **1** from adjacent molecules in the solid state, but it also apparently affects the internal coordination of the allyl ligands. Computational modeling of the parent [Al(C₃H₅)₃] indicates that the binding mode of the ligands is a sensitive function of the level of theory employed. At the Hartree-Fock level with the def2-TZVP basis set (Figure 5a), the ligands are clearly σ-bonded with localized bonding, e.g., all Al–C_α–C_β angles are >105°, and there is an average 0.18 Å difference between the single and double carbon-carbon bond lengths. The Al–C bond lengths (1.983 Å, ave.) are close to those in **1**.

In contrast, a DFT calculation using a functional that provides some accounting for dispersion effects (M06-L) leads to a conformation with ligands of clearly mixed hapticity, i.e., (η¹-C₃H₅)₂(η³-C₃H₅)Al (Figure 5b). The Al–C bonds to the two η¹-bonded allyls average to 1.974 Å, with a C4–Al–C7 angle of 122.4°. The π-electrons are also strongly localized, with average C–C and C=C distances of 1.477 Å and 1.331 Å, respectively. The third allyl ligand has moved into a π-bonded arrangement; the Al–C distances vary only from 2.13–2.16 Å, and the carbon-carbon distances in the ligand are almost identical, at 1.400 and 1.408 Å. Complexes with allyl ligands of mixed hapticity are known in both main-group¹¹⁹ and d- and f-block chemistry,¹²⁰⁻¹³⁰ but [Al(C₃H₅)₃] is one of the few neutral homoleptic complexes that is predicted to adopt such a conformation.¹³¹ The calculated appearance of π-bonding in an allyl ligand is not observed in the solid-state structure of **1**.¹³²

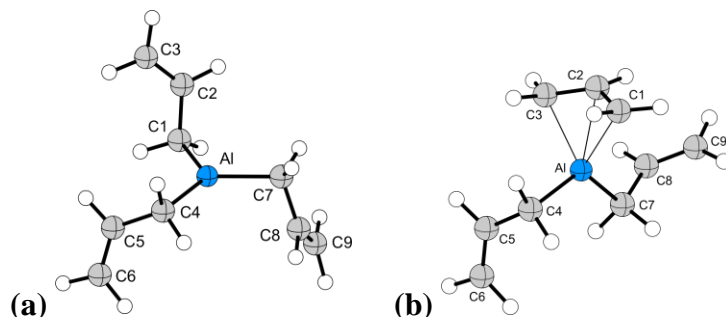
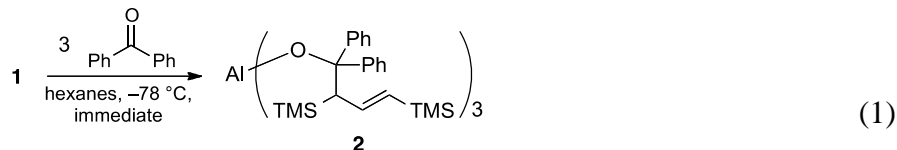


Figure 5. Optimized geometries of $\text{Al}(\text{C}_3\text{H}_5)_3$. Selected bond distances (\AA) for (a) with HF/def2TZVP: Al–C1, 1.981; Al–C4, 1.984; Al–C7, 1.984. (b) with M06-L/def2TZVP: Al–C4, 1.976; Al–C7, 1.971; Al–C1, 2.127; Al–C2, 2.136; Al–C3, 2.159 (Appendix C, Section C1).

As the first example of a base-free tri(allyl)aluminum compound, several survey reactions were conducted with **1** to determine how the bulky allyl ligands might affect its reactivity. Initially, reactivity surveys focused on comparisons to closely related compounds, specifically $[\text{Al}(\text{C}_3\text{H}_5)_3(\text{thf})]$.¹³³ Later surveys focused on the ability of **1** to act as an A' source in the synthesis of other $[\text{MA}'_x]$ complexes of more easily reduced metal centers. No reaction is observed when **1** is treated with an equivalent of HOCPPh_3 . Even with 3 equivalents, there is negligible evidence of interaction, and no new product can be isolated. The inhibited reactivity may stem from the combined bulk of the alcohol and allyl ligands.

In a direct comparison to $[\text{Al}(\text{C}_3\text{H}_5)_3(\text{thf})]$, the reaction of **1** with benzophenone was conducted to test the ability of the bulky A' ligand to add to a ketone.¹³³⁻¹³⁴ In contrast to the behavior with HOCPPh_3 , $[\text{Al}(\text{A}'\text{Ph}_2\text{CO})_3]$ (**2**) is readily formed from the treatment of Ph_2CO with **1** in hexanes (eq 1). Notable are the faster reaction and larger scale of **1** compared to those reported for $[\text{Al}(\text{C}_3\text{H}_5)_3(\text{thf})]$, despite the bulk of the A' ligand. Reactions of $[\text{Al}(\text{C}_3\text{H}_5)_3(\text{thf})]$ took up to 10 min at room temperature for NMR scale reactions.¹³³

Upon addition of **1** the reaction proceeds rapidly at $-78\text{ }^\circ\text{C}$, as demonstrated by the immediate appearance of a light orange color. Additionally, **2** was produced on the hundred milligram scale in quantitative yield, as there was no evidence in NMR spectra for residual **1**.



The difference in reactivity is likely the result of **1** being a base-free 3-coordinate complex, as compared to the 4-coordinate $[\text{Al}(\text{C}_3\text{H}_5)_3(\text{thf})]$. Preliminary DFT calculations concerning a major mechanistic reaction step, the formation of an Al-O bond between Ph_2CO and $[\text{Al}(\text{C}_3\text{H}_5)_3]$ or $[\text{Al}(\text{C}_3\text{H}_5)_3(\text{thf})]$, support coordination number as a prominent factor in reactivity. For the unsolvated $[\text{Al}(\text{C}_3\text{H}_5)_3]$, the formation of the Al-O bond to create a four-coordinate complex is an energetically favored process, with a ΔG° of $-9.8 \text{ kcal mol}^{-1}$ (Figure 6).

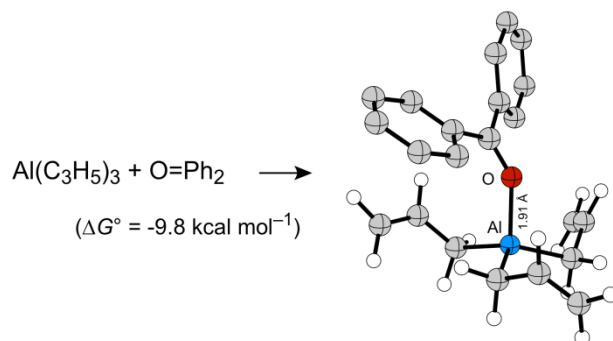


Figure 6. Calculated reaction product (M06/def2TZVP) of benzophenone with the parent $[\text{Al}(\text{C}_3\text{H}_5)_3]$ (Appendix C, Section C1).

The solvated four-coordinate $[\text{Al}(\text{C}_3\text{H}_5)_3(\text{thf})]$ complex already contains an Al-O bond from the coordinated and strongly donating THF molecule. The formation of a second Al-O interaction from Ph_2CO to form a five-coordinate complex is actually an unfavorable process, with a ΔG° of $+4.5 \text{ kcal mol}^{-1}$ (Figure 7).

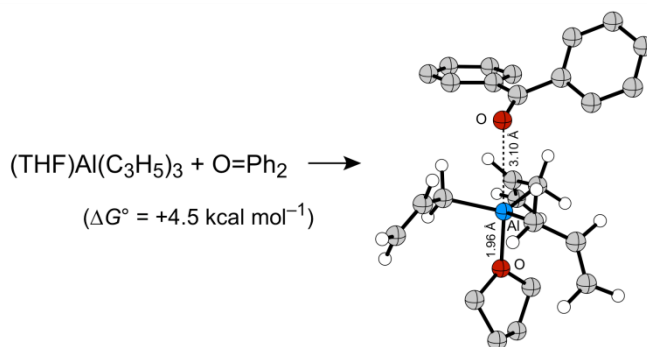


Figure 7. Calculated reaction product (M06/def2TZVP) of benzophenone with the solvated $[\text{Al}(\text{C}_3\text{H}_5)_3(\text{thf})]$ complex. (Appendix C: Section C1)

It should be noted that the unsubstituted $[\text{Al}(\text{C}_3\text{H}_5)]$ was used in place of **1** for these calculations. While the extra bulk of the A' ligands might in principle impede the reactivity, the speed of observed reaction suggests that this is a minor concern. The highly fluxional nature of the A' ligands presumably contributes to minimizing the steric influence by allowing an A' ligand to shift orientations, thereby allowing ready access to the Al center.

In a test of the interaction of a rare earth halide with **1**,¹³⁵ the latter was ball milled with ScCl_3 and the ground mixture extracted with hexanes. Only the starting **1** was evident in the ^1H NMR spectrum. In contrast, repeating the procedure with $\text{K}[\text{A}']$ and ScCl_3 yields the allyl complex $[\text{ScA}'_3]$ (**3**). Although **3** can be synthesized in THF from $\text{K}[\text{A}']$ and ScCl_3 , it offers an interesting comparison to **1**. The overall yields of **3**, in both solution and milling syntheses, are lower (~50%) than those observed for **1**. The ^1H NMR spectrum of **3** at room temperature displays the resonances expected for a typically π -bound A' ligand;¹³⁶ this is also true of the unsolvated parent complex, $[\text{Sc}(\text{C}_3\text{H}_5)_3]$, although the THF-solvated versions exhibit various combinations of η^1 - and η^3 -bonded ligands.¹²² The single crystal X-ray structure of **3** (Figure 8), like that of the $[\text{YA}'_3]$ homologue,⁶⁶ suffers from considerable disorder in the allyl ligands, rendering it essentially of connectivity-only quality. Nevertheless, the ligands are clearly π -bound, and the average Sc–C distance of 2.38(3) Å is shorter than the equivalent distance in $[\text{TmA}'_3]$ (2.53(1) Å) by roughly the difference in ionic radii (0.14 Å).¹³⁷ No reactivity studies have been performed for **3**. The synthesis of **3** provided one of the initial proofs of concept syntheses for our ball milling techniques.

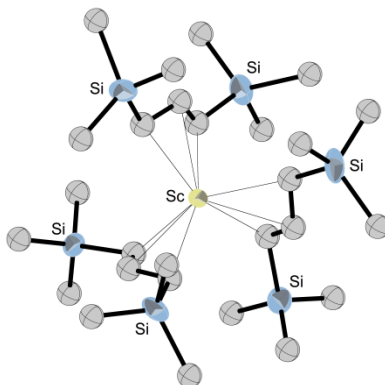


Figure 8. Plot of the non-hydrogen atoms of **3**; only one conformation of the disordered allyl ligands is shown. Thermal ellipsoids for Sc and Si are drawn at the 50% level, and carbons have been assigned an arbitrary radius (Appendix B, Section B1).

The ability to synthesize multigram quantities of **1** in high yield and purity, without further purification, allowed us to consider **1** as a possible reagent for additional syntheses. In our examination of the mechanochemical synthesis of $[MA'_x]$ complexes, discussed further in Chapter 5, we found that the techniques were largely unsuccessful when easily reduced metal centers were involved. Easily accessible reduction potentials combined with the oxidative coupling of A' to $[A'_2]$ appeared to be amplified when milling. Similar trends had been observed previously in solution when $K[A']$ was in the presence of a more easily reduced metal, such as Tl, Pb, and the 2nd and 3rd row transition metals. As the metal-ligand interactions of **1** are significantly more covalent than those of $K[A']$, it was believed that **1** might allow access to $[MA'_x]$ complexes that cannot be synthesized from our standard A' source.

Initial investigations offered mixed results ranging from no reactivity, such as with $ScCl_3$, to the successful synthesis of new complexes such as $[BiA'_3]$, discussed in Chapter 3.³⁷ While results as definitive as those of $ScCl_3$ and $[BiA'_3]$ were rare, the majority of reactions suggested **1** could be used as an A' source. Though no conclusive identification of the desired $[MA'_x]$ complexes could be made, ¹H NMR spectra indicate disappearance of **1** and the appearance of new A' ligands. These results and the ease of reactions in both hexanes and by ball milling warrant more in depth investigations of “second generation” mechanochemical products.

Attempted Syntheses of p-Block Metal Complexes

Attempts to mechanochemically synthesize $[SnA'_4]$ from $K[A']$ demonstrated a strong tendency towards reduction of the tin center, yielding complex mixtures of $[A'_2]$ and unidentifiable products. Thus treatment of SnI_4 with **1** in hexanes or by ball milling yielded intensely-colored yellow products containing A' ligands, confirmed with ¹H NMR. While the presence of an A' containing complex could be established, the NMR spectra showed that highly complex mixtures of products were present. The prominent products appeared to be liquids; however, a non-crystalline yellow solid with low hydrocarbon solubility was also present. Adding to the complication of the systems was that the products varied with the synthesis method.

The most complex spectra were obtained from reactions conducted in hexanes, with a reaction time less than 24 hours. The major product was free flowing yellow oil, although small amounts of the yellow solid were deposited on the walls of the flask. NMR spectra of the oil indicated the presence of at least six distinct A' environments, all of which were clearly σ -bound, of roughly equal intensity (Appendix A, Figure A8). COSY NMR was utilized for assignment of chemical shifts to individual ligands, from which interesting deviations from predicted chemical shift ranges could be observed. The greatest deviation was a doublet near

δ 1.4 corresponding to the $H_{(\alpha)}$ of the ligand labeled $[A_A']$. The other doublets corresponding to the other five A' ligands appear within the expected range, δ 2.3–2.8. The signal at δ 1.4 is significantly more upfield than expected and, through analysis of the patterns in COSY spectra and the trend in coupling constants, is clearly consistent with σ -bound A' . The chemical shifts for $[A_A']$'s $H_{(\beta)}$ and $H_{(\gamma)}$ are on the edges of the expected ranges, δ 5.2–5.8 and δ 6.0–6.4, respectively. The spectra were not unlike those of $[EA'_3]$ ($E = \text{As, Sb, Bi}$)³⁷, discussed in Chapter 3, but of significantly greater complexity (Figure 9).

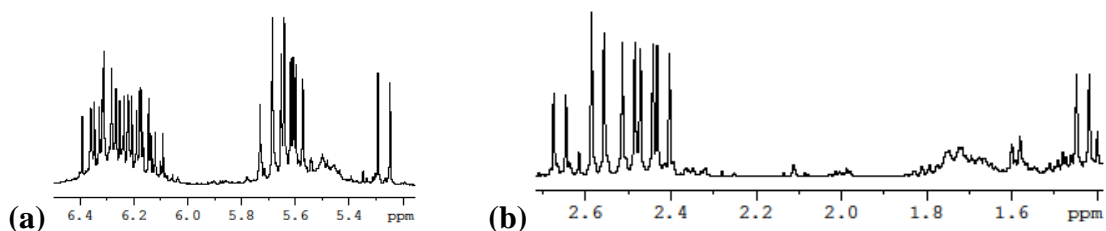


Figure 9. Selected portions of the ^1H NMR spectrum from the $[\text{SnA}'_x]$ oil, containing resonances for $[A'_A]$, $[A'_B]$, $[A'_C]$, $[A'_D]$, $[A'_E]$, and $[A'_F]$; **(a)** the $H_{(\beta)}$ (leftmost multiplet) and $H_{(\gamma)}$ ranges; **(b)** the $H_{(\alpha)}$ range.

Spectra of the oil also contained a complex set of four overlapping quartets, centered near δ 3.7, and a triplet centered at δ 0.7, labeled as $[q/t]$ (Figure 10). COSY NMR spectra show these signals to be splitting each other, and their equal coupling constants confirm the analysis. The chemical shifts and coupling constants, $J = 7.0$ Hz, are more consistent with alkanes than what is expected for A' ($J = 10\text{--}12$ Hz). Additionally, the A' ligand cannot give rise to the observed splitting, specifically four quartets adjacent to a triplet. The lack of appropriately intense peaks in the TMS region, centered at δ 0.0, suggest that the compound (or ligand) giving rise to these signals does not contain TMS and is therefore not derived from an A' ligand. Due to these factors, this product cannot be identified, but warrants continued investigation. As this is only part of the initial investigation of **1** as an A' source, it is also possible that this could be a heterometallic species.

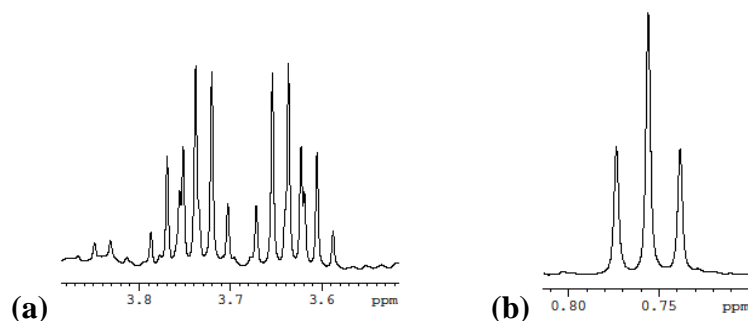


Figure 10. Selected portions of the ^1H NMR spectrum from the $[\text{SnA}'_x]$ oil of $[\text{q/t}]$; **(a)** four overlapping quartets and **(b)** triplet split by all quartets (analysis from COSY spectra).

The oil likely contains several $[\text{SnA}'_x]$ complexes of varying substitution and conformation. The ability to bind four A' ligands offers high degrees of freedom in terms of the orientation and symmetry of final complexes. However, an accurate identification of the products cannot be made solely based on NMR. Given samples of sufficient concentration, it may be possible to encourage the oil to crystallize over an extended period of time or at a reduced temperature. A crystal structure of one of the products would greatly aid in identifying the components of the mixture.

Further complicating this system, the NMR spectra of the yellow solid are significantly different from those of the oil (Figure 11). Only two A' ligands, labeled $[A'_A]$ and $[A'_B]$, of equal intensity are found in the ^1H NMR spectra. These ligands display coupling constants and chemical shifts similar to those of the ligand $[A'_B]$ found in the oil. It should be noted that the greatest similarity is found between $[A'_A]$ and $[A'_B]$, while there is no evidence of $[A'_B]$ within the oil sample. Based on this data, it is believed that the solid is a distinctly different product from the oil, though whether or not the oil contains any dissolved solid cannot be determined.

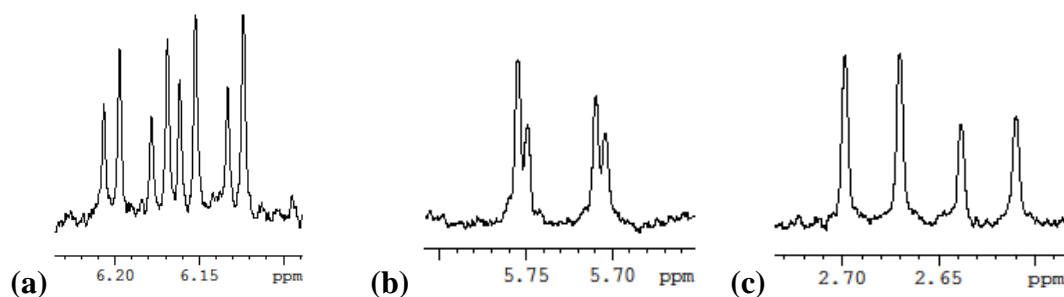


Figure 11. Selected portions of the ^1H NMR spectrum from the $[\text{SnA}'_x]$ solid, containing resonances for $[A'_A]$ and $[A'_B]$; **(a)** $\text{H}_{(\beta)}$ overlapping doublet of doublets; **(b)** $\text{H}_{(\gamma)}$ overlapping doublets; **(c)** $\text{H}_{(\alpha)}$ doublets.

If the reaction is performed by ball milling or is allowed to continue in solution for up to 48 hours, a different mixture of products can be isolated. Both reactions produced the same mixture of a yellow oil and yellow solid, observed by ^1H NMR. The mixture contains the same yellow solid found from the 24 hour solution reaction, as indicated by the presence of the $[\text{A}'_{\text{A}}]$ and $[\text{A}'_{\text{B}}]$ ligands.

Two additional sets of peaks could be observed in the mixtures that were not present in the solid obtained in the 24 h reaction. One set is identical to the quartets and triplets, $[\text{q/t}]$, discussed previously (Figure 12a). The final set was found to correspond to the ligand, or ligand environment, previously identified as $[\text{A}'_{\text{A}}]$ (Figure 12b, c, d). These ligands are likely part of the complex, or complexes, that make up the yellow oil. What these complexes are cannot yet be determined.

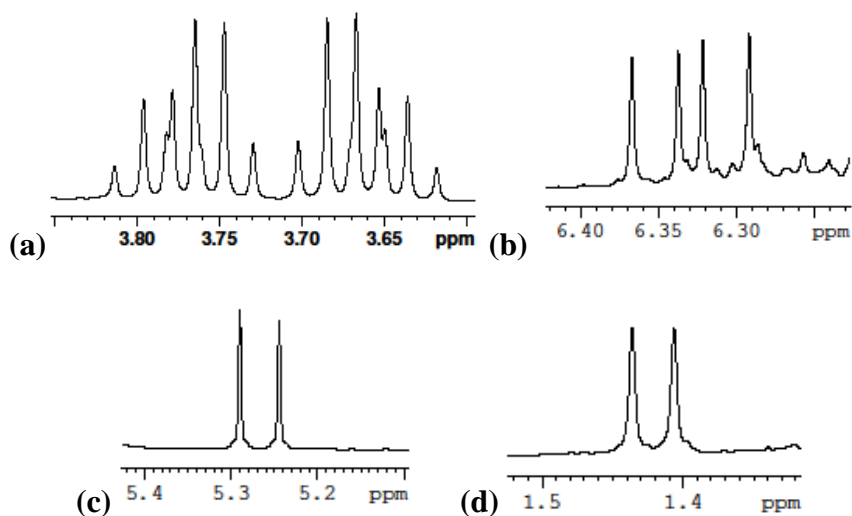


Figure 12. Selected portions of the ^1H NMR spectrum from the $[\text{SnA}'_{\text{x}}]$ mill, containing resonances for (a) $[\text{q/t}]$ environment, and $[\text{A}'_{\text{A}}]$; (b) $\text{H}_{(\beta)}$ (doublet of doublets); (c) $\text{H}_{(\gamma)}$ doublet; (d) $\text{H}_{(\alpha)}$ doublet.

The reactions conducted for 48 h or by ball milling should logically represent a more “complete” reaction, since ball milling imparts such high energy into the system and the products from the two reaction conditions are identical. It stands to reason then that the mixture of compounds observed after the 24 hour reaction represent reactive intermediates. Whether these are stable themselves, or continue to react, cannot currently be said. Additionally it is currently unknown whether the products are polymetallic or monometallic. More extensive investigation of synthesis with **1** is needed to determine this, most likely requiring single crystal structures of products. Based on its limited solubility it may be possible to

isolate the yellow solid; however, the oil mixture will likely prove significantly more difficult to characterize.

A preliminary investigation suggests that treatment of TeI_4 with **1** under ball milling conditions produces a mixture of $[\text{TeA}'_x]$ complexes. The reaction generated a yellow residue in very low yield, only sufficient for analysis by ^1H NMR. The spectra indicate the presence of two σ -bound A' ligands of a difference in intensity of roughly four to one. The difference in intensity suggests that these correspond to two different complexes but is not definitive. Additional signals representing overlapping quartets and triplets, similar to those from $[\text{SnA}'_x]$ mixtures, are also present. Their presence here implies that they may be a result of reactions incorporating **1** or an Al metal center into the formula, but further investigation is needed to determine what is creating these sets of signals. A substantial amount of $[\text{A}'_2]$ is present, suggesting that decomposition is not completely avoided. In contrast, if $\text{K}[\text{A}']$ is used in place of **1**, only $[\text{A}'_2]$ can be isolated.

In the case of the reaction of TiCl_4 with $[\text{AlA}'_3]$, only decomposition products (e.g., $[\text{A}'_2]$) were obtained. While a $[\text{TIA}']$ complex is not produced, these results do provide a reference point for the reducing ability of **1**. This provides an important factor for reaction considerations when employing **1** as a reagent, as the decomposition pathways observed for $\text{K}[\text{A}']$ are still possible.

Attempted Syntheses of Transition Metal Allyl Complexes

Whereas no reactivity was observed with ScCl_3 and $[\text{AlA}'_3]$, this was not the case for other transition metals. Titanium, nickel, palladium, and platinum were reactive in the presence of **1**, either in hexane solutions or when ball milling. Reactions performed with TiBr_4 in hexanes solution produced rapid and distinct color changes but ultimately yielded $[\text{A}'_2]$ after several hours. The observed color changes accompanied by the formation of $[\text{A}'_2]$ imply the formation of a $[\text{TiA}'_x]$ or a mixed Al-Ti complex of low thermal stability. Alterations of the reaction conditions to shorter times or lower temperatures may allow for the isolation of this complex. It is likely that milling of TiBr_4 and **1** will produce $[\text{A}'_2]$, as the high energy of the mill reactions may promote the formation of decomposition products.

Attempted syntheses of A' complexes of palladium and platinum from $\text{K}[\text{A}']$, employing both solution and ball milling techniques, promoted the formation of $[\text{A}'_2]$. Due to the ease of reduction for both metals, these results from ball milling were not unexpected. However reactivity was observed for both MCl_2 salts ($\text{M} = \text{Pd}, \text{Pt}$) when treated with **1**. The products were not visually consistent with the formation of decomposition products, and the ^1H NMR spectra were significantly more complicated than that of pure **1**. Spectra of each indicated that

a complex mixture of products containing several σ -bonded A' ligands was present. Additionally, the distinctive chemical shifts of **1** were not present. While it may not be possible to isolate or separate a single product from these reactions, the presence of the mixture does imply that **1** could be used in place of K[A'] when dealing with second and third row transition metals.

Trials conducted with NiCl₂ and NiBr₂(dme) offer a very interesting point of comparison for the difference of reactivity between **1** and K[A']. The synthesis and reactivity of [NiA'₂] had been well documented and requires the use of NiBr₂(dme) in place of NiCl₂ when conducted in THF solution.^{113, 138} Nickel halides were found to be largely insoluble in THF and promoted the formation of [A'₂]. However, if the more THF soluble NiBr₂(dme) was used, [NiA'₂] could be isolated in high yield. The insoluble NiX₂ salts were believed to promote the coupling of ligands. This hypothesis was further examined when syntheses using both NiCl₂ and NiBr₂(dme) were conducted mechanochemically. When either Ni(II) source was milled in the presence of K[A'], the only isolated product was [A'₂]. However, milling either in the presence of **1** promotes in completely different reactivity.

A yellow-orange oil was isolated from the reaction of NiBr₂(dme) and **1**; under the same conditions, **1** and NiCl₂ yielded a yellow-brown oil. Unlike the reported [NiA'₂] complex, neither product solidified.¹³⁸ The yellow-orange oil appeared reasonably stable, whereas the yellow-brown oil deposited grey solid over a period of days, very similar to the decomposition of [NiA'₂(CO)].¹¹³ NMR spectra of the yellow-orange oil indicated that a complex mixture was present that included **1** along with several unidentifiable signals within the appropriate shift ranges of the A' ligand. A suitable ¹H NMR spectrum of the yellow-brown oil could not be obtained as the relative instability of the compound resulted in the formation of solids during the experiment. The recorded spectra were consistent with the presence of a ferromagnetic metal, suggesting the formation of nickel metal. It should be noted that the relative colors, orange and yellow, of the two products are consistent with the reported colors of the two reported [NiA'₂] diastereomers.¹³⁸ If these products could be isolated and more fully characterized, it may provide an invaluable comparison between the behavior of reactions concerning bulky allyls and the difference between solution-based techniques and ball milling techniques, as well as furthering the possible applications of **1** as a reagent.

Results obtained from the treatment of U_L4(dioxane) with **1** in hexanes are very similar to those described above. A distinct color change to red was witnessed upon the addition of **1**, and throughout the remainder of the 72 h reaction a shift towards orange was observed. A brown oil was isolated as the final product and the ¹H NMR spectra indicated a complex mixture of several species containing A' ligands. Chemical shifts corresponding to A'₂ could be identified but were of very low intensity. Most importantly, no evidence of **1** could be found

in the spectra. The formation and disappearance of the red and orange solutions may indicate the presence of reactive complexes initially formed during the reaction and consumed later to produce the brown oil. The low amount of $[A'_2]$ implies that the reduction of U^{4+} to U^{3+} did not occur. Future investigations would likely benefit from significantly shorter reaction times to try and isolate the red and orange species, if these are in fact distinct compounds. If these are indeed reactive, separation from other mixture components may allow their characterization. The lack of reduction from **1**, as opposed to the formation of purple solid in the presence of $K[A']$, further supports the use of **1** as a gentler A' source.

Conclusions

In summary, the first unsolvated tri(allyl) complex of aluminum and its monomeric scandium analogue have been isolated through a mechanochemical route. This sidesteps the formation of either solvated complexes or ill-defined ‘-ate’ species. Preliminary results indicate that the aluminum compound displays the reactivity expected of an allyl complex, although the combination of an unsolvated metal center and bulky ligands may moderate it in unanticipated ways. In addition to the expected reactivity, the aluminum compound has been employed as a reagent for the transfer of the ligands onto other metals of interest. In some cases this has allowed the isolation of potentially new metal allyl complexes of easily reduced metal centers, leading to “second generation” mechanochemical complexes. It is possible that with further investigation, the aluminum complex could be used to synthesize metal allyl complexes of transition and heavy p-block metals. These results suggest that mechanochemical approaches should be more widely explored to expand the palette of other base-free/low-coordinate organometallic complexes.

Chapter 3

Mechanochemical Influence on Stereoisomer Formation in the Syntheses of Group 15 Bis(1,3-trimethylsilyl)allyl Complexes (As–Bi)

Introduction

Allyl ligands in main-group complexes display a remarkable range of bonding modes (σ , π , μ_x , and various combinations), and the complexes themselves have found diverse uses as allyl transfer agents and polymerization initiators.¹³⁹⁻¹⁴¹ In addition to their conformational flexibility, substituted allyls can introduce additional stereochemical possibilities to structures and reactions.^{109, 142-143} The *ansa*-tris(allyl) complex $[\text{MeSi}\{(\text{C}_3\text{H}_3\text{SiMe}_3)\text{Li}(\text{tmeda})\}_3]$ (Figure 13a), for example, displays a mix of *exo*, *endo* configurations; the central [*endo*, *exo*] allyl ligand exhibits asymmetric η^2 -bonding, whereas the flanking [*exo*, *exo*] ligands possess η^1 -bonding.^{85, 142} With the p-block elements, for which σ -bonded allyls are the rule, the $[\text{1,3}-(\text{SiMe}_3)_2\text{C}_3\text{H}_3]^-$ (A^-) anion appears in various diastereomeric configurations. The complexes $[\text{AlA}^-_3]$ and $[\text{GaA}^-_3]$ possess [*R,S,S*] (or [*S,R,R*]) configurations around the $\text{C}_{(\alpha)}$ of the allyl ligands in the solid state (Figure 13b).^{38, 67} In solution, the molecules are highly fluxional, appearing π -bound in ^1H NMR spectra (Figure 14a); there is a single doublet for the three $\text{H}_{(\alpha)}$ and three $\text{H}_{(\gamma)}$ protons, a triplet for the three $\text{H}_{(\beta)}$ protons, and all SiMe_3 groups are equivalent. The tris(allyl) complex $[\text{Sn}(\text{1,3-SiMe}_3)_2\text{C}_3\text{H}_3)_3\text{K}(\text{thf})]$ (Figure 13c) possesses C_3 symmetry in the solid state and solution; all three $\text{H}_{(\alpha)}$ protons exhibit the same stereochemical arrangement, [*R,R,R*] (or [*S,S,S*]).⁸⁵ The same configuration is observed in the solid state for the zincates $[\text{Zn}(\text{1,3-SiMe}_3)_2\text{C}_3\text{H}_3)_3\text{M}]$ ($\text{M} = \text{Li}, \text{Na}, \text{K}$); they are highly fluxional in solution, however, displaying “ π -bound” ligands.⁸⁶ These examples were synthesized with solution-based methods, and in each case were the sole isolated products.

Mechanochemical methods of synthesis, which employ grinding or milling with little or no solvent, are intrinsically high energy in nature.¹² To a first approximation, such syntheses might be thought to favor thermodynamically preferred products. As reaction conditions during milling may be far from equilibrium, however, and mass transport effects are considerably different from those in solution, ball milling can generate either the thermodynamic or kinetic products of a reaction.¹⁴⁴ Furthermore, even thermodynamically controlled reactions in the solid state may yield a different distribution of products from those produced in solution.^{80, 145-146}

Our interest both in silyl-substituted allyls^{38, 67, 70, 74, 147-150} and Group 15 element chemistry¹⁵¹⁻¹⁵² led us to consider whether mechanochemistry could be used to generate allyl-based stereoisomers unattainable through solution approaches. There have been no reports of silyl-substituted allyl complexes with the heavier Group 15 elements (As–Bi), however, and in anticipation of possible synthetic difficulties, we wanted to explore the use of mechanochemical methods of synthesis. Such an approach has been used to synthesize a substituted aluminum allyl that could not be produced in ethereal or hydrocarbon solvents.³⁸ Even though this precaution was unnecessary, as synthesis could be accomplished in solution, there are still differences in the outcomes depending on the synthesis method used.

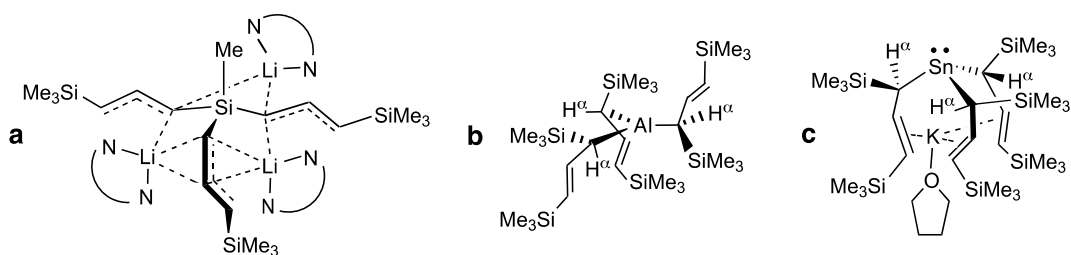


Figure 13. Structure and bonding configuration of (a) $[\text{MeSi}\{(\text{C}_3\text{H}_3\text{SiMe}_3)\text{Li}(\text{tmeda})\}_3]$; (b) $[\text{AlA}'_3]$; (c) $[\text{Sn}(1,3\text{-SiMe}_3)_2\text{C}_3\text{H}_3]_3\text{K}(\text{thf})$.

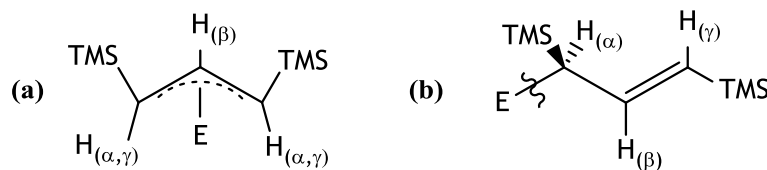


Figure 14. (a) Labeling for π -bonded allyl; in a “pseudo- π ” (rapidly fluxional) situation, the $\text{H}_{(\alpha)}$ and $\text{H}_{(\beta)}$ of a π -bonded allyl become equivalent, appearing as one doublet. (b) labeling for σ -bonded allyl

Experimental

General Considerations. All syntheses were conducted under rigorous exclusion of air and moisture using Schlenk line and glovebox techniques. Proton (^1H), carbon (^{13}C), and COSY NMR spectra were obtained at ambient temperature on an Advance AV-400 MHz spectrometer. Proton and carbon spectra were referenced to residual resonances of C_6D_6 (δ 7.15 and δ 128). Variable temperature ^1H NMR was obtained on a Bruker DRX-500 instrument and referenced to residual resonances of tol-d_8 . Metal and combustion analyses were performed by ALS Environmental, Tucson, AZ.

Materials. Anhydrous AsI₃, SbCl₃, SbI₃, and BiCl₃ were purchased from Strem Chemicals and used as received. Anhydrous inhibitor-free tetrahydrofuran (THF) was used as obtained. Hexanes and toluene were distilled under nitrogen in the presence of potassium metal prior to use. Deuterated benzene and deuterated toluene (tol-d₈) were purchased from Cambridge Isotopes and were distilled from Na/K (22/78) alloy prior to use. The K[A'] reagent was synthesized as previously described.¹¹² [AlA'₃] was synthesized with the previously reported mechanochemical method.³⁸ Stainless steel (440 grade) ball bearings (³/₈ in, 6 mm) were thoroughly cleaned with hexanes and acetone prior to use. Planetary milling was performed with a PM100 mill, 50 mL stainless steel grinding jar type C, and safety clamp for air sensitive grinding, all purchased from Retsch. ¹H NMR spectra of HA', K[A'], and [A']₂ available in Appendix A: Figures A1, A2, and A3, respectively.

Synthesis of [AsA'₃] by ball milling. Solid AsI₃ (0.176 g, 0.386 mmol) and K[A'] (0.286 g, 1.27 mmol) were added to a 50 mL stainless steel grinding jar (type C). The jar was charged with stainless steel ball bearings (6 mm dia, 50 count) and closed tightly with the appropriate safety closer device under an N₂ atmosphere. The reagents were milled for 5 min at 600 rpm, resulting in a light yellow solid. The product was extracted with minimal hexanes (< 100 mL) and filtered through a medium porosity ground glass frit, providing a pale yellow filtrate. Drying under vacuum yielded yellow crystals (0.194 g, 80%), mp 52 °C. Crystals were identified as the asymmetric (C₁) compound [AsA'₃], supported with elemental analysis and NMR spectra. Chemical shift assignments were identified with COSY NMR. A set of peaks visible in ¹H and ¹³C NMR were assigned to the C₃ diastereomer of [AsA'₃] as a minor product. The observed ratio of isomers was approximately 10:1 C₁ to C₃. Variations of mill time from 30 s to 2 h had no effect on isomer ratio. C₃-Symmetric [AsA'₃]: ¹H NMR (400 MHz, 298 K, C₆D₆): δ = 0.14 (br s, 9H, SiMe₃), 0.18 (br s, 9H, SiMe₃), 2.53 (d, 3H, J = 11.1 Hz, C_(α)-H), 5.61 (d, 3H, J = 18.1 Hz, C_(γ)-H), 6.08 (dd, 3H, J₁ = 18.2 Hz, J₂ = 11.1 Hz, C_(β)-H). ¹³C NMR (100 MHz, 298K, C₆D₆): δ = -1.03 (SiMe₃), -0.45 (SiMe₃), 33.90 (C_(α)), 130.48 (C_(γ)), 145.78 (C_(β)). C₁-Symmetric [AsA'₃]*: ¹H NMR (400 MHz, 298 K, C₆D₆): δ = 0.18–0.22 (br s, 54H, SiMe₃); [A'_(A)]: δ = 2.47 (d, 1H, J = 11.0 Hz, C_(α)-H), 5.65 (d, 1H J = 18.3 Hz, C_(γ)-H), 6.47 (dd, 1H, J₁ = 18.4 Hz, J₂ = 11.0 Hz, C_(β)-H); [A'_(B)]: δ = 2.26 (d, 1H, J = 11.0 Hz, C_(α)-H), 5.56 (d, 1H J = 18.2 Hz, C_(γ)-H), 6.34 (dd**, 1H, J₁ = 18.2 Hz, J₂ = 10.9 Hz, C_(β)-H); [A'_(C)]: δ = 2.60 (d, 1H, J = 11.2 Hz, C_(α)-H), 5.68 (d, 1H J = 18.2 Hz, C_(γ)-H), 6.31 (dd**, 1H, J₁ = 18.3 Hz, J₂ = 11.2 Hz, C_(β)-H). ¹³C NMR (100 MHz, 298K, C₆D₆): δ = -0.99 (SiMe₃), -0.85 (SiMe₃), -0.67 (SiMe₃), -0.35 (SiMe₃), -0.29 (SiMe₃), -0.17 (SiMe₃), 34.79 (C_(α)), 35.51 (C_(α)), 38.34 (C_(α)), 128.71 (C_(γ)), 128.82 (C_(γ)), 130.19 (C_(γ)), 145.00 (C_(β)), 147.45 (C_(β)), 147.45 (C_(β)). C₃-Symmetric [AsA'₃]: ¹H NMR (500 MHz, 363K, tol-d₈): δ = 0.15–0.23 (br s, 66H, SiMe₃), 2.52 (d, 1H, J = 11.1 Hz, C_(α)-H), 5.72 (d, 1H, J = 18.5 Hz, C_(γ)-H), 6.09 (dd,

1H, $J_1 = 18.2$ Hz, $J_2 = 11.2$ Hz, C_(β)-H). C₁-Symmetric [AsA'₃]*: ¹H NMR (500 MHz, 363K, tol-d₈): δ = 0.151–0.225 (br s, 66H, SiMe₃); [A'_(A)]: δ = 2.46 (d, 1H, $J = 11.3$ Hz, C_(α)-H), 5.65 (d, 1H $J = 18.4$ Hz, C_(γ)-H), 6.47 (dd, 1H, $J_1 = 18.3$ Hz, $J_2 = 11.1$ Hz, C_(β)-H); [A'_(B)]: δ = 2.25 (d, 1H, $J = 11.0$ Hz, C_(α)-H), 5.54 (d, 1H $J = 18.2$ Hz, C_(γ)-H), 6.33 (dd**, 1H, $J_1 = 17.2$ Hz, $J_2 = 11.0$ Hz, C_(β)-H); [A'_(C)]: δ = 2.59 (d, 1H, $J = 11.3$ Hz, C_(α)-H), 5.65 (d, 1H $J = 18.5$ Hz, C_(γ)-H), 6.30 (dd**, 1H, $J_1 = 18.2$ Hz, $J_2 = 11.3$ Hz, C_(β)-H). Anal. Calcd for C₂₇H₆₃AsSi₆ (631.23 g mol⁻¹): C, 51.38; H, 10.06, As, 11.87. Found: C, 49.52; H, 10.37; As, 10.87. (*Labels A'_(A), A'_(B), and A'_(C) indicate H assignments to specific [A'] ligands; **Coincident peaks give the appearance of overlapping triplets; i.e., [A'_(B)]: δ 6.35 (t, $J_1 = 22$ Hz, $J_2 = 11$ Hz C_(β)-H), [A'_(C)]: δ 6.30 (t, $J_1 = 22$ Hz, $J_2 = 11$ Hz C_(β)-H). The peak assignments listed above were obtained through COSY analysis. Full ¹H NMR spectrum available in Appendix A: Figure A15.

Synthesis of [AsA'₃] in hexanes: AsI₃ (0.145 g, 0.318 mmol) was partially dissolved in hexanes in a 50 mL Erlenmeyer flask with magnetic stir bar to yield a golden colored solution. K[A'] (0.210 g, 0.935 mmol) was added slowly to the AsI₃ solution over 5 min. The reaction mixture between the AsI₃ solution and K[A'] slurry was stirred for 72 h at room temperature. During the course of the reaction, the solution became more intensely yellow. The mixture was filtered through a medium porosity ground glass frit, providing a pale yellow filtrate. Drying under vacuum yielded pale yellow crystals (0.125 g, 64%), identified as [AsA'₃] with ¹H and ¹³C NMR. ¹H NMR spectra confirmed the presence of both the C₁ and C₃ diastereomers, and a high content of [A']₂. The ratio of C₁ to C₃ was found to be approximately 3:1. Full ¹H NMR spectrum available in Appendix A: Figure A16.

Attempted C₁ to C₃ conversion of [AsA'₃]: [AsA'₃] (0.128 g, 0.20 mmol), synthesized by ball milling, was dissolved in minimal toluene in a 50 mL Schlenk flask with magnetic stir bar to yield a pale yellow solution. The flask was sealed with a condenser and refluxed for 4 h under a nitrogen atmosphere. During the reflux, the solution changed from the initial pale yellow to a pale brown. Removal of toluene under vacuum yielded an orange-brown residue that consisted mainly of insoluble decomposition products. The residue that could be extracted with hexanes was found to possess a ratio of C₁ to C₃ of approximately 8:1, suggesting that no substantial thermal conversion between the isomers had occurred.

Attempted synthesis of [AsA'₃] in THF: Attempts to synthesize [AsA'₃] by salt metathesis of AsI₃ and K[A'] in THF were unsuccessful. Work up yielded a mixture consisting prominently of [A'₂] and unidentifiable products (¹H NMR). The expected peaks for [AsA'₃] were not present. Analogous attempts at synthesis at a reduced reaction temperature (-78 °C) were similarly unsuccessful.

Synthesis of [SbA'₃] by ball milling: Solid SbCl₃ (0.213 g, 0.938 mmol) and K[A'] (0.645 g, 2.87 mmol) were added to a 50 mL stainless steel grinding jar (type C). The jar was charged with stainless steel ball bearings (3/8 in dia, 9 count) and closed tightly with the appropriate safety closer device under an N₂ atmosphere. The reagents were milled for 5 min. at 300 rpm, resulting in a light yellow solid. The product was extracted with minimal hexanes (< 100 mL) and filtered through a medium porosity ground glass frit, providing a pale yellow filtrate. Drying under vacuum initially yielded a mixture of pale yellow-brown crystals suitable for single crystal X-ray diffraction, and low-viscosity yellow oil (0.53 g, 82%). The low viscosity of the oil allowed for the isolation of a crystalline solid, mp 90 °C (0.27 g, 42%), identified with ¹H, ¹³C, and COSY NMR spectra and single crystal X-ray analysis as the asymmetric (C₁) [SbA'₃]. The isolated oil (0.10 g, 16%) was identified as a mixture of the asymmetric [SbA'₃] dissolved in the C₃-symmetric [SbA'₃] (¹H, ¹³C, and COSY NMR). Analysis of ¹H NMR peaks in the oil sample displayed an approximate ratio of 3:2 for the C₁ to C₃ isomers. C₃-symmetric [SbA'₃]: ¹H NMR (400 MHz, 298 K, C₆D₆): δ = 0.19 (s, ~27H, SiMe₃), 0.22 (s, ~27H, SiMe₃), 2.58 (d, 3H, *J* = 11.7 Hz, C_(α)-H), 5.59 (d, 3H, *J* = 18.1 Hz, C_(γ)-H), 5.95 (dd, 3H, *J*₁ = 18.1 Hz, *J*₂ = 11.7 Hz, C_(β)-H). ¹³C NMR (100 MHz, 298 K, C₆D₆): δ = -0.73 (SiMe₃), -0.37 (SiMe₃), 30.18 (C_(α)), 129.79 (C_(γ)), 146.68 (C_(β)). C₁-symmetric [SbA'₃]*: ¹H NMR (400 MHz, 298 K, C₆D₆): δ = 0.188, δ 0.193; δ 0.202, δ 0.212, δ 0.215, δ 0.222 (br s, 54 H, SiMe₃); [A'₍A₎]: δ = 2.20 (d, 1H, *J* = 11.2 Hz, C_(γ)-H), 5.57 (d, 1H *J* = 18.1 Hz, C_(ω)-H), 6.40 (dd, 1H, *J*₁ = 18.1 Hz, *J*₂ = 11.2 Hz, C_(β)-H); [A'₍B₎]: δ = 2.53 (d, 1H, *J* = 11.6 Hz, C_(γ)-H), 5.65 (d, 1H *J* = 18.2 Hz, C_(α)-H), 6.36 (dd, 1H, *J*₁ = 18.1 Hz, *J*₂ = 11.6 Hz, C_(β)-H); [A'₍C₎]: δ = 2.34 (d, 1H, *J* = 11.6 Hz, C_(γ)-H), 5.60 (d, 1H *J* = 18.0 Hz, C_(ω)-H), 6.14 (dd, 1H, *J*₁ = 18.0 Hz, *J*₂ = 11.6 Hz, C_(β)-H). ¹³C NMR (100 MHz, 298 K, C₆D₆): δ = -0.69 (SiMe₃), -0.07 (SiMe₃), -0.30 (SiMe₃), -0.25 (SiMe₃), -0.21 (SiMe₃), 0.05 (SiMe₃), 29.59 (C_(α)), 31.87 (C_(α)), 32.04 (C_(ω)), 127.88 (C_(γ)), 128.44 (C_(γ)), 129.15 (C_(γ)), 145.82 (C_(β)), 146.85 (C_(β)), 147.94 (C_(β)). Anal. Calcd for C₂₇H₆₃SbSi₆ (678.07 g mol⁻¹): C, 47.83; H, 9.36; Sb, 17.96. Found: C, 47.29; H, 9.79; Sb, 17.80. (*Labels A'₍A₎, A'₍B₎, and A'₍C₎ indicate H assignments to specific [A'] ligands). Full ¹H NMR spectra of [SbA'₃] crystal-oil mixture, [SbA'₃] crystals, and [SbA'₃] oil available in Appendix A: FiguresA17-A19, respectively.

Synthesis of [SbA'₃] in THF: SbI₃ (0.106 g, 0.211 mmol) was dissolved in a 125 mL Schlenk flask, containing a magnetic stir bar, in minimal THF to give a yellow solution. K[A'] (0.168 g, 0.748 mmol) was dissolved in a 50 mL Schlenk flask in minimal THF to give a pale orange solution. Both flasks were attached to a Schlenk line and cooled to -78 °C in dry ice-acetone baths. Once cooled, the K[A'] solution was cannulated into the 125 mL Schlenk flask containing SbI₃ solution. Upon addition of K[A'], the solution became orange-peach. The mixture was stirred and warmed to room temperature overnight, during which time the

solution turned dark brown. THF was removed under vacuum and the product extracted with hexanes. The extract was filtered through a medium porosity ground glass frit to yield a pale brown filtrate and black solid. The filtrate was dried under vacuum to yield a brown oil (90 mg, 63%) that did not solidify over a period of days. The product was identified as a mixture of $[\text{SbA}'_3]$ diastereomers C_1 and C_3 in 3:2 ratios, with ^1H and ^{13}C NMR. Separation of the diastereomers was not possible as no solid formed, they displayed identical solubility, and the C_3 oil served to dissolve the C_1 solid. Full ^1H NMR spectrum available in Appendix A. Figure A20.

Synthesis of $[\text{SbA}'_3]$ in hexanes: SbCl_3 (87.8 mg, 0.385 mmol) was dissolved in minimal hexanes in a 50 mL Erlenmeyer flask, containing a magnetic stir bar, to give a yellow solution. $\text{K}[\text{A}']$ (0.274 g, 1.22 mmol) was slurried in hexanes and added dropwise to the 50 mL flask with stirring over 5 min. After addition of $\text{K}[\text{A}']$, the solution took on a grey tint. After stirring for 2 h, the solution became dark grey and was filtered through a medium porosity ground glass frit to yield a yellow filtrate and a gray-brown solid. Drying the filtrate under vacuum yielded a mixture of yellow oil and solid (0.195 g, 80%). The product was identified with ^1H NMR as a mixture of $[\text{SbA}'_3]$ C_1 and C_3 diastereomers, in 3:2 ratio.

Attempted C_1 to C_3 conversion of $[\text{SbA}'_3]$: $[\text{SbA}'_3]$ (46 mg, 0.073 mmol), primarily of the C_1 isomer, was dissolved in minimal toluene in a 50 mL Schlenk flask with magnetic stir bar, yielding a pale yellow solution. The flask was sealed with a condenser and refluxed for 4 h under a nitrogen atmosphere. During the reflux, the solution changed from the initial pale yellow to a pale brown. Removal of toluene under vacuum yielded a yellow-brown residue that was identified as the C_1 and C_3 isomers in approximately 8:1 ratio with ^1H NMR spectra, suggesting that no substantial thermal conversion between the isomers had occurred. Additionally, a substantial amount of $[\text{A}']_2$ was also observed in the spectra.

Attempted synthesis of $[\text{BiA}'_3]$: Attempts to synthesize $[\text{BiA}'_3]$ by salt metathesis from BiI_3 and $\text{K}[\text{A}']$ were unsuccessful. In both solution (hexanes and THF) and ball milling (IKA tube disperser) synthesis attempts, products consistent with Bi^0 and $[\text{A}']_2$ were obtained. The coupled allyl diastereomer A'_2 was identified with ^1H NMR.

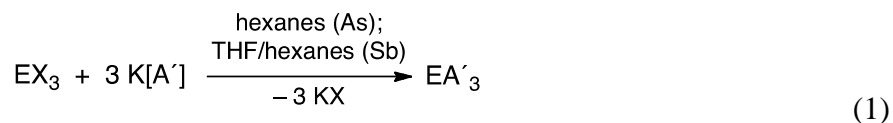
Synthesis of $[\text{BiA}'_3]$ from $[\text{AlA}'_3]$ in hexanes: BiI_3 (0.138 g, 0.438 mmol) was suspended in a 50 mL Erlenmeyer flask with magnetic stir bar in hexanes. $[\text{AlA}'_3]$ (0.245 g, 0.419 mmol) was readily dissolved in hexanes in a 20 mL vial, forming a pale yellow solution, and added dropwise to the flask over 5 min. The mixture was stirred for 24 h in the dark to yield a bright yellow solution, which was filtered through a medium porosity ground glass frit, providing a yellow filtrate. Drying under vacuum yielded a low-viscosity bright yellow oil (0.320 g). The collected product was identified as a complex mixture, with $[\text{BiA}'_3]$ being the major product (^1H NMR); the C_1 and C_3 diastereomers were present in an approximately

1:3.5 ratio. The product was found to be photosensitive and thermally unstable, with complete decomposition occurring within 72 hours. C₃-symmetric [BiA'₃]: ¹H NMR (400 MHz, 298 K, C₆D₆): δ = 0.21 (br s, 27H, SiMe₃), 0.22 (br s, 27H, SiMe₃), 2.85 (d, 3H, *J* = 12.0 Hz, C_(α)-H), 5.30 (d, 3H, *J* = 18.0 Hz, C_(γ)-H), 6.08 (dd, 3H, *J*₁ = 18.0 Hz, *J*₂ = 12.1 Hz, C_(β)-H). ¹³C NMR (100 MHz, 298K, C₆D₆): δ = 0.23 (SiMe₃), 0.27 (SiMe₃), 47.85 (C_(α)), 130.57 (C_(γ)), 146.98 (C_(β)). C₃-symmetric [BiA'₃]*: ¹H NMR (400 MHz, 298 K, C₆D₆): δ = 0.12–0.23 (br s, 54H, SiMe₃); [A'_(A)]: δ = 2.38 (d, 1H, *J* = 11.5 Hz, C_(α)-H), 5.35 (d, 1H *J* = 18.2 Hz, C_(γ)-H), 6.65 (dd, 1H, *J*₁ = 18.1 Hz, *J*₂ = 11.3 Hz, C_(β)-H); [A'_(B)]: δ = 2.85 (d, 1H, *J* = 12.0 Hz, C_(α)-H), 5.40 (d, 1H *J* = 17.9 Hz, C_(γ)-H), 6.46 (dd, 1H, *J*₁ = 18.1 Hz, *J*₂ = 11.7 Hz, C_(β)-H); [A'_(C)]: δ = 2.66 (d, 1H, *J* = 11.7 Hz, C_(α)-H), 5.30 (d, 1H *J* = 18.2 Hz, C_(γ)-H), 6.24 (dd, 1H, *J*₁ = 18.5 Hz, *J*₂ = 11.7 Hz, C_(β)-H). ¹³C NMR (100 MHz, 298K, C₆D₆): δ = -0.52 (SiMe₃), -0.45 (SiMe₃), -0.11 (SiMe₃), -0.072 (SiMe₃), -0.042 (SiMe₃), -0.30 (SiMe₃), 43.66 (C_(α)), 44.67 (C_(α)), 47.09 (C_(α)), 128.79 (C_(γ)), 129.05 (C_(γ)), 130.06 (C_(γ)), 146.61 (C_(β)), 147.20 (C_(β)), 147.50 (C_(β)). The instability of the compound precluded obtaining elemental analysis. Full ¹H NMR spectrum available in Appendix A: Figure A21. (*Labels A'_(A), A'_(B), and A'_(C) indicate H assignments to specific [A'] ligands.)

Synthesis of [BiA'₃] from [AlA'₃] by ball milling: BiI₃ (0.120 g, 0.38 mmol) and [AlA'₃] (0.212 g, 0.36 mmol) were added to a 50 mL stainless steel grinding jar (type C). The jar was charged with stainless steel ball bearings (3/8 in dia, 10 count) and closed tightly with the appropriate safety closer device under an N₂ atmosphere. The reagents were milled for 5 min. at 600 rpm, resulting in a brown-orange solid. The product was extracted with minimal hexanes (< 100 mL) and filtered through a medium porosity ground glass frit, providing a brown-yellow filtrate. Drying under vacuum yielded brown-yellow oil (0.225 g). The collected product was identified as a complex mixture of [BiA'₃], [A'₂], and unidentified side products. Both the C₁ and C₃ [BiA'₃] diastereomers were present in approximately a 1:2.5 ratio. Full ¹H NMR spectrum available in Appendix A: Figure A22.

Results and Discussion

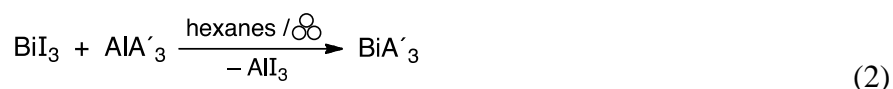
The reaction of trihalides of As (X = I) and Sb (X = Cl, I) with K[A'] was conducted either in solution (THF, hexanes) or by mechanochemical methods (ball milling), followed by extraction in hexanes (eq 1). Although tris(allyl) complexes could be produced with both metals, the outcomes differed in several details.



The tris(allyl)arsenic product [AsA'₃] (**1**) could not be formed from THF solutions. The coupled hexadiene ([A'₂])⁷⁰ was the major identified product (¹H NMR), accompanied by reduced arsenic-containing byproducts. From hexanes, however, crystalline yellow **1** could be isolated in 64% yield. It could also be isolated in slightly higher yield (80%) by ball milling AsI₃ with K[A'] (5 min/600 rpm), followed by extraction in hexanes.

The tris(allyl)antimony product [SbA'₃] (**2**) could be formed in the same manner as **1**, but its synthesis was compatible with a wider range of solvents (THF, toluene, hexanes). From a THF-based reaction, **2** was isolated in ca. 60% yield as a brown oil that did not solidify. Ball-milling solid SbCl₃ and K[A'] (5 min/300 rpm) produced a light yellow solid, which could be extracted into hexanes. A mixture of transparent pale yellow-brown crystals and low-viscosity yellow oil, in a total yield of 82%, was isolated from the extract. The oil could be drained from the crystals, but both were found to consist of **2**.

Attempts to synthesize [BiA'₃] (**3**) by the reaction of BiI₃ with K[A'] were unsuccessful. Reactions conducted in THF, hexanes, or by milling produced a dark gray powder consistent with the presence of bismuth metal. Extraction of the gray powder with hexanes yielded [A'₂]⁷⁰ as the only identifiable product (¹H NMR). However in either hexanes or by ball milling, **3** can be formed from treatment of BiI₃ with the mechanochemically produced [AlA'₃] (eq 2).³⁸ **3** was isolated as a light-sensitive, thermally unstable yellow oil in 95% yield, completely decomposing within three days at room temperature. The [AlA'₃] evidently serves as a less strongly reducing substrate than does the more ionic K[A']. The generation of [BiA'₃] from [AlA'₃] is a type of “second generation” mechanochemical synthesis.



NMR spectra (¹H/¹³C) of [EA'₃] from both the solution and mechanochemical preparations clearly indicate the presence of σ-bound allyl ligands, but are unexpectedly complex (see full spectra in Appendix A). A portion of the spectra that contains the resonances associated with the H_(α) protons for **1** and **2** is given in Figure 15. The σ-bound [A'] (Figure 15b) has five unique proton environments: two inequivalent trimethylsilyl groups and three distinct protons of the allyl. The resulting splitting pattern consists of a doublet, doublet of doublet, and doublet for H_(α), H_(β), and H_(γ) protons, respectively. Spectra of [EA'₃] suggested the presence of σ-bound ligands but deviated from the expected patterns.

In the case of **1** (Figure 15a, b), the doublets of $H_{(\alpha)}$, arising from coupling to $H_{(\beta)}$ ($^1J = 11$ Hz), are observed in the expected range (2–3 ppm). A maximum of three doublets would be expected for a molecule with no symmetry, but four are observed. Three of the doublets are of equal intensity, whereas the relative intensity of the doublet at δ 2.53 varies with the mode of synthesis. Analogous complications are observed in the region of the $H_{(\beta)}$ resonance (6–7 ppm), which contains what appears as overlapping sets of triplets.

Interpretation of COSY NMR spectra indicate that **1** is a mixture of two diastereomers, one with no symmetry (C_1) giving rise to the three equal intensity doublets, and another with an apparent three-fold axis (C_3), accounting for the single resonance at δ 2.53. The overlapping triplets in the 6–7 ppm region were identified as two overlapping doublets of doublets from $H_{(\beta)}$ of the C_1 diastereomer.

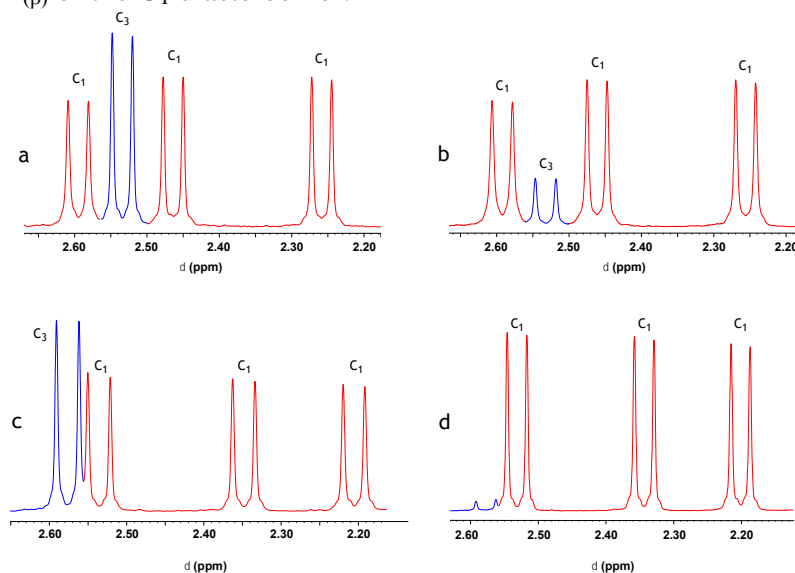


Figure 15. ^1H NMR of the $H_{(\alpha)}$ region of: **a**) $[\text{AsA}'_3]$ from solution; **b**) $[\text{AsA}'_3]$ from ball milling; **c**) $[\text{SbA}'_3]$ from solution; **d**) $[\text{SbA}'_3]$ of the crystals obtained from ball milling; they were drained of the C_3 oil, leaving the nearly pure C_1 diastereomer.

The ratio of diastereomers depends upon the method of synthesis; for **1**, the $C_1:C_3$ ratio is approximately 3:1 from hexanes solution, increasing to 10:1 from ball mill reactions (Table 1). Variation of milling times (30 s to 2 h) did not alter the observed diastereomer ratios, suggesting the product ratio is set very early in the reaction. Variable temperature ^1H NMR spectra (up to 90 °C) show significant broadening of peaks, but no change in the diastereomer ratio is observed. Refluxing in toluene promoted sample decomposition with no significant change of the ratio.

Similar behavior is observed for **2**. Figure 15c displays four doublets within the $H_{(\alpha)}$ region for **2** obtained in THF. Three of the resonances correspond to a C_1 diastereomer, while the resonance at $\delta 2.58$ corresponds to the C_3 diastereomer. The $H_{(\beta)}$ region of the NMR spectra was highly complex due to the presence of an apparent octet of equal intensity peaks that could be resolved with COSY as overlapping doublets of doublets of the C_1 diastereomer. The C_1 to C_3 ratio is 3:2 from solution and 3:1 from ball milling. The ratios were consistent across variations of reaction time in both solution (2-12 h) and milling reactions (5-30 min). The mechanochemical synthesis allowed for the nearly complete isolation of the C_1 diastereomer as crystals, as shown in Figure 15d. The oil drained from the crystals was a mixture of C_1 and C_3 . A pure sample of the C_3 diastereomer could not be obtained, as the oil dissolved the C_1 form. No conversions between the C_1 and C_3 diastereomers of **2** were observed.

The products from the bismuth reactions also contain a mixture of C_1 and C_3 -symmetric forms of **3**, but with the C_3 form in excess. Reactions conducted in hexanes and by ball milling yielded **3** with C_1 : C_3 ratios of 1:3.5 and 1:2.5, respectively. No conversion between diastereomers was observed, however the instability of **3** prevented thermal conversion attempts. The relative amounts of the isomers for all three $[EA'_3]$ produced under the different reaction conditions are summarized in Table 1.

Table 1. Relative amounts of the C_1 and C_3 -symmetric isomers (C_1 : C_3) of $[EA'_3]$ obtained through solution and ball milling methods.

E	Solution	Ball milling
As	3:1	10:1
Sb	3:2	3:1
Bi	1:3.5	1:2.5

The source of the difference in the relative ratios of the C_1 and C_3 -symmetric diastereomers is not immediately obvious. A few points, however, are clear: (a) the ratio of C_1 to C_3 is independent of time for reactions conducted either in solution or by ball milling; (b) once formed, there is no evidence for diastereomer interconversion; and (c) there is a metal center dependency on the C_1 / C_3 ratio. The latter is manifested in two ways. Firstly, mechanochemical synthesis increases the C_1 / C_3 ratio relative to that produced in solution for all three elements, although the enhancement decreases from As (230%) to Bi (40%). Secondly, the C_1 form becomes less favored moving down group 15, switching from the major diastereomer for **1** and **2**, to the minor isomer for **3**.

In order to help interpret these results, single crystals of **1** and **2** were grown from hexane. The complexes were found to be monomeric in the solid state, with the arsenic (antimony) atom σ -bound to the A' ligands in a trigonal pyramidal manner (Figure 16).¹⁵³ They have no molecular symmetry, and are consistent with the C₁ diastereomers found in NMR spectra. They represent the first crystal structures of uncoordinated homoleptic arsenic and antimony allyl complexes.¹⁵⁴⁻¹⁵⁵ In the case of **1**, two of the ligands are roughly parallel to a line between the As and the center of the C₃ pyramid base (C1–C10–C19), but the third (involving C1–C2–C3) is approximately parallel to the C₃ plane. The average As–C distance of 2.010(5) Å is typical for arsenic-carbon single bonds; cf. those of the mononuclear tri(neopentyl)arsenic (1.998(10) Å),¹⁵⁶ (2,4,6-*i*-Pr)₃C₆H₂)₃As (1.986(7) Å),¹⁵⁷ and perhaps especially, the As(C₃H₅)₃ ligands in PdCl₂[As(C₃H₅)₃]₂ (1.96(1) Å).¹⁵⁵ The average C–As–C' angle of 100.59(2)° in [AsA'₃] is somewhat wider than found in tri(neopentyl)arsenic (94.6(4)°),¹⁵⁶ but is similar to that in (4-MeC₆H₄)₃As (99.3(2)°);¹⁵⁸ the values in tri(mesityl)arsenic (107.6(4)°)¹⁵⁹ or (2,4,6-*i*-Pr)₃C₆H₂)₃As (109.2(2)°)¹⁵⁷ are notably wider. The differences have been ascribed to steric crowding. The fully localized carbon-carbon bonding in the allyl ligands in **1** is indicated by the average C=C and C–C bond distances of 1.321(7) and 1.496(6) Å, respectively.

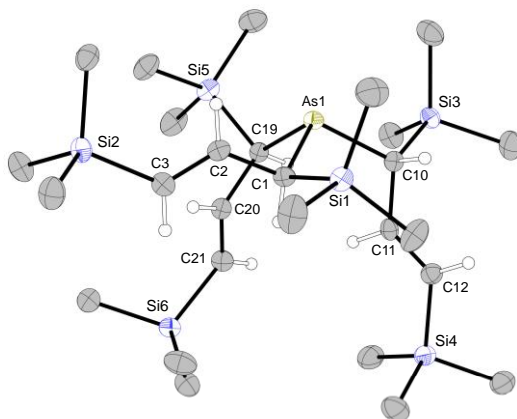


Figure 16. Thermal ellipsoid plot of [AsA'₃], illustrating the numbering scheme used in the text. Thermal ellipsoids are drawn at the 50% level, and for clarity, hydrogen atoms have been removed from the trimethylsilyl groups. List of bond angles and distances available in Appendix B, Section B2.

Compound **2** is isostructural with **1** (Appendix B: Section B3). The same mix of parallel and perpendicular ligand arrangement relative to the C₃ pyramid base is present. The average Sb–C distance of 2.206(5) Å is on the upper end for antimony-carbon single bonds, and is similar to those in the mononuclear tri(neopentyl)antimony (2.18(3) Å)¹⁶⁰ and

tribenzylantimony (2.175(3) Å).¹⁶¹ The average C–Sb–C' angle of 98.7(2)° in **2** is wider than found in tri(neopentyl)antimony (93.5(3)°),¹⁶⁰ or tribenzylantimony (94.9(6)°),¹⁶¹ which may be the result of steric crowding.

DFT calculations of the relative energies of the [EA₃] complexes were completed to compare them with the experimentally observed product ratios. The central metal was varied (As–Bi, with Al added for comparison), and three conformations were considered (Figure 17). For the C₁ form (**a**), the coordinates from the crystal structures of **1** and **2** were used as starting points. The C₃ form (**b**) was modelled after the configuration found in [M(1,3-SiMe₃)₂C₃H₃)₃E(thf)_n].⁸⁵⁻⁸⁶ The conformation found for [AlA₃] and [GaA₃],^{38, 67} in which the three ligands are roughly perpendicular to the AlC₃ plane, with one antiparallel to the other two (1U2D) served as the basis for configuration **c**. The C₁ and 1D2U forms (both of which are of C₁ symmetry) possess [R,S,S] arrangements at the C_(α) centers, while the C₃ diastereomer exhibits [R,R,R] symmetry. It should be noted that these three forms do not exhaust the possibilities for the symmetries (e.g., *endo,exo* forms of the ligands were not studied). The calculations were completed with three different functionals (M06-L,¹⁶² APF-D,¹⁶³ ωB97X-D¹⁶⁴), all of which include some accounting for dispersion interactions; the def2TZVP basis set was used on the metal atoms, and def2SVP was used on all the others.¹⁶⁵ All the conformations were found to be minima on their respective potential energy surfaces. Relative energy differences for the conformations were averaged from the three functionals and were plotted for each metal center in Figure 18.

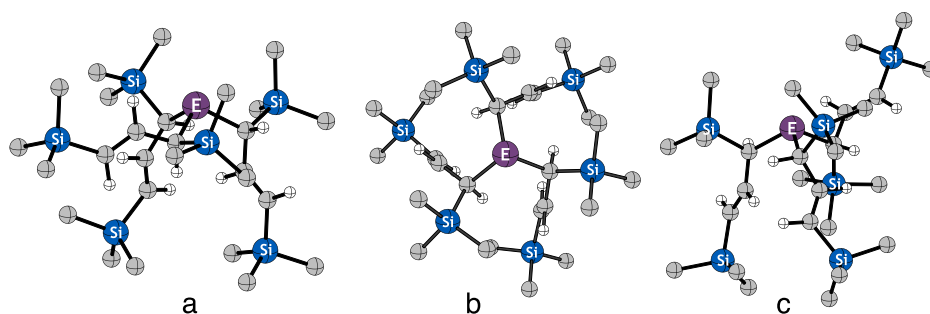


Figure 17. Basic structural types considered for geometry optimization; **a**, the C₁ form, modeled after the [(As,Sb)A₃] crystal structures; **b**, the C₃ form, viewed down its major axis; **c**, the 1U2D form, modeled after the configuration found in [AlA₃] and [GaA₃] (Appendix C: Section C2).

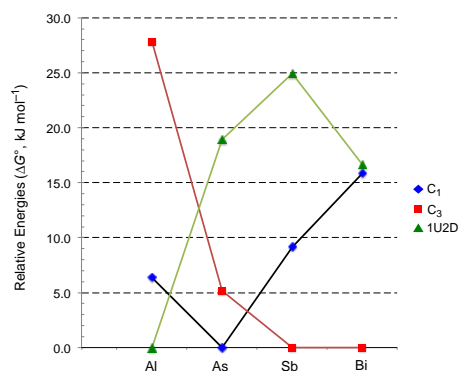


Figure 18. Relative energies of the [EA'₃] diastereomers; those at 0.0 kJ mol⁻¹ represent the most stable form for each metal (Appendix C: Section C2).

There is a substantial dependence of the relative energies of the conformations on the identity of the metal center. The 1U2D is the lowest energy conformation for [AlA'₃], but is the highest energy of the three conformations for **1** and **2**. This may be a consequence of intramolecular close contacts generated by the pyramidal coordination around the center element, a feature absent in the trigonal planar environments of [(Al, Ga)A'₃].^{38, 67} For **3**, the 1U2D conformation is only 0.7 kJ mol⁻¹ above that of C₁, which is insignificant at this level of theory. The longer M–C bonds in **3** reduce the interligand crowding in the 1U2D conformation; there are no methyl-methyl contacts less than 4.0 Å.

For **1**, all three DFT functionals agree in placing the C₁ form lower in energy than C₃; the average difference is 5.1 kJ mol⁻¹. For **2** and **3**, the preference is reversed, with the C₃ form lower in energy than C₁ by an average of 9.2 and 15.9 kJ mol⁻¹, respectively. The calculated stability of the C₁ and C₃ forms of **2** is reversed relative to the experimentally observed product ratios. Although C₃ is predicted to be the more stable form for **3**, the energy difference of 15.9 kcal mol⁻¹ between C₃ and C₁ would be equivalent to a diastereomer ratio difference of roughly 1:600, if they were in true thermodynamic equilibrium, and not the 1:(2.5–3.5) ratios experimentally observed.

The calculations are qualitatively consistent with the experimentally isolated ratios of products if: a) the C₁ forms are the kinetically preferred products for **1** and **2**; and b) milling promotes the kinetic products. In the case of **1**, this reinforces the thermodynamically preferred product, and contributes to the C₁:C₃ ratio of 10:1 from milling. Although the C₁ diastereomer is still the predominantly isolated form for **2**, despite its calculated lower stability, the C₁:C₃ ratio from solution is half that for **1**, and less than a third from the mechanochemical synthesis. The observed isomer ratios for **3** are consistent with the higher thermodynamic stability of the C₃ form, but whether this reflects true thermodynamic control is not certain. Once

again, ball milling increases the relative amount of the unsymmetrical C_1 isomer. The different reaction conditions for the formation of **3**, ligand transfer from the covalently bonded $[AlA'_3]$ rather than from the more salt-like $K[A']$, makes comparisons with the lighter Group 15 counterparts difficult.

Conclusions

In summary, trimethylsilylated tris(allyl) complexes of arsenic, antimony, and bismuth have been prepared in high yield through both solution and mechanochemical methods. The complexes of arsenic and antimony represent the first crystal structures of such uncomplexed compounds. The unstable tris(allyl) bismuth complex could only be generated by treatment with the mechanochemically produced $[AlA'_3]$. The latter may prove to be a valuable reagent in the preparation of other redox sensitive complexes of the heavier p- and d-block metals. The $[EA'_3]$ complexes were isolated as mixtures of diastereomers of C_1 and C_3 -symmetry, the ratio of which depends on the metal center and synthesis method. Mechanochemical syntheses shift the diastereomer ratio to promote the unsymmetrical C_1 product of these systems. These results suggest mechanochemical syntheses can moderate the isomer ratios in metal allyl complexes, an influence that may be useful in other systems where stereocontrol must be exerted.

Chapter 4

Organometallic Mechanochemistry of s-Block Metal Complexes

Introduction

The synthesis and reactivity of alkaline earth metal complexes containing the bulky allyl ligand A' have occupied a large portion of our investigations for the past several years.^{37-38, 65-67, 74, 84, 140, 150, 166} With an ultimate goal of mimicking the catalytic properties of rare earth metal complexes with the alkaline earth metals, the catalytic reactivity of group 2 complexes were investigated and compared to rare earth metal (lanthanide) counterparts.^{65, 73, 140, 150, 166} As the group 2 metals are significantly more abundant and of comparable size and charge, it is believed that the alkaline earth metals could in many cases offer a cheaper alternative than the more expensive and less abundant rare earth metals for catalysis.

Previous investigations in our group led to the successful synthesis, characterization, and in some cases catalytic screening of several bulky allyl metal complexes containing A'.^{140, 166} Among these were the mononuclear $[MA'_2(thf)_x]$ (M = Be, Mg, Ca, Sr) complexes and the binuclear $[K(thf)Ba_2A'_5]$.^{84, 140, 147, 166} Attempts to remove THF from the final products were unsuccessful in all cases, and as demonstrated by synthesis of a THF-free $[MgA'_2]_2$ complex, base free complexes could only be obtained by excluding THF from the synthesis route.^{140, 166} Unlike $[AlA'_3]$ (Chapter. 2), the complexes could still be formed in the presence of THF; once coordinated, THF did not appear to have any other effect.

It was not until the investigation of catalytic activity that THF was suspected as not being as benign as originally expected. The complex $[MgA'_2(thf)_2]$ was inactive towards the polymerization of MMA. The base free $[MgA'_2]_2$ complex, however demonstrated a modest turnover rate ($\sim 3,000\text{ h}^{-1}$).^{140, 166} Apart from the monomer vs. dimer distinction (which is not as apparent in solution, owing to fluxional behavior), the only appreciable difference between these complexes is the presence, or lack thereof, of coordinated THF. The presence of THF evidently inhibits catalytic activity, presumably by occupying coordination sites on the magnesium center. This principle should be applicable to other s-block complexes as well.

The calcium complex $[CaA'_2(thf)_2]$ is of particular interest as it displays significant activity even with THF coordination (TOF $\sim 19,000\text{ h}^{-1}$).¹⁶⁶ If a $[CaA'_2]$ complex could be isolated without coordinated THF, it makes sense that an increase of activity could be observed. Complications arise when attempting to synthesize $[CaA'_2]$ by our standard salt metathesis routes, however, which require ethereal solvents in the form of Et₂O or THF. Due to the strength of the THF coordination to Ca, THF cannot be removed from the final product.

Unlike the Mg system, $[\text{CaA}'_2]$ could not be synthesized in Et_2O , and thus appeared inaccessible through our traditional solvent-based methods.

The successful synthesis of $[\text{AlA}'_3]$ provided a previously unconsidered approach to the formation of a base-free p-block metal allyl complex.³⁸ The negative influence of coordinating solvents is especially deleterious in the case of $[\text{AlA}'_3]$, as the compound cannot even be formed in either THF or diethyl ether. The successful mechanochemical synthesis of the base-free aluminum complex suggested that it might serve as a model for the preparation of alkaline-earth counterparts. It seemed reasonable that, as with $[\text{AlA}'_3]$, the removal of coordinating solvents should allow the straightforward synthesis of homoleptic $[\text{MA}'_x]_y$ complexes. This last assumption was found to be incorrect. While the removal of coordinating solvents does allow for the isolation of base-free complexes, these are not the monometallic variants expected.

Described here are the applications of mechanochemical synthesis techniques, specifically ball milling, towards the formation of base free s-block metal allyl complexes. The compositions of the complexes demonstrate that mechanochemical syntheses cannot routinely be expected to follow the patterns set by solution-based routes. Instead, new complexes are formed to compensate for the lack of coordinating solvents; these may not reflect the stoichiometries of the starting reagents, for example, and in some cases display deceptively simple NMR spectra.

Experimental

General Considerations. All syntheses were conducted under rigorous exclusion of air and moisture using Schlenk line and glovebox techniques. Proton (^1H), carbon (^{13}C), and COSY spectra were obtained on an Advance AV-400 MHz spectrometer. Proton and carbon were referenced to residual resonances of C_6D_6 (δ 7.15 and δ 128). Variable temperature ^1H NMR was obtained on a Bruker DRX-500 and referenced to residual resonances of tol-d_8 . Metal analysis was obtained with ICP-OES on a Perkin Elmer Optima 7000 DV. Combustion analysis was performed by ALS Environmental, Tucson, AZ.

Materials. All anhydrous metal salts were previously purchased from Strem and Sigma-Aldrich, stored under an N_2 atmosphere and used as received. Anhydrous inhibitor-free tetrahydrofuran (THF) was used as obtained from Aldrich. Other commercially available reagents were used without additional purification. Toluene, hexanes, and diethyl ether were distilled under nitrogen from potassium benzophenone ketyl.¹¹¹ Deuterated benzene (C_6D_6) was distilled from Na/K (22/78) alloy prior to use. Deuterated toluene (tol-d_8) was purchased from Cambridge Isotopes and dried over molecular sieves prior to use. The HA' and $\text{K}[\text{A}']$

(A' = 1,3-(SiMe₃)₂C₃H₃) reagents were synthesized as previously described.¹¹² Stainless steel (440 grade) ball bearings (6mm, 3/8 in, and 1/2 in dia) were thoroughly cleaned with hexanes and acetone prior to use. Disperser milling was performed with an Ultra-Turrax Tube Drive and BMT-20-S tubes, both purchased from IKA. Planetary milling was performed with a Retsch model PM100 mill, 50 mL stainless steel grinding jar type C, and safety clamp for air-sensitive grinding. ¹H NMR spectra of HA', K[A'], and [A']₂ available in Appendix A: Figures A1, A2, and A3, respectively.

Nonstoichiometric Synthesis of K[BeA'₃]: Solid BeCl₂ (0.393 g, 4.96 mmol) and K[A'] (2.246 g, 10.01 mmol) were added to a 50 mL stainless steel grinding jar (type C). The jar was charged with stainless steel ball bearings (6 mm dia, 150 count) and closed tightly with the appropriate safety closer device under an N₂ atmosphere. The reagents were milled for 15 min at 600 rpm, resulting in a light orange solid. The product was extracted with minimal hexanes (< 100 mL) and filtered through a medium porosity ground glass frit, providing a dark orange filtrate. Drying under vacuum yielded a dark orange solid (0.1967 g, 25% yield of K[BeA'₃]) which was recrystallized by the slow evaporation of toluene over 1 month to provide dark orange-brown crystals suitable for single crystal X-ray diffraction. The product was identified as K[BeA'₃]. A second set of peaks, of an identical splitting pattern to K[BeA'₃], were present in NMR spectra but were marginally above baseline intensity. Tentative assignments were made based on known data, though integrations were not reliable due to low intensity and overlap. Anal. Calcd (%) for C₂₇H₆₃BeKSi₆: C, 53.65; H, 10.51; Be, 1.49; K, 6.47. Found: C, 52.09; H, 9.79; Be, 1.04; K, 4.44. **Major K[BeA'₃] product.** ¹H NMR (400 MHz, C₆D₆, 298K): δ 0.216 (s, 54H, SiMe₃); δ 3.209 (d, 6H, J = 13.12 Hz, H_(α,γ)); δ 6.999 (t, 3H, J₁ = 15.6 Hz, H_(β)). ¹³C NMR (100 MHz, C₆D₆, 298K): δ 1.024 (s, SiMe₃); δ 70.71 (s, C_(α,γ)); δ 166.09 (s, C_(β)). **Minor K[BeA'₃] product.** ¹H NMR (400 MHz, C₆D₆, 298K): δ 0.2433 (s, SiMe₃); δ 2.766 (d, J = 16.0 Hz, H_(α,γ)); δ 6.662 (t, J = 16.0 Hz, H_(β)). ¹³C NMR (100 MHz, C₆D₆, 298K): δ 2.0405 (s, SiMe₃); δ 70.62 (s, C_(α,γ)); δ 153.63 (s, C_(β)). The full ¹H NMR spectrum can be found in Appendix A: Figure A23

Attempted Stoichiometric Synthesis of K[BeA'₃]: Solid BeCl₂ (0.293 g, 3.70 mmol) and K[A'] (2.628 g, 11.72 mmol) were added to a 50 mL stainless steel grinding jar (type C). The jar was charged with stainless steel ball bearings (6 mm dia, 150 count) and closed tightly with the appropriate safety closer device under an N₂ atmosphere. The reagents were milled for 15 min at 600 rpm, resulting in a burnt-orange solid. Multiple extractions were performed, through a medium porosity ground glass filtration frit, in an attempt to collect products showing lower solubility in hexanes. Both extractions yielded large amounts of brown solid in the filter frit. Initial extraction was performed with hexanes yielding a dark orange filtrate after filtration. Removal of hexanes under vacuum initially precipitated a light brown solid and

complete removal yielded an orange-brown oil. The oil was highly soluble in hexanes and could be extracted, while the brown solid was insoluble once precipitated from hexanes. The oil slowly solidified into a dark orange-brown solid, though no crystals were observed. The solid was identified as $\text{K}[\text{BeA}'_3]$ by ^1H NMR. As such this method allowed for the isolation of pure $\text{K}[\text{BeA}'_3]$ in low yield (0.0805 g, 9.3% yield). The hexane insoluble solid demonstrated marginal solubility in C_6D_6 , and the NMR spectra were consistent with the minor product identified in the nonstoichiometric reaction. A second filtration and extraction was performed with toluene on the remaining brown solid of the filtration frit. The brown solid was only partially soluble, yielding a red-orange filtrate. The filtrate was dried to an orange-brown solid composed of brittle flakes (0.187 g). The NMR spectra of this product were consistent with the minor product of the non-stoichiometric reaction. It should be noted the chemical shifts of the minor product are identical to those observed for $\text{K}[\text{A}']$, which is soluble in toluene. However, due to $\text{K}[\text{A}']$'s being insoluble in hexanes, the minor product is clearly not the same material. The full ^1H NMR spectrum can be found in Appendix A, Figure A24.

Non-stoichiometric Synthesis of $[\text{K}(\text{tol})(\mu\text{-A}')\text{K}(\text{tol})][\text{Mg}(\text{A}')(\mu\text{-A}')_2]$. Solid MgBr_2 (0.556 g, 3.02 mmol) and $\text{K}[\text{A}']$ (1.224 g, 5.46 mmol) were added to a 50 mL stainless steel grinding jar (type C). The jar was charged with stainless steel ball bearings (6 mm dia, 50 count) and closed tightly with the appropriate safety closer device under an N_2 atmosphere. The reagents were milled for 10 min at 600 rpm, resulting in a hard, dark pink solid caked along the walls of the jar and a large sticky mass of pink solid and ball bearings. Hexanes were used to soften and begin extraction of product directly from the jar. Filtering through a medium porosity ground glass frit separated a pink solid from a yellow filtrate. The solid was dried and milled a second time for 10 min at 600 rpm yielding a white-pink solid. The solid was extracted with hexanes, filtered, and added to the initial filtrate. Removal of hexanes under vacuum yielded an orange oil in low yield, which solidified to orange microcrystals overnight. A reaction yield was not obtained. The sample was dissolved in toluene and allowed to slowly evaporate to dryness over the course of one month to form small orange block crystals suitable for single crystal x-ray analysis. Due to complications in handling the best crystals were lost, however a structure was obtained for a second set of crystals. The product was identified as the bimetallic complex $[\text{K}(\text{tol})(\mu\text{-A}')\text{K}(\text{tol})][\text{Mg}(\text{A}')(\mu\text{-A}')_2]$, not the initially predicted $[\text{MgA}'_x]_y$ based on stoichiometric reaction ratios. The ^1H NMR spectra of both the initial product and $[\text{K}(\text{tol})(\mu\text{-A}')\text{K}(\text{tol})][\text{Mg}(\text{A}')(\mu\text{-A}')_2]$ are identical in C_6D_6 , indicating that toluene only helped to promote large crystal formation and the microcrystals are of the form $[\text{K}(\mu\text{-A}')\text{K}][\text{Mg}(\text{A}')(\mu\text{-A}')_2]$. Considering the complexity of the molecule, the ^1H NMR spectra are remarkably simple and clean, displaying the expected splitting pattern of two π -bound

or highly fluxional A' ligands in roughly a two to one ratio. Due to low yield and product loss, insufficient sample was obtained for microanalysis. **Major A'**. ^1H NMR (400 MHz, C_6D_6 , 298K): δ 0.262 (s, 36H, SiMe_3); δ 3.218 (d, 4H, $J = 15.8$ Hz, $\text{H}_{(\alpha,\gamma)}$); δ 6.945 (t, 2H, $J_1 = 15.8$ Hz, $\text{H}_{(\beta)}$). ^{13}C NMR (100 MHz, C_6D_6 , 298K): δ 1.598 (s, SiMe_3); δ 71.66 (s, $\text{C}_{(\alpha,\gamma)}$); δ 157.21 (s, $\text{C}_{(\beta)}$). **Minor A'**. ^1H NMR (400 MHz, C_6D_6 , 298K): δ 0.223 (s, 18H, SiMe_3); δ 2.727 (d, 2H, $J = 16.0$ Hz, $\text{H}_{(\alpha,\gamma)}$); δ 6.644 (t, 1H, $J_1 = 16.0$ Hz, $\text{H}_{(\beta)}$). ^{13}C NMR (100 MHz, C_6D_6 , 298K): δ 2.413 (s, SiMe_3); δ 70.57 (s, $\text{C}_{(\alpha,\gamma)}$); δ 153.75 (s, $\text{C}_{(\beta)}$). The full ^1H NMR spectrum can be found in Appendix A: Figure A25.

Stoichiometric Synthesis of $[\text{K}(\text{tol})(\mu\text{-A}')\text{K}(\text{tol})][\text{Mg}(\text{A}')(\mu\text{-A}')_2]$. Solid MgBr_2 (0.094 g, 0.511 mmol) and $\text{K}[\text{A}']$ (0.533 g, 2.38 mmol) were added to a 50 mL stainless steel grinding jar (type C). The jar was charged with stainless steel ball bearings (3/8 in dia, 10 count) and closed tightly with the appropriate safety closer device under an N_2 atmosphere. The reagents were milled for 10 min at 600 rpm, resulting in a pale orange solid. The product was extracted with hexanes and filtered through a medium porosity ground glass frit to isolate a pale orange filtrate. When dried under vacuum, two solid, but non-crystalline products were isolated, one pink and the other yellow-orange (0.101 g total, 24% yield if calculated as $[\text{K}(\mu\text{-A}')\text{K}][\text{Mg}(\text{A}')(\mu\text{-A}')_2]$). Due to similar solubility the solids could not be separated. The ^1H NMR spectrum of a sample containing the predominantly red solid was identical to that obtained for $[\text{K}(\text{tol})(\mu\text{-A}')\text{K}(\text{tol})][\text{Mg}(\text{A}')(\mu\text{-A}')_2]$, however the major and minor products were reversed. This implies that the solids are two discrete compounds and a tentative correlation between samples and chemical shifts can be made. Integrations were based upon the peak at δ 6.945 being set to 1H. An exact ratio cannot be calculated without knowing the identity of both products. **Major A' (red solid).** ^1H NMR (400 MHz, C_6D_6 , 298K): δ 0.223 (s, 72H, SiMe_3); δ 2.727 (d, 8H, $J = 16.0$ Hz, $\text{H}_{(\alpha,\gamma)}$); δ 6.644 (t, 4H, $J_1 = 16.0$ Hz, $\text{H}_{(\beta)}$). ^{13}C NMR (100 MHz, C_6D_6 , 298K): δ 2.413 (s, SiMe_3); δ 70.57 (s, $\text{C}_{(\alpha,\gamma)}$); δ 153.75 (s, $\text{C}_{(\beta)}$). **Minor A' (yellow-orange solid).** ^1H NMR (400 MHz, C_6D_6 , 298K): δ 0.262 (s, 18H, SiMe_3); δ 3.218 (d, 2H, $J = 15.8$ Hz, $\text{H}_{(\alpha,\gamma)}$); δ 6.945 (t, 1H, $J = 15.8$ Hz, $\text{H}_{(\beta)}$). ^{13}C NMR (100 MHz, C_6D_6 , 298K): δ 1.598 (s, SiMe_3); δ 71.66 (s, $\text{C}_{(\alpha,\gamma)}$); δ 157.21 (s, $\text{C}_{(\beta)}$). The full ^1H NMR spectrum can be found in Appendix A: Figure A26.

Synthesis of $\text{K}[(\mu\text{-A}')\text{CaA}'_2]$. In a typical reaction, CaI_2 (0.0714 g, 2.43 mmol) and $\text{K}[\text{A}']$ (1.705 g, 7.60 mmol) were added to a 50 mL stainless steel grinding jar (type C). The jar was charged with stainless steel ball bearings (6 mm dia, 50-70 count) and closed tightly with the appropriate safety closer device under an N_2 atmosphere. The reagents were milled for 15 min at 600 rpm, resulting in a mixture of solids closely resembling the starting materials. The ground mixture was extracted with hexanes and filtered through a medium porosity

ground glass frit to isolate a pale-colored filtrate. Removal of hexanes under vacuum provided a pale yellow residue, in low yield, which grew into microcrystals overnight not suitable for single crystal x-ray diffraction. Approximately 72 h after isolation, the yellow microcrystals turned orange under an inert atmosphere. The change was found to occur whether the product was dry or dissolved in hexanes, turning a yellow tinted solution to orange. Both the yellow and orange solids were air- and moisture-sensitive. Once formed, the orange solid was stable indefinitely under an inert atmosphere. As with $\text{K}[\text{BeA}'_3]$, a white solid was often left in the flask upon removal of the product that was insoluble in the available solvents (toluene, hexanes, pentane, and C_6D_6). Variations in the ratio of reagents used (up to 4 equivalents $\text{K}[\text{A}']$) did not have a significant impact on yield; in some cases yields were lower when the $\text{K}[\text{A}']/\text{CaI}_2$ ratio was higher. This, however, may be more of a factor of the mass ratio between the reagents and ball bearings. The ^1H NMR spectra of both the yellow solid, taken immediately after isolation, and the orange solid were characteristic of π -bound or highly fluxional A' ligands. The yellow solid appeared to contain only a single A' environment, while the orange solid contained two. The set of greater intensity A' peaks from the orange solid were identical in splitting and chemical shift to those of the yellow. This suggests that only some of the ligands in the complex do not undergo a detectable change in environment while other are shifted significantly more downfield and result in the color change. The chemical shifts of the yellow solid were consistent with those of the previously reported $[\text{CaA}'_2(\text{thf})_2]$.^{147, 166} After 6 months, the product became primarily orange and the maximum ratio between the peaks for the two colored solids was 2:1. Single crystals suitable for x-ray crystal analysis were grown over the course of 6 months, by the slow evaporation of hexanes in a heavily etched 20 mL glass vial. The orange product was identified as $\text{K}[(\mu\text{-A}')\text{CaA}'_2]$, deviating significantly from the structures found for beryllium and magnesium, but having an allyl arrangement around the metal center similar to that found for $[\text{ScA}'_3]$.³⁸ Yellow $[\text{CaA}'_x]$ complex. ^1H NMR (400 MHz, C_6D_6 , 298K): δ 0.242 (s, 18H, SiMe_3); δ 2.774 (d, 2H, $J = 16.0$ Hz, $\text{H}_{(\alpha,\gamma)}$); δ 6.664 (t, 1H, $J_1 = 16.0$ Hz, $\text{H}_{(\beta)}$). ^{13}C NMR (100 MHz, C_6D_6 , 298K): δ 2.398 (s, SiMe_3); δ 70.72 (s, $\text{C}_{(\alpha,\gamma)}$); δ 153.76 (s, $\text{C}_{(\beta)}$). The full ^1H NMR spectrum can be found in Appendix A: Figure A27. $\text{K}[(\mu\text{-A}')\text{CaA}'_2]$. ^1H NMR (400 MHz, C_6D_6 , 298K): δ 0.279 (s, 36H, SiMe_3); δ 0.344 (s, 18H, SiMe_3); δ 2.715 (d, 4H, $J = 15.9$ Hz, $\text{H}_{(\alpha,\gamma)}$); δ 3.393 (d, 2H, $J = 16.1$ Hz, $\mu\text{-H}_{(\alpha,\gamma)}$); δ 6.623 (t, 2H, $J = 15.9$ Hz, $\text{H}_{(\beta)}$). δ 7.245 (t, 1H, $J = 16.2$ Hz, $\mu\text{-H}_{(\beta)}$). The full ^1H NMR spectrum can be found in Appendix A, Figure A28.

Attempted Syntheses of [CaA'_x] Complexes from CaX₂ (X = F, Cl, Br). Reactivity was observed between CaX₂ (X = Cl, Br) and K[A'] under mechanochemical conditions. The products were confirmed with ¹H NMR as identical to the products observed from reactions with CaI₂, but in lower yields. Variations of reaction and grinding parameters, such as ball size, ball composition, milling time (up to 20 min), and reagent ratios, did not improve the yield from either calcium source. Milling times on the scale of hours may be able to increase yields, but these have yet to be investigated. Attempts to utilize CaF₂ as a reagent were unsuccessful. No reactivity with excess K[A'] was observed, likely due to the high lattice energy of CaF₂. Variations on grinding parameters were similarly unsuccessful.

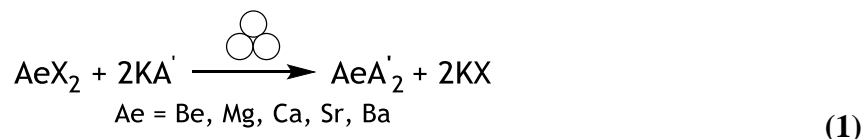
Attempted Mechanochemical Synthesis of an [SrA'_x] Complex: Solid SrBr₂ (0.244 g, 0.986 mmol) and K[A'] (0.4761 g, 2.122 mmol) were added to a 50 mL stainless steel grinding jar (type C). The jar was charged with stainless steel ball bearings (6 mm dia, 100 count) and closed tightly with the appropriate safety closer device under an N₂ atmosphere. The reagents were milled for 5 min at 600 rpm, resulting in an off-white solid resembling starting material. The solid was extracted with minimal hexanes (< 100 mL) and filtered through a medium porosity ground glass frit, providing a near colorless filtrate. Drying under vacuum produced a small amount (0.015 g) of a white solid. The solid was soluble in C₆D₆ and ¹H NMR spectra suggested the presence of π -bound or highly fluxional [A'] ligands. Due to the low yield, assignment of carbons by ¹³C NMR could not be made. Only a single set of [A'] peaks were visible, unlike those observed with Be, Mg, and Ca. ¹H NMR (400 MHz, C₆D₆, 298K): δ 0.246 (s, 18H, SiMe₃); δ 2.780 (d, 2H, J = 16.0 Hz, H_(α , γ)); δ 6.680 (t, 1H, J = 16.0 Hz, H_(β)). The full ¹H NMR spectrum can be found in Appendix A: Figure A29.

Synthesis of Cs_{0.5}K_{0.5}[A']. Solid CsI (0.157 g, 0.602 mmol) and K[A'] (0.445 g, 1.986 mmol) were added to a 50 mL stainless steel grinding jar (type C). The jar was charged with stainless steel ball bearings (1/2 in dia, 3 count) and closed tightly with the appropriate safety closer device under an N₂ atmosphere. The reagents were milled for 15 min at 600 rpm, resulting in a pale yellow-orange solid. The solid was extracted with hexanes and filtered through a medium porosity ground glass frit, providing a nearly colorless, yellow tinted filtrate. Removal of hexanes under vacuum resulted in a cloudy yellow-white solution that deposited a precipitate as the product was concentrated. Removal of hexanes yielded a yellow solid in negligible yield (0.012 g). The solid was dissolved in hexanes, which were slowly evaporated over the course of a week to promote crystal growth. During this time, the solution became significantly darker, taking on a more prominent orange color, not unlike what is observed for the [CaA'_x] system, resulting in orange-red crystals being collected. X-ray analysis of the crystals revealed them to be the bimetallic Cs_{0.5}K_{0.5}[A'] complex. The product was

highly soluble in C₆D₆, giving a bright red solution. The ¹H NMR was consistent with a single π-bound or highly fluxional A' ligand. ¹H NMR (400 MHz, C₆D₆, 298K): δ 0.272 (s, 18H, SiMe₃); δ 2.707 (d, 2H, J = 16.0 Hz, H_(α,γ)); δ 6.575 (t, 1H, J₁ = 32 Hz, J₂ = 16.0 Hz, H_(β)). ¹³C NMR (100 MHz, C₆D₆, 298K): δ 2.322 (s, SiMe₃); δ 73.08 (s, C_(α,γ)); δ 153.51 (s, C_(β)). The full ¹H NMR spectrum can be found in Appendix A: Figure A30.

Results and Discussion

The procedures used for the synthesis of [AlA'₃], encompassing the round bottom flask mill, the tube disperser mill, and the planetary ball mill, were adapted for use with the various s-block elements of interest.³⁸ The reactions of the metal halides (M = Be, Mg, Ca, Sr, Ba, Cs) and K[A'] were conducted mechanochemically (ball milling), primarily with the planetary mill, followed by an extraction of hexanes (eq. 1). Metal allyl products could be isolated from all elements except for barium, which even in solution is known to provide products whose formula is not directly related to the stoichiometry of reagents. As such, the lack of an isolable product from mechanochemical methods of synthesis was not entirely surprising.



Initial investigations used stoichiometric ratios of K[A'] based on charge; 2:1 for alkaline earth metals and 1:1 for Cs. Milling typically resulted in low yields of products, identifiable by ¹H NMR, and the collection of the starting material K[A'] during extraction. Due to the simple nature of ¹H NMR spectra obtained for early samples of reactions with CaX₂ and MgBr₂, products were tentatively identified as [MA'₂] complexes. The spectra displayed two sets of patterns expected of π-bound or highly fluxional A' ligands and were partially consistent with values reported for the [MA'₂(thf)₂] (M = Ca, Mg) complexes.^{84, 140, 147, 166-167}

Many of the observed chemical shifts also showed strong agreement with K[A'], which was present after milling and collected during extraction with hexanes. K[A'] is insoluble in hexanes, so it should be completely removed upon filtration. Grinding pure samples of K[A'] followed by extraction with hexanes produced no change, as expected. Analysis by ¹H NMR indicated trace amounts of HA', an unreacted starting material from the K[A'] synthesis, as the only identifiable compound. The milled K[A'] was collected in the frit during filtration and was not present in the isolated "product". The removal of K[A'] suggests that, while the ¹H NMR spectra are highly similar, [AeA'_x] complexes are being isolated in the final prod-

ucts. The similarity of the chemical shifts between $K[A']$ and various products stems, in part, from the similar ionicities of complexes of the s-block metals.

The largest variations between the various complexes were their physical properties, specifically their color, and the intensity of a minor set of A' peaks in the NMR. The majority of the complexes were yellow to dark orange, or in the case of Ca and Cs were initially yellow and become orange over a period of days. While the greater intensity set of peaks showed strong agreement with the reported values, the lesser intensity set showed significant deviation. It was not until we obtained crystal structures of Mg and Be products that we realized our initial assumptions that monometallic species had formed was incorrect.

$K[BeA'_3]$ complex. The orange product isolated from milling $BeCl_2$ in the presence of $K[A']$ was not $[BeA'_2]$ but rather the tris(allyl)berylate $K[BeA'_3]$ (**1**) (Figure 19). Dark orange crystals of **1** were obtained from a non-stoichiometric reaction using only two equivalents of A' ; however reactions conducted with the proper ratio produced identical products (eq 2). In the solid state **1** exhibits approximate C_3 -symmetry with σ -bound A' ligands, with the potassium cation situated between the three double bonds of the allyl ligands, and is isostructural with the previously reported $M[ZnA'_3]$ ($M = Li, Na, K, Cs$) and $K[SnA'_3]$ complexes.⁸⁵⁻⁸⁶ The beryllium center is in a nearly perfectly planar trigonal planar environment (sum of angles C-Be-C angles = 357.7°).

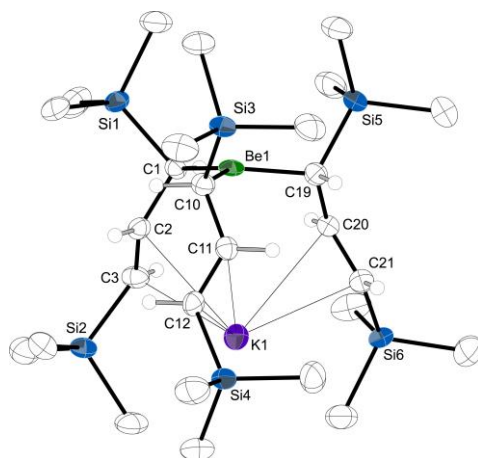
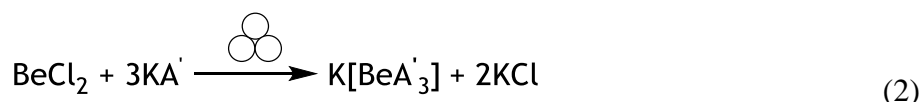


Figure 19. Structure of $K[BeA'_3]$, with thermal ellipsoids drawn at the 50% level. Hydrogen atoms have been removed from the trimethylsilyl groups for clarity. (Appendix B: Section B4)

The average Be–C distance of 1.805(10) Å is not directly comparable to that in other beryllium compounds, as **1** represents the first crystallographically characterized trialkylberyllate. The Be–C length is similar to the Be–C_{carbene} length of 1.816(2) Å in the [Me₂Be·(IPr)] (IPr = 1,3-bis(2,6-di-isopropylphenyl)imidazol-2-ylidene) complex, which also has a 3-coordinate Be center.¹⁶⁸ The charged methyl groups in [Me₂Be(IPr)] are at a noticeably shorter distance (1.742(3) Å), however. A comparison could also be made with the Be–C distance of 1.84 Å in lithium tetramethylberyllate, Li₂[BeMe₄], although the bond distance would be expected to be slightly longer in the latter owing to the higher coordination number on beryllium and the higher negative charge.¹⁶⁹ The C–C and C=C bonds in the alkyl groups are localized at 1.475(5) Å and 1.353(9) Å, respectively. The K⁺⋯C(olefin) contacts average 3.153(7) Å and 2.940(7) Å to the carbon atoms β (C2, C11, C20) and γ (C3, C12, C21) to the beryllium atom, respectively. These distances are comparable to, but slightly shorter than, the range of K⁺⋯C contacts found in the comparable zincate structure (3.205(3) Å and 2.945(3) Å, respectively), which reflects the shorter M–C_(o) bonds in **1**. The distance between Be and K, about 3.59 Å, is long enough to rule out significant metal-metal interactions.

The composition of **1** is obviously completely different from that of [BeA'₂(Et₂O)] (**2**) (Figure 20), even though the same stoichiometric ratio of reagents was used for the Et₂O syntheses (eq 3) and the initial mechanochemical attempts.⁸⁴ Whereas **2** formed colorless crystals, those of **1** were orange, a possible result of the anionic charge on the metal center.

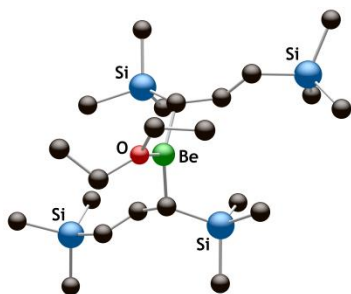
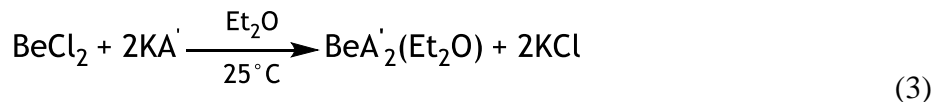


Figure 20: Crystal structure of [BeA'₂(Et₂O)]. Hydrogen atoms have been removed for clarity

The ^1H NMR of **1** shows a distinctly π -bound A' with a triplet representing $\text{H}_{(\beta)}$, a doublet representing the equivalent $\text{H}_{(\alpha)}$ and $\text{H}_{(\gamma)}$, and a singlet for the two equivalent TMS groups (Appendix A: Figure A24). When compared to the σ -bound ligands of the crystal structure, the A' ligands of **1** are highly fluxional. The triplet of **1**, at δ 7.00, is significantly more downfield than the triplet of $[\text{Be}A'_2(\text{Et}_2\text{O})]$ at δ 6.53. No significant difference in chemical shift is present for the doublets and singlets between the two complexes. However, the spectra of **1** does display a second set of lower intensity signals corresponding to another π -bound or highly fluxional A' environment. The second set of resonances show close agreement with those of $\text{K}[A']$, but since $\text{K}[A']$ is not soluble in hexanes, these lower intensity peaks likely correspond to a minor beryllium allyl complex of unknown composition.

Regardless of the reaction ratio of BeCl_2 to $\text{K}[A']$, **1** is the major product. Formation of **1** suggests this structure is highly favored and could be adopted by the other group 2 metals. **1** is highly air and moisture sensitive but stable indefinitely under an inert atmosphere. The intense orange color of the products is visible immediately after ball milling and persists during extraction and isolation of the final products. No color change is observed during this process, giving no indication that an additional product is formed during the work up. Due to their differing solubility, the major and minor products can be separated from each other.

Removal of hexanes from the filtrate precipitates a pale orange solid followed by a darker orange solid, once all hexanes have been removed. The dark orange solid is highly soluble in hexanes, allowing for the isolation of pure **1**. The pale orange minor product is insoluble in hexanes once precipitated, but can be dissolved in toluene.

In attempt to isolate more of either product, an extraction with toluene was attempted on the solid collected in the hexanes extraction. These attempts were largely ineffective. A light orange-brown solid could be isolated from the toluene filtrate, but ^1H NMR spectra displayed a mixture of **1**, the minor product, and likely unreacted $\text{K}[A']$. The corresponding peaks of the minor product showed significant overlap with those of $\text{K}[A']$. As $\text{K}[A']$ is relatively soluble in toluene, this is not unexpected.

The presence of **1** in the toluene filtrate implies the need for a more thorough initial extraction. Due to its composition as a beryllate salt, **1** may be less soluble in hexanes than initially thought, despite the presence of the nonpolar trimethylsilyl groups. By lengthening the extraction process and allowing more time for **1** to enter solution, it may be possible to increase its yield. A second extraction with hexanes will be needed, once the filtrate from the first is dry, to separate and isolate both products. As the initial extraction should remove any unreacted $\text{K}[A']$, toluene can be used when working with the minor product.

K₂[MgA'₄] complex A situation similar to that observed for **1**, was encountered when milling MgBr₂ and with two equivalents of K[A']. Milling yielded an orange oil that crystallized overnight to produce orange microcrystals in low yield. They were found to be highly air- and moisture-sensitive but stable indefinitely under an inert atmosphere. Crystals suitable for x-ray crystal diffraction had to be grown by the slow evaporation of toluene. Owing to complications during handling, and the highly sensitive nature of the product, initial samples containing the most prominent and well-formed crystals were lost on exposure to air. Due to the simplicity of ¹H NMR spectra, prior to the crystallographic characterization of **1**, the product was tentatively identified as a [MgA'_x]_y complex. A dimeric product was believed possible due to the previously reported base-free [MgA'₂]₂ complex, although the ¹H NMR spectra were not a perfect match.^{140, 166}

Crystallographic analysis of the crystals identified them as the polymetallic complex [K(tol)(μ-A')K(tol)][Mg(A')(μ-A')₂] (**3**) (Figure 21); the structure is only of sufficient quality to provide connectivity information. Three bridging π-bound A' ligands link the two potassiums and single magnesium. A single σ-bound A' ligand is present on the magnesium. The coordination sphere of the potassiums is completed by capping toluenes, derived from the crystallization solvent. The highly complex structure of **3** indicates a reaction requiring four equivalents of K[A'] (eq 4) as opposed to the two that were provided.

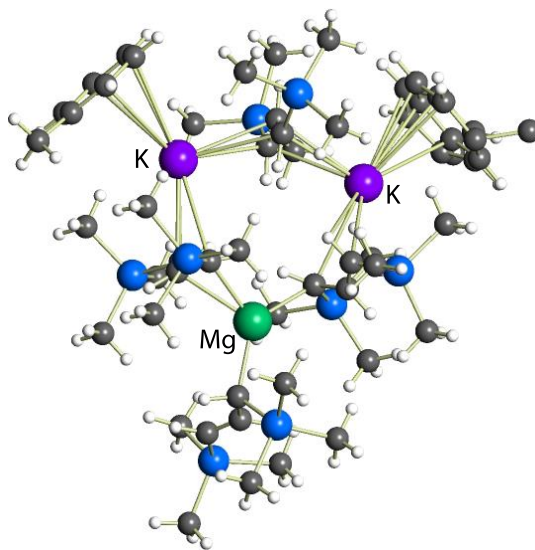
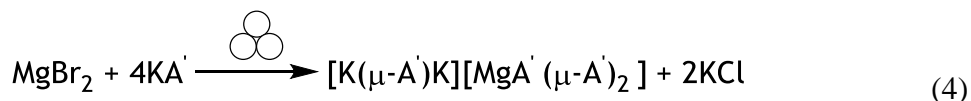


Figure 21. Structure of (A')Mg(μ-A')₂K(tol)(μ-A')K(tol). Only a major conformation is shown; owing to extensive disorder, the structure is of connection-quality only.

It is believed the inclusion of the toluene molecules, while disordered, assisted in the crystal growth by filling the coordination sphere of K. The identical ^1H NMR spectra of **3** and the microcrystals, obtained prior to the addition of toluene, further supports this conclusion. This implies that the microcrystals were likely the toluene free product $[\text{K}(\mu\text{-A}')\text{K}][\text{Mg}(\text{A}')(\mu\text{-A}')_2]$ (**4**).

Given the complexity of **3** and **4**, their (identical) ^1H NMR spectra are deceptively simple (Appendix A: Figures A25 (**3**), A26 (**4**)). The spectra display the expected splitting pattern of π -bound or highly fluxional A' ligands. Interestingly, the spectra of **3** and **4** are closer in agreement to spectra of $[\text{MgA}'_2(\text{thf})_2]$ than the significantly more complex spectra of $[\text{MgA}'_2]_2$.^{140, 166} The reason for this is currently unclear. It may arise from the cation- π interactions in $[\text{MgA}'_2]_2$, which are absent in **3**.

As with **1**, two major sets of different intensity A' ligands are observed. The more intense set are in close agreement with the reported chemical shifts $[\text{MgA}'_2(\text{thf})_2]$, while the less intense are consistent with $\text{K}[\text{A}']$. Again, due to the solubility of $\text{K}[\text{A}']$ it is unlikely that this is from unreacted starting material collected during extraction. The minor product may be the release of $\text{K}[\text{A}']$ from **3** and **4** in solution or may correspond to an alternate $[\text{MgA}'_x]$ complex. A more in-depth investigation of this system would be needed for a definitive identification.

Another possibility exists for the identity of the products obtained in the Mg system. Close inspection of the crystal structure of **3** shows the presence of a $[\text{Mg}(\text{A}')(\mu\text{-A}')_2]^-$ unit which is not unlike the structure of **1**. As such, the initial product or products may include the complex $\text{K}[\text{MgA}'_3]$ (**5**). The presence of toluene may promote the crystallization of **3** or some mixture of **4** and **5**. It remains highly possible that initial crystal samples were **5**, which preliminary calculations suggest as a stable configuration, and not **3** (Figure 22).

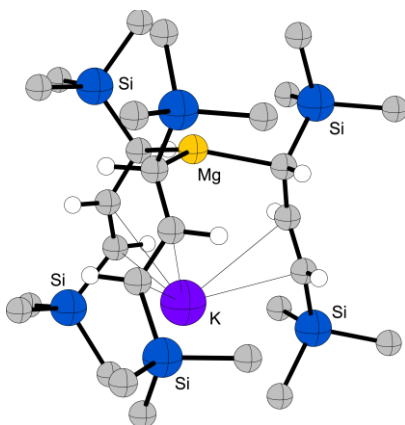
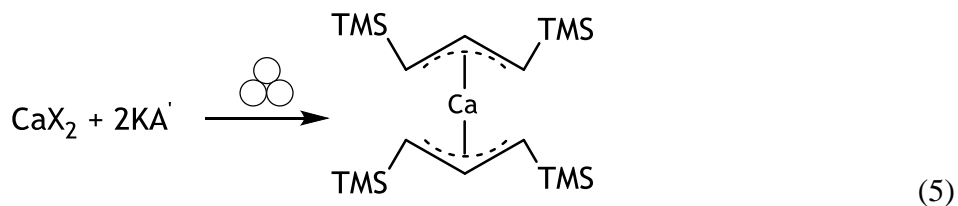


Figure 22. Calculated structure ($\omega\text{B97x-D/def2tzvp}$ (Mg,K); def2svp (C,H,Si)) of $\text{K}[\text{MgA}'_3]$, with hydrogens removed from the trimethylsilyl groups for clarity. The structure was optimized under C_3 symmetry, and is a minimum on the potential energy surface. (Appendix C: Section C3)

Future investigations using three equivalents of $K[A']$ may prove beneficial for understanding this system. A focus should be placed on identification of the initial microcrystals as **4**, **5**, or a still different product. These investigations will likely require optimization of synthetic conditions and the avoidance of toluene to limit the possible formation of **3**. Additionally, the reactivity of **3** remains largely unexplored and could provide a useful comparison to the previous investigations of $[MgA'_2(thf)_2]$ and $[MgA'_2]_2$. The complexity of this system adds support to the thesis that that removal of solvent from reactions involving coordinately under-saturated metal complexes can lead to the formation of unpredictable products.

Synthesis of $[CaA'_x]$ complexes. By far the most interesting system observed thus far concerns the formation of calcium complexes. The high catalytic activity of $[CaA'_2(thf)_2]$ and the observed difference in activity between $[MgA'_2(thf)_2]$ and $[MgA'_2]_2$ suggested a base-free calcium complex would be very highly reactive.^{140, 147, 166} The differences between the beryllium and magnesium allyl structures obtained by mechanochemical methods made it unlikely that the results of analogous reactions with calcium allyls could be predicted with confidence. This turned out to be true.

Synthesis attempts, prior to the determination of the crystal structures of **1** and **3**, consisted of milling a calcium halide with two equivalents of $K[A']$ (eq 5). Extraction and isolation with hexanes yielded yellow microcrystals, an expected color for group 2 complexes but a significant deviation from the orange **1** and **3**. The 1H NMR spectra of the product displayed the expected triplet (δ 6.66), doublet (δ 2.77), singlet (δ 0.24) pattern of a single π -bound or highly fluxional A' (Figure 23). The chemical shifts were consistent with the values reported for $[CaA'_2(thf)_2]$ ¹⁴⁷ and were not with those of **1** and **3**. As such, the yellow product was believed to be the coordinately unsaturated $[CaA'_2]$ (**6**), and will be discussed according to this identification. While the exact structure and composition are unknown, the chemical shifts indicate that **6** is likely not a bimetallic complex as seen with **1** and **3**.



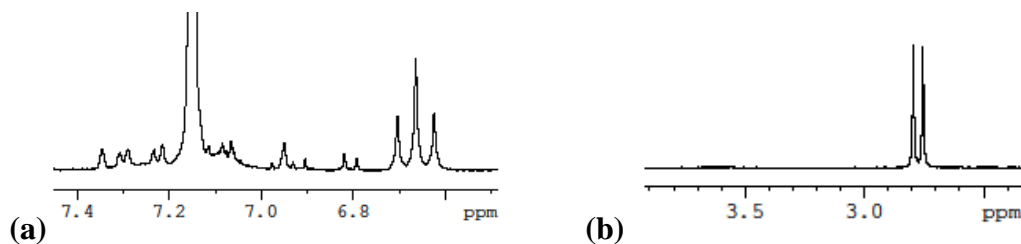


Figure 23: Selected portions of the ^1H NMR spectrum of $[\text{CaA}'_2]$ (**6**) containing the resonances (a) $\text{H}_{(\beta)}$; (b) $\text{H}_{(\alpha)}$ and $\text{H}_{(\gamma)}$. Full ^1H NMR Spectrum can be found in Appendix A: Figure A27.

When solid **6** was stored under an inert atmosphere, a dramatic color change occurred over the course of several days; i.e., orange microcrystals formed from the yellow **6**. Approximately 72 h after isolation, only an orange product was visible and the color remained stable for several months. The same color change occurred when the product was dissolved in hexanes, turning a light yellow solution orange. The orange coloration was similar to that found with **1** and **3**, and the relative cleanliness of the NMR spectra did not suggest that the yellow to orange transformation was the result of decomposition.

Spectra of the orange solid indicated the presence of two A' ligands, the more intense of which were consistent with the hypothetical **6**. The triplet (δ 7.25, $\text{H}_{(\beta)}$), doublet (δ 3.39, $\text{H}_{(\alpha,\gamma)}$) and singlet (δ 0.34, $\text{H}_{(\text{TMS})}$) of the less intense A' were shifted downfield by a considerable margin (Figure 24). The typical chemical shift of the $\text{H}_{(\beta)}$ is centered around δ 6.5 to δ 6.8 for both σ - and π -bound A' ligands.^{37-38, 67, 70, 84-85, 112, 147, 170} As such, the $\text{H}_{(\beta)}$ of the orange solid is approximately 0.6 ppm downfield of its expected range. The ratio between the peaks corresponding to **6** and those more downfield was found to be 2:1.

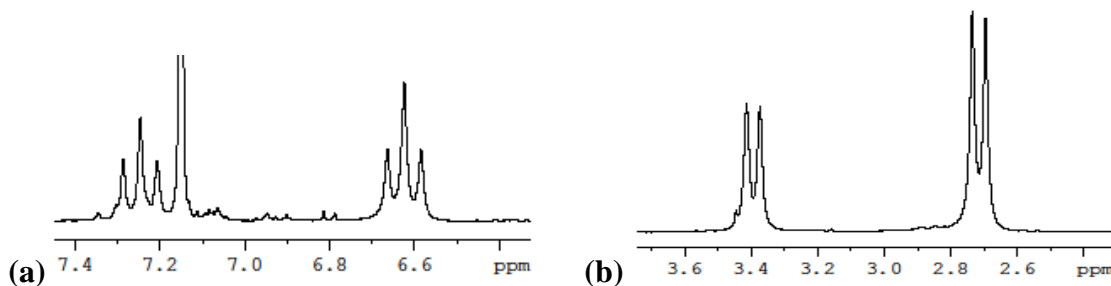


Figure 24: Selected portions of the ^1H NMR spectrum of the orange $\text{K}[\text{CaA}'_3]$ product containing the resonances (a) $\text{H}_{(\beta)}$; (b) $\text{H}_{(\alpha)}$ and $\text{H}_{(\gamma)}$. Full ^1H NMR Spectrum can be found in Appendix A: Figure A28.

There are few A' complexes that display H_(β) chemical shifts downfield near C₆D₆ (δ 7.15). To the best of our knowledge, the only reported examples are for [YA₃]⁶⁶, [ScA'₃]³⁸, and K[ZnA'₃].⁸⁶ All of the reported complexes in solution contained three highly fluxional A' ligands. The H_(β) chemical shifts of [ScA'₃] (δ 7.60), and [YA₃] (δ 7.46) are considerably more downfield than is typically observed. The chemical shifts are a possible result of the combined effect of three π-bound A' ligands (both solution and solid state) on highly electropositive M³⁺ centers.

The H_(β) chemical shift of K[ZnA'₃] (δ 7.05) is just downfield of the expected range.⁸⁶ If the presence of three A' ligands causes a deshielding of protons, as suggested by [YA'₃] and [ScA'₃], downfield chemical shifts might be expected. Since K[ZnA'₃] contains a Zn(II) metal center and σ-bound A' ligands in the solid state, less deshielding could be expected. Additionally, the presence of the anionic [ZnA'₃]⁻ center may introduce a competing shielding effect. The resulting combination of these influences likely gives rise to the chemical shifts on the downfield border of typically observed ranges. As **1** is isostructural with K[ZnA'₃], similar reasoning may account for the H_(β) resonance at δ 7.00. The appearance of the H_(β) chemical shift at δ 7.25 of the orange calcium complex may be the result from a blending of these factors.

To aid in the identification of the orange calcium product, crystals were grown over the course of several months. Those suitable for single crystal x-ray analysis were identified as {K[(μ-A')CaA'₂]}_∞ (**7**). Though the chemical formula of **7** is the same, it is far from isostructural with **1** (Figure 25). {K[(μ-A')CaA'₂]}_∞ forms a coordination polymer in the solid state, with the three A' ligands of **7** π-bound to the metal center, as was observed with the structures of [YA'₃]⁶⁶ and [ScA'₃].³⁸ The potassium counter ion interacts with two of the A' ligands of **7**.

Around the calcium, the allyl ligands are arranged in an irregular fashion, with Ca–C distances ranging from 2.573–2.751 Å, with an average of 2.67 Å. Despite the geometrically irregular shape of the substituted allyl anion, metal–ligand distances in monomeric lanthanide and alkaline-earth allyl complexes have previously been shown to be reasonably predictable based on metal radius and oxidation state.⁶⁵ This is an expected consequence of a high degree of ionic character in the bonding (i.e., $DM-L = r_+ + r_-$). Subtracting the value of the radius of 6-coordinate Ca²⁺ (1.00 Å)¹³⁷ from 2.67 Å leaves 1.67 Å for the 'radius' of the A' anion. This is a value that is slightly long for a neutral complex with a divalent metal center (MA'₂L_x, ca. 1.64 Å), but matches the value obtained from, e.g., the allyl-bridged dimeric complex [Sm(A')₃{μ-K(THF)₂}]₂ (i.e., 2.84 Å - 1.17 Å (for Sm²⁺)).¹⁷¹ Thus, the packing of the A' ligands around the calcium center appears to be typical for such a metal/ligand combination.

The six K–C contacts are highly variable, 2.923–3.327 Å ($\Delta = 0.40$ Å), averaging to 3.12 Å. This is a broader range than that observed in the polymeric $\{K[A^{\wedge}]\}_{\infty}$ (2.87–3.15 Å; $\Delta = 0.28$ Å),¹⁷² which itself is larger than usually observed in complexes containing extended $A^{\wedge}(\mu\text{-K})A^{\wedge}$ arrays (e.g., $\{K[A^{\wedge}](\text{THF})_{3/2}\}_{\infty}$ (2.93–3.12 Å; $\Delta = 0.19$ Å).¹⁶⁷ It is difficult to attach much significance to the variation in **7**, other than to note that it is perhaps not entirely surprising, given that the potassium ions are linking the large and highly asymmetric $[\text{Ca}(A^{\wedge})_3]^{-}$ fragments, rather than A^{\wedge} ligands alone.

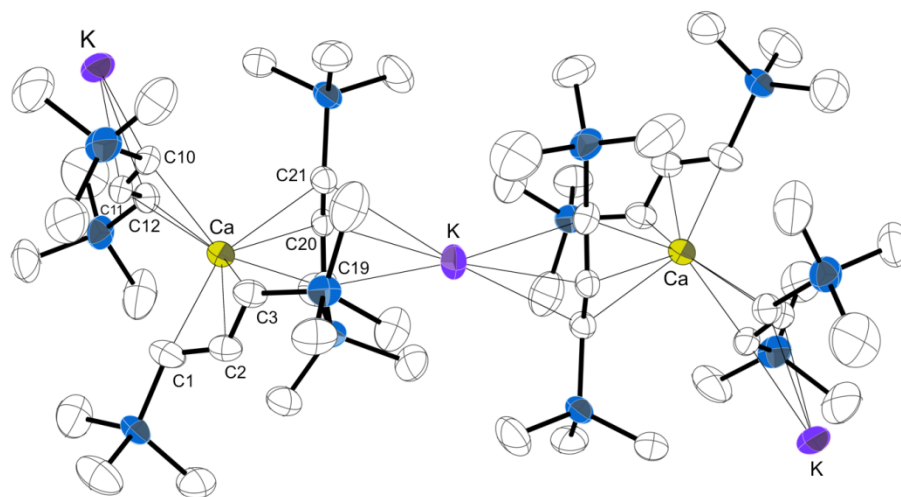


Figure 25. Portion of the structure of $[K[(\mu\text{-}A^{\wedge})\text{Ca}A^{\wedge}_2]]_{\infty}$, with thermal ellipsoids drawn at the 50% level. Hydrogen atoms have been removed for clarity. (Appendix B: Section B5)

Determination of the structure of **7** has allowed for a more accurate analysis of the ^1H NMR spectra and accounts for the number of resonances and their respective intensities. The non-bridging A^{\wedge} ligands would be in an environment similar to the ligands of **6**; likely accounting for the $H_{(\beta)}$ resonance at δ 6.62. The presence of the $\mu\text{-}A^{\wedge}$ ligands accounts for the $H_{(\beta)}$ resonance at δ 7.25 and the observed 2:1 allyl ligand ratio. The $\mu\text{-}A^{\wedge}$ ligands generate a MA^{\wedge}_3 environment around Ca, so corresponding resonances would be expected to appear more downfield of typical ranges. As with the case of **1**, the M^{2+} center and shielding from the $[\text{Ca}A^{\wedge}_3]^{-}$ anion likely are the reasons the resonances are not as far downfield as those of $[\text{Y}A^{\wedge}_3]^{66}$ and $[\text{Sc}A^{\wedge}_3]^{38}$.

Preliminary calculations of the $\text{K}[\text{CaA}'_3]$ composition suggest that a structure isostructural with **1** (i.e., $\text{K}[\text{Ca}(\sigma\text{-A}'_3)]$) would in fact be a minimum on the potential energy surface. An isolated fragment of **7** (i.e., $\text{K}[\text{Ca}(\pi\text{-A}'_3)]$) would be approximately $5.9 \text{ kcal mol}^{-1}$ lower in energy (ΔG°) when compared to a calcium complex isostructural with **1** (Figure 26). The structure of **7** is, likely due to the π -bound A' ligands. Previous investigations show Ca^{2+} complexes largely favor π -bound A' ligands and require considerable steric and electronic constraints to promote σ -bonding.^{86, 140, 166}

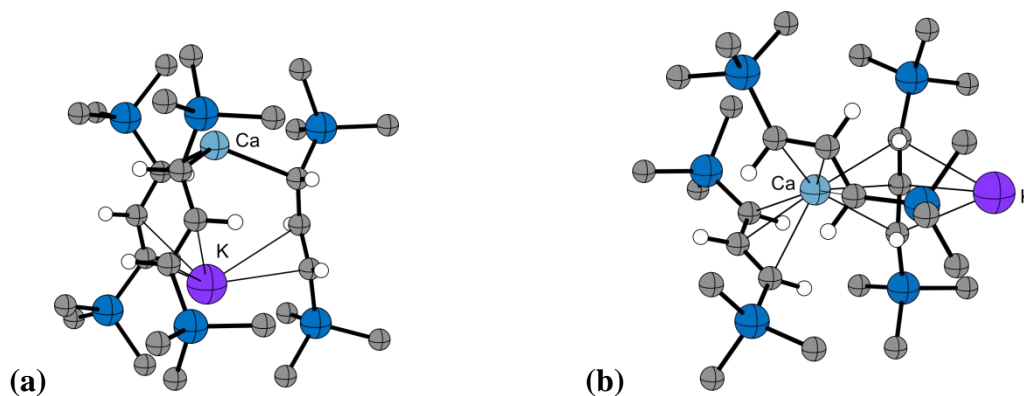
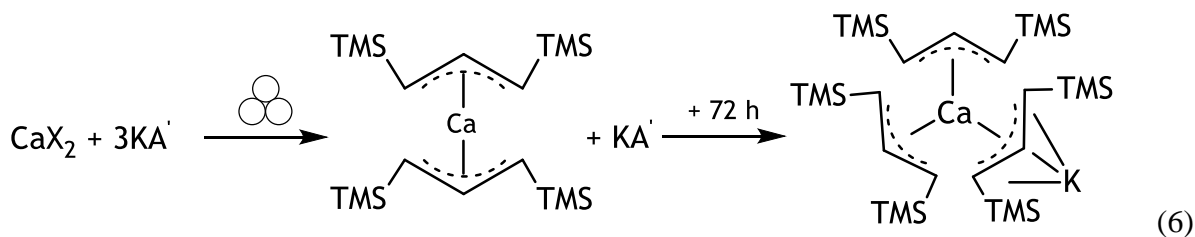


Figure 26: Calculated structures ($\omega\text{B97x-D/def2tzvp}$ (Ca,K); def2svp (C,H,Si)) of $\text{K}[\text{CaA}'_3]$, with hydrogens removed from the trimethylsilyl groups for clarity. Structure **(a)** was optimized under C_3 symmetry; **(b)** structure was modeled after the crystal structure; both are minima on their respective potential energy surfaces. (Appendix C: Section C3)

What cannot be readily explained, however, is the manner in which **7** is formed. It is obvious thus far that the overall process involves the initial isolation of **6**, followed by the slow formation of **7** (eq 6). The isolation of and continued reactivity of **6** demonstrates it is a highly reactive, but marginally stable unsaturated calcium complex. If **6** reacts with any $\text{K}[\text{A}']$ present after isolation then the formation of **7** seems reasonable. This formation could be expected to occur slowly as there would be an overall loss of entropy and a significant rearrangement of ligands would be needed to ease steric interactions.



While the reaction presented by stoichiometry is straightforward, the presence of any significant amount of $K[A']$ after isolation is unlikely. $K[A']$ is insoluble in hexanes, as demonstrated by its isolation from a hexane solution during synthesis.¹¹² This was further confirmed by milling samples of $K[A']$ with a disperser mill. Attempted extraction and filtration, with hexanes, of the samples resulted only the isolation of trace amounts of HA' . These results indicate that the standard extraction procedures effectively remove free $K[A']$ after samples are milled. If any free $K[A']$ is present it would be in extremely trace amounts.

One possible source of $K[A']$ may be from reactivity similar to that of **3**. This polymetallic complex demonstrates that $K[A']$ can be extracted as part of a larger product and a similar situation may be present for the calcium system. The major difference between these systems is that **6** is likely isolated immediately after extraction; however, the presence of less soluble aggregates or complexes may account for the precipitate encountered on work up. The amount of $K[A']$ is likely far from the stoichiometric equivalent needed but may be enough to promote reactivity.

It is also possible that **7** is not the only product produced. As **6** is highly reactive, it may continue to react with any compounds present. The formation of the orange complex may in fact be only one of several generated, taking roughly the same amount of time. This would account for the near uniform color change of yellow to orange. However, more information is needed concerning how **7** is formed.

It seems obvious that this calcium system is more complex than initially predicted. Combined with the results from beryllium and magnesium, these three metals present a wide range of possible reactivity. What can be said is that these complexes are highly reactive, most likely due to their unsaturated nature. As demonstrated by the formation of **7**, **6** continues to slowly react after isolation. Continued investigation of this system will be required to completely understand the intricacies of reactivity. If the more of the final products present with **7** could be identified, a better picture of the sample composition immediately following milling may be possible.

[SrA'_x] complex. The initial investigations of the mechanochemical reactivity of $SrBr_2$ and $K[A']$ showed significantly less reactivity when compared to beryllium, magnesium, and calcium. Although a product could be isolated from reactions using two equivalents of $K[A']$, the low yield only allowed analysis by 1H NMR. In general, isolations yielded near negligible amounts of a residue whose 1H NMR spectrum was consistent with the presence of a metal complex containing π -bound or highly fluxional A' ligands. The spectra are similar to those of $K[A']$, but this simply points to existence of a highly ionic metal-allyl interaction, as $K[A']$ itself is removed during workup prior to NMR analysis. Unlike the previously

discussed systems of the lighter Group 2 metals, no crystals or microcrystals could be grown from the reaction residue.

The presence of a single A' environment in the ^1H NMR spectrum of the product residue provides too little information to make an accurate identification of its composition without additional analysis methods (Appendix A, Figure A29). Increasing the reaction sizes and reactant ratio may offer the best chances for isolation of greater amounts of product. Using three equivalents of $\text{K}[\text{A}']$ seems the most likely starting point for further investigations, however, as has been demonstrated predicting the reaction ratios of these systems can be problematic. The strontium system may follow more in line with calcium by demonstrating some form of self-rearrangement or reactivity after initial isolation. If this is the case, a complex such as $[\text{SrA}'_2]$ may form and react slowly with adjacent complexes to form an orange product. As with **6**, the chemical shifts of the immediately isolated strontium product are upfield of what is has been observed for **1** and **3**.

Attempted formation of a $[\text{BaA}'_x]$ complex Preliminary investigations of ball milling BaX_2 ($\text{X} = \text{Br}, \text{I}$) with two equivalents of various A' sources ($\text{K}[\text{A}']$, $\text{Li}[\text{A}']$, $[\text{AlA}'_3]$) were not successful in the promotion of any reactivity. No visible changes could be observed immediately after milling and only a side product from the $\text{M}[\text{A}']$ ($\text{M} = \text{Li}, \text{K}$) synthesis, $\text{H}[\text{A}']$, could be isolated and identified by ^1H NMR. Only starting material was isolated when $[\text{AlA}'_3]$ was used as a reagent. Attempts using the previously reported reaction ratios for $\text{K}[\text{Ba}_2\text{A}'_5]$ were similarly unsuccessful.¹⁶⁶ Reaction utilizing the ratios observed in the crystal structures of **1** and **3** could prove more successful in future investigations. However as the even the solution reactivity of this system deviates significantly from other group 2 elements, this may not hold true.

The near identical ionic radii of barium and potassium may contribute to this issue and in some way prevent or hinder reactivity. As the possible mechanism, or mechanisms, of ball milling are not known, the impact of similar ionic radii cannot be fully determined. This does continue the general trend observed for the mechanochemical synthesis of group 2 A' complexes; i.e., that the reactivity of such systems under mechanochemical conditions decreases moving down the group.

$[(\text{Cs}/\text{K})\text{A}']$ complex. When CsI is milled in the presence of 3 equiv of $\text{K}[\text{A}']$, followed by an extraction with hexanes, a pale yellow solid is isolated in low yield. After several days, the yellow solid darkened to orange, similar to what was observed for the calcium complex. During this time fragile red-orange crystals, suitable for single crystal x-ray diffraction, formed. The product was identified as the coordination polymer $[(\text{Cs}/\text{K})\text{A}']$ (**9**) (Figure 27).

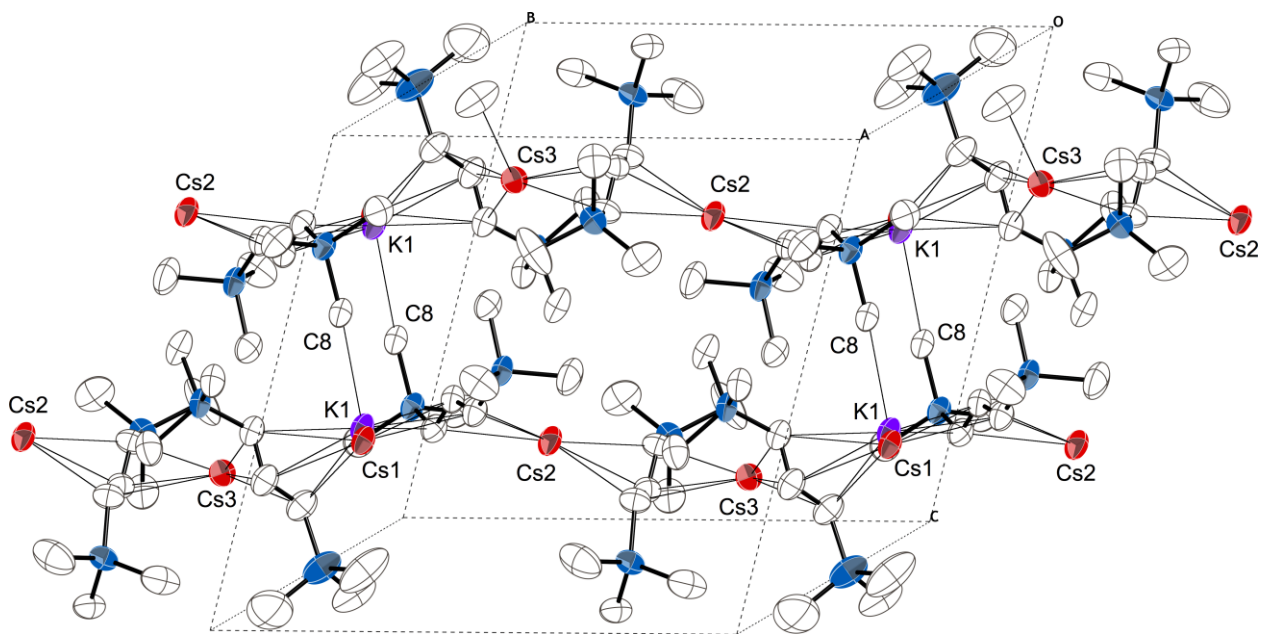
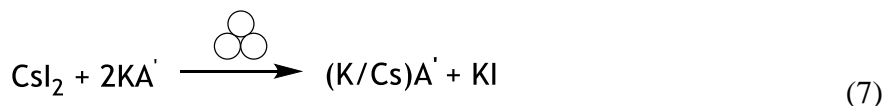


Figure 27. Packing diagram of $\text{Cs}_{0.5}\text{K}_{0.5}[\text{A}']$, with thermal ellipsoids drawn at the 50% level. Hydrogen atoms have been removed for clarity. The asymmetric unit contains three alkali metal cations and three substituted allyl anions, all in general positions. Each of the three metal sites is modeled as a site disorder of atoms types K and Cs. Two distinct peaks were found in the difference Fourier map for the site containing atoms Cs1 and K1, and their positions were refined freely, but their anisotropic displacement parameters were constrained to be equivalent. For the other two site disorders (atom pairs Cs2/K2 and Cs3/K3), the atoms were constrained to be isopositional and their anisotropic displacement parameters were constrained to be equivalent. The ratios of Cs to K in the three sites refined to 0.60:0.40, 0.29:0.71, and 0.61:0.39, respectively, for atom pairs Cs1/K1, Cs2/K2, and Cs3/K3. The structure is polymeric in two dimensions; contacts such as $\text{K1} \cdots \text{C8}$ (3.20 Å) are responsible for generating the 2-D arrangement. (Appendix B: Section B6)

Following the trends of the other s-block complexes, **9** appears to be the result of a non-stoichiometric reaction ratio. It appears as if **9** is formed from CsI reacting with approximately two equivalents of $\text{K}[\text{A}']$ (eq 7), however the exact ratio is more difficult to determine. As seen from the structure, both Cs^+ and K^+ are present in the structure and, for all intents and purposes, are completely interchangeable. Remarkably, very little ligand disorder is present even with the partial substitution of metal ions.



The crystal structure of **9** is similar to what has been reported for $\text{K}[\text{A}']$.¹⁶⁷ Both structures are coordination polymers of interchanging M^+ ions and the A' ligand. However, likely owing to the presence of Cs^+ , **9** demonstrates significantly more interactions between the lay-

ers of the coordination polymer. These interactions, promoting the formation of layers, help to explain the highly fragile crystals and the length of time needed for crystal formation.

Unsurprisingly, only a single set of resonances corresponding to a π -bound or highly fluxional A' ligand is present in ^1H NMR spectra of the complex. The chemical shifts of this complex are identical to those of $\text{K}[\text{A}']$, which is not entirely unexpected given the inclusion of $\text{K}[\text{A}']$ and Cs^+ in the final structure. All the observed shifts are upfield of those for complexes of the other s-block complexes. Unlike the previously described complexes, **9** forms a red solution when dissolved in C_6D_6 , which suggests that the cation- π interactions are maintained in nonpolar media.

Future investigations will likely focus on attempts to increase the reaction yield so that more of **9** can be analyzed. Based on the crystal structure the more likely reaction to be successful will utilize two equivalents of $\text{K}[\text{A}']$, in place of the 3 equiv excess described here. It seems unlikely that a distinct complex such as $[\text{CsA}'_x]$ could be isolated from halide metathesis under mechanochemical conditions, due to the inclusion of K^+ in the final product. It should be noted that the known $[\text{CsA}'(\text{thf})]$ complex was prepared from direct reaction of the elemental cesium with HA' .¹⁶⁷

The investigation of the mechanochemical synthesis of a $[\text{RbA}'_x]$ complex will likely add another valuable data point to this current set. It may follow the behavior demonstrated by **9**. If so, we may be able to begin predicting to some extent, the consequences of solvent removal from these large, highly electropositive metal centers.

Conclusion

Mechanochemical techniques can be used to successfully synthesize highly reactive A' complexes of Be, Mg, Ca, Sr, and Cs, from both stoichiometric and non-stoichiometric ratios of reagents. The results of these reactions are not easily predicted as merely the base-free equivalents of their THF coordinating counterparts. The confirmed products $\text{K}[\text{BeA}'_3]$, $[\text{K}(\mu\text{-A}')\text{K}][\text{Mg}(\text{A}')(\mu\text{-A}')_2]$, $[\text{K}[(\mu\text{-A}')\text{CaA}'_2]]_\infty$, and $[(\text{Cs}/\text{K})\text{A}']$ exemplify how coordinating solvents are not as benign as originally believed. In the absence of coordinating solvents, products are formed that serve to maximize the saturation of the metal coordination spheres. All products appear to be highly reactive, and may open the doorway to more highly active catalysts of MA'_x complexes than previously observed. While efforts towards the synthesis and characterization of strontium and barium systems have been relatively unsuccessful, an examination of a wider range of reagent ratios will likely make these efforts more fruitful.

Chapter 5:

Mechanochemical Investigations of d-Block and p-Block Metal Centers

Introduction

The application and development of organometallic mechanochemical techniques has potential well beyond what has been discussed in previous chapters. There, the focus was on complexes and trends in highly specific areas of the period table. In addition to these areas, considerable efforts have been made into the mechanochemical formation of A' complexes of the transition metals and select p-block metals.

The transition metals offered an expansive list of possible comparison due to past research on transition metal A' complexes.^{67, 70, 73-75, 138, 173-174} Additionally, it was hoped that new techniques would allow for the isolation of second and third row transition metal complexes. While solvent coordination was not an issue for transition metal complexes, the tendency of the second and third rows towards reduction has severely hindered past work. At the time, a mechanochemical approach towards A' complexes seemed a viable synthetic route. This investigation spanned the near entirety of the transition metals and was largely unsuccessful in the isolation of $[MA'_x]$ complexes due to reduction of the metal centers. The immediate result was a tendency to favor reduction of more easily reduced metal centers over the formation of A' complexes. The same was observed in the investigation of the p-block metals. The only definitive success, not including aluminum and group 15, was the synthesis of a previously published $[GaA'_3]$ ⁶⁷ by mechanochemical methods.

Described here are the mechanochemical investigations of the transition metals and selected p-block metals. For the transition metals, it was found that the vast majority underwent reduction when milled in the presence of $K[A']$. The areas where this trend was not followed were for metals in groups 3, 4, and 12. Group 4 provides the most interesting point of comparison as a distinct difference was observed between the reactivity of zirconium and hafnium. The p-block displayed an interesting mix of reactivity with certain metals favoring reduction pathways while others favored the formation of A' complexes. Correlation of the transition metals and selected p-block metals allow for increased understanding of the rules dictating mechanochemical synthesis.

Experimental

General Considerations. All syntheses were conducted under rigorous exclusion of air and moisture using Schlenk line and glovebox techniques. Proton (^1H), carbon (^{13}C), and COSY spectra were obtained on an Advance AV-400 MHz spectrometer. Proton and carbon were referenced to residual resonances of C_6D_6 (δ 7.15 and δ 128). Variable temperature ^1H NMR was obtained on a Bruker DRX-500 and referenced to residual resonances of tol-d_8 . Metal analysis was obtained with ICP-OES on a Perkin Elmer Optima 7000 DV. Combustion analysis was performed by ALS Environmental, Tucson, AZ.

Materials. All anhydrous metal salts were previously purchased from Strem and Sigma-Aldrich, stored under an N_2 atmosphere and used as received. Anhydrous inhibitor-free tetrahydrofuran (THF) was used as obtained from Aldrich. Other commercially available reagents were used without additional purification. Toluene, hexanes, and diethyl ether were distilled under nitrogen from potassium benzophenone ketyl.¹¹¹ Deuterated benzene (C_6D_6) was distilled from Na/K (22/78) alloy prior to use. Deuterated toluene (tol-d_8) was purchased from Cambridge Isotopes and dried over molecular sieves prior to use. The HA' and $\text{K}[\text{A}']$ ($\text{A}' = 1,3\text{-(SiMe}_3)_2\text{C}_3\text{H}_3$) reagents were synthesized as previously described.¹¹² Stainless steel (440 grade) ball bearings (6mm, 3/8 in, and 1/2 in dia) were thoroughly cleaned with hexanes and acetone prior to use. Disperser milling was performed with an Ultra-Turrax Tube Drive and BMT-20-S tubes, both purchased from IKA. Planetary milling was performed with a Retsch model PM100 mill, 50 mL stainless steel grinding jar type C, and safety clamp for air-sensitive grinding. ^1H NMR spectra of HA' , $\text{K}[\text{A}']$, and $[\text{A}']_2$ available in Appendix A. Figures A1, A2, and A3, respectively.

Attempted Mechanochemical Synthesis of Transition Metal $[\text{M}^*\text{A}'_x]$ complexes:

Attempts towards the synthesis of $[\text{M}^*\text{A}'_x]$ complexes of transition metals by ball milling were largely unsuccessful. Save for the cases list below, grinding a transition metal halide in the presence of $[\text{KA}']$ yields black powder and $[\text{A}'_2]$, identified by NMR. It appears that under mechanochemical conditions, an easily reduced metal center will promote the coupling of $[\text{A}']$ to $[\text{A}'_2]$. ($\text{M}^* = \text{Ti, V, Cr, Fe, Co, Ni, Cu, Ag, Nb, Mo, Ru, Pd, Ag, Ta, W, Re, and Pt}$).

Mechanochemical Synthesis of $[\text{YA}'_3]$: A 20 mL dispersing tube (IKA BMT-20) was charged with YCl_3 (0.066 g, 0.376 mmol), KA' (0.224 g, 0.999 mmol), and stainless steel ball bearings (6 mm dia, 20 count) under a nitrogen atmosphere and tightly sealed. The tube was connected to the dispersing unit and milled for 15 min at a high rate, yielding a yellow solid. The mixture was extracted with minimal hexanes (< 50 mL) and filtered through a medium porosity ground glass frit, providing a bright yellow filtrate. Removal of hexanes under vacuum gave a yellow solid that did not crystallize. No yield was recorded; however,

^1H NMR chemical shifts were consistent with those previously reported.¹⁷⁴ It should be noted that that splitting from ^{89}Y can be observed in ^1H NMR spectra. ^1H NMR (400 MHz, C_6D_6 , 298K): δ 0.221 (s, 54H, SiMe_3); δ 3.575 (dd, 6H, $J = 16.2$ Hz, $^2J_{\text{Y-H}} = 3.3$ Hz, $\text{H}_{(\alpha,\gamma)}$); δ 7.456 (td, 3H, $J = 16.2$ Hz, $^2J_{\text{Y-H}} = 1.5$ Hz, $\text{H}_{(\beta)}$). ^{13}C NMR (100 MHz, C_6D_6 , 298 K): δ 1.108 (s, SiMe_3); δ 95.507 (s, $\text{C}_{(\alpha,\gamma)}$); δ 163.130 (s, $\text{C}_{(\beta)}$). The full ^1H NMR spectrum can be found in Appendix A. Figure A31

Group 4 Complexes Containing the A' Ligand

Attempted Synthesis of $[\text{ZrA}'_4]$: ZrCl_4 (0.158 g, 0.678 mmol) was dissolved in minimal THF in a 125mL Schlenk flask, equipped with magnetic stir bar and sealed under an $\text{N}_2(\text{g})$ atmosphere with a septum, to give a near colorless solution. $\text{K}[\text{A}']$ (0.611 g, 2.724 mmol) was dissolved in minimal THF in a 50 mL Schlenk flask, and sealed under an $\text{N}_2(\text{g})$ atmosphere with a septum, to give an orange solution. Both flasks were attached to a Schlenk line and cooled to -78°C in a dry ice-acetone bath. As the $\text{K}[\text{A}']$ solution was cannulated into the 125 mL flask, no color change was observed. The solution was stirred for 24 h and gradually warmed to room temperature, yielding a red-brown solution. Removal of THF under vacuum produced dark brown oil that was extracted with hexanes. The hexane soluble product of the oil was filtered through a medium porosity ground glass frit, providing an orange-brown filtrate. Drying under vacuum yielded orange-brown oil (0.335 g, 59.4%), tentatively identified as $[\text{ZrA}'_4]$ with ^1H NMR. Slow evaporation of solvent did not result in crystal formation. ^1H NMR (400 MHz, C_6D_6 , 298 K): δ 0.281 (s, 72H, SiMe_3); δ 3.565 (d, 8H, $J = 15.5$ Hz, $\text{H}_{(\alpha,\gamma)}$); δ 6.605 (t, 4H, $J = 15.5$ Hz, $\text{H}_{(\beta)}$). ^{13}C NMR (100 MHz, C_6D_6 , 298K): δ 1.027 (s, SiMe_3); δ 95.98 (s, $\text{C}_{(\alpha,\gamma)}$); δ 149.61 (s, $\text{C}_{(\beta)}$). The full ^1H NMR spectrum can be found in Appendix A. Figure A32.

Attempted Mechanochemical Synthesis of $[\text{ZrA}'_4]$: Attempts to synthesize $[\text{ZrA}'_4]$ from ZrCl_4 and $\text{K}[\text{A}']$ by disperser milling resulted in a grey solid consistent with Zr metal and $[\text{A}'_2]$, identified by ^1H NMR. The reaction went to complete decomposition within a few minutes. Synthesis in a planetary mill (PM100) was not attempted, as it introduces significantly more energy than the disperser, which already results in decomposition.

Synthesis of $[\text{HfA}'_4]$ in solution: HfCl_4 (0.247 g, 0.771 mmol) was dissolved in minimal THF in a 125mL Schlenk flask, equipped with magnetic stir bar and sealed under an $\text{N}_2(\text{g})$ atmosphere with a septum, to give a near colorless solution. $\text{K}[\text{A}']$ (0.692 g, 3.085 mmol) was dissolved in minimal THF in a 50mL Schlenk flask, sealed under an $\text{N}_2(\text{g})$ atmosphere with a septum, to give an orange solution. Both flasks were attached to a Schlenk line and cooled to -78°C in a dry ice-acetone bath. As the $\text{K}[\text{A}']$ solution was cannulated into the

125 mL flask, no color change was observed. The solution was stirred for 24 h and gradually warmed to room temperature, yielding a yellow solution. Removal of THF under vacuum produced a yellow oil, which was extracted with hexanes. The hexane soluble product of the oil was filtered through a medium porosity ground glass frit, providing a pale yellow filtrate. Drying under vacuum yielded a viscous yellow oil (0.408 g) believed to be [HfA'₄]. Slow evaporation of solvent did not result in crystal formation. NMR spectra of the oil were found to contain a significant amount of [A'₂] as well as product. The ¹H and ¹³C NMR spectra were not completely consistent with those obtained from products of mechanochemical syntheses. ¹H NMR (400 MHz, C₆D₆, 298 K): δ 0.269 (s, 72H, SiMe₃); δ 3.434 (d, 8H, J = 15.3 Hz, H_(α,γ)); δ 6.547 (t, 4H, J = 15.3 Hz, H_(β)). ¹³C NMR (100 MHz, C₆D₆, 298K): δ 0.949 (s, SiMe₃); δ 98.49 (s, C_(α,γ)); δ 148.28 (s, C_(β)). The full ¹H NMR spectrum can be found in Appendix A, Figure A33.

Synthesis of [HfA'₄] by ball milling: Solid HfCl₄ (0.258 g, 0.805 mmol) and K[A'] (0.730 g, 3.25 mmol) were added to a 50 mL stainless steel grinding jar (type C). The jar was charged with stainless steel ball bearings (6 mm dia, 100 count) and closed tightly with the appropriate safety closer device under an N₂ atmosphere. The reagents were milled for 5 min at 600 rpm, resulting in dark brown solid. The product was extracted with minimal hexanes (< 100 mL) and filtered through a medium porosity ground glass frit, providing a brown filtrate. Drying under vacuum yielded a brown solid (0.164, 22% yield, tentatively identified as [HfA'₄]). Attempts to crystallize the product from the slow evaporation of solvent were unsuccessful. NMR spectra indicate the presence of π-bound or highly fluxional [A'] ligands. Syntheses conducted on smaller scales by disperser milling yielded similar results. ¹H NMR (400 MHz, C₆D₆, 298 K): δ 0.273 (s, 72H, SiMe₃); δ 3.740 (d, 8H, J = 14.96 Hz, H_(α,γ)); δ 6.670 (t, 4H, J = 14.88 Hz, H_(β)). ¹³C NMR (100 MHz, C₆D₆, 298 K): δ 0.859 (s, SiMe₃); δ 114.77 (s, C_(α,γ)); δ 145.81 (s, C_(β)). The full ¹H NMR spectrum can be found in Appendix A, Figure A34.

Group 12 Complexes Containing the A' Ligand

Synthesis of a [ZnA'_x] Complex: A 50 mL round-bottom flask was charged with ZnF₂ (0.163 g, 1.58 mmol), [KA'] (0.707 g, 3.15 mmol), and stainless steel ball bearings (6 mm, 100 count). The contents were milled by attaching the flask to a rotary evaporator. The reactants were milled for 2 h at a low rotational speed, to prevent breaking the flask, resulting in a dark brown-red mixture. The reaction mixture was extracted with minimal hexanes and filtered through a medium porosity ground glass frit. Drying of the filtrate resulted in the isolation of a red-brown solid in low yield. Although the chemical shifts of the ¹H NMR

spectrum match those reported for [KA'], this must be an accidental agreement, as K[A'] is insoluble in hexanes, and would have been completely removed during the extraction. The splitting and chemical shifts are consistent with a π -bound or highly fluxional [A'] ligand. Repeating this reaction with three equivalents of [KA'] in the PM100 may result in the isolation and crystallization to help confirm the identity of the isolated product. ^1H NMR (400 MHz, C_6D_6 , 298K): δ 0.250 (s, 18H, SiMe₃); δ 2.768 (d, 2H, J = 16.0 Hz, H_(α , γ)); δ 6.676 (t, 1H, J = 16.0 Hz, H_(β)). The full ^1H NMR spectrum can be found in Appendix A. Figure A35.

Synthesis of a [CdA'_x] complex: A 20 mL dispersing tube (IKA BMT-20) was charged with CdI₂ (0.152 g, 0.410 mmol), KA' (0.183 g, 0.816 mmol), and stainless steel ball bearings (6 mm dia, 20 count) under a nitrogen atmosphere, tightly sealed, and wrapped in electrical tape to exclude light. The tube was connected to the dispersing unit and milled for 15 min at a high rate. The mixture was extracted with minimal hexanes (< 50 mL) and filtered through a medium porosity ground glass frit, providing a yellow filtrate. Removal of hexanes under vacuum gave a light-sensitive yellow solid that decomposed overnight. The solid is tentatively identified as a [CdA'_x] complex with a ^1H NMR spectrum consistent with a π -bound or highly fluxional [A']. ^1H NMR (400 MHz, C_6D_6 , 298K): δ 0.208 (s, 18H, SiMe₃); δ 3.411 (very broad s, 2H, H_(α , γ)); δ 6.763 (broad t, 1H, J = 15.1 Hz, H_(β)). The full ^1H NMR spectrum can be found in Appendix A, Figure A36.

Synthesis of a [Hg₂A'_x] complex: A 20 mL dispersing tube (IKA BMT-20) was charged with Hg₂Cl₂ (0.156 g, 0.331 mmol), KA' (0.209 g, 0.932 mmol), and stainless steel ball bearings (6 mm dia, 20 count) under a nitrogen atmosphere and tightly sealed. The tube was connected to the dispersing unit and milled for 15 min at a high rate, yielding a yellow oil. The mixture was extracted with minimal hexanes (< 50 mL) and filtered through a medium porosity ground glass frit, providing a pale yellow filtrate. Removal of hexanes under vacuum gave a low viscosity colorless to pale yellow oil, tentatively identified as [Hg₂A'₂] by ^1H NMR. Cooling the oil at -30.0 °C overnight resulted in a dramatic increase in viscosity but no solid formation, suggested that the temperature may have been above the compound's freezing point. NMR spectra suggest the presence of two highly similar σ -bound [A'] ligands of equal intensity. Interpretation of COSY NMR spectra allowed for a correlation between the protons of the ligands, where possible, labeled as A and B. ^1H NMR (400 MHz, C_6D_6 , 298K): δ 0.086 (s, 9H, SiMe₃); δ 0.096 (s, 9H, SiMe₃); δ 0.147 (s, 9H, SiMe₃); δ 0.152 (s, 9H, SiMe₃); δ 1.920 (d, 1H, J = 10.6 Hz, H_(α -A)); δ 1.967 (d, 1H, J = 10.6 Hz, H_(α -B)); δ 5.4624 (d, 1H, J = 18.0 Hz, H_(γ -A)); δ 5.479 (d, 1H, J = 18.0 Hz, H_(γ -B)); δ 6.4968 (dd, 2H, J₁ = 18.0 Hz, J₂ = 10.9, H_(β -A/B)). ^{13}C NMR (100 MHz, C_6D_6 , 298K): δ -0.465 (s, SiMe₃); δ 0.330 (s, SiMe₃); δ 57.95 (s, C_(α)); δ 58.60 (s, C_(α)); δ 125.19 (s, C_(γ)); δ 125.33 (s, C_(γ)); δ 147.69 (s, C_(β)). The full ^1H NMR spectrum can be found in Appendix A. Figure A37.

Synthesis of a [HgA'_x] complex: A 20 mL dispersing tube (IKA BMT-20) was charged with HgCl₂ (0.102 g, 0.376 mmol), KA' (0.167 g, 0.744 mmol), and stainless steel ball bearings (6 mm dia, 20 count) under a nitrogen atmosphere and tightly sealed. The tube was connected to the dispersing unit and milled for 15 min at a high rate yielding yellow oil. The mixture was extracted with minimal hexanes (< 50 mL) and filtered through a medium porosity ground glass frit, providing a pale yellow filtrate. Removal of hexanes under vacuum gave a low viscosity colorless to pale yellow oil, tentatively identified as [HgA'₂] by ¹H NMR. NMR spectra suggest the presence of two similarly σ-bound [A'] ligands of equal intensity, labeled as [A'_A] and [A'_B]. ¹H NMR (400 MHz, C₆D₆, 298K): δ 0.074 (s, 9H, SiMe₃); δ 0.081 (s, 9H, SiMe₃); δ 0.131 (s, 9H, SiMe₃); δ 0.137 (s, 9H, SiMe₃); δ 1.908 (d, 1H, J = 10.6 Hz, H_(α-B)); δ 1.953 (d, 1H, J = 10.6 Hz, H_(α-A)); δ 5.434 (d, 1H, J = 18.0 Hz, H_(γ-B)); δ 5.452 (d, 1H, J = 18.0 Hz, H_(γ-A)); δ 6.470 (dd, 1H, J₁ = 18.1 Hz, J₂ = 10.7, H_(β-B)); δ 6.473 (dd, 1H, J₁ = 18.0 Hz, J₂ = 10.6, H_(β-A)). ¹³C NMR (100 MHz, C₆D₆, 298K): δ -0.428 (s, SiMe₃); δ 0.355 (s, SiMe₃); δ 57.95 (s, C_(α)); δ 58.29 (s, C_(ω)); δ 125.18 (s, C_(γ)); δ 125.32 (s, C_(γ)); δ 147.65 (s, C_(β)); δ 147.68 (s, C_(β)). The full ¹H NMR spectrum can be found in Appendix A. Figure A38.

P-Block (In, Ga) Complexes Containing the A' Ligand

Attempted Mechanochemical Synthesis of p-Block [MA'_x] complexes: Attempts to prepare [M*A'_x] complexes of the heavy p-block metals by ball milling were largely unsuccessful. Milling metal halides of Ge, Pb, Tl, and Te yielded [A'₂]. Similar results were observed from Sn(IV) metal halides; however ¹H NMR spectra suggesting possible reactivity were collected from reactions that employed Sn(II) metal halides. Products collected from reactions utilizing Sn(II) halides suggest the presence of multiple σ-bound [A'] ligands and are highly similar to those obtained from reactions with [AlA'₃]. Reactions performed with Ga(III) and In(III) are discussed below, and Group 15 complexes are discussed in Chapter 3.

Mechanochemical Synthesis of [GaA'₃]: A 20 mL dispersing tube (IKA BMT-20) was charged with GaI₃ (0.159 g, 0.353 mmol), KA' (0.238 g, 0.1.06 mmol), and stainless steel ball bearings (6 mm dia, 20 count) under a nitrogen atmosphere and tightly sealed. The tube was connected to the dispersing unit and milled for 15 min at a high rate, yielding a yellow solid. The mixture was extracted with minimal hexanes (< 50 mL) and filtered through a medium porosity ground glass frit, providing a yellow filtrate. Removal of hexanes under vacuum gave a yellow to white solid that did not crystallize. The solid was identified as [GaA'₃] and ¹H NMR chemical shifts were consistent with those previously reported.⁶⁷ ¹H NMR (400 MHz, C₆D₆, 298K): δ 0.176 (s, 54H, SiMe₃); δ 3.938 (d, 6H, J = 14.8 Hz, H_(α,γ)); δ 6.383 (t, 3H, J = 14.8 Hz, H_(β)). The full ¹H NMR spectrum can be found in Appendix A. Figure A39.

Synthesis of an [InA'_x] complex: A 20 mL dispersing tube (IKA BMT-20) was charged with InI₃ (0.107 g, 0.216 mmol), KA' (0.150 g, 0.667 mmol), and stainless steel ball bearings (6 mm dia, 15 count) under a nitrogen atmosphere and tightly sealed. The tube was connected to the dispersing unit and milled for 15 min at a high rate yielding yellow solid. The mixture was extracted with minimal hexanes (< 50 mL) and filtered through a medium porosity ground glass frit, providing a yellow filtrate. Removal of hexanes under vacuum gave yellow oil that solidified overnight. No yield was recorded NMR spectra suggest the presence of three σ -bound [A'] ligands. Accurate identification, correlation, and coupling constants could not be obtained due to heavy overlap of all observed signals. Variable temperature ¹H NMR may allow for a better separation of the observed signals. ¹H NMR (400 MHz, C₆D₆, 298K): δ 0.192 - δ 0.237 (broad singlets, 54H, SiMe₃); δ 2.499 (m, 3H, H_(α)); δ 5.770 (m, 3H, H_(γ)), δ 6.446 (m, 3H, H_(β)). The full ¹H NMR spectrum can be found in Appendix A. Figure A40.

Results and Discussion

The majority of transition metal halides underwent reduction when milled with K[A'] to yield metallic powders and [A'₂]. Reduction of the metal and coupling of the A' ligand could be accomplished by both flask and tube disperser milling. Because of this, [MA'₂] (M = Fe, Co, Ni, Mn, Cr)^{70, 73-75} complexes synthesized in THF could not be made mechanochemically.¹³⁸ While the difference in reactivity was disappointing, ultimately this investigation helped to define the limitations of milling as a synthetic methodology, and in the process helped to confirm a previous hypothesis concerning the [NiA'₂] complex.¹³⁸

During attempts to synthesize [NiA'₂], the product could be obtained from the THF soluble NiBr₂(dme), but not the THF-insoluble NiCl₂.¹³⁸ It was originally believed that solid NiCl₂ acted as a platform for the formation of [A'₂], and that by switching to a more soluble salt this issue could be avoided. NiCl₂ milled in the presence of K[A'] yielded nickel metal and [A'₂], as previously observed in solution with NiCl₂. The same reactivity was witnessed upon milling with NiBr₂(dme), confirming the role of solvent for this system; i.e., that solvated Ni²⁺ ions are required to avoid decomposition reactions. Since milling reactions are done in the solid state, both NiCl₂ and NiBr₂(dme) are able to promote A' coupling. In this case the presences, or lack thereof, of solvent effects dictate the final products.

Mechanochemical Synthesis of [YA'3]. Parallel reactivity between solution based and milling techniques was witnessed with the synthesis of [YA'3] (**1**). **1** can be made by mixing solutions of YCl₃ and K[A'] in THF or by milling the solid reagents in a tube disperser.⁶⁶ The ¹H NMR spectrum of the mechanochemical product is nearly identical to the previously reported spectra of **1**, synthesized in THF.¹⁷⁴ The spectra of **1** produced mechanochemically have additional splitting of the doublet and triplet, not observed in the original spectra (figure 28). The coupling constants of these additional peaks correspond to the secondary coupling between the allyl protons and ⁸⁹Y (spin ½, 100% abundance) (Appendix A. Figure A31). The discrepancy between the spectra likely results from different NMR strengths between the mechanochemical sample (400 MHz) and the reported sample (300 MHz).¹⁷⁴ Like [ScA'3], **1** falls into the category of complexes which can be made by both solution and milling techniques. The lack of readily accessible reduction states and absence of coordination sites around the metal that could accommodate a coordinating solvent are likely the reasons that the solution and solid-state syntheses yield the same product.

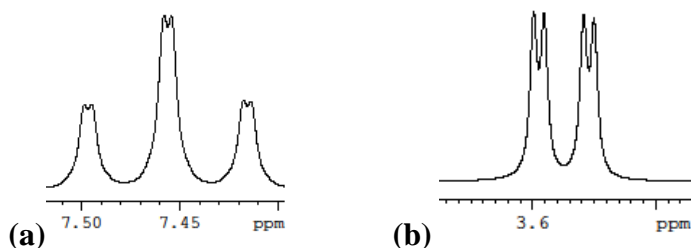
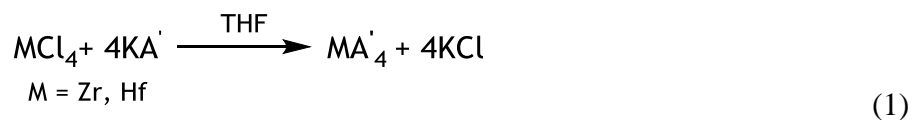


Figure 28: Selected portions of the ¹H NMR spectrum of [YA'3] containing resonances of (a) H_(β) split by ⁸⁹Y; (b) H_(α/γ) split by ⁸⁹Y.

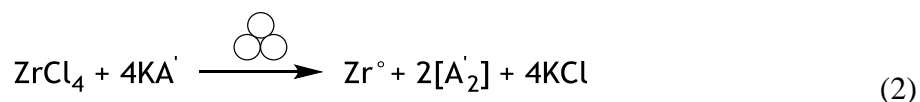
Mechanochemistry of Group 4 Complexes. The heavy Group 4 elements, zirconium and hafnium, are among the most interesting systems investigated within the transition metals. The synthesis of either [ZrA'4] (**2**) or [HfA'4] (**3**) have not been reported, so both solution-based and mechanochemical synthetic techniques could be investigated simultaneously. The initial assumption was that both zirconium and hafnium should react similarly through either method in the presence of K[A'] to yield **2** and **3**. Generally speaking, complexes of Zr(IV) and Hf(IV) display closely similar reactivity, should not be easily reduced, and are unlikely to incorporate coordinating solvents. We expected **2** and **3** to provide additional examples of identical reactivity in solution and solid state, in a manner similar to that of **1** and [ScA'3].

Both **2** and **3** can be readily formed in THF at low temperature in approximately 60% crude yield (eq 1). Though crystals of sufficient quality for x-ray crystal analysis could not be obtained for definitive identification, these represent the most likely products. The ¹H NMR

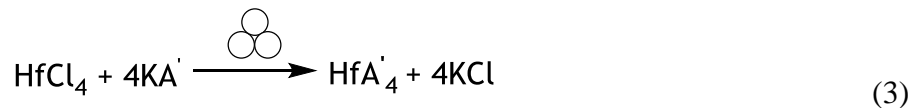
spectra display splitting and chemical shifts consistent with a single π -bound, or highly fluxional, A' ligand environment, and confirm the absence of any coordinating THF and starting materials. The spectra indicate highly symmetric molecules and are consistent with previous investigations.¹⁷⁵



In contrast to the solution reactions, the mechanochemical attempts to synthesize **2** and **3** provided highly unexpected results. When ZrCl_4 was milled with 4 equivalents of $\text{K}[\text{A}']$ in a tube disperser mill, a black solid rapidly formed. Work up provided a black powder from which only $[\text{A}'_2]$ could be extracted and identified by ^1H NMR (eq 2). Since $[\text{A}'_2]$ was the only identifiable product, it is likely the black solid was zirconium metal. This alone was surprising as we were not expected to be able to reduce $\text{Zr}(\text{IV})$; however, this reduction was consistent with the other transition metals.



Milling of HfCl_4 with four equivalents of $\text{K}[\text{A}']$, however, yielded a dark brown solid (eq 3). The brown solid was consistently formed by milling in both the tube disperser and planetary ball mill. Work up of the brown solid yielded a brown non-crystalline solid. Efforts to crystallize the brown solid from the slow evaporation of solvent (hexanes, toluene) over the course of several weeks were unsuccessful. The ^1H NMR spectra suggested that **3** was the isolated product from this reaction. Slight discrepancies in the NMR spectra were noted between the product produced from solution methods and that generated mechanochemically (resonances in the latter were consistently 0.1–0.3 ppm more downfield). Coupling constants, splitting patterns, and integral ratios were consistent between both methods, however, and the products were judged the same. As such, the mechanochemical product was identified as **3**.



These results mark a very distinct difference between zirconium and hafnium, and offers insight into the impact removing solvent has on a reaction. The exact reasons for the difference in the outcomes between the two metals is not readily apparent. The fact that **2** can be formed in THF but not by milling suggests very different metal-A' interactions when solvent is removed. THF may in some way be regulating the possibility of reduction, thus promoting the formation of **2** over that of [A'₂]. As was observed with the nickel system, Ni(II) can act as a solid-state platform to promote the coupling of A' ligands. While it is possible this occurs with Zr(IV), one would expect it to apply to Hf(IV) as well. It seems apparent that the A' anion in THF is not a strong enough reducing agent to promote the reduction of Zr(IV) as it does when milling. It is clear that this was not a thermal process due to the rapid reactivity observed in the low energy tube disperser. These relatively low energy collisions, compared to a planetary ball mill, were enough to promote reactivity within the early minutes of the reaction.

These results further demonstrate a unique difference in reactivity between solution-based and mechanochemical methods. Here we saw the reduction of a metal center that could not be predicted from solution-based analogies. It seems mechanochemical reactions may amplify a tendency towards reduction that is otherwise mitigated by solvent. The direct cause of this is unknown but it does seem that standard solution reduction potentials are not immediately applicable to mechanochemical synthesis.

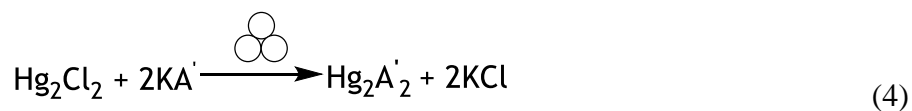
Group 12 Complexes Containing the A' Ligand

The group 12 metals displayed very similar mechanochemical reactivity to that observed with Y(III) and Sc(III). Milling the metal halides (ZnF₂, HgCl₂, Hg₂Cl₂, CdI₂) with two equivalents of K[A'] yielded isolable products with no indication of reduction or coupling of ligands to [A'₂]. The yields for all reactions were low and the isolated products from each metal center were considerably different from each other. The low yields are likely due the inherently low yields associated with round bottom flask and tube disperser milling.

The exact identity of the Zn(II) product is currently unknown and will require a crystal structure for an accurate identification. Past work with zinc A' complexes yielded the previously published zincate K[ZnA'₃], whose ¹H NMR chemical shifts were more downfield than those of K[A'].¹⁷⁶ The product from the mill reaction gave spectra more consistent with K[A'], though the physical characteristics and solubility were more consistent with K[ZnA'₃].¹⁷⁶ Examination of this [ZnA'_x] system with different reaction ratios and higher energy milling methods, either with a planetary or mixer mill, may allow for a more accurate analysis of the products.

An apparent $[\text{CdA}'_x]$ complex was formed when milling CdI_2 in the presence of $\text{K}[A']$. Analysis of the isolated product was greatly hindered by its light sensitivity and likely low thermal stability. The product, a yellow solid, decomposed completely to a black solid and $[A'_2]$ within approximately 12 h of isolation. The ^1H NMR spectra that could be obtained displayed considerable broadening, most likely due to decomposition prior or during the NMR experiment. The spectra do however suggest the presence of a $[\text{CdA}'_x]$ complex containing π -bound, or highly fluxional, A' ligands. This was based prominently on the presence of a triplet at δ 6.77, within the expected $\text{H}_{(\beta)}$ range, with roughly half the intensity of the signal at δ 3.41. The signal at δ 3.41 is an extremely broad and displays no splitting, but is within the range expected for $\text{H}_{(\alpha)}$ and $\text{H}_{(\gamma)}$ (δ 2.0- δ 3.5). The low stability prevents further analysis and a more accurate determination. From this, however, it does appear that $\text{Cd}(\text{II})$ is able to react mechanochemically to produce a $[\text{CdA}'_x]$ complex and not follow the decomposition pathway largely favored by the transition metals.

Milling of either Hg_2Cl_2 or HgCl_2 in the presence of two equivalents of $\text{K}[A']$ allows for the isolation of a mobile pale yellow oil in low yield (eq 4 and 5). The products, with respect to their starting materials, were tentatively identified as $[\text{Hg}_2\text{A}'_2]$ (**4**) and $[\text{HgA}'_2]$ (**5**). Storing **4** and **5** at -30°C for 12-24 h greatly increased viscosity but produced no solid. Warming back to room temperature returned the oils to their previous low viscosity states. The ^1H NMR, for both **4** and **5**, indicated samples of high purity containing two A' ligands in nearly identical environments. These A' ligands are distinctly σ -bound, of equal intensity, and provide no indication of fluxional behavior.



Spectra of **4** and **5** are virtually identical, with only slight differences between chemical shifts ($\sim\delta$ 0.02). The spectra of **5** does display two distinct and heavily overlapping doublets of doublets for the $\text{H}_{(\beta)}$ that not visible in spectra of **4**. It should be noted that the peaks in **4** are noticeably broader than those of **5**, possibly accounting for a loss of splitting or is the result of subtle differences between the Hg_2^{2+} ion and $\text{Hg}(\text{II})$.

The behavior of the Hg_2^{2+} ion and $\text{Hg}(\text{II})$ is remarkably different than what has been observed for the other complexes of transition metals when milled. The clearly σ -bound A'

ligands are more in line with those of Group 15³⁷, discussed in chapter 3, and other heavy p-block metals, than anything observed in the d-block. As these samples are oils, temperatures below -30°C will be required to promote the formation of any crystals. Elemental analysis will likely be the most diagnostic for distinguishing between **4** and **5**, due to the dramatic change in percent composition accompanying the addition or removal of a single Hg atom. However, higher yields are needed for proper analysis. It is currently unknown whether this system will be compatible with a planetary ball mill, due to possible interactions of **4** and **5** with the stainless steel milling jars. If no interactions occur then higher yields should be possible.

Group 12 Complexes Containing the A' Ligand of the p-Block Elements

Mechanochemical investigations of the p-block metals, not including aluminum and Group 15, were largely reminiscent of the transition metals. Attempts to mill halide salts of germanium, thallium, lead, and tellurium, in the presence of K[A'], lead to rapid reduction and the isolation of [A'₂]. As with many of the transition metals, the tendency towards reduction of the metal center and coupling of A' ligands appears highly favorable. It is not known how much of this is intrinsic to the metal centers and how much can be ascribed to mechanochemical processing, as there have been no attempts to prepare many of these metal-A' complexes with solution-based techniques. Synthetic attempts with tin offered a highly complex mixture containing numerous σ -bound A' ligands and decomposition products. Syntheses using [AlA'₃] in place of K[A'] may prove beneficial for the synthesis of [GeA'_x] and [PbA'_x] complexes similar to those isolated for tellurium and tin, as discussed in chapter 2.

The synthesis of [GaA'₃] (**6**), by milling GaI₃ and stoichiometric amounts of K[A'], offers another example of a product unaffected by the inclusion or removal of solvent from the synthesis. The ¹H NMR spectra of **6** are identical to those previously reported from solution-based techniques.⁶⁷ As observed with [YA'₃], [ScA'₃], and [HoA'₃], **6** remains base-free even when synthesized from solutions of THF.^{38, 174, 176} These three complexes represent the only examples we currently have of identical reactivity between solution-based and mechanochemical techniques.

The results of ball mill reactions of InI₃ and K[A'] produced a yellow oil that solidified overnight to a non-crystalline yellow solid. The ¹H NMR spectra of this product suggested the possible presence of an [InA'_x] complex, but were largely inconclusive due to excessive peak broadening. The location and integration of the broad multiplets at δ 2.50, δ 5.77, and δ 6.45 are all within the ranges expected for the H_(α), H_(γ), and H_(β), respectively, of a σ -bound A'.³⁷

The number of peaks per multiplet suggests several A' ligands are present, though the exact number cannot be determined.

This suggests the A' ligands of the $[\text{InA}'_x]$ complex are σ -bound in solution, a notable deviation from the previous group 13 complexes $[\text{AlA}'_3]$ and **6**. Both $[\text{AlA}'_3]$ and **6** are σ -bound in the solid state but highly fluxional in solution, even down to -70°C .^{38, 176} It seems reasonable to expect that the $[\text{InA}'_x]$ complex will retain its σ -bound ligands in the solid state. As such, indium may mark the point at which the transition between highly fluxional “ π -bound” to σ -bound A' ligands occurs in solution.

If viewed as a transition point between these two behaviors, the extremely broad splitting observed appears reasonable. It is possible that while the A' ligands are σ -bound in solution, they are not locked into position, such as those observed for the $[\text{EA}'_3]$ (E = As, Sb, Bi) complexes.³⁷ (Chapter 3) Although their resting state is not π -bound, the A' ligands of $[\text{InA}'_x]$ do not rearranged their conformations as rapidly as with the lighter metals, resulting in an overall broadening of signals. Analysis by low temperature NMR may allow the ligand motion to be frozen out, and the presence of σ -bound fluxional behavior could be confirmed and quantified.

Conclusion

Mechanochemical investigations into the transition and selected p-block metals present an interesting mix of reactivity. The vast majority of the transition metals, along with thallium, lead, germanium, and tellurium are incompatible with the milling techniques, at least in the presence of $\text{K}[\text{A}']$. Reactivity was still observed for these metal centers; however, $[\text{MA}'_x]$ complexes were not the result. Milling resulted in the oxidative formation of $[\text{A}'_2]$ with reduction of the metal center. Access to $[\text{MA}'_x]$ complexes of these metals will likely require a less reducing source of A', such as $[\text{AlA}'_3]$. Only when reduction of metal salts to the elements is chemically difficult (e.g., with Group 3 and 12 metals and hafnium), it appears that milling of $\text{K}[\text{A}']$ in the presence of metals with easily accessible oxidation states will favor the redox pathway.

Reactions of the metal centers where the decomposition did not occur were themselves widely varied. Allyl complexes of gallium and yttrium could be synthesized by ball milling and were identical to previously reported complexes, and add to the class of compounds where removal of solvent leaves identical reactivity. A noticeable difference in reactivity between Zr(IV) and Hf(IV) was observed in milling reactions but not those conducted in THF, suggesting a difference of reduction potentials or reaction mechanisms are operative in the solid state.

Mechanochemical reactions allowed for the isolation of likely $[MA']_x$ complexes of zinc, cadmium, mercury, and indium. The presence of coordinated A' ligands could be confirmed but owing to reaction and stability difficulties, accurate identifications could not be made. More in-depth investigation of these systems is needed for the identification and analysis of their characteristics and reactivity. As these metals have only been briefly studied through solution-based efforts, few direct comparisons are available. Investigations using both solid-state and solution routes would provide valuable information concerning the effects of mechanochemistry and the removal of solvent from the synthesis of late d-block and early p-block metal complexes.

Chapter 6

Balancing Adduct Formation and Ligand Coupling with the Bulky Allyl Complexes

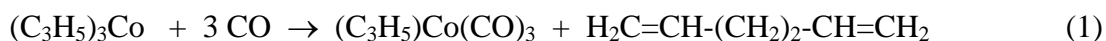


Introduction

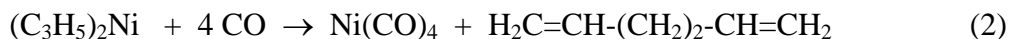
The field of π -allyl transition metal chemistry was inaugurated with the synthesis of $[(\text{C}_3\text{H}_5)\text{PdCl}]_2$ by Smidt and Hafner in 1959,¹⁷⁷ and two years later Wilke had prepared a first-row allyl complex, $(\text{C}_3\text{H}_5)_2\text{Ni}$.¹⁷⁸ Since that time, π -allyl metal complexes have become broadly useful as reagents in organic chemistry and catalysis,^{179-193,139, 194-198} and numerous examples have been synthesized for these purposes.

Despite this, many poly(allyl) complexes of the first row transition metals are not easily handled; for example, the pyrophoric $(\text{C}_3\text{H}_5)_2\text{Ni}$ decomposes at 20 °C,¹⁹⁹ and $(\text{C}_3\text{H}_5)_3\text{Fe}$ and $(\text{C}_3\text{H}_5)_3\text{Co}$ are even less stable (dec. at -40 °C).¹⁹⁹ The instability is often driven by the operation of low-energy decomposition pathways involving the coupling of the allyl ligands. Furthermore, the presence of additional donor ligands that could help saturate the metal coordination sphere and inhibit ligand loss may not lead to stable $(\text{C}_3\text{H}_5)_n\text{ML}_m$ species. Although $(\text{C}_3\text{H}_5)_2\text{NiPMe}_3$ is stable enough to be crystallographically characterized, for example,⁷¹ the corresponding PPh_3 adduct begins to dissociate in solution at -60 °C; at 0 °C, coupling of the allyl ligands occurs to give a hexadiene complex.⁷¹ Similarly, the 18-electron species $(\text{C}_3\text{H}_5)_2\text{Fe}(\text{CO})_2$ evolves 1,5-hexadiene on standing at room temperature, and requires storage at low temperature (-76 °C) under an inert atmosphere.²⁰⁰⁻²⁰¹

Allyl coupling reactions are often induced during reactions of poly(allyl) complexes. Treatment of $(\text{C}_3\text{H}_5)_3\text{Co}$ with CO leads to the production of $(\pi\text{-allyl})\text{cobalt tricarbonyl}$, for example, which is stable against further loss of the allyl ligand (eq 1).^{199, 202}

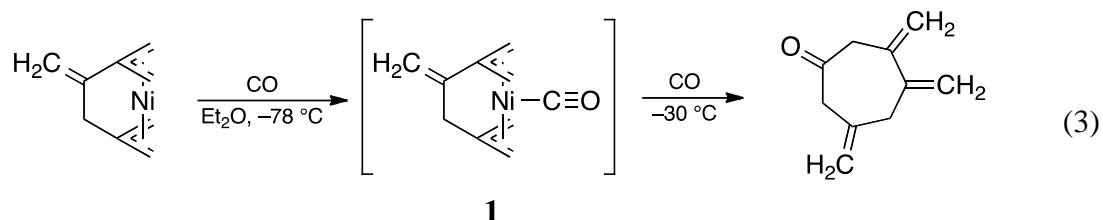


In contrast, Wilke found that the direct reaction of $(\text{C}_3\text{H}_5)_2\text{Ni}$ with carbon monoxide goes completely to $\text{Ni}(\text{CO})_4$ and 1,5-hexadiene, rather than yielding $(\text{C}_3\text{H}_5)_2\text{Ni}(\text{CO})$ (**1**) (eq 2).¹⁷⁸



There is some evidence that $(2\text{-MeC}_3\text{H}_4)_2\text{Ni}$ reacts with an equivalent of CO at $-80\text{ }^\circ\text{C}$ to produce an unstable 1:1 adduct $(2\text{-MeC}_3\text{H}_4)_2\text{Ni}(\text{CO})$.¹⁹⁹ Nevertheless, warming the reaction in the presence of additional CO leads to the production of $\text{Ni}(\text{CO})_4$ and the coupling product 2,5-dimethylhexa-1,5-diene, or to the insertion product phorone (diisopropylidene acetone) if excess CO is present.

Spectroscopic evidence for a bis(allyl)nickel carbonyl complex was obtained when Baker treated the bridged nickel allyl complex derived from 2,3,5-tris(methylene)hexamethylene with CO at $-78\text{ }^\circ\text{C}$; the resulting red solution displayed a strong IR resonance at 2000 cm^{-1} .²⁰³ Warming the reaction to $-30\text{ }^\circ\text{C}$ in the presence of additional CO caused the signal to disappear, however, and the cyclic insertion product 3,4,6-trimethylenecycloheptanone was identified (eq 3). The unisolated, thermally unstable species **1** was proposed as the source of the transient IR resonance.



As hinted at by the reactions of substituted bis(allyl)nickel compounds with CO noted above, it is possible to improve the kinetic stability of allyl complexes and their donor adducts by employing substituted allyl ligands. For example, $(2\text{-MeC}_3\text{H}_4)_2\text{Fe}(\text{PMe}_3)_2$ ²⁰⁴ is stable in solution to at least $30\text{ }^\circ\text{C}$ (cf. $0\text{ }^\circ\text{C}$ for the $(\text{C}_3\text{H}_5)_2\text{Fe}(\text{PMe}_3)_2$ analog),²⁰⁵ and unlike $(\text{C}_3\text{H}_5)_2\text{Ni}$, the tetrasubstituted substituted bis(1,1,3,3-tetraphenylallyl)nickel is stable indefinitely at $20\text{ }^\circ\text{C}$.²⁰⁶ The trimethylsilyl groups of the $[1,3\text{-(SiMe}_3)_2\text{C}_3\text{H}_3]^-$ (A') ligand²⁰⁷ provide even more robust complexes, and A' has been used to synthesize a variety of bis(allyl')M species of the first row transition metals, even in cases where the unsubstituted analog is not known (e.g., $\text{A}'_2\text{Fe}$,⁷⁴ $\text{A}'_2\text{Co}$ ^{75, 188}).^{109, 166} Furthermore, substituted allyl halide species of nickel (i.e., $[\text{A}'\text{Ni}(\mu\text{-Br})_2]$, $[\text{A}'\text{Ni}(\mu\text{-I})_2]$) are known that do not undergo Schlenk redistribution reactions.⁷⁰

Below we describe the efforts made towards adduct formation by the direct addition of CO to $\text{A}'_2\text{Ni}$ and an alternative synthesis developed to confirm the presence of products synthesized from $\text{A}'_2\text{CO}$. Previous work within the group focused on the reactivity of $\text{A}'_2\text{Fe}$ and $\text{A}'_2\text{Co}$ with CO and resulted in the characterization of their CO adducts. Additionally, initial synthetic work surrounding $\text{A}'_2\text{Ni}$ treatment with CO was performed; however, owing to both synthetic and stability issues of the resulting product, a complete analysis could not be obtained. The results of the previous work and newest are described together to offer the

complete picture concerning the formation of CO adducts from these A_2M ($M = \text{Fe, Co, Ni}$) complexes.

Experimental

General Considerations. All manipulations were performed with the rigorous exclusion of air and moisture using high vacuum, Schlenk, or glovebox techniques. Proton and carbon (^{13}C) NMR spectra were obtained on Bruker AV-I-400 at 400 and 101 MHz, respectively, and were referenced to the residual proton and ^{13}C resonances of C_6D_6 . Infrared data were obtained on an ATI Mattson–Genesis FT–IR spectrometer between as KBr plates. Combustion analyses were performed by Columbia Analytical Services, Tucson, AZ. ICP-OES measurements were made on a Perkin Elmer Optima 2000 DV instrument.

Materials. A_2M ($M = \text{Fe},^{74}\text{Co},^{75}\text{Ni}^{70}$) and $A\text{Br}^{138}$ were prepared as previously described. Carbon monoxide (CP grade) was passed through a drying column (anhydrous CaSO_4) before use. A Schlenk-line adapted needle, which was purged with CO for several minutes, was used to introduce CO to solutions. THF and hexanes were distilled under nitrogen from potassium benzophenone ketyl.¹¹¹ Deuterated solvents were vacuum distilled from Na/K (22/78) alloy prior to use. ICP-OES samples were digested in 4% HNO_3 at 85 °C and diluted with deionized water until a clear colorless solution was obtained. Other reagents were obtained from commercial sources and used as received.

Alternate synthesis of $[\text{CoA}(\text{CO})_3]$.²⁰⁸ A 250 mL Schlenk flask equipped with a magnetic stir bar was charged with $\text{PhCH}_2\text{N}(\text{C}_2\text{H}_5)_3^+\text{Cl}^-$ (0.293 g, 1.29 mmol) dissolved in 40 mL of 5 M NaOH. The resulting clear colorless solution was degassed using the freeze-pump-thaw method. A 125 mL Schlenk flask with a magnetic stir bar was charged with $\text{Co}_2(\text{CO})_8$ (0.461 g, 1.35 mmol), $A\text{Br}$ (0.367 g, 1.38 mmol), and 50 mL of hexanes to yield a dark brown solution. The solution in hexanes was cannulated into the NaOH solution at room temperature. The mixture was stirred vigorously for 2 h, resulting in an orange benzene solution above a blue aqueous layer. A liquid-liquid extraction was performed under argon to collect the benzene solution. The solution was dried with MgSO_4 , and gravity filtered to remove any solid. The extracted orange solution was dried under vacuum and collected under an N_2 atmosphere, yielding a dark orange oil (0.115 g, 26%). The product showed limited stability in solution and under an N_2 atmosphere. Both in solution and when dry, complete decomposition to a blue-green solid occurred within 12 h. Prior to decomposition, both products **3a** and **3b** were identified in the ^1H and ^{13}C NMR spectra. Their instability prevented the acquisition of elemental analysis data.

Reaction of A₂Ni and CO. A 125 mL Schlenk flask containing a magnetic stir bar was charged with A₂Ni (0.20 g, 0.56 mmol) and 50 mL of hexanes. The flask was cooled to -78 °C in a dry ice-acetone bath under nitrogen. A needle was purged with CO for 10 min, submerged into the solution, and CO was added for 15 min. Addition of CO resulted in a slight color change in the solution from dark brown to a red-brown. The solution was degassed using the freeze-pump-thaw method, filtered, and the hexanes were removed immediately under reduced pressure. A dark red-orange oil (0.18 g, 80% yield) was collected. Anal. Calcd for C₁₉H₄₂NiOSi₄: Ni, 12.8. Ni analysis (ICP-OES): 11.2. Complete decomposition was observed within a week of synthesis without solvent and after 2–3 h in solution. ¹H NMR (C₆D₆, 298K): δ 0.08 (s, 18H, Si(CH₃)₃); 0.10 (s, 18H, Si(CH₃)₃); 3.39 (d, *J* = 9.8 Hz, 2H, *syn* C-H); 5.43 (dd, *J* = 18.5 Hz, 2H, *anti*-C-H) 6.81 (dd, *J* = 18.0 Hz, *J* = 10.4 Hz, 2H, C₍₂₎-H). ¹³C NMR (C₆D₆, 298 K): δ -2.50 ppm (Si(CH₃)₃); -1.00 (Si(CH₃)₃); 61.10 (*syn* C-H); 128.62 (*anti* C-H); 143.01 (C₍₂₎); 204.14 (CO). Principle IR bands (cm⁻¹): 2955 (s), 2898 (m), 2005 (m), 1655 (m), 1619 (s), 1597 (s), 1404 (m), 1341 (m), 1247 (s), 1210 (m), 1099 (s), 1020 (s), 945 (m), 908 (m), 840 (s, br), 753 (m), 690 (m), 637 (m).

Computational Details. Geometry optimization calculations were performed using the *Gaussian* 03 and 09 suites of programs.²⁰⁹⁻²¹⁰ The PW91PW91 functional, which employs the 1991 gradient-corrected functional of Perdew and Wang for both correlation and exchange,²¹¹ was used. The triple- ζ polarized def2-TZVP basis set¹⁶⁵ and an ultrafine grid were used for all calculations. Stationary points were characterized by the calculation of vibrational frequencies, and unless otherwise noted, all geometries were found to be minima ($N_{\text{imag}} = 0$). Use of the PW91PW91 functional in conjunction with the Def2-TZVP basis set predicts CO stretching frequencies with good accuracy even without scaling; the predicted values are generally lower than experimental ones by 10–15 cm⁻¹. This functional/basis set combination was used to calculate $\nu(\text{CO})$ for CO itself and several benchmark carbonyl complexes; the values (cm⁻¹) for CO (2135), Fe(CO)₅ (2012, 2029), (CO)₃Co(μ -CO)₂Co(CO)₃ (2033, 2040, 2041, 2065, 2102, terminal only), and Ni(CO)₄ (2048) are in good agreement with the experimentally determined values (CO (2143); Fe(CO)₅ (2013, 2034); Co₂(CO)₈ (2031, 2044, 2059, 2071, 2112), and Ni(CO)₄ (2057)).²¹²

Results and Discussion

Reactions with carbon monoxide. After carbon monoxide is passed through solutions of A₂M (M = Fe, Co, Ni) in hexanes, removal of the solvent leaves liquids that are the result of the addition of CO to the allyl complex.

Reaction of A'_2Fe and CO. The bis(allyl)iron complex $(C_3H_5)_2Fe$ is unknown, but the dicarbonyl complex $(C_3H_5)_2Fe(CO)_2$ has been prepared from the carbonyl halide $(C_3H_5)Fe(CO)_3I$,²⁰¹ which in turn is derived from $Fe(CO)_5$. The trimethylsilylated version can be prepared directly from carbon monoxide and A'_2Fe . A CO purge at atmospheric pressure through an orange solution of A'_2Fe in hexanes eventually causes the solution to become yellow. Removal of the solvent yields a viscous yellow liquid that was characterized with elemental and spectroscopic analysis as the dicarbonyl species $A'_2Fe(CO)_2$ (**2**). It does not crystallize after weeks at room temperature or for one week at low temperature ($-40\text{ }^\circ\text{C}$). Although stable as the pure liquid under a nitrogen atmosphere, **2** quickly decomposes in air. A solution of **2** in hexanes is also unstable, and a black precipitate is observed after standing overnight at room temperature.

Only one set of resonances is found in the proton NMR spectrum for **2**, indicating that there is only a single orientation of the allyl ligands present (i.e., eclipsed or staggered). The proton NMR spectral pattern (s, s, d, d, dd; from the two $SiMe_3$ groups, the terminal hydrogens, and the central hydrogen, respectively) is indicative of a *syn*, *anti* arrangement of trimethylsilyl groups on the allyl ligands, as observed in the crystallographically characterized A'_2Fe (Figure 29).⁷⁴

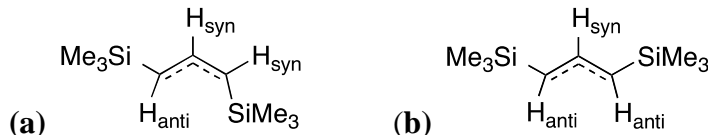


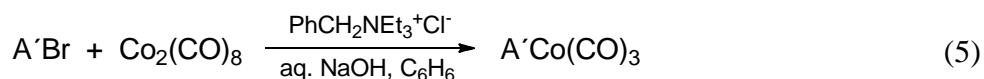
Figure 29. (a) The *syn*, *anti* arrangement of $SiMe_3$ groups on the A' ligand, following the naming convention used for the hydrogens; **b**. the corresponding *syn*, *syn* arrangement of $SiMe_3$ groups.

The J values for the two doublets in the proton NMR spectrum of **2** are both 13.5 Hz, so the *syn* and *anti* protons cannot be distinguished on that basis (in A'_2Ni , in contrast, the J values are not the same (16 and 10 Hz); the larger coupling constant is associated with the *anti* proton of the allyl ligand).⁷⁰ If the order observed in A'_2Ni is followed, the upfield proton doublet is assignable to the *anti* protons of the allyl ligands in **2**. There is only one peak in the ^{13}C NMR spectrum for the CO ligands of **2** (216.8 ppm); the two carbonyls are, as expected, equivalent on the NMR timescale.

Two CO stretching peaks are present in the IR spectrum of **2** at 1931 cm⁻¹ and 1986 cm⁻¹, which correspond to asymmetric and symmetric stretching modes, respectively. They are both 34 cm⁻¹ lower than those reported for (C₃H₅)₂Fe(CO)₂ (1965, 2020 cm⁻¹),²⁰¹ and indicate that the SiMe₃ groups on the allyl ligands are net electron donors. This point is discussed in more detail below.

Reaction of A'Co and CO. As noted above (eq 1), the orange red (C₃H₅)Co(CO)₃ (mp -33 to -32 °C).^{202, 213} can be synthesized from the direct reaction of CO with (C₃H₅)₃Co, but the usual routes start from the more conveniently obtained [Co(CO)₄]⁻ anion,^{202, 213-214} which is derived from Co₂(CO)₈. A direct route is available for the synthesis of the trimethylsilylated version of the allyl cobalt complex. As carbon monoxide is added to an orange solution of A'Co in hexanes, the solution turns dark red but eventually returns to orange. Removal of solvent results in an orange oil, which contains the spectroscopically identifiable cobalt complex A'Co(CO)₃ (**3**) in addition to the allyl coupling product 1,3,4,6-tetrakis(trimethylsilyl)-1,5-hexadiene. Colorless crystals of the latter grow out of the oil over several days at room temperature. The similar solubility of **3** and the hexadiene has prevented the isolation of analytically pure samples. Nevertheless, the general chemical properties of **3** are consistent with the other allyl complexes described here. For example, like **2**, **3** quickly decomposes in air, and it also decomposes in solution overnight, with the formation of a black precipitate.

Owing to the complications involved in the synthesis of **3** by direct addition of CO, a more conventional route was used to confirm its properties. A known phase transfer catalyzed method for the synthesis of (C₃H₅)Co(CO)₃²⁰⁸ was adapted for the synthesis of **3**. Addition of a dark brown benzene solution of equimolar Co₂(CO)₈ and 1,3-(SiMe₃)₂C₃H₃Br (A'Br)¹³⁸ to a colorless NaOH(aq) solution containing PhCH₂NEt₃⁺Cl⁻ gradually produced an orange benzene layer above a blue aqueous layer. After extraction and drying of the upper layer, the dark orange **3** was isolated (eq 5).



The product matches the physical appearance and spectroscopic properties of the product from the treatment of A'Co with CO, although as the second synthesis reveals, **3** can tolerate brief exposure to water during synthesis. Nevertheless, even after drying, complete decomposition to a blue-green solid occurs within 12 h, perhaps accelerated by traces of remaining water.

Regardless of the method of preparation of **3**, there are two different cobalt allyl species that can be identified from NMR data. One of them (**3a**) has a proton NMR spectral pattern consistent with trimethylsilyl groups in *syn* and *anti* positions on the allyl ligands (i.e., s, s, d, d, dd; see Figure 29). The two sets of doublets at 2.30 ppm and 3.10 ppm have *J* values of 12.9 and 8.7 Hz, respectively. As in the proton NMR spectrum of A₂Ni, the upfield doublet resonance, with its larger *J* value, is considered to reflect the *anti* proton position, while the downfield one is associated with the *syn* protons. The corresponding carbons coupled to the *syn* and *anti* protons in **3a** follow this trend in the ¹³C NMR spectrum.

The other cobalt allyl species present (**3b**) has an NMR spectral pattern typical of allyl ligands with trimethylsilyl substituents in *syn, syn* positions (i.e., s, d, t; see Fig. 1). The *J* value of 12.3 Hz for the doublet and triplet resonances is smaller than that either for K[A⁺] (15.6 Hz) or for the *anti* proton *J* value for A₂Ni (16 Hz), but is similar to the *anti* proton *J* value for **3a**. The ratio of the *syn, syn* species to the *syn, anti* species in the proton NMR spectra varies somewhat from preparation to preparation, but the *syn, syn* complex is always the major product (note that in the formation of (1,3-Me₂C₃H₃)Co(CO)₃ from K[Co(CO)₄] and 1,3-pentadiene, both *syn, syn*, and *syn, anti* forms are generated, with the *syn, syn* form the major species²¹⁵). Although the *syn* (or *syn, syn*) forms of (allyl)Co(CO)₃ complexes have been assumed to be more thermodynamically stable than the corresponding *anti* (or *syn, anti*) conformations,²¹⁶ DFT calculations (discussed below) indicate that **3a** and **3b** are of almost the same energy (within ~1 kcal mol⁻¹). Kinetic factors evidently play a role in the synthesis.

The ¹³C NMR spectrum of **3** displays one peak at 204.5 ppm that corresponds to coordinated CO, suggesting that the ligands are in fast exchange and/or that the CO environments of **3a** and **3b** are nearly equivalent. The FT-IR data for **3** exhibits carbonyl peaks at 1984 and 2053 cm⁻¹. As the carbonyl resonance at 1984 cm⁻¹ is roughly twice the width of the sharp peak at 2053 cm⁻¹, the broad CO peak may reflect the presence of two unresolved, closely spaced peaks. The IR spectrum is available in Appendix A Figure A41.

Reaction of A₂Ni and CO. Given the anticipated low thermal stability of an allyl nickel complex, carbon monoxide was added to a solution of A₂Ni in hexane at -78 °C. The solution became red-brown, and removal of solvent produced a dark red-orange oil that was characterized as A₂Ni(CO) (**4**). Synthesis of **4** in THF was not successful; addition of CO to A₂Ni in THF produced a black reaction mixture from which no product could be isolated. In air, **4** rapidly decomposes, but even under a nitrogen atmosphere, decomposition is obvious after a few days, and complete decomposition is observed in approximately 7-10 days. Like **2** and **3**, solutions of **4** are unstable; decomposition is evident within a few hours.

As with **2**, only one set of resonances is observed in the NMR data of **4**. The ^1H NMR spectrum contains a set of resonances that is consistent with trimethylsilyl substituents in *syn*, *anti* positions on the allyl ligands (i.e., s, s, d, d, dd; see Fig. 1). In the proton NMR spectrum, the two sets of doublets at δ 3.39 ppm and δ 5.43 ppm have J values of 9.8 Hz and 18.5 Hz, respectively. Since the proton resonance for the allyl framework's *anti* proton of $\text{A}'_2\text{Ni}$ is associated with a larger J value than is that for its *syn* proton, the proton resonance at δ 5.43 is assigned to the *anti* proton in **4**. Interestingly, this peak position is downfield from the resonance for the *syn* proton, making the relative positions of the peaks opposite to that observed for $\text{A}'_2\text{Ni}$.⁷⁰ The ^{13}C NMR peaks that are coupled to the corresponding proton peaks also follow the trend of upfield *syn* and downfield *anti* positions for **4**.

There is one peak in the ^{13}C NMR spectrum that corresponds to bound CO (δ 204.1). The FT-IR data for **4** contains one CO stretching frequency at 2005 cm^{-1} . It is close to the value of 2000 cm^{-1} reported for the CO stretch in **1**, adding support to the latter's identification as a nickel carbonyl complex.

Calculations

Density functional theory calculations (PW91PW91/Def2-TZVP) were performed on model allyl carbonyl complexes with both the parent and the trimethylsilylated allyl ligands in order to clarify the effects of the substituents on ligand conformations and CO stretching frequencies.¹³¹ A variety of conformations were examined for the various complexes; only those that were found to be minima on the potential energy surface (as indicated by the absence of negative vibrational frequencies) are discussed in detail here. The lowest energy conformer in each case is depicted in Figure 30; illustrations of the others are available in Appendix C: Section C4.

Iron Complexes. Several conformations of $(\text{C}_3\text{H}_5)_2\text{Fe}(\text{CO})_2$ were examined, but only the eclipsed arrangement depicted in Figure 30(a) was found to be a minimum on the potential energy surface ($N_{\text{imag}} = 0$). A summary of its structural parameters is provided in Table 1. The calculated CO stretching frequencies of 1968 cm^{-1} (asymmetric) and 2009 cm^{-1} (symmetric) are close to the experimentally reported CO stretching frequencies ($1965, 2020\text{ cm}^{-1}$).²⁰¹

In contrast, calculations on **2** indicate that several local energy minima exist for it (Table 1). The angles between the C_3 allyl planes differ substantially among the three conformations, but the calculated CO stretching frequencies are in the narrow spread of $1943\text{--}1947\text{ cm}^{-1}$ (asymmetric) and $1985\text{--}1993\text{ cm}^{-1}$ (symmetric). The C_2 -symmetric "eclipsed-front" conformation (Figure 30(b)) is the lowest in energy (ΔG°) by at least 6 kcal mol^{-1} , and it shares the same basic arrangement as the stable form of $(\text{C}_3\text{H}_5)_2\text{Fe}(\text{CO})_2$. Taking it as the most likely

approximation to the solution structure of $A_2Fe(CO)_2$, the $\nu(CO)$ are calculated to be 21 cm^{-1} and 24 cm^{-1} lower for the asymmetric and symmetric frequencies, respectively, than in $(C_3H_5)_2Fe(CO)_2$. This decrease parallels the 34 cm^{-1} drop for both frequencies observed experimentally between $(C_3H_5)_2Fe(CO)_2$ and $A_2Fe(CO)_2$, and supports the conclusion that the $SiMe_3$ groups on the allyl ligands are net electron donors.

Cobalt Complexes. The conformation of $(C_3H_5)Co(CO)_3$ with the CO group oriented distally to the center carbon of the allyl group was found to be a minimum on the potential energy surface (Figure 2(c), Table 1); with the $(CO)_3$ group rotated by 180° , a transition structure is obtained with a single imaginary frequency ($\nu = -76\text{ cm}^{-1}$). CO stretching frequencies of 2004 cm^{-1} (asymmetric), 2006 cm^{-1} (asymmetric), and 2059 cm^{-1} (symmetric) are predicted for the complex; these compare favorably with the experimental values of 1998 cm^{-1} (asymmetric; the individual stretches are not resolved) and 2065 cm^{-1} (symmetric).²¹⁷

DFT calculations were performed on both the proposed *syn, syn* and *syn, anti* structures of **3**. In the case of the *syn, syn* conformer (Figure 30(d), Table 2), a structure with no symmetry (C_1) displays three calculated CO stretching frequencies at 1984 cm^{-1} (asymmetric), 1995 cm^{-1} (asymmetric), and 2044 cm^{-1} (symmetric). These values are close to the experimental CO stretching frequencies in **3** (1984 cm^{-1} and 2053 cm^{-1}), taking into account that the two asymmetric stretching frequencies may be overlapping to produce the observed broad peak at 1984 cm^{-1} .²¹⁸

The calculated structure of *syn, anti* **3** (Figure 30(e), Table 2) is higher in energy than the *syn, syn* structure by only 1.2 kcal mol^{-1} in ΔG° and 0.4 kcal mol^{-1} in ΔH° ; i.e., they are essentially equienergetic. The *syn, anti* **3** has three CO stretching frequencies at 1986 cm^{-1} (asymmetric), 1993 cm^{-1} (asymmetric), and 2044 cm^{-1} (symmetric); there is a $15\text{--}18\text{ cm}^{-1}$ reduction in the values in the trimethylsilylated versions compared to the unsubstituted complex. As in the case of **2** and **4** (below), this reflects greater electron donation from the trimethylsilylated ligands relative to the parent species; the effect is less in **3** as only a single allyl ligand is contributing.

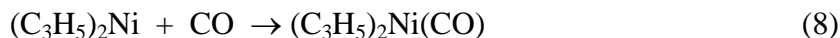
Nickel Complexes. An “eclipsed-front” geometry is found in the structurally characterized $(C_3H_5)_2NiPMe_3$ complex,⁷¹ and although this conformation was determined by DFT calculations to be the lowest energy of the three $(C_3H_5)_2Ni(CO)$ complexes that were examined (Figure 30(f), Table 2), all of them are minima on their potential energy surfaces ($N_{imag} = 0$). The calculated $\nu(CO)$ are also similar ($2005\text{--}2015\text{ cm}^{-1}$). The Ni–C(allyl) bond lengths and allyl bending angle in the eclipsed-front structure are close to those of $(C_3H_5)_2NiPMe_3$ ($1.998(5)\text{--}2.092(5)\text{ \AA}$ and 3.6° , respectively).

A calculation on the bridged **1** (Figure 30(g)) converged to a structure with features similar to those of $(\text{C}_3\text{H}_5)_2\text{Ni}(\text{CO})$. Tellingly, its calculated $\nu(\text{CO})$ of 2014 cm^{-1} is close to the value of 2000 cm^{-1} reported for **1**, and supports the assignment of the latter as an allyl carbonyl complex.

DFT calculations were also conducted on several forms of **4** (Table 2), but the “eclipsed-front structure” (Figure 30(h)) is the lowest in energy. The calculated Ni–C(allyl) bonding range ($2.038\text{--}2.193\text{ \AA}$) and the allyl bending angle (12.9°) are somewhat larger than those calculated for the parent $(\text{C}_3\text{H}_5)_2\text{Ni}(\text{CO})$; these changes reflect the increased steric strain imposed by the trimethylsilyl-substituted groups. The calculated bond lengths are also longer than those of the solid-state structure of $\text{A}'_2\text{Ni}$ ($1.944(3)\text{--}2.037(3)\text{ \AA}$), although the allyl bending angle is smaller (cf. 49.1° in $\text{A}'_2\text{Ni}$ (exp.)).⁷⁰ However, the Ni–CO bond length is 1.789 \AA , which is similar to that calculated for $(\text{C}_3\text{H}_5)_2\text{Ni}(\text{CO})$, and shorter than that in $\text{Ni}(\text{CO})_4$ ($1.836(2)\text{ \AA}$, gas-phase).²¹⁹

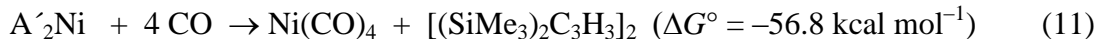
The eclipsed-front structure has a CO stretching frequency of 1989 cm^{-1} ; this value is lower than that predicted for the unsubstituted allyl complexes, again reflecting the enhanced electron donation from the trimethylsilyl groups. The stretching frequency is close to the experimental CO stretching frequency measured for **4** (2005 cm^{-1}).

Formation of $(\text{C}_3\text{R}_2\text{H}_3)_2\text{Ni}(\text{CO})$. A series of calculations was performed to provide a measure of the thermodynamic driving force associated with the formation of an $(\text{C}_3\text{R}_2\text{H}_3)_2\text{Ni}(\text{CO})$ complex, historically the most elusive of the first row allyl carbonyls. The reaction of $(\text{C}_3\text{H}_5)_2\text{Ni}$ with CO (eq 8) is predicted to have a ΔG° of $-10.1\text{ kcal mol}^{-1}$; this is reduced to $-7.6\text{ kcal mol}^{-1}$ for the analogous reaction with $\text{A}'_2\text{Ni}$ (eq 9).

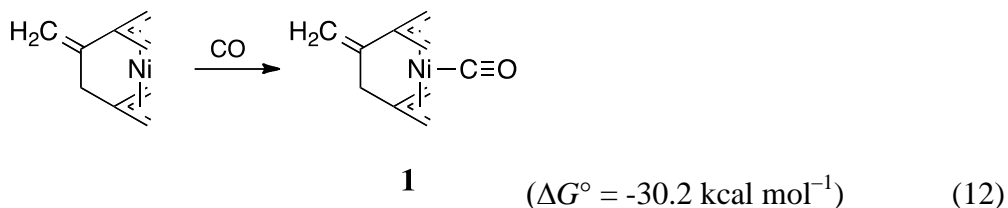


These modest driving forces reflect competition between the stable pseudo-square planar 16-e^- $(\text{C}_3\text{R}_2\text{H}_3)_2\text{Ni}$ species¹³¹ and their 18-e^- derivatives. An alternative reaction of $(\text{C}_3\text{R}_2\text{H}_3)_2\text{Ni}$ with CO to form $\text{Ni}(\text{CO})_4$ and the corresponding hexadienes (eq 10, 11) is strongly favored for both allyl ligands:





The fact that the reaction in eq 10 is experimentally observed,¹⁷⁸ whereas eq 11 is not, or not immediately, is clearly a consequence of kinetic stabilization provided by the trimethylsilyl groups, rather than the result of major thermodynamic differences between the two systems. In this context, it is interesting to note that the reaction to form **1** (eq 12) is calculated to be more strongly favored ($\Delta G^\circ = -30.2 \text{ kcal mol}^{-1}$) than when the allyl ligand is C_3H_5 or A' ; apparently the preorganization provided by the bridge optimizes the complex for subsequent reaction with CO.



Donor properties of the A' ligand. The electronic effect of trimethylsilyl substituents in organometallic systems is not always easily predictable. In consonance with the lower electronegativity of silicon compared to carbon, the group electronegativity of $-\text{SiMe}_3$ compared to $-\text{CH}_3$ is calculated to be lower (e.g., 1.92 vs. 2.56, respectively,²²⁰ although other values have been suggested²²¹). This might, perforce, indicate that that $-\text{SiMe}_3$ would be a better donor than hydrogen, and indeed, a comparison of the free energies of ionization of substituted ruthenocene complexes suggest that the $-\text{SiMe}_3$ group is comparable to $-\text{CH}_3$ as an electron donor.²²² Measurement of the inner-shell electron binding energies in $[(\text{SiMe}_3)_n\text{C}_5\text{H}_{5-n}]_2\text{MCl}_2$ ($\text{M} = \text{Zr}$, $n = 0-3$; $\text{M} = \text{Hf}$, $n = 0$ and 3) indicates that $-\text{SiMe}_3$ is ca. 1.25 times as strong a donor as is $-\text{CH}_3$.²²³ In contrast to this evidence, however, the reduction potential ($E_{1/2}^{\text{red}}$) of substituted $\text{Cp}'_2\text{ZrCl}_2$ compounds increases in the order $((\text{SiMe}_3)_2 < \text{SiMe}_3 < \text{H} < \text{Me} < \text{Et})$, indicating that $-\text{SiMe}_3$ is functioning as an electron *acceptor* relative to hydrogen.²²⁴⁻²²⁵ In other cases, especially when the steric bulk of the $-\text{SiMe}_3$ comes into play, its electronic effect appears to be negligible.²²⁶

In the present case, the $-\text{SiMe}_3$ groups on A' are evidently electron-donating relative to the protons on the unsubstituted allyl ligand, as manifest in the lowered CO stretching frequencies in both **2** and **3** relative to their parent complexes. In this regard, the $-\text{SiMe}_3$ group has an effect similar to that observed with the cyclobutadienyl ligand (e.g., CO stretches of 1995 and 2061 cm^{-1} are observed in $(\text{C}_4\text{H}_4)\text{Ru}(\text{CO})_3$,²²⁷ but stretches of 1980 and 2046 cm^{-1} are found in $(\text{C}_4(\text{SiMe}_3)_4)\text{Ru}(\text{CO})_3$ ²²⁸).

Figure 30.

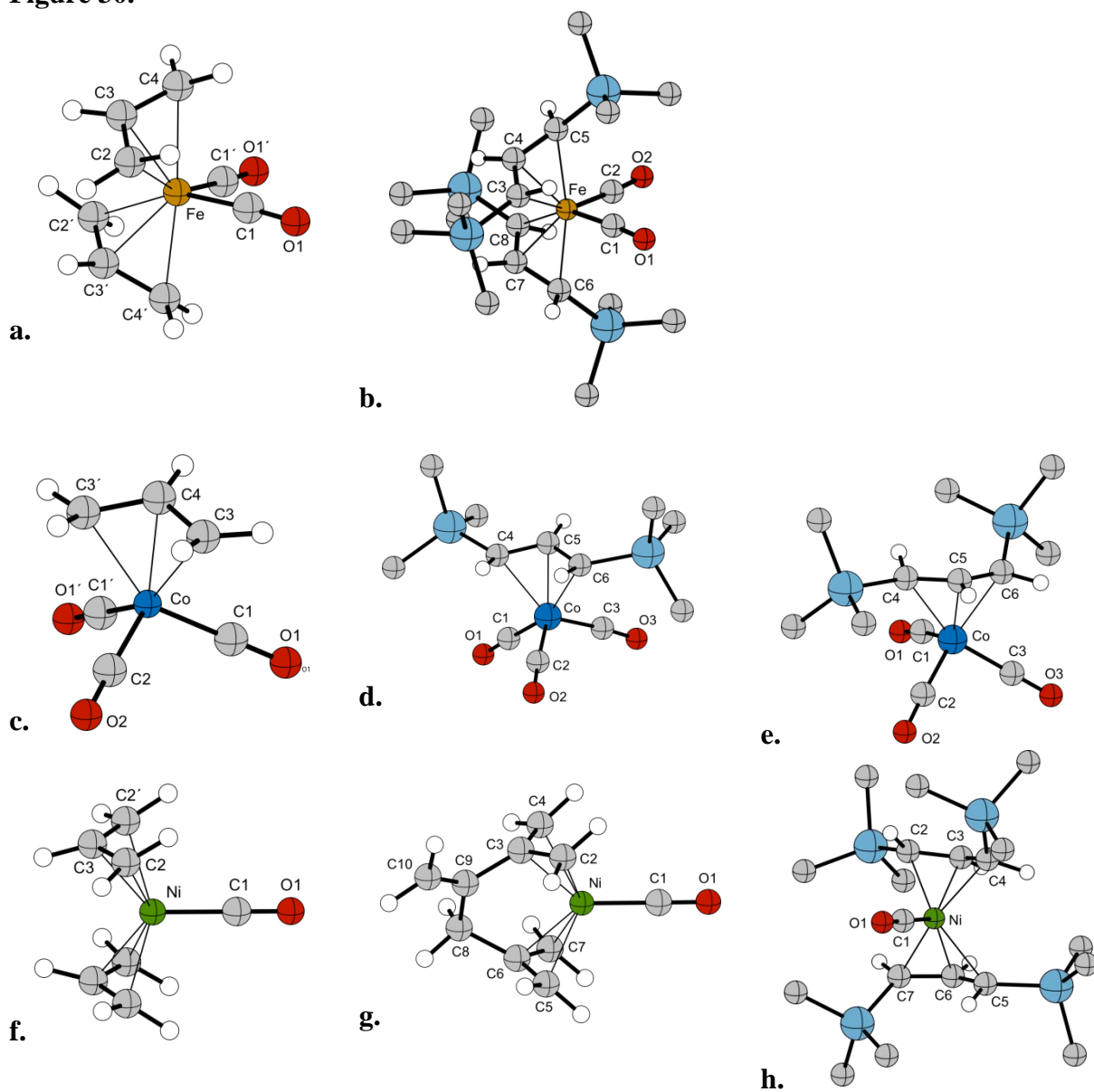


Figure 30. Calculated structures of (a) eclipsed $(C_3H_5)_2Fe(CO)_2$ (C_2); (b) eclipsed $A'_2Fe(CO)_2$ (C_2); (c) distal $(C_3H_5)Co(CO)_3$ (C_1); (d) *syn, syn* $A'Co(CO)_3$ (C_1); (e) *syn, anti* $A'Co(CO)_3$ (C_1); (f) eclipsed-front $(C_3H_5)_2NiCO$ (C_{2v}); (g) $[\eta^6-2,3,5\text{-tris(methylene)-1,6-hexanediyl}]$ -nickel carbonyl; (h) eclipsed-front A'_2NiCO (C_2). For clarity, hydrogen atoms have been omitted from trimethylsilyl groups. (Appendix C: Section C4)

Table 2. Selected calculated structural parameters and $\nu(\text{CO})$ values in $(\text{R}_2\text{C}_3\text{H}_3)_x\text{M}(\text{CO})_y$ Complexes

Complex	M–C range (Å)	M–CO (Å)	Angle between allyl planes (°)	$\nu(\text{CO})$ (cm^{-1})	Relative energy (kcal mol^{-1})
a. $(\text{C}_3\text{H}_5)_2\text{Fe}(\text{CO})_2$ (C_2 , eclipsed-front)	2.059–2.185	1.761	23.8	1968 cm^{-1} (asymm); 2009 cm^{-1} (symm)	—
b. $\text{A}'_2\text{Fe}(\text{CO})_2$ (C_2 , eclipsed-front)	2.077–2.274	1.753	25.6	1947 cm^{-1} (asymm); 1985 cm^{-1} (symm)	0.0 (ΔH°) 0.0 (ΔG°)
c. $\text{A}'_2\text{Fe}(\text{CO})_2$ (C_2 , eclipsed-back)	2.083–2.255	1.761	83.2	1943 cm^{-1} (asymm); 1993 cm^{-1} (symm)	16.2 (ΔH°) 15.7 (ΔG°)
d. $\text{A}'_2\text{Fe}(\text{CO})_2$ (C_1 , staggered)	2.078–2.285	1.754, 1.759	58.8	1946 cm^{-1} (asymm); 1990 cm^{-1} (symm)	6.6 (ΔH°) 6.3 (ΔG°)
e. $(\text{C}_3\text{H}_5)\text{Co}(\text{CO})_3$ (C_s , distal)	2.021–2.116	1.811 (center); 1.771 (side)	—	2004 cm^{-1} (asymm); 2006 cm^{-1} (asymm); 2059 cm^{-1} (symm);	—
f. <i>syn, syn</i> $\text{A}'\text{Co}(\text{CO})_3$ (C_1)	2.039–2.195	1.760 (Co–C1); 1.800 (Co–C2); 1.775 (Co–C3)	—	1984 cm^{-1} (asymm); 1995 cm^{-1} (asymm); 2044 cm^{-1} (symm)	0.0 (ΔH°) 0.0 (ΔG°)
g. <i>syn, anti</i> $\text{A}'\text{Co}(\text{CO})_3$ (C_1)	2.035–2.157	1.802 (Co–C1); 1.777 (Co–C2); 1.761 (Co–C3)	—	1986 cm^{-1} (asymm); 1993 cm^{-1} (asymm); 2044 cm^{-1} (symm);	0.4 (ΔH°) 1.2 (ΔG°)

Table 2. (cont.)

Complex	M–C range (Å)	M–CO (Å)	Angle between allyl planes (°)	$\nu(\text{CO})$ (cm^{-1})	Relative energy (kcal mol^{-1})
h. $(\text{C}_3\text{H}_5)_2\text{Ni}(\text{CO})$ (C_{2v} , eclipsed-front)	2.021–2.103	1.795	8.6	2015	0.0 (ΔH°) 0.0 (ΔG°)
i. $(\text{C}_3\text{H}_5)_2\text{Ni}(\text{CO})$ (C_2 , eclipsed-back)	2.032–2.194	1.794	85.0	2005	7.4 (ΔH°) 7.2 (ΔG°)
j. $(\text{C}_3\text{H}_5)_2\text{Ni}(\text{CO})$ (C_s , staggered)	1.995–2.087	1.818	54.0	2008	4.0 (ΔH°) 3.3 (ΔG°)
k. $[\eta^6\text{-}2,3,5\text{-}$ $\text{tris}(\text{methylene})\text{-}1,6\text{-}$ $\text{hexanediyl}]\text{-nickel}$ carbonyl	2.014–2.138	1.782	28.0	2014	—
l. $\text{A}'_2\text{Ni}(\text{CO})$ (C_2 , eclipsed-front)	2.038–2.193	1.789	12.9	1989	0.0 (ΔH°) 0.0 (ΔG°)
m. $\text{A}'_2\text{Ni}(\text{CO})$ (C_2 , eclipsed-back)	2.017–2.187	1.859	71.6	1979	16.3 (ΔH°) 15.0 (ΔG°)
n. $\text{A}'_2\text{Ni}(\text{CO})$ (C_1 , staggered)	2.020–2.334	1.795	40.7	1992	10.60 (ΔH°) 8.5 (ΔG°)

Conclusion

This work has shown that first-row A'_2M complexes can be used to form kinetically stabilized carbonyl derivatives by direct reaction with CO. A'_2Fe and A'_2Ni accept carbon monoxide as a donor ligand to form the 18-electron carbonyl adducts $A'_2Fe(CO)_2$ and $A'_2Ni(CO)$, respectively. The addition of CO to A'_2Co generates the 18-electron $A'Co(CO)_3$, along with the corresponding trimethylsilylated hexadiene, $[(SiMe_3)_2C_3H_3]_2$; in the process, a one-electron reduction of Co(II) to Co(I) occurs. The CO stretching frequencies observed in $A'_2Fe(CO)_2$ and $A'Co(CO)_3$ are consistent with the A' ligand's being a better electron donor than the unsubstituted allyl.

All of the carbonyl derivatives are air-sensitive, and degrade rapidly in solution. That they can be isolated at all, if even for a limited time, at room temperature is clearly a consequence of the presence of the trimethylsilyl substituents. The similar calculated thermodynamics for the reactions of CO with $(C_3R_2H_3)_2Ni$ suggests that $(C_3R_2H_3)_2Ni(CO)$ is only an intermediate on the way to forming nickel tetracarbonyl and the corresponding hexadienes for both $R = H$ and $SiMe_3$.

Appendix A
Selected Spectra

Section A1
Reference Spectra

Figure A1. ^1H NMR Spectrum of HA'

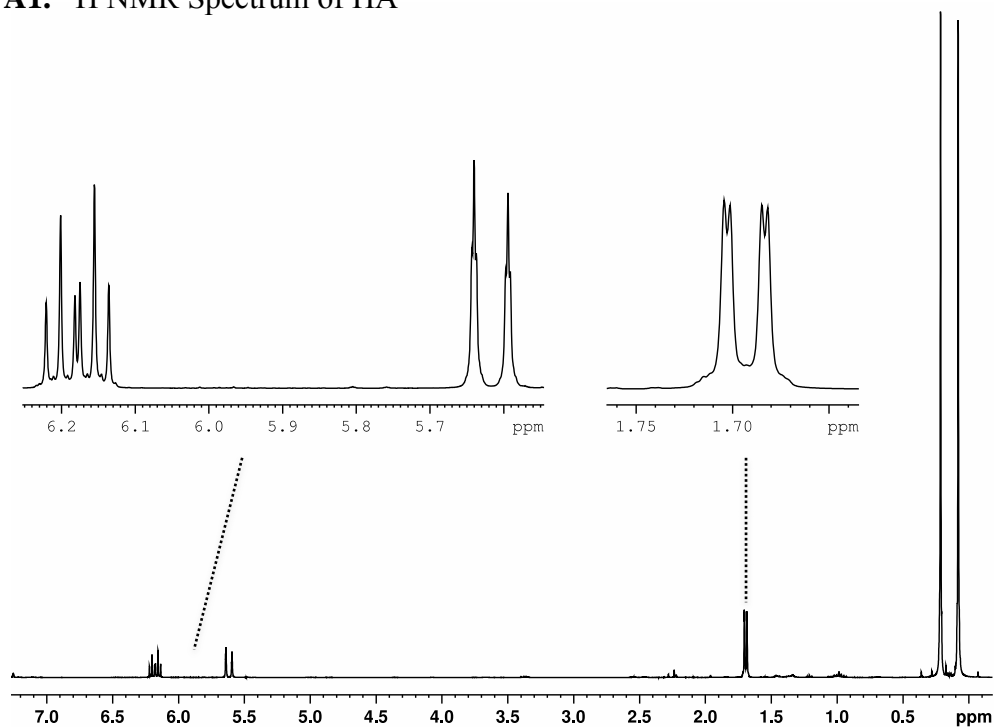


Figure A2. ^1H NMR Spectrum of K[A']

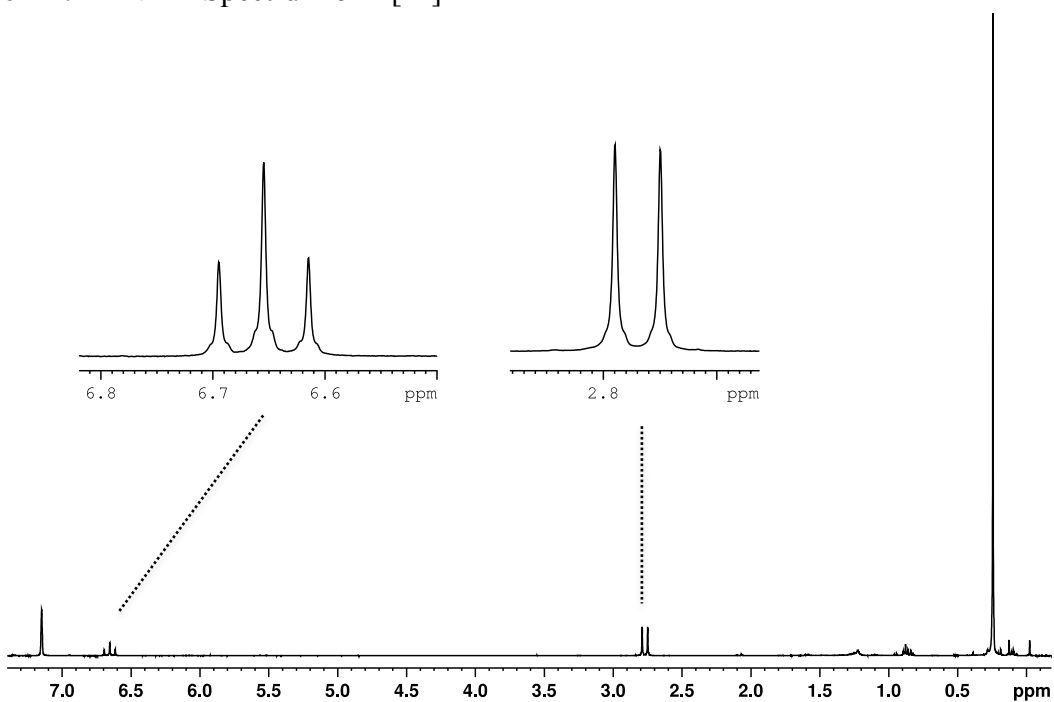
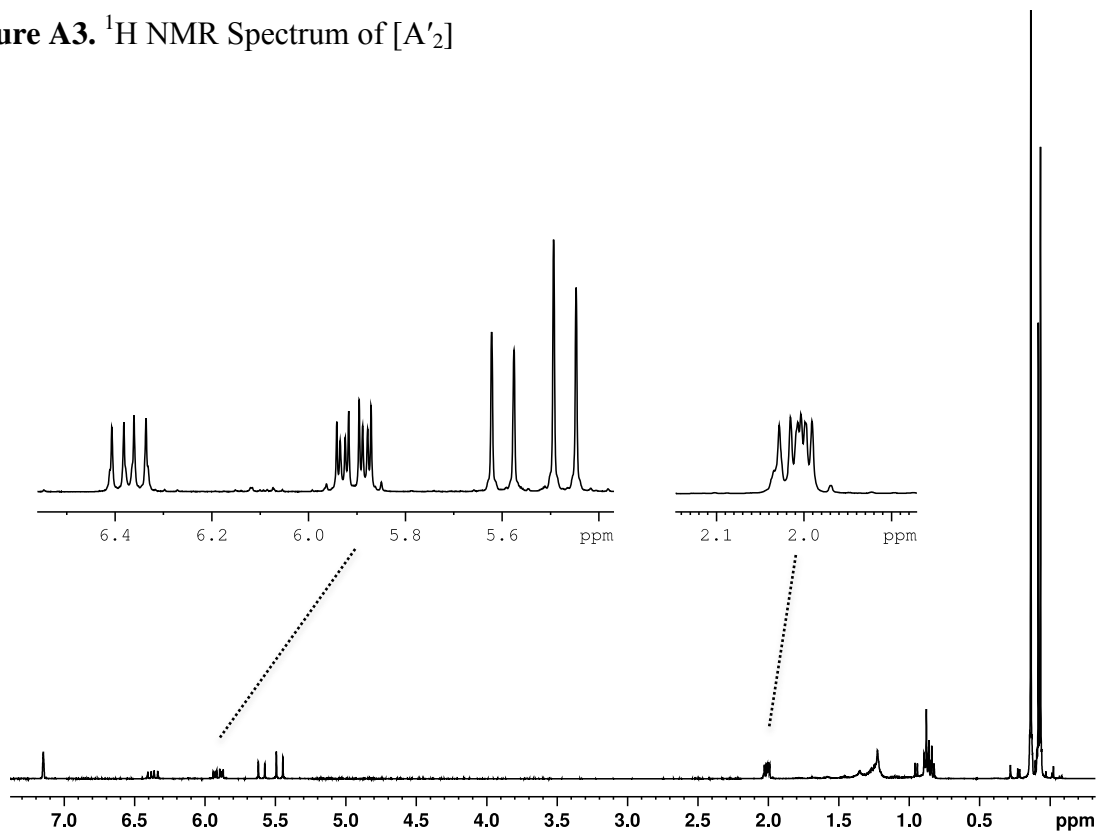


Figure A3. ^1H NMR Spectrum of $[\text{A}'_2]$



Section A2

Mechanochemical Synthesis and Investigations as a Potential Allyl Transfer Agent of the Base-Free Tris(allyl)aluminum Complex $[\text{Al}(\text{1,3}-(\text{SiMe}_3)_2\text{C}_3\text{H}_3)_3]$

Figure A4. ^1H NMR Spectrum of $[\text{AlA}'_3]$

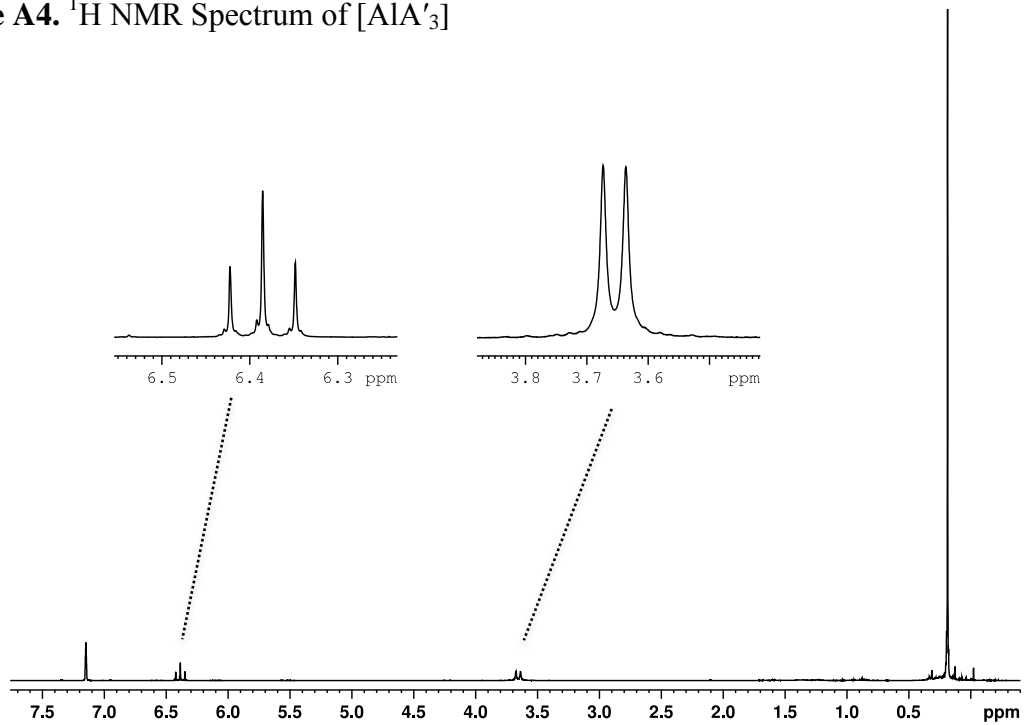


Figure A5. ^1H NMR Spectrum of $[\text{Al}(\text{A}'\text{Ph}_2\text{CO})_3]$

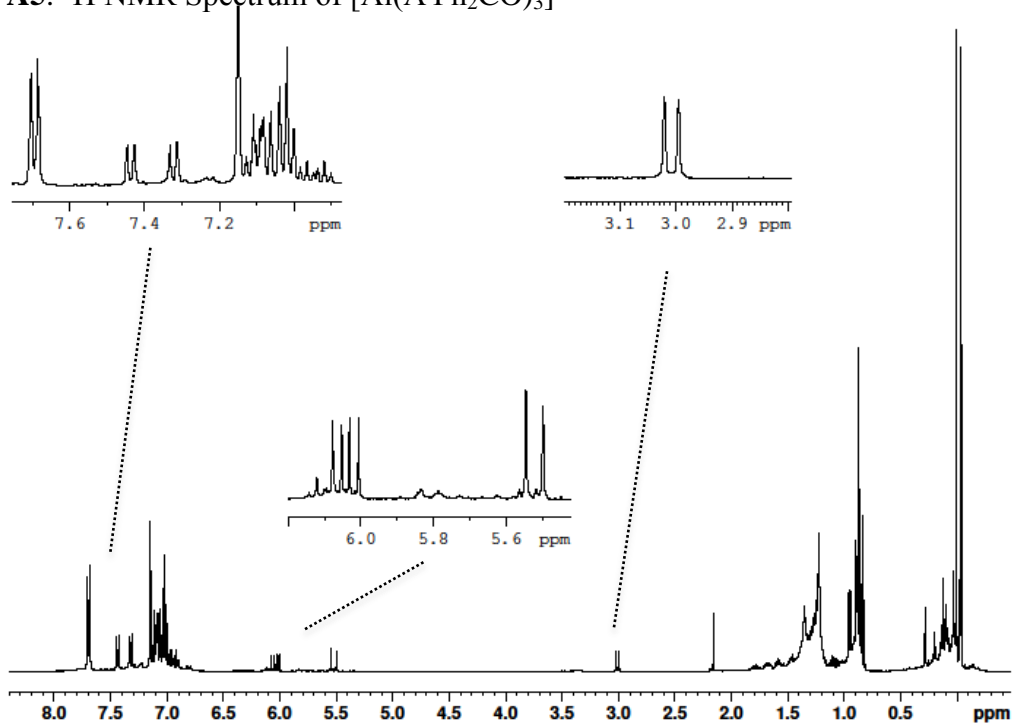


Figure A6. ^1H NMR Spectrum of AlA'_3 at -70°C

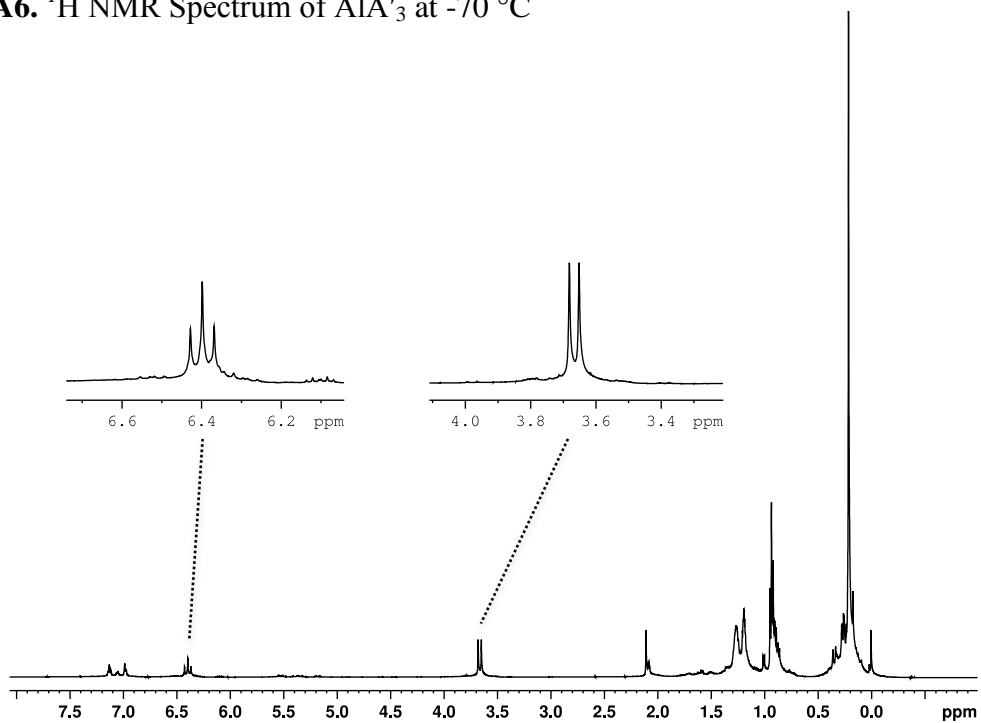


Figure A7. ^1H NMR Spectrum of $[\text{ScA}'_3]$

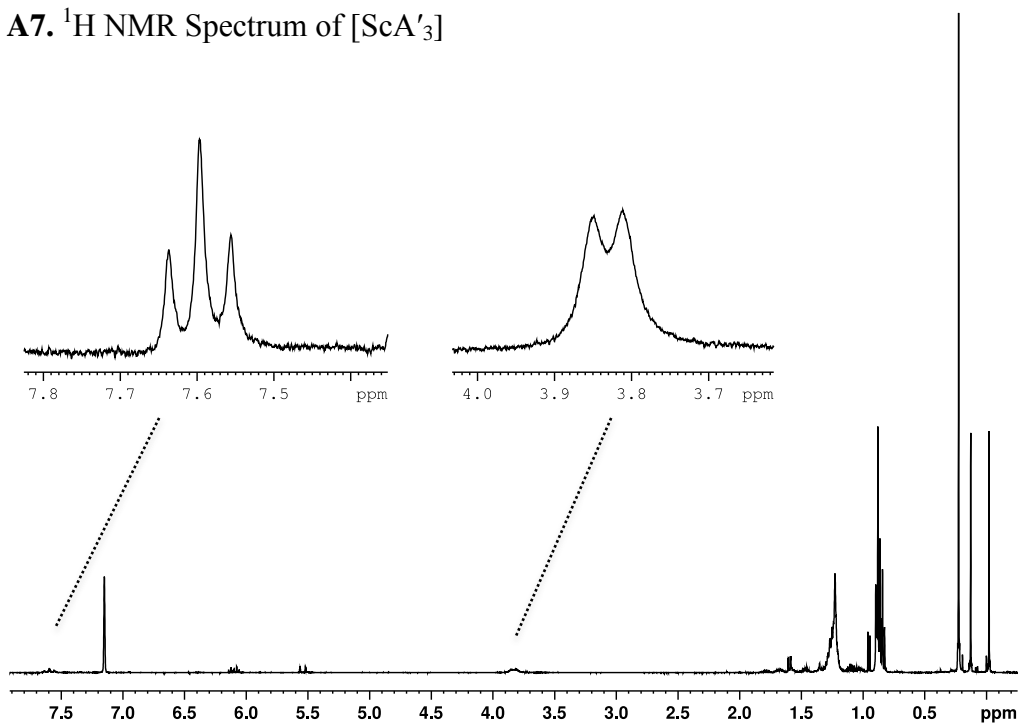


Figure A8. ^1H NMR Spectrum of $[\text{SnA}'_x]$ yellow oil from 24 h reaction in hexanes

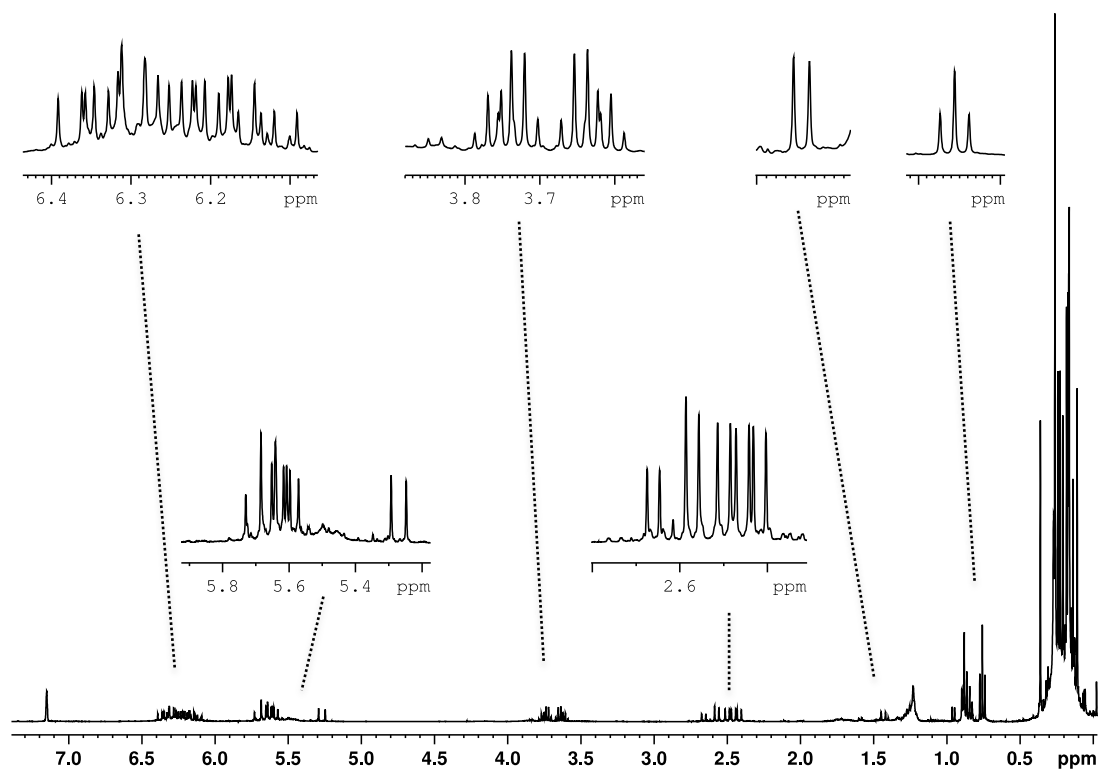


Figure A9. ^1H NMR Spectrum of $[\text{SnA}'_x]$ yellow solid from 24 h reaction in hexanes

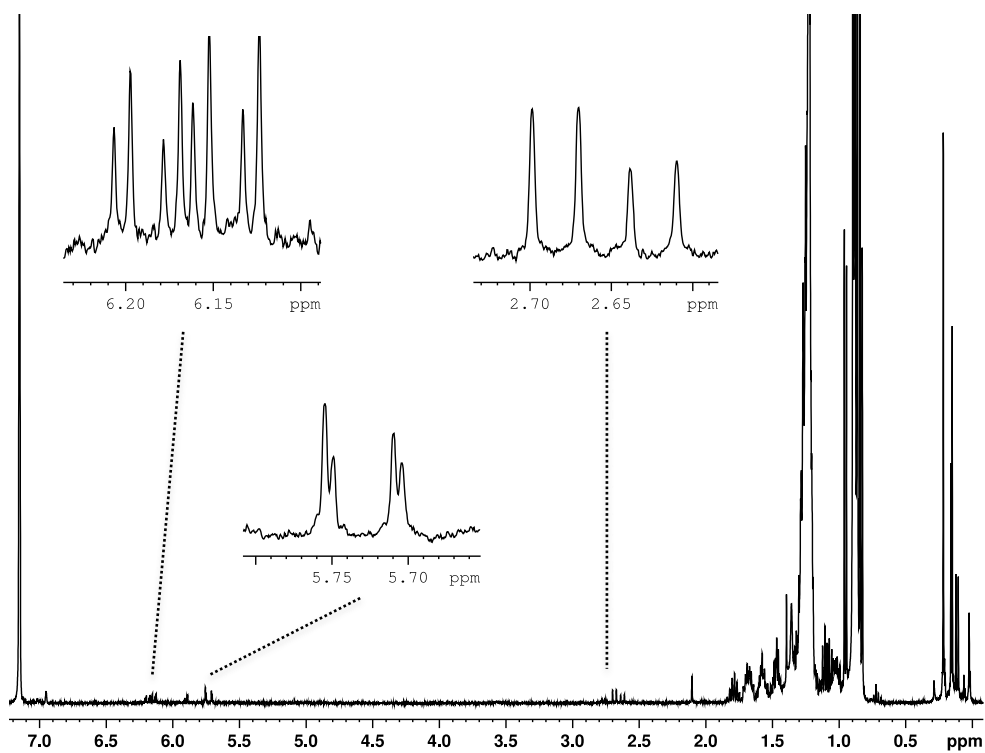


Figure A10. ^1H NMR Spectrum of $[\text{SnA}'_x]$ yellow product from 48 h reaction in hexanes

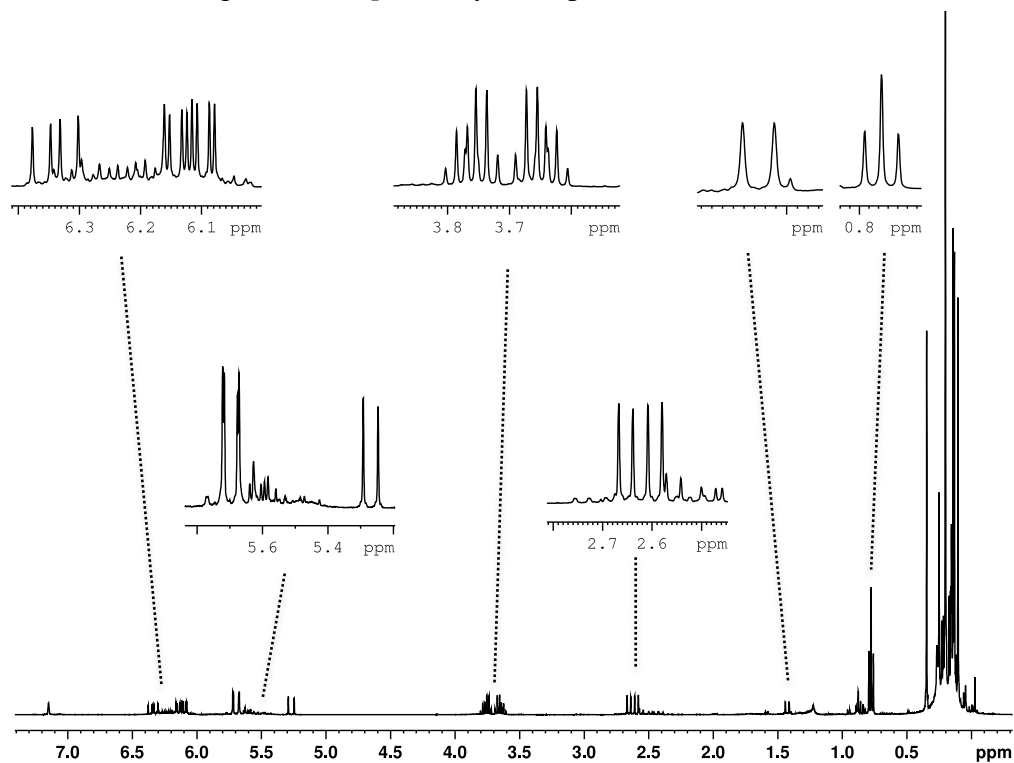


Figure A11. ^1H NMR Spectrum of $[\text{SnA}'_x]$ yellow product from ball mill

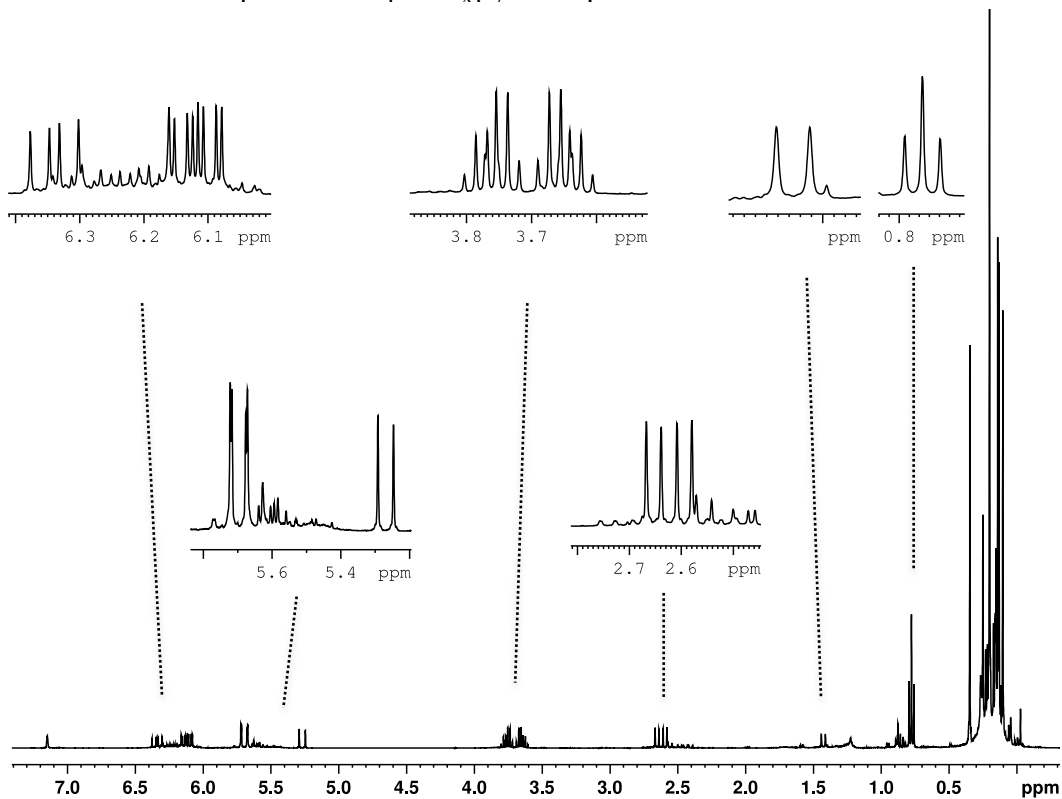


Figure A12. ^1H NMR Spectrum of $[\text{PtA}'_x]$ complex

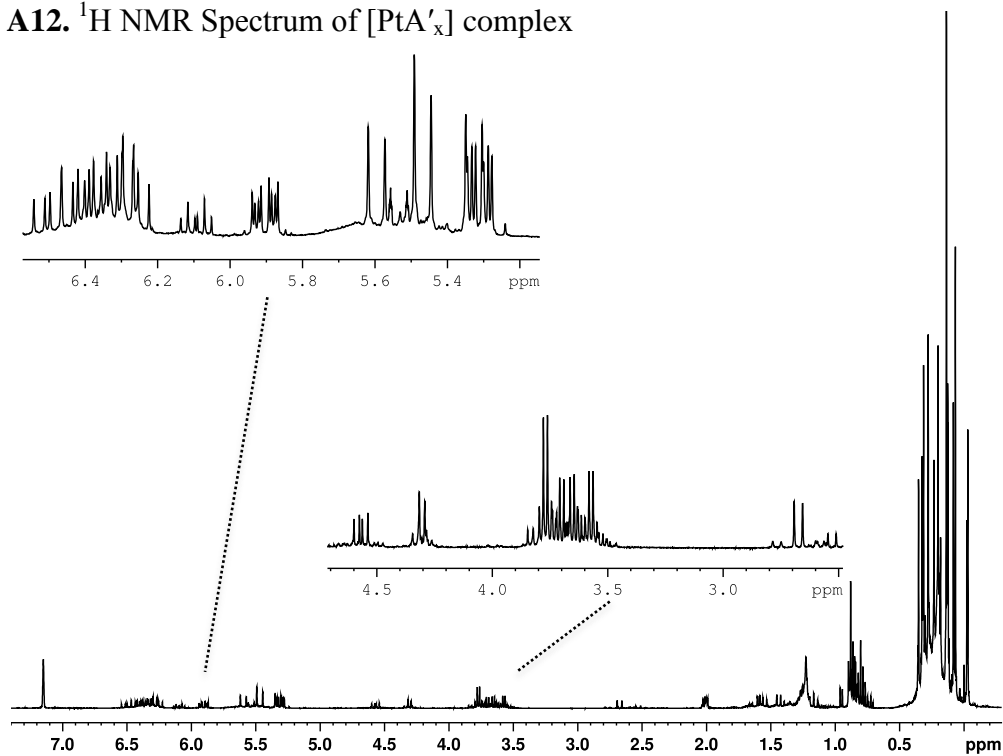


Figure A13. ^1H NMR Spectrum of $[\text{TeA}'_x]$ complex

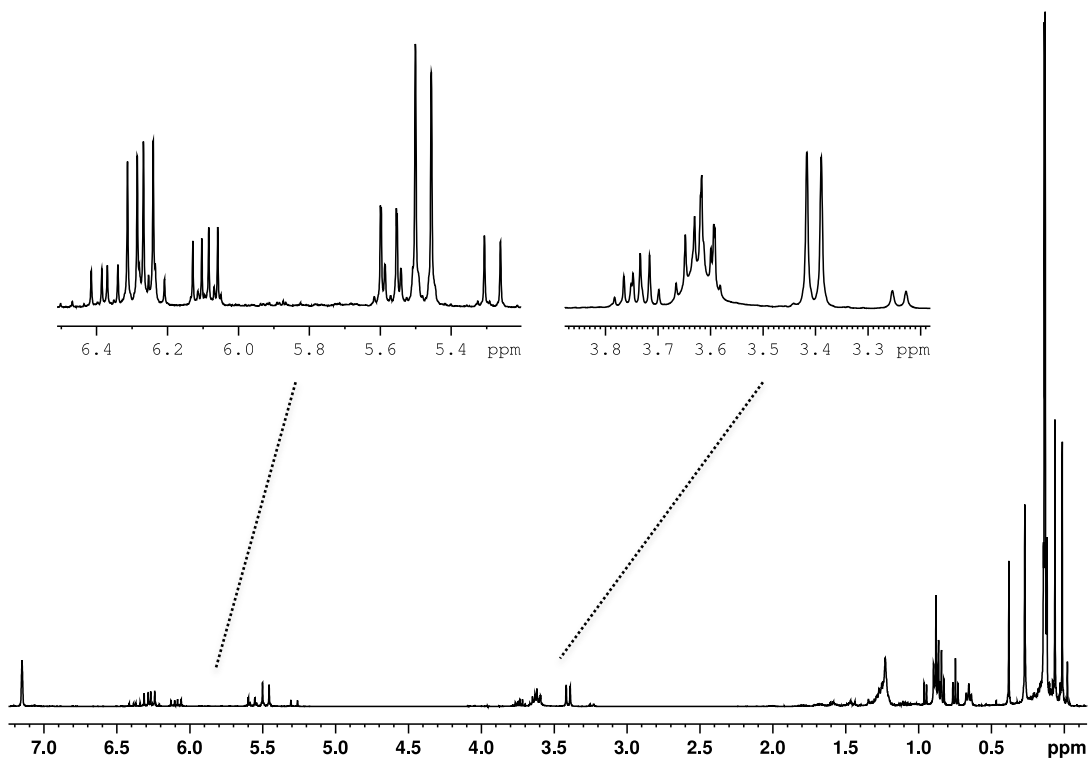
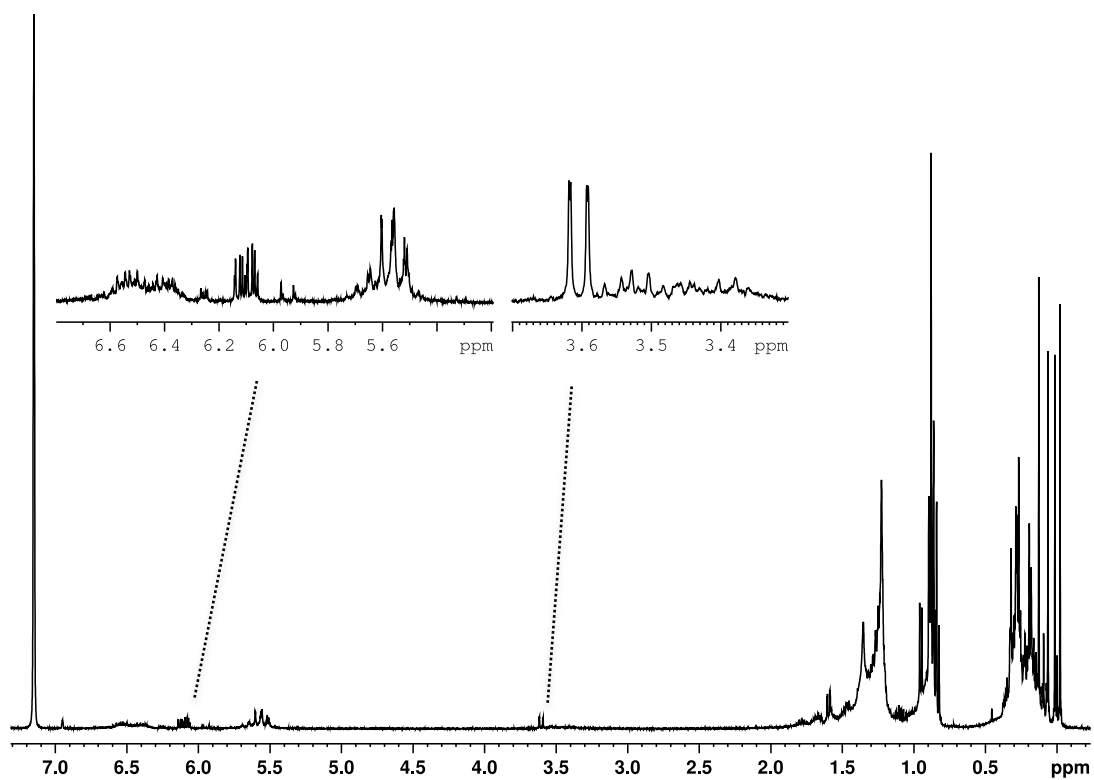


Figure A14. ^1H NMR Spectrum of $\text{UI}_4(\text{dioxane})$ reaction



Section A3

Mechanochemical Influence on Stereoisomer Formation in the Syntheses of Group 15 Bis(1,3-trimethylsilyl)allyl Complexes (As–Bi)

Figure A15. ^1H NMR Spectrum of $[\text{AsA}'_3]$ from ball milling

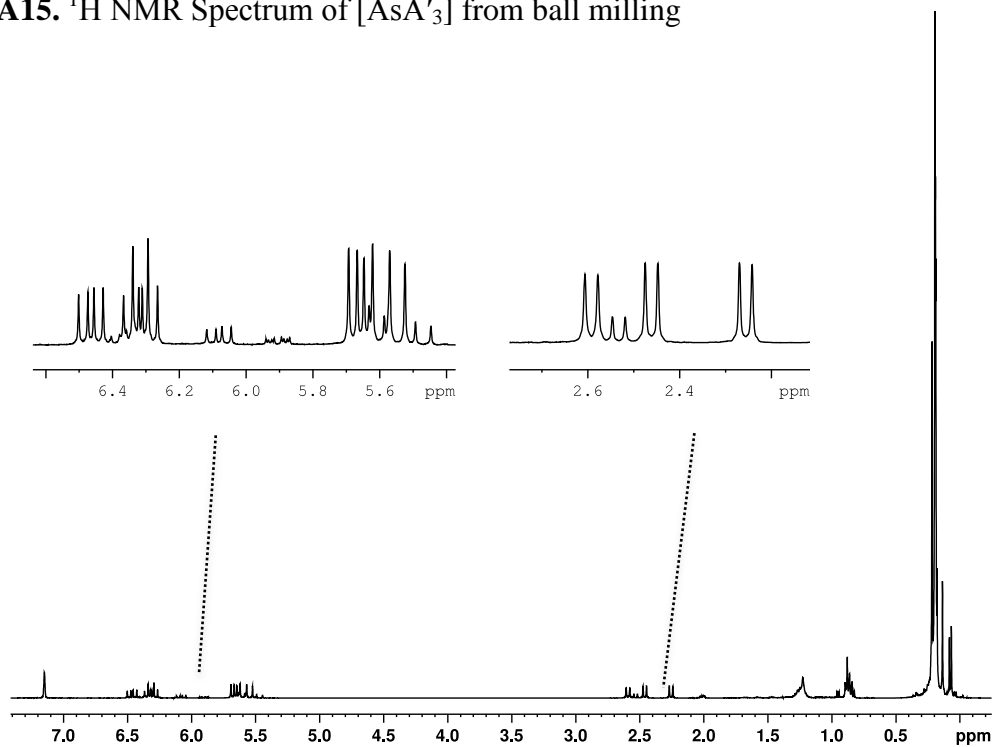


Figure A16. ^1H NMR Spectrum of $[\text{AsA}'_3]$ from solution

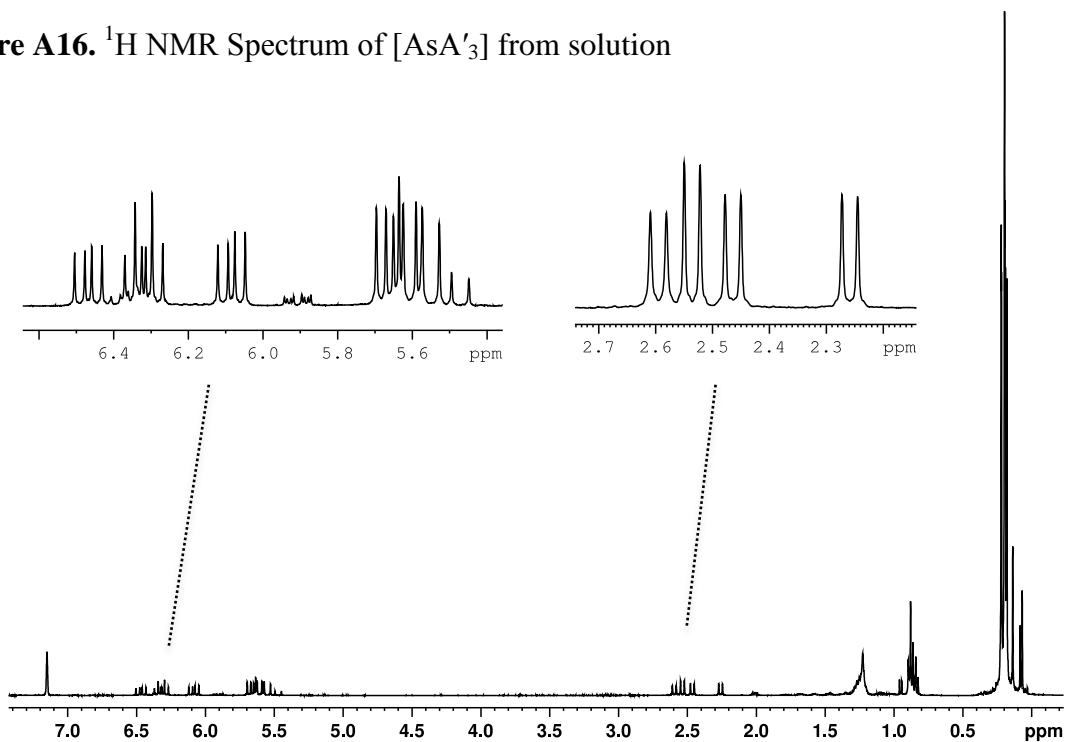


Figure A17. ^1H NMR Spectrum of $[\text{SbA}'_3]$ from ball milling

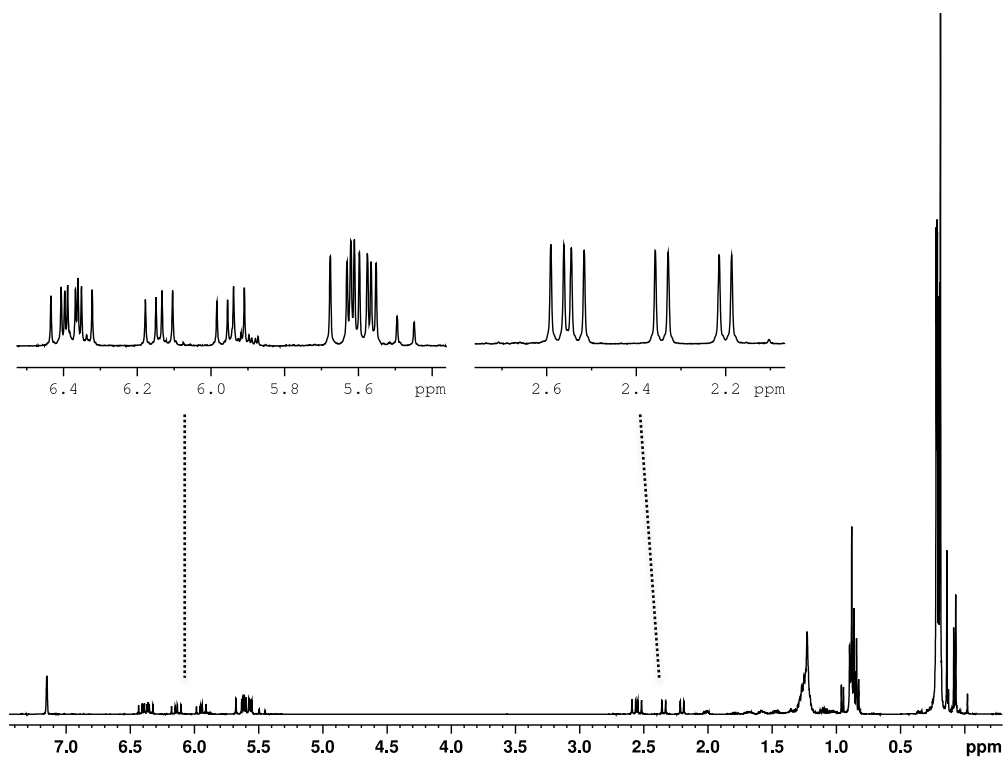


Figure A18. ^1H NMR Spectrum of $[\text{SbA}'_3]$ crystals from ball milling

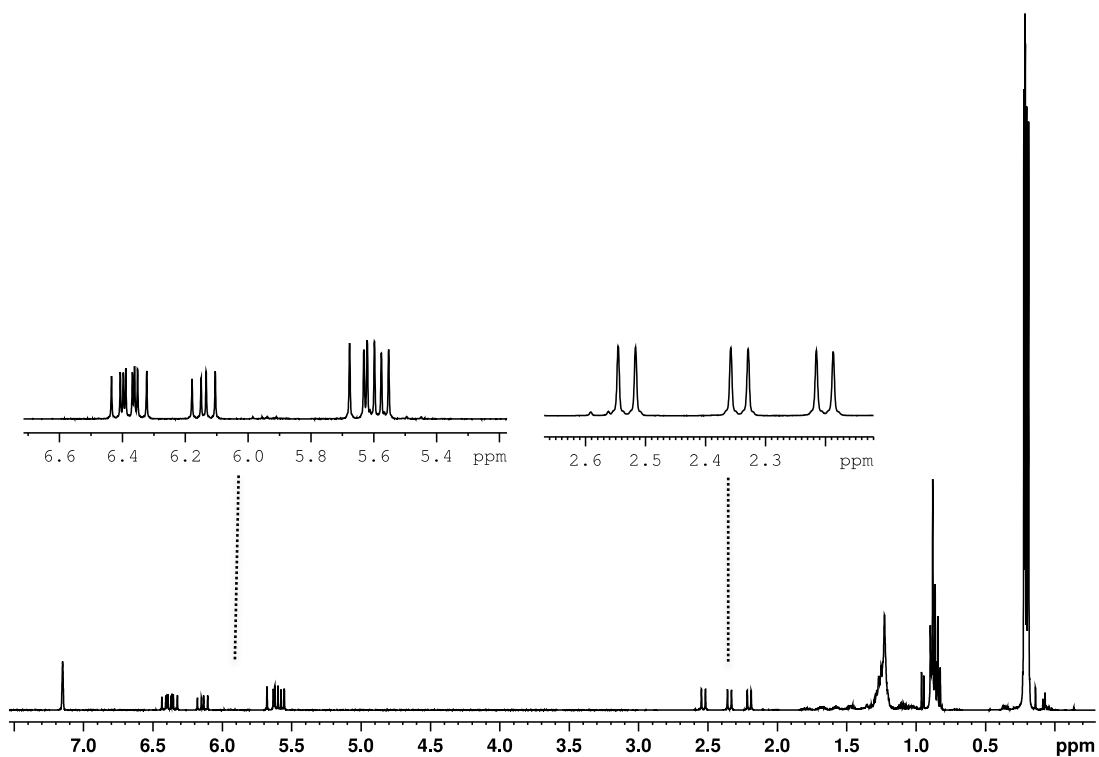


Figure A19. ^1H NMR Spectrum of $[\text{SbA}'_3]$ oil from ball milling

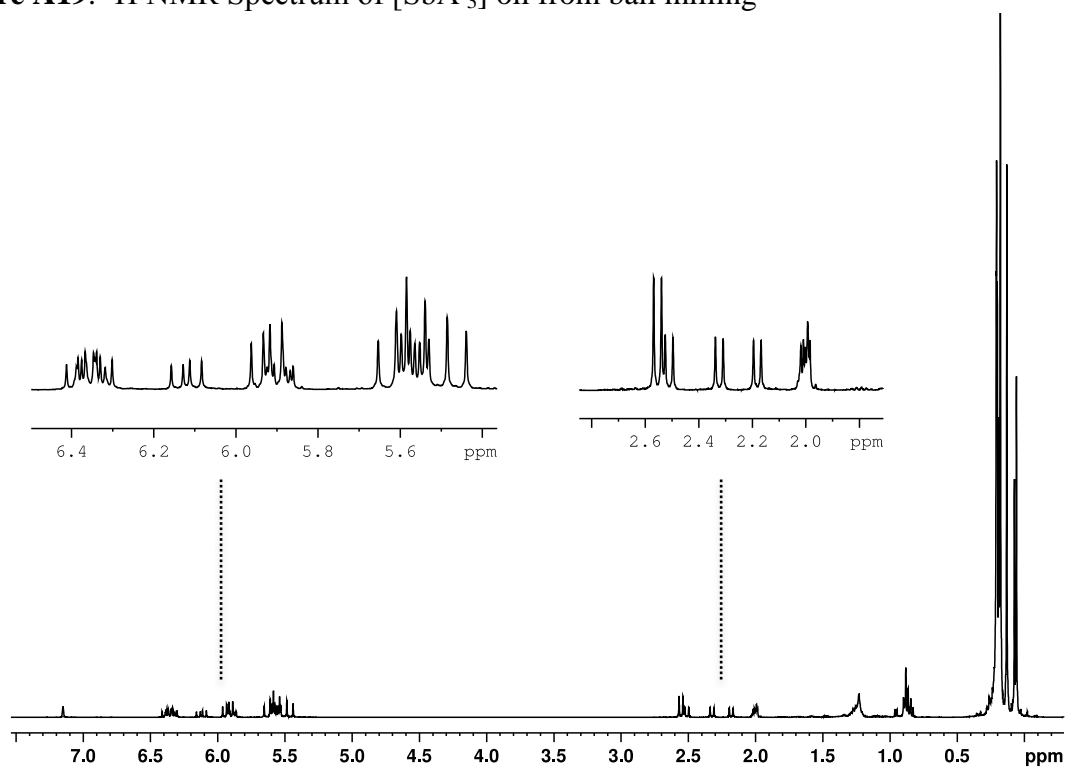


Figure A20. ^1H NMR Spectrum of $[\text{SbA}'_3]$ from solution

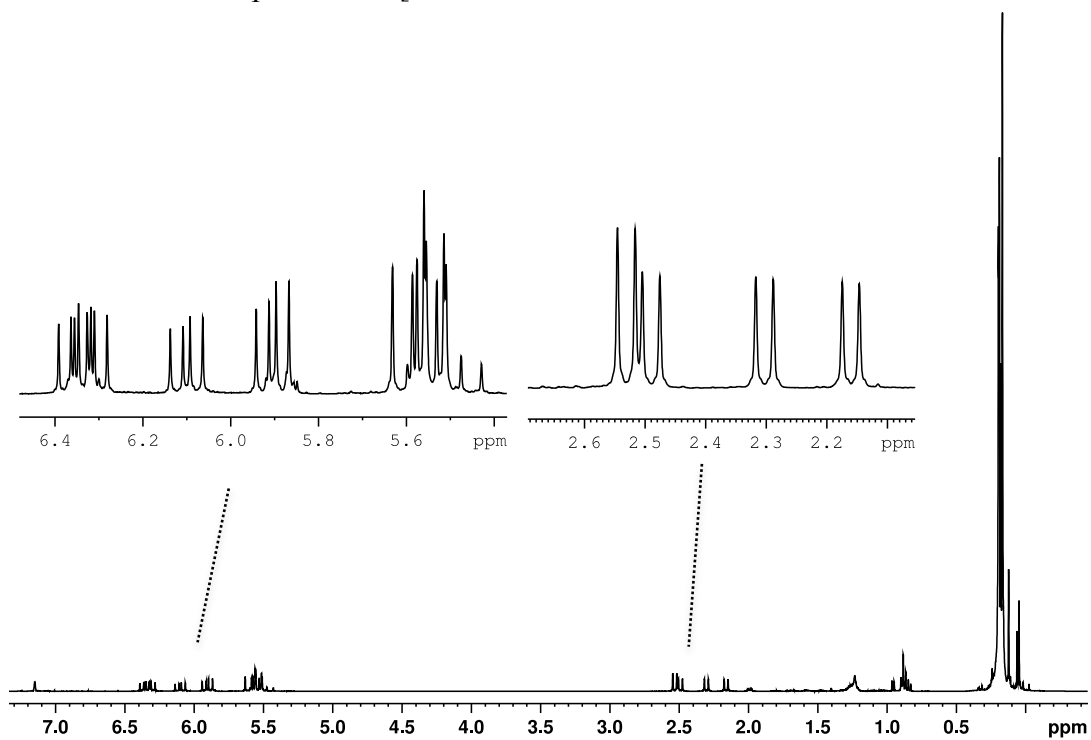


Figure A21. ^1H NMR Spectrum of $[\text{BiA}'_3]$ from solution

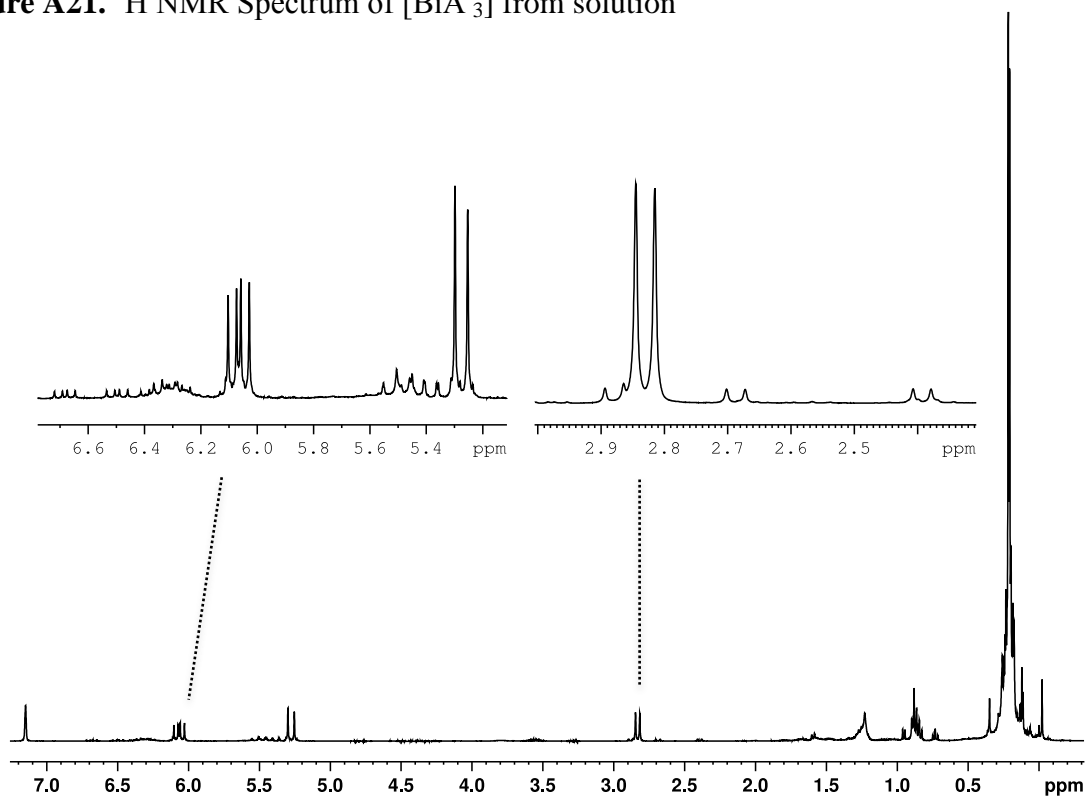
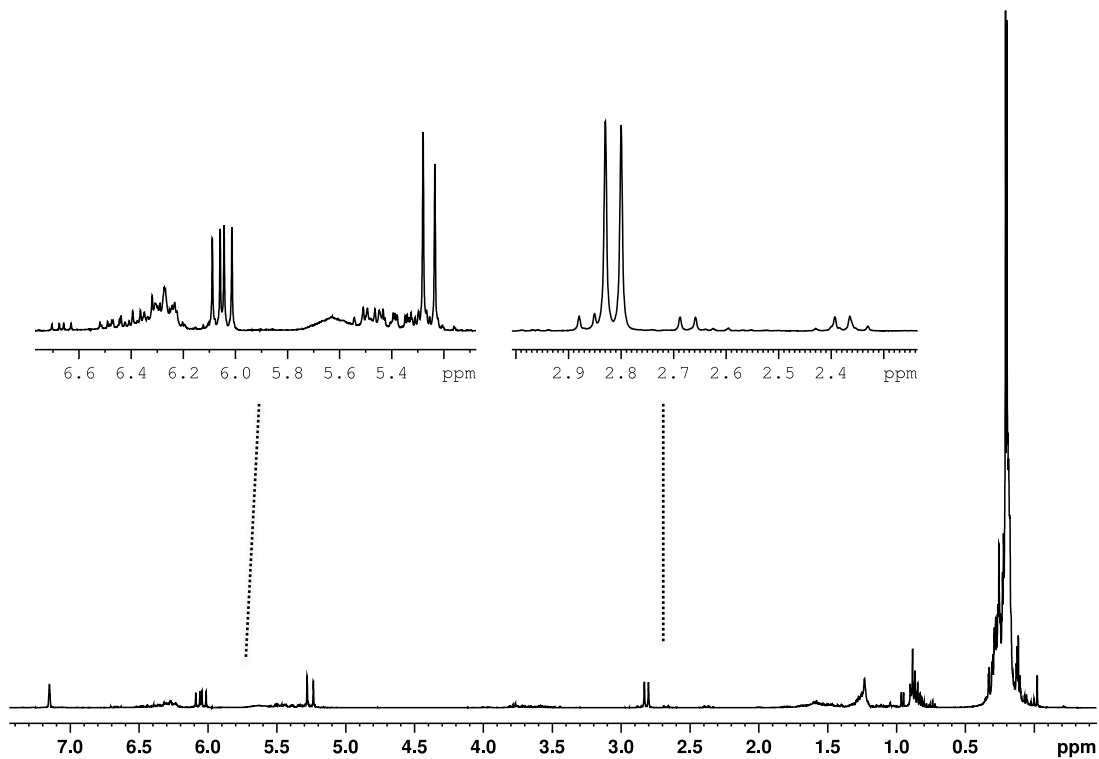


Figure A22. ^1H NMR Spectrum of $[\text{BiA}'_3]$ from ball milling



Section A4

Organometallic Mechanochemistry of s-Block Metal Complexes

Figure A23. ^1H NMR Spectrum of $\text{K}[\text{BeA}'_3]$ from Nonstoichiometric Synthesis

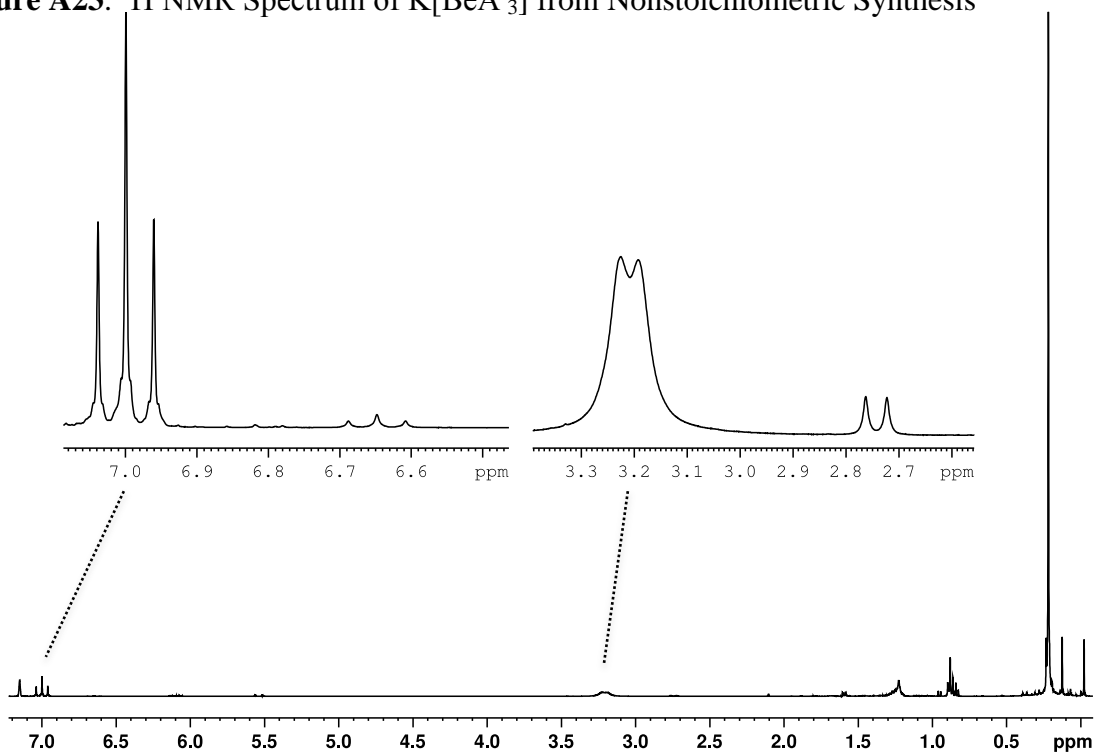


Figure A24. ^1H NMR Spectrum of $\text{K}[\text{BeA}'_3]$ from Stoichiometric Synthesis

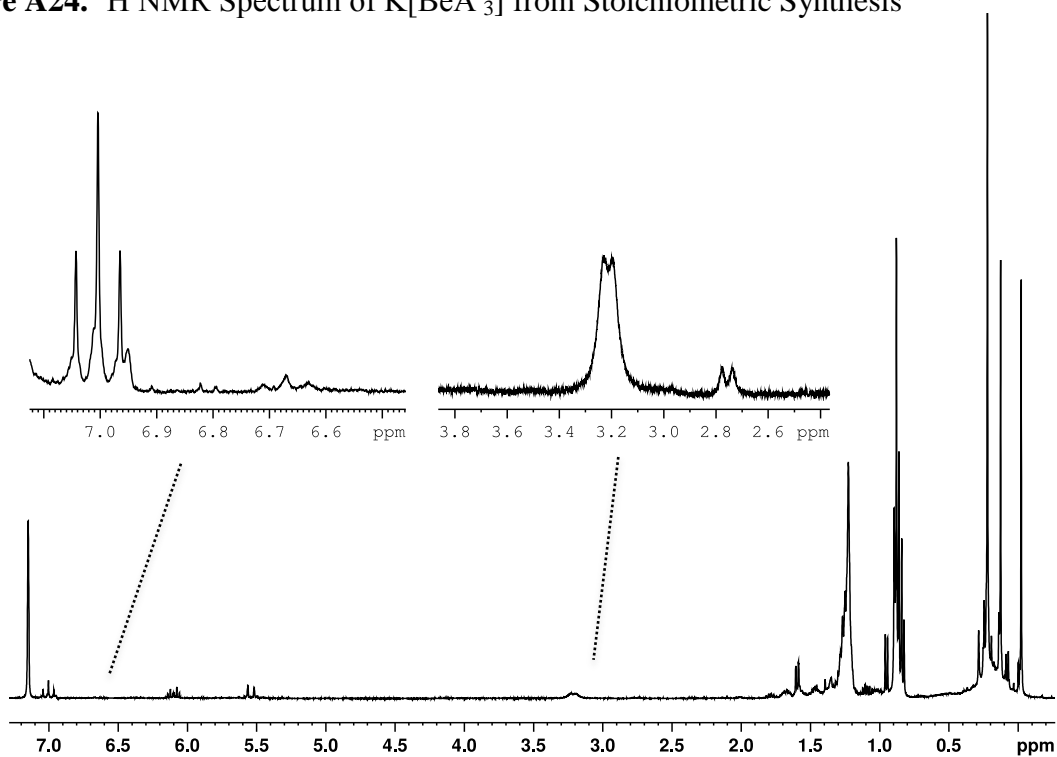


Figure A25. ^1H NMR Spectrum of $[\text{K}(\text{tol})(\mu\text{-A}')\text{K}(\text{tol})][\text{Mg}(\text{A}')(\mu\text{-A}')_2]$ from Nonstoichiometric Synthesis

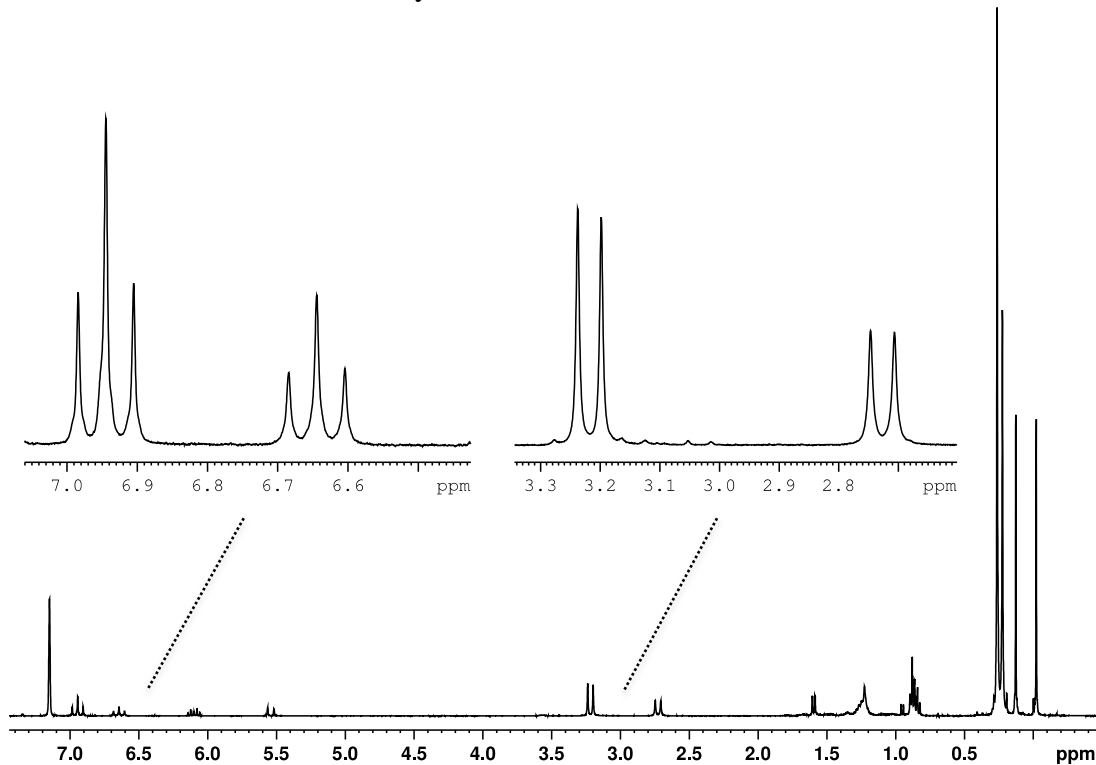


Figure A26. ^1H NMR Spectrum of $[\text{K}(\text{tol})(\mu\text{-A}')\text{K}(\text{tol})][\text{Mg}(\text{A}')(\mu\text{-A}')_2]$ from Stoichiometric Synthesis

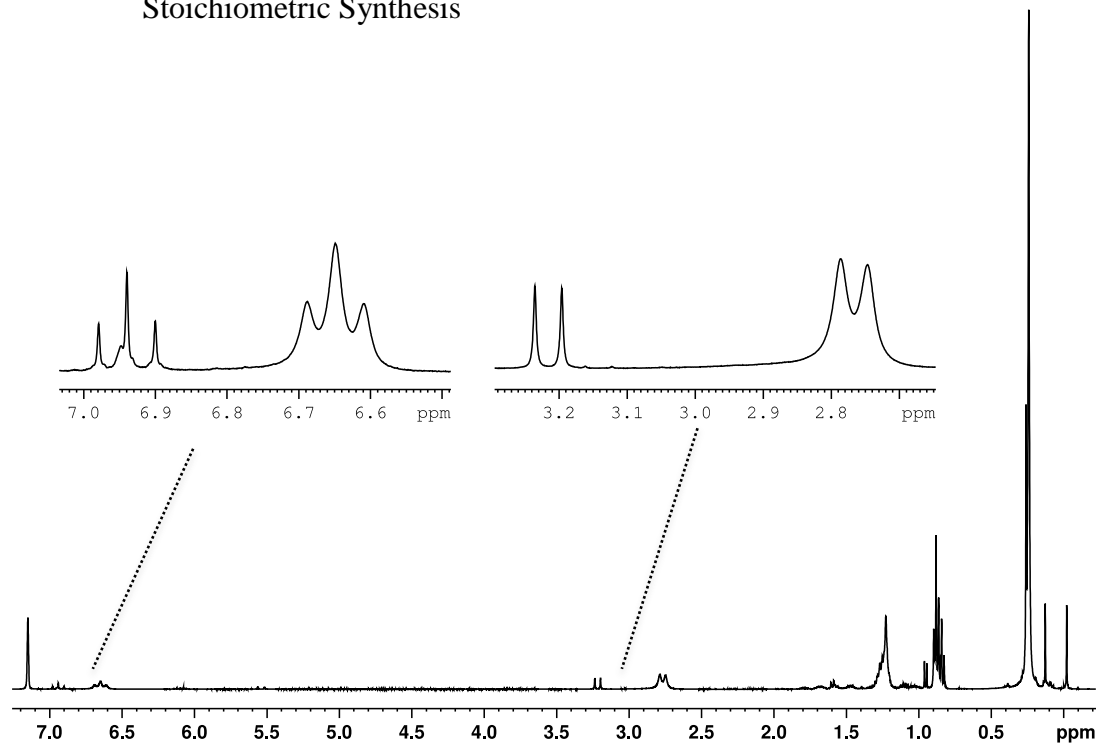


Figure A27. ^1H NMR Spectrum of yellow $[\text{CaA}'_x]$ complex

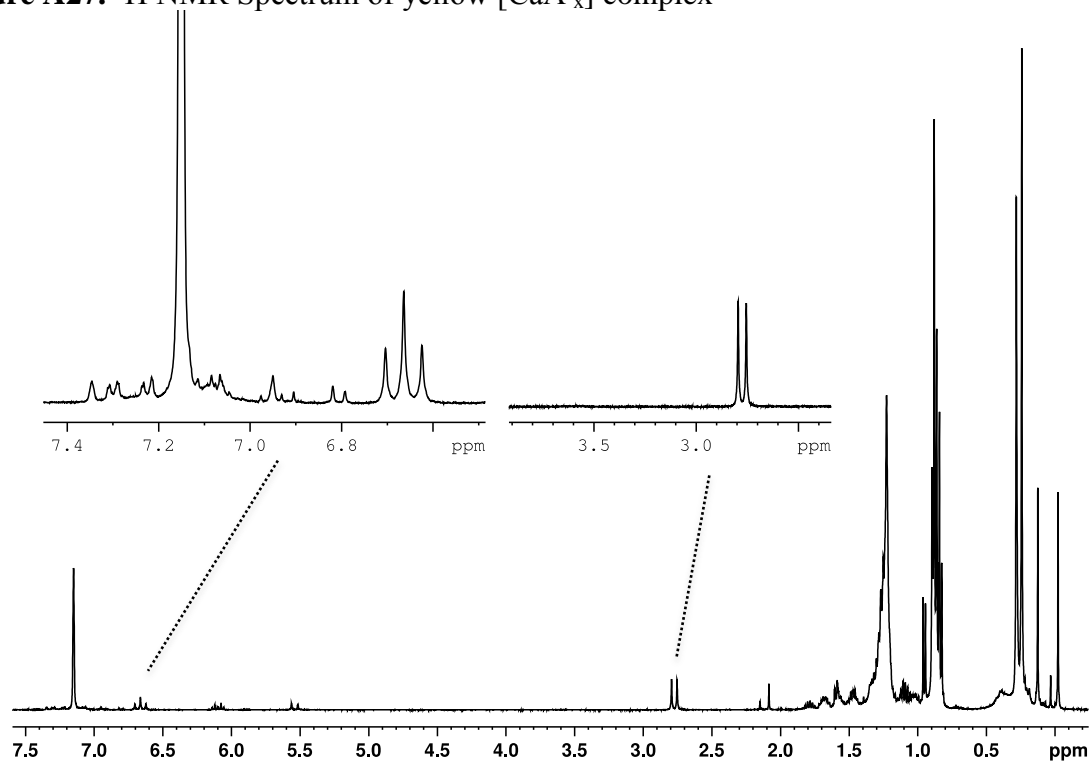


Figure A28. ^1H NMR Spectrum of orange $[\text{CaA}'_x]$ complex

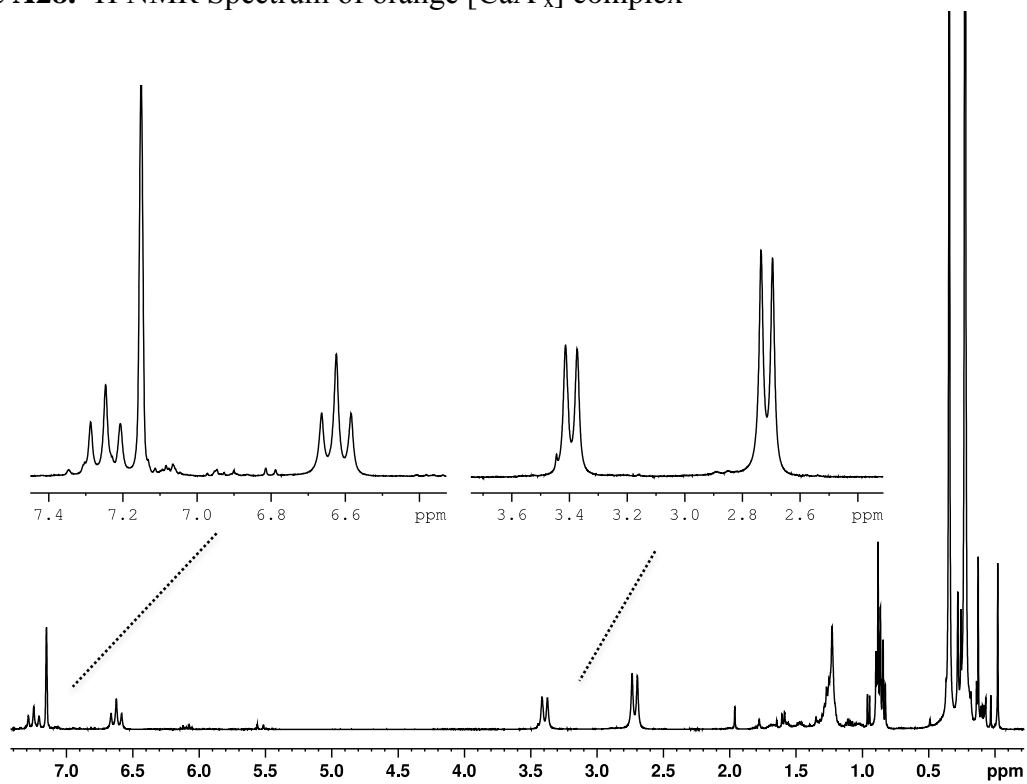


Figure A29. ^1H NMR Spectrum of $[\text{SrA}'_x]$ Complex

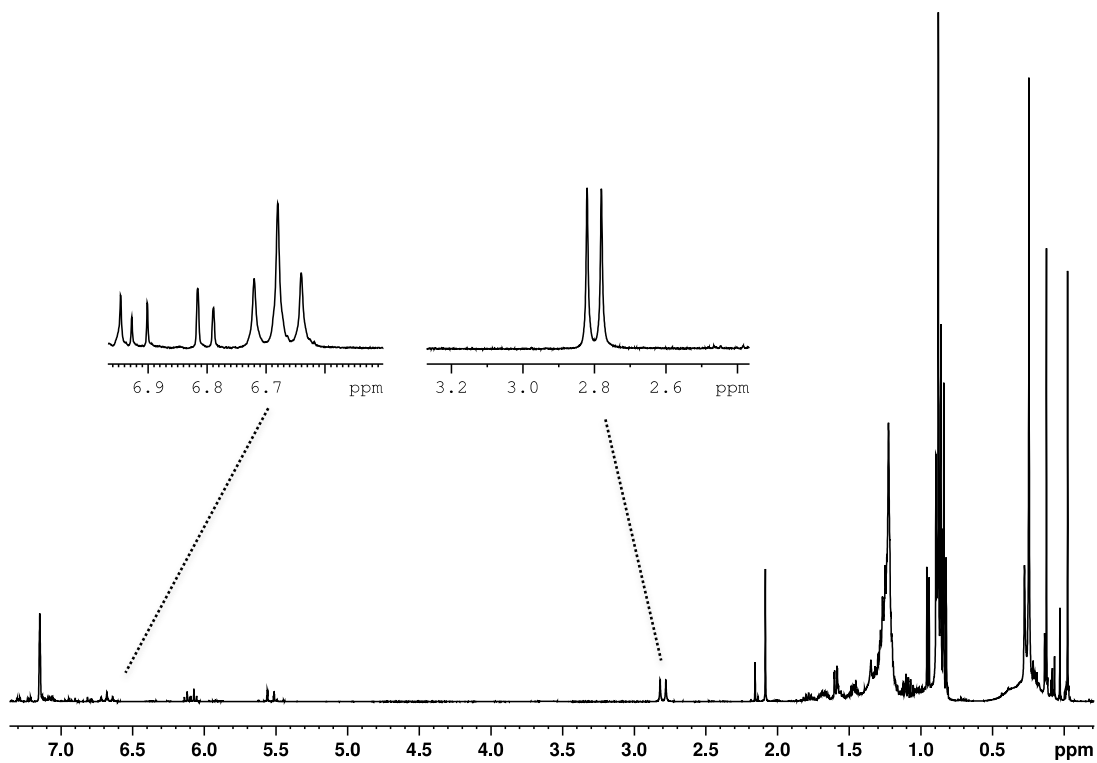
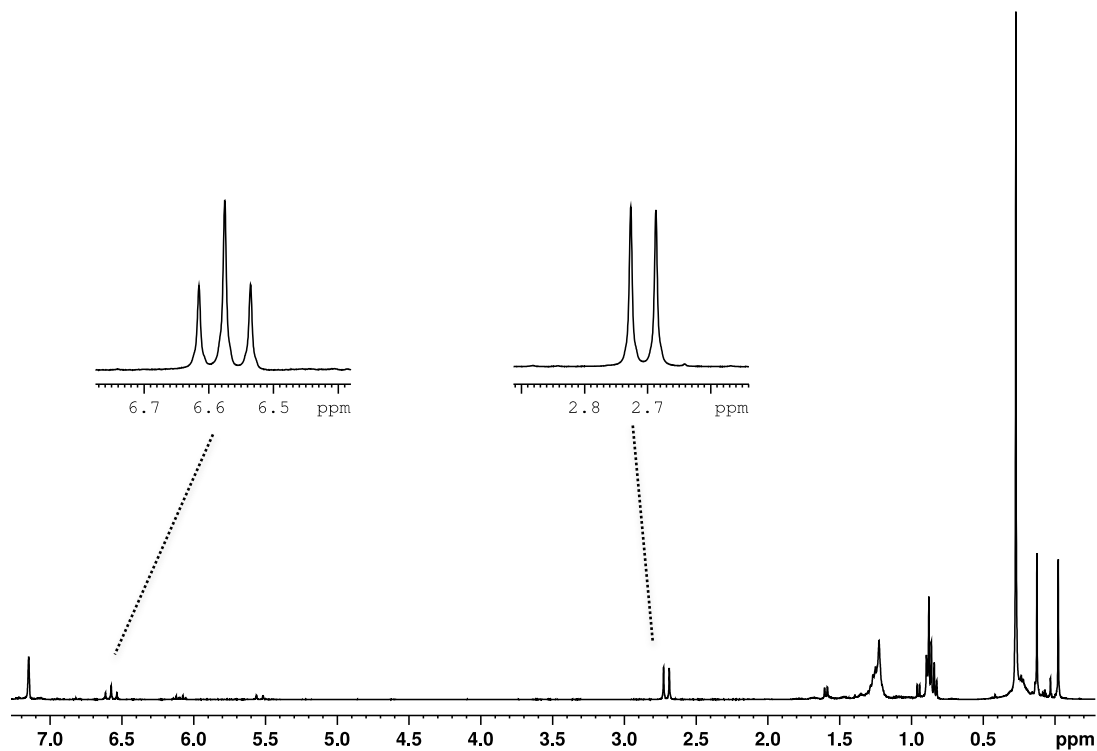


Figure A30. ^1H NMR Spectrum of $[\text{CsA}'_x]$ Complex



Section A5

Mechanochemical Investigations of d-Block and p-Block Metal Centers

Figure A31. ^1H NMR Spectrum of $[\text{YA}'_3]$

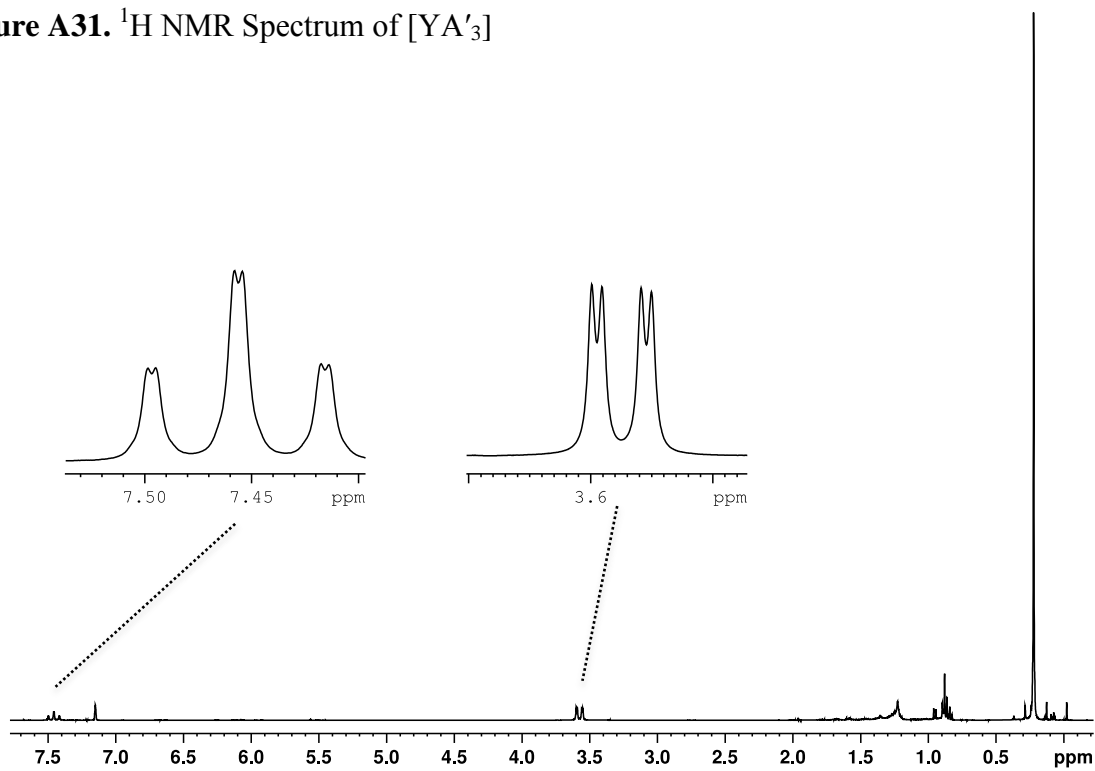


Figure A32. ^1H NMR Spectrum of $[\text{ZrA}'_4]$

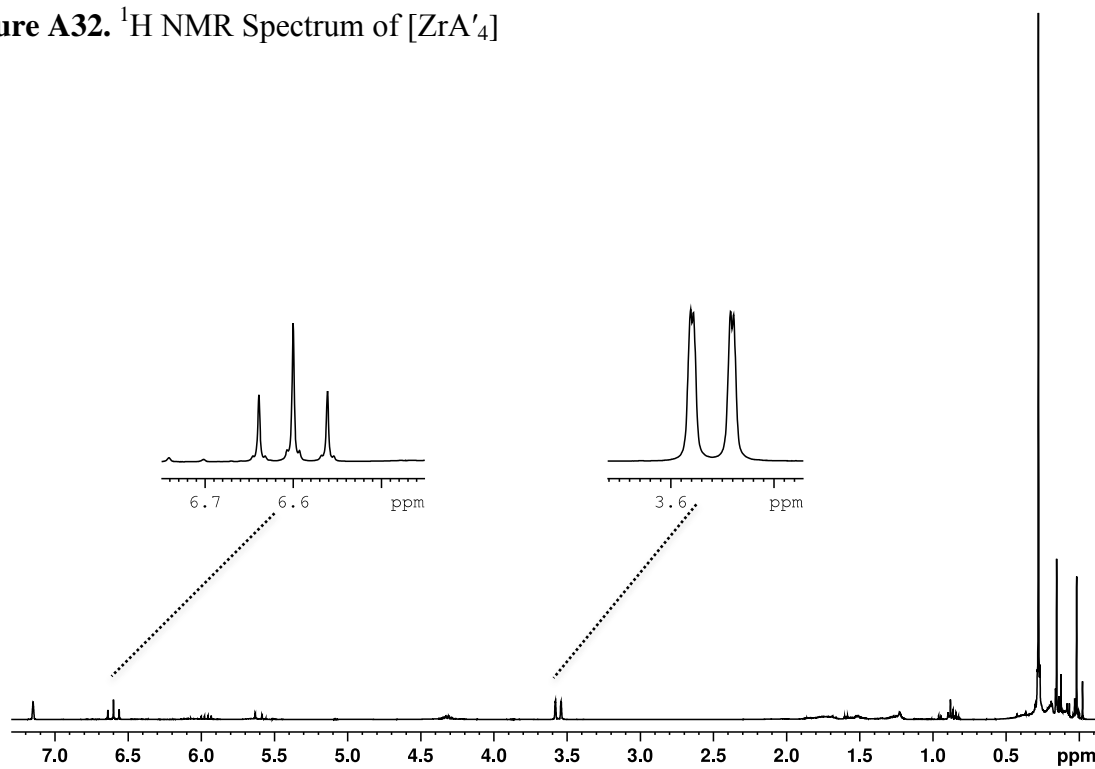


Figure A33. ^1H NMR Spectrum of $[\text{HfA}'_4]$ by ball milling

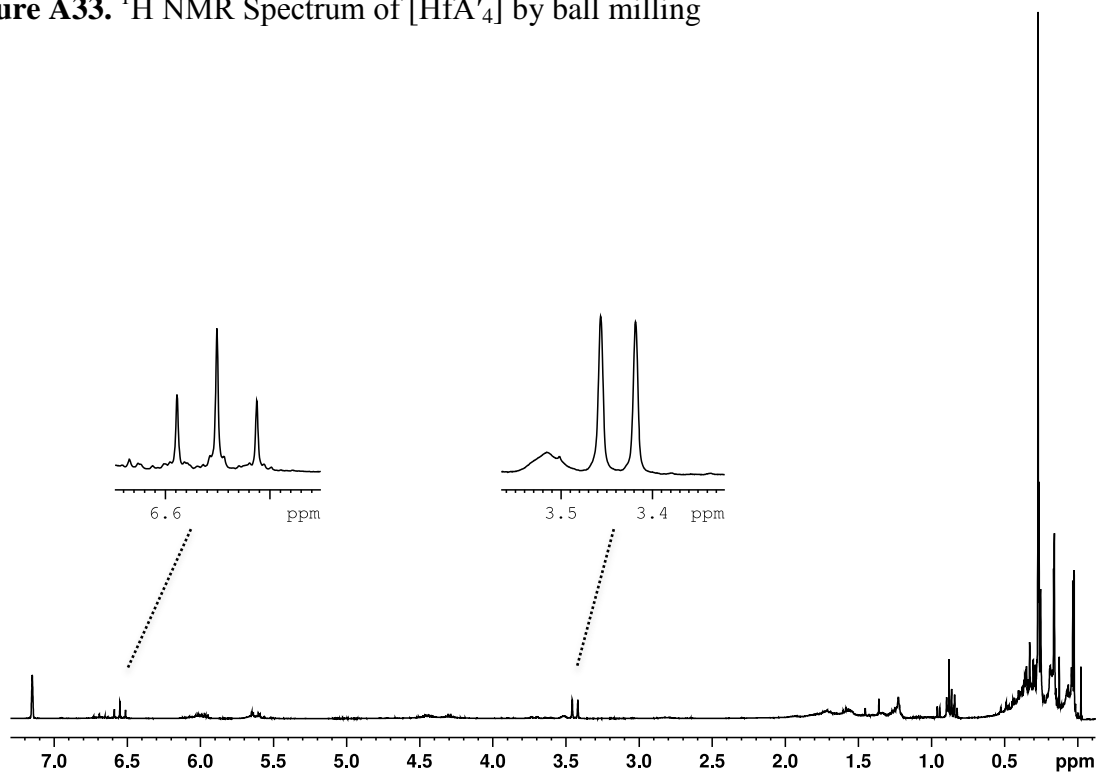


Figure A34. ^1H NMR Spectrum of $[\text{HfA}'_4]$ in solution

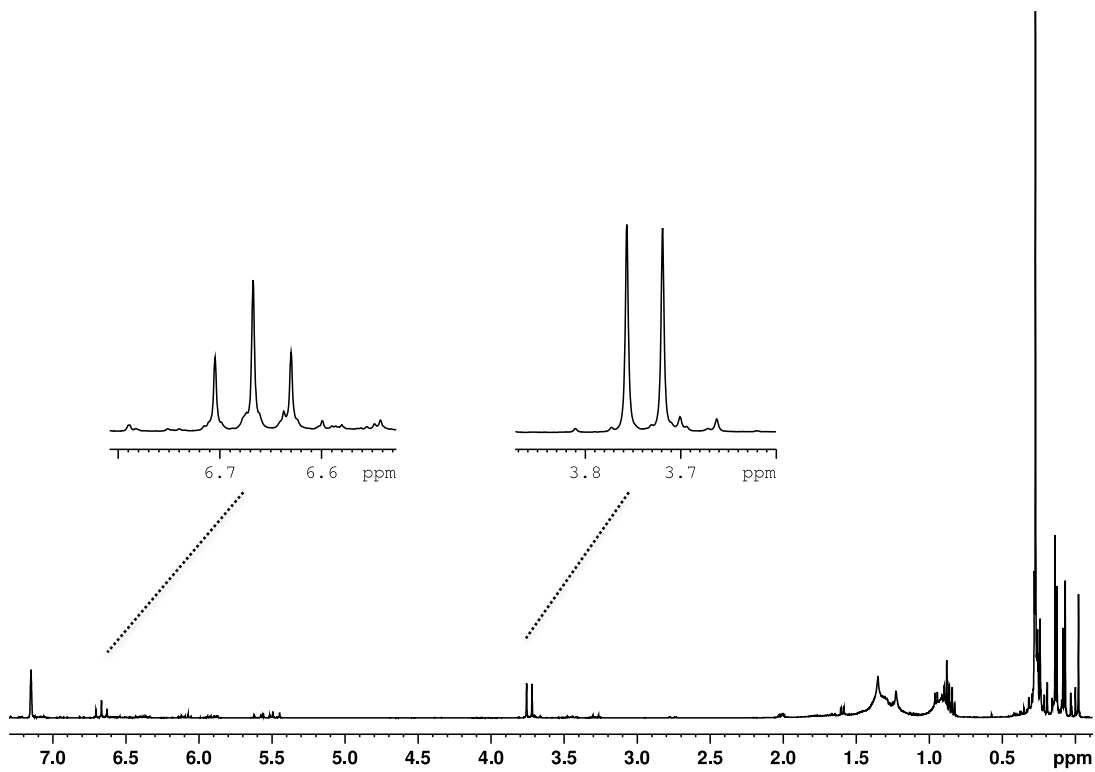


Figure A35. ^1H NMR Spectrum of a $[\text{ZnA}'_x]$ Complex

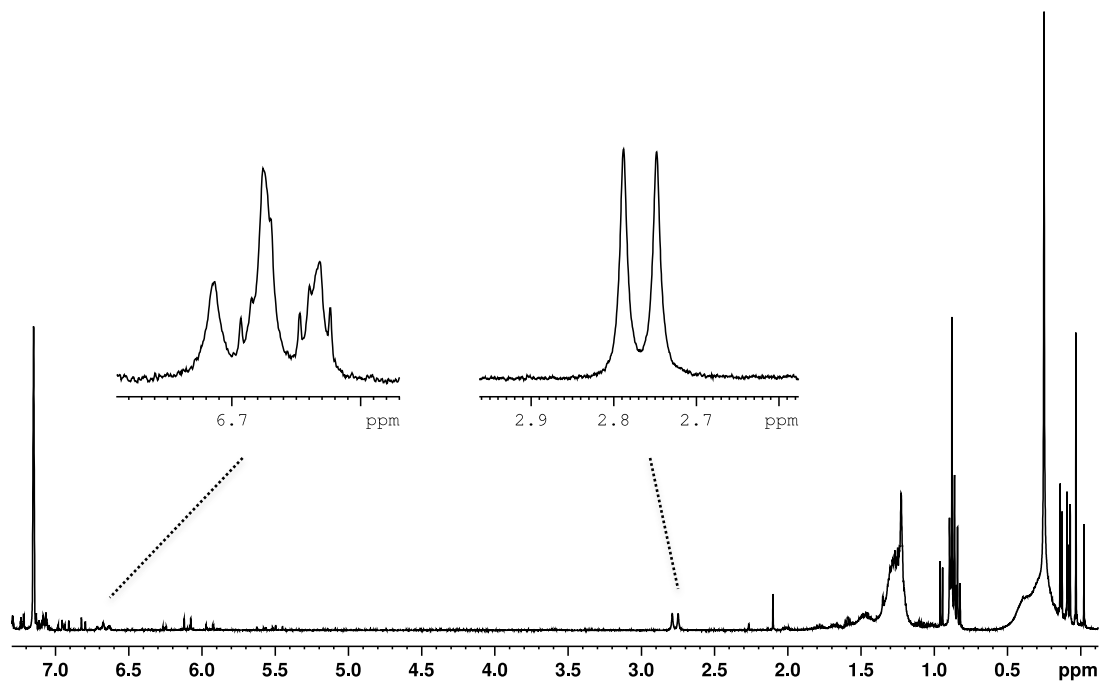


Figure A36. ^1H NMR Spectrum of a $[\text{CdA}'_x]$ complex

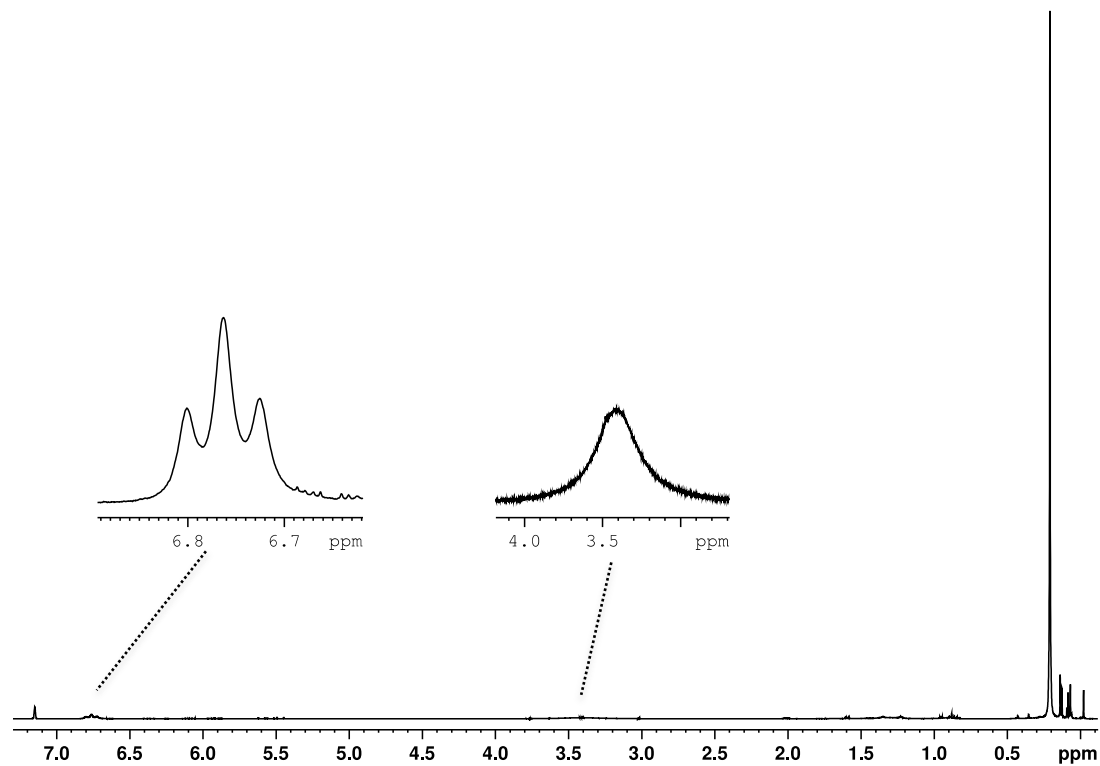


Figure A37. ^1H NMR Spectrum of a $[\text{Hg}_2\text{A}'_x]$ complex

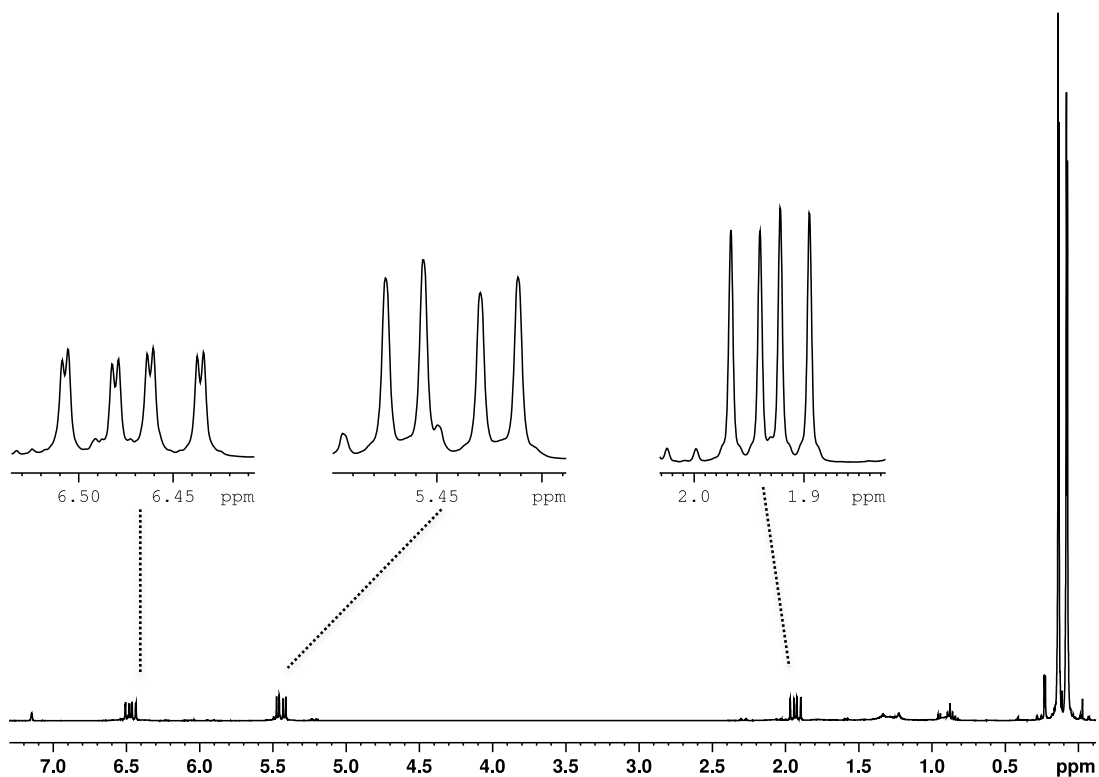


Figure A38. ^1H NMR Spectrum of a $[\text{HgA}'_x]$ complex

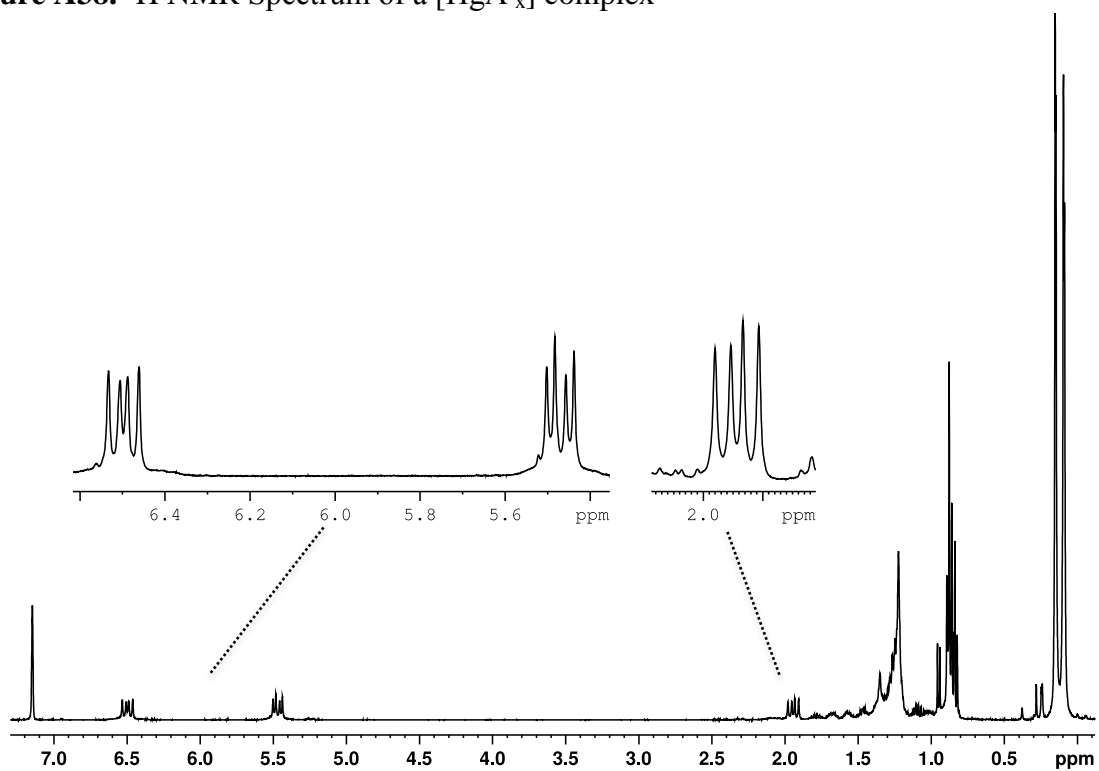


Figure A39. ^1H NMR Spectrum of $[\text{GaA}'_3]$

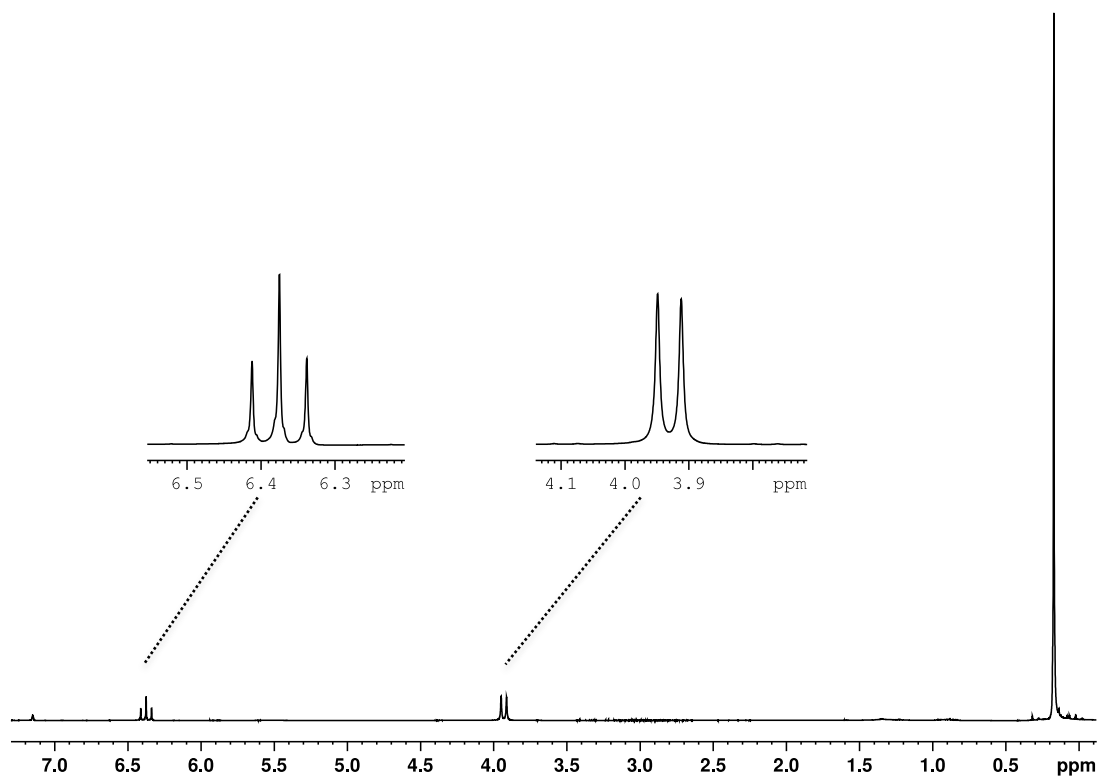
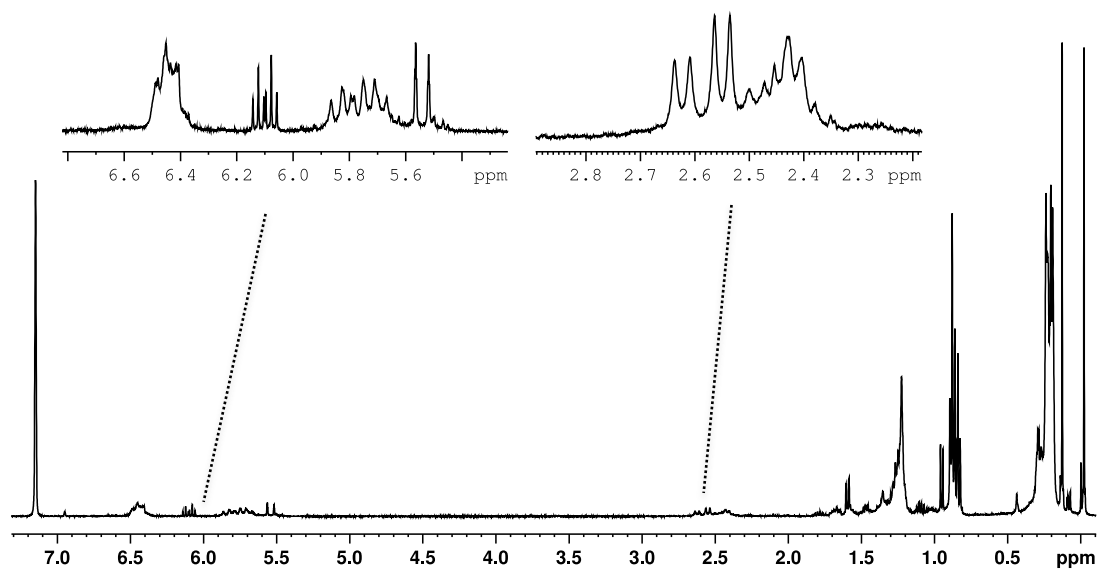


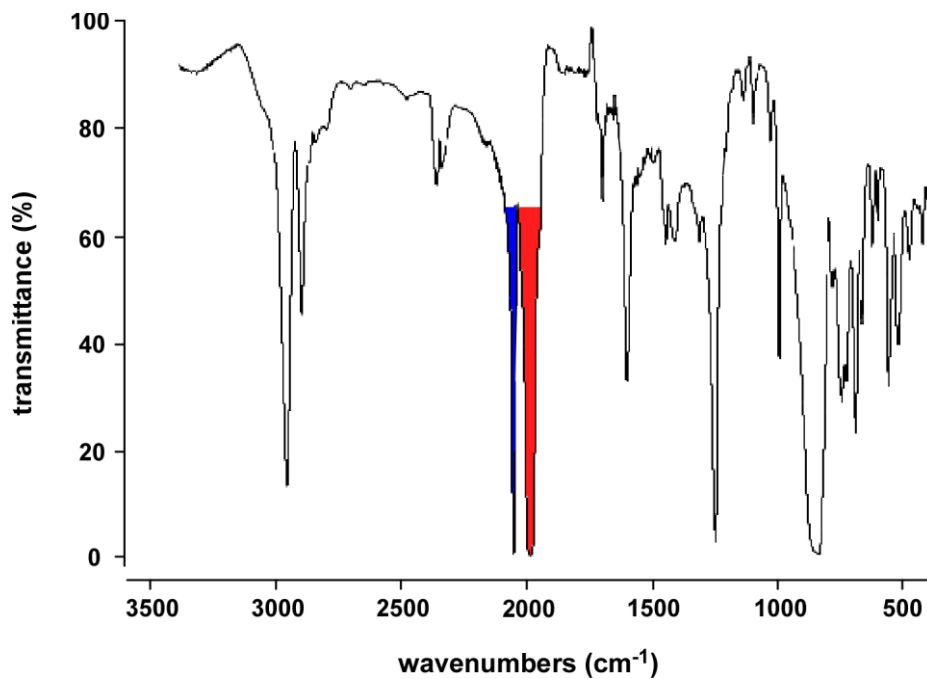
Figure A40. ^1H NMR Spectrum of an $[\text{InA}'_x]$ complex



Section A6

Balancing Adduct Formation and Ligand Coupling with the Bulky Allyl Complexes [1,3-(SiMe₃)₂C₃H₃]₂M (M = Fe, Co, Ni)

Figure A41. FT-IR spectrum of [1,3-(SiMe₃)₂C₃H₃]₂Co(CO)₃ (A'Co(CO)₃), with CO stretching frequencies (2053 cm⁻¹ (blue) and 1984 cm⁻¹ (red)). The broad 1984 cm⁻¹ peak likely represents two partially overlapped stretches.



Appendix B

Crystallographic Data

Section B1

Single Crystal Analyses of [Al(1,3-(SiMe₃)₂C₃H₃)₃] and [Sc(1,3-(SiMe₃)₂C₃H₃)₃]

General Procedures for X-ray Crystallography.

A suitable crystal of each sample was located, attached to a glass fiber, and mounted on a Bruker diffractometer for data collection at 100 K. Data collection and structure solutions for all molecules were conducted at the University of California, San Diego by Prof. Arnold L. Rheingold (Al) or at the X-ray Crystallography Facility at the University of Rochester by Dr. William W. Brennessel (Sc). The intensity data were corrected for absorption and decay (SADABS). All calculations were performed using the SHELXTL suite of programs.^[1] Final cell constants were calculated from a set of strong reflections measured during the actual data collection. The space groups were determined based on systematic absences (for ScA₃) and intensity statistics. For both the compounds, a direct-methods solution was calculated that provided most of the non-hydrogen atoms from the E-map. Several full-matrix least squares/difference Fourier cycles were performed that located the remainder of the non-hydrogen atoms. All hydrogen atoms were placed in ideal positions and refined as riding atoms with relative isotropic displacement parameters.

[ScA₃] was refined as a two-component twin, with a merohedral twin law of [0 -1 0 / -1 0 0 / 0 0 -1]. The scandium and silicon atoms were refined with anisotropic displacement parameters; the carbon and hydrogen atoms were refined with isotropic displacement parameters. The structure suffers from multiple orientations about the scandium center, two of which have been modeled (occupancy ratio, 60:40). Each potential orientation is based on the scandium center and the six silicon atoms in an approximate octahedron about it. The allyl moieties then connect the silicon atoms. In addition to all these permutations, there were peaks in the difference Fourier map which suggested that some of the allyls were also disordered over the same site, but angled in the opposite direction. The allyl C–C bond lengths were restrained to be 1.40 Å and the Si–C bond lengths were restrained to be 1.85 Å. Corresponding bond lengths and angles in each ligand were restrained to be similar. Additionally, the Sc–C(outer) bond lengths and Sc–C(inner) bond lengths were restrained to be similar.

[1] Lu, Y.; Kim, I. S.; Hassan, A.; Del, V.; David, J.; Krische, M. J., *Angew. Chem.* 2009, 121, 5118.

Table 3. Crystal Data and Summary of [Al(1,3-(SiMe₃)₂C₃H₃)₃] and [Sc(1,3-(SiMe₃)₂C₃H₃)₃]

compound	[1,3-(SiMe ₃) ₂ C ₃ H ₃] ₃ Al	[1,3-(SiMe ₃) ₂ C ₃ H ₃] ₃ Sc	
formula	C ₂₇ H ₆₃ AlSi ₆	C ₂₇ H ₆₃ ScSi ₆	
formula weight	583.29	601.27	
color of cryst	colorless	yellow	
cryst dimens, mm	0.29 x 0.24 x 0.10	0.38 x 0.24 x 0.16	
space group	<i>P</i> $\bar{1}$	<i>Pna</i> 2 ₁	
cell dimens	<i>a</i> , Å	10.2630(4)	20.353(4)
	<i>b</i> , Å	12.7306(5)	10.3936(19)
	<i>c</i> , Å	15.8391(6)	18.749(3)
	α , deg	76.9090(14)	90
	β , deg	87.3960(15)	90
	γ , deg	81.8680(15)	90
volume, Å ³	1995.20(13)	3966.2(12)	
<i>Z</i>	2	4	
calcd density, Mg/m ³	0.971	1.007	
abs coeff, mm ⁻¹	0.244	0.380	
<i>F</i> (000)	644	1320	
radiation type	Mo- <i>K</i> α (0.71073 Å)	2.00 to 25.03°	
temperature, K	100(2)	100.0(5) K	
limits of data collection	2.005 $\leq \theta \leq$ 28.304°	2.00 $\leq \theta \leq$ 25.03°	
index ranges	-13 $\leq h \leq$ 13, -14 $\leq k \leq$ 16, -15 $\leq l \leq$ 21	-24 $\leq h \leq$ 24, -12 $\leq k \leq$ 12, -22 $\leq l \leq$ 22	
total reflcns collected	12686	47647	
unique reflcns	9092 (<i>R</i> _{int} = 0.0197)	7017 (<i>R</i> (int) = 0.1035)	
transmission factors	0.932–0.976	0.8690–0.9417	
data/restraints/param	9092 / 0 / 325	7017 / 979 / 276	
<i>R</i> indices (<i>I</i> > 2 σ (<i>I</i>))	<i>R</i> ₁ = 0.0438, <i>wR</i> ₂ = 0.0657	<i>R</i> ₁ = 0.1306, <i>wR</i> ₂ = 0.3318	
<i>R</i> indices (all data)	<i>R</i> ₁ = 0.1004, <i>wR</i> ₂ = 0.1115	<i>R</i> ₁ = 0.2251, <i>wR</i> ₂ = 0.4041	
goodness of fit on <i>F</i> ²	1.014	1.189	
max/min peak in final diff map, e ⁻ /Å ³	0.791/-0.297	0.870/-0.271	
abs structure parameter	n/a	0(8)	

Table 4. Atomic coordinates ($\times 10^4$) and equivalent isotropic displacement parameters ($\text{\AA}^2 \times 10^3$) for $[1,3-(\text{SiMe}_3)_2\text{C}_3\text{H}_3]_3\text{Al}$. U_{eq} is defined as one third of the trace of the orthogonalized U_{ij} tensor.

	<i>x</i>	<i>y</i>	<i>z</i>	U_{eq}
Al(1)	3977(1)	7555(1)	7351(1)	15(1)
Si(1)	6565(1)	3641(1)	8350(1)	22(1)
Si(2)	1866(1)	6145(1)	8584(1)	17(1)
Si(3)	1832(1)	11101(1)	8377(1)	26(1)
Si(4)	6466(1)	8533(1)	7949(1)	21(1)
Si(5)	7351(1)	6241(1)	5092(1)	21(1)
Si(6)	2426(1)	8419(1)	5509(1)	20(1)
C(1)	5505(2)	4831(2)	8622(1)	24(1)
C(2)	4472(2)	5402(2)	8174(1)	21(1)
C(3)	3616(2)	6400(1)	8351(1)	18(1)
C(4)	6071(2)	3362(2)	7315(1)	31(1)
C(5)	8302(2)	3940(2)	8265(2)	34(1)
C(6)	6447(2)	2397(2)	9224(1)	32(1)
C(7)	1132(2)	5836(2)	7624(1)	24(1)
C(8)	883(2)	7371(2)	8877(1)	29(1)
C(9)	1838(2)	4937(2)	9502(1)	27(1)
C(10)	3072(2)	10386(2)	7743(1)	26(1)
C(11)	3802(2)	9421(1)	8017(1)	19(1)
C(12)	4765(2)	8821(1)	7497(1)	19(1)
C(13)	1837(3)	10373(2)	9534(2)	49(1)
C(14)	182(2)	11151(2)	7915(2)	54(1)
C(15)	2189(2)	12520(2)	8287(2)	39(1)
C(16)	7126(3)	9845(2)	7844(2)	45(1)
C(17)	7536(2)	7652(2)	7331(2)	41(1)
C(18)	6455(2)	7836(2)	9116(1)	35(1)
C(19)	5715(2)	6337(2)	5637(1)	21(1)
C(20)	4995(2)	7250(2)	5760(1)	19(1)
C(21)	3661(2)	7371(1)	6184(1)	17(1)
C(22)	7782(2)	7626(2)	4618(2)	39(1)
C(23)	7286(2)	5482(2)	4216(1)	39(1)
C(24)	8662(2)	5485(2)	5862(1)	32(1)
C(25)	1125(2)	8992(2)	6206(2)	40(1)
C(26)	1645(2)	7784(2)	4745(2)	40(1)
C(27)	3258(2)	9557(2)	4865(2)	37(1)

Table 5. Atomic coordinates ($\times 10^4$) and equivalent isotropic displacement parameters ($\text{\AA}^2 \times 10^3$) for $[1,3-(\text{SiMe}_3)_2\text{C}_3\text{H}_3]_3\text{Sc}$. U_{eq} is defined as one third of the trace of the orthogonalized U_{ij} tensor.

	<i>x</i>	<i>y</i>	<i>z</i>	U_{eq}
Sc1	3762(1)	1074(1)	2674(2)	80(1)
C1	4258(14)	4250(20)	4153(14)	265(16)
C2	5499(12)	4000(30)	4111(15)	282(18)
C3	4588(15)	1890(20)	4844(10)	223(13)
Si1	4729(6)	3018(9)	4106(4)	167(4)
C4	4628(7)	2096(13)	3295(5)	122(6)
C5	4633(6)	2687(13)	2621(5)	113(5)
C6	4578(9)	2080(16)	1963(6)	214(12)
Si2	4643(4)	2857(11)	1105(5)	162(4)
C7	5515(8)	3290(30)	1024(17)	272(16)
C8	4019(13)	4120(30)	932(17)	231(12)
C9	4420(19)	1950(30)	459(13)	770(100)
C10	5478(10)	-1120(20)	2042(12)	210(11)
C11	4953(12)	-3320(20)	1953(14)	237(14)
C12	5250(12)	-2010(30)	3460(10)	225(12)
Si3	4967(4)	-1888(6)	2536(5)	121(3)
C13	4175(6)	-1084(12)	2611(8)	147(6)
C14	3855(6)	-1016(13)	3270(7)	105(5)
C15	3247(6)	-476(15)	3415(7)	157(7)
Si4	2849(5)	-740(12)	4269(5)	135(3)
C16	2123(9)	-1700(20)	4018(12)	164(8)
C17	2763(16)	700(30)	4836(15)	320(17)
C18	3315(13)	-1520(30)	4804(13)	290(19)
C19	2514(15)	5198(19)	2279(18)	430(30)
C20	2542(14)	4350(30)	3570(12)	253(16)
C21	1600(9)	3120(30)	2396(18)	289(17)
Si5	2395(5)	3828(11)	2643(9)	169(3)
C22	2973(6)	2640(12)	2310(9)	161(7)
C23	2756(7)	1512(13)	1982(8)	112(5)
C24	3164(7)	668(14)	1598(7)	132(6)
Si6	2791(6)	-716(14)	1161(7)	148(3)
C25	2117(15)	-1170(40)	1760(20)	470(30)
C26	3398(12)	-1920(20)	859(15)	208(10)
C27	2518(16)	-350(30)	387(13)	370(30)
C1'	1909(11)	-1050(30)	4079(16)	164(8)
C2'	2480(20)	650(40)	4843(15)	320(17)
C3'	3237(18)	-1830(40)	4250(20)	290(19)
Si1'	2649(9)	-510(20)	4125(7)	135(3)
C4'	2871(10)	208(19)	3276(8)	157(7)
C5'	2876(9)	-530(18)	2657(7)	125(7)
C6'	3115(9)	-330(20)	1976(7)	132(6)
Si2'	2615(10)	-490(20)	1179(8)	148(3)
C7'	1928(17)	-1520(50)	1460(20)	470(30)
C8'	3091(18)	-880(40)	365(12)	208(10)
C9'	2350(20)	870(40)	900(20)	370(30)
C10'	5652(12)	-2180(30)	2350(15)	210(11)
C11'	4698(15)	-3280(20)	2980(20)	237(14)
C12'	5459(18)	-860(30)	3649(14)	225(12)
Si3'	5085(6)	-1687(11)	2884(7)	121(3)
C13'	4587(7)	-468(14)	2458(11)	147(6)

C14'	4837(8)	611(18)	2119(12)	135(10)
C15'	4486(8)	1510(20)	1715(13)	214(12)
Si4'	4928(6)	2692(17)	1186(9)	162(4)
C16'	5310(30)	3770(40)	1840(20)	770(100)
C17'	4466(16)	3360(50)	420(19)	272(16)
C18'	5472(15)	1990(40)	702(18)	231(12)
C19'	2730(19)	5600(20)	2770(30)	430(30)
C20'	2064(17)	4030(40)	3536(19)	253(16)
C21'	2227(19)	3640(50)	1864(19)	289(17)
Si5'	2585(8)	4087(17)	2728(12)	169(3)
C22'	3347(9)	3185(16)	2777(10)	161(7)
C23'	3685(9)	3029(19)	3414(10)	124(9)
C24'	4258(9)	2333(19)	3550(10)	122(6)
Si6'	4737(9)	2579(15)	4350(7)	167(4)
C25'	4184(19)	3500(40)	4935(16)	265(16)
C26'	5581(13)	3190(50)	4200(20)	282(18)
C27'	4967(18)	1280(30)	4733(17)	223(13)

Section B2

Single Crystal Analysis of [As(1,3-(SiMe₃)₂C₃H₃)₂]

Data Collection

A crystal (0.24 x 0.14 x 0.08 mm³) was placed onto the tip of a 0.1 mm diameter glass capillary tube or fiber and mounted on a Bruker SMART APEX II CCD platform diffractometer for a data collection at 100.0(5) K.^[1] A preliminary set of cell constants and an orientation matrix were calculated from reflections harvested from three orthogonal wedges of reciprocal space. The full data collection was carried out using MoK α radiation (graphite monochromator) with a frame time of 90 seconds and a detector distance of 4.02 cm. A randomly oriented region of reciprocal space was surveyed: six major sections of frames were collected with 0.50° steps in ω at six different ϕ settings and a detector position of -38° in 2θ . The intensity data were corrected for absorption.^[2] Final cell constants were calculated from the xyz centroids of 4079 strong reflections from the actual data collection after integration.³

Structure Solution and Refinement

The structure was solved using SIR2011^[4] and refined using SHELXL-2014.^[5] The space group $P-1$ was determined based on intensity statistics. A direct-methods solution was calculated which provided most non-hydrogen atoms from the E-map. Full-matrix least squares / difference Fourier cycles were performed which located the remaining non-hydrogen atoms. All non-hydrogen atoms were refined with anisotropic displacement parameters. All hydrogen atoms were placed in ideal positions and refined as riding atoms with relative isotropic displacement parameters. The final full matrix least squares refinement converged to $R1 = 0.0493$ (F^2 , $I > 2\sigma(I)$) and $wR2 = 0.1067$ (F^2 , all data). The asymmetric unit contains one [As(1,3-(SiMe₃)₂C₃H₃)₃] molecule in a general position.

[1] APEX2, version 2013.10-0; Bruker AXS: Madison, WI, 2013.

[2] G. M. Sheldrick, SADABS, version 2012/1; University of Göttingen: Göttingen, Germany, 2012.

[3] SAINT, version 8.34A; Bruker AXS: Madison, WI, 2013.

[4] M. C. Burla, R. Caliendo, M. Camalli, B. Carrozzini, G. L. Cascarano, C. Giacovazzo, M. Mal-lamo, A. Mazzone, G. Polidori, R. Spagna, SIR2011: a new package for crystal structure determination and refinement, version 1.0; Istituto di Cristallografia: Bari, Italy, 2012.

[5] G. M. Sheldrick, SHELXL-2014/3; University of Göttingen: Göttingen, Germany, 2014.

Table 6. Crystal Data and Summary of [As(1,3-(SiMe₃)₂C₃H₃)₃] and [Sb(1,3-(SiMe₃)₂C₃H₃)₃]

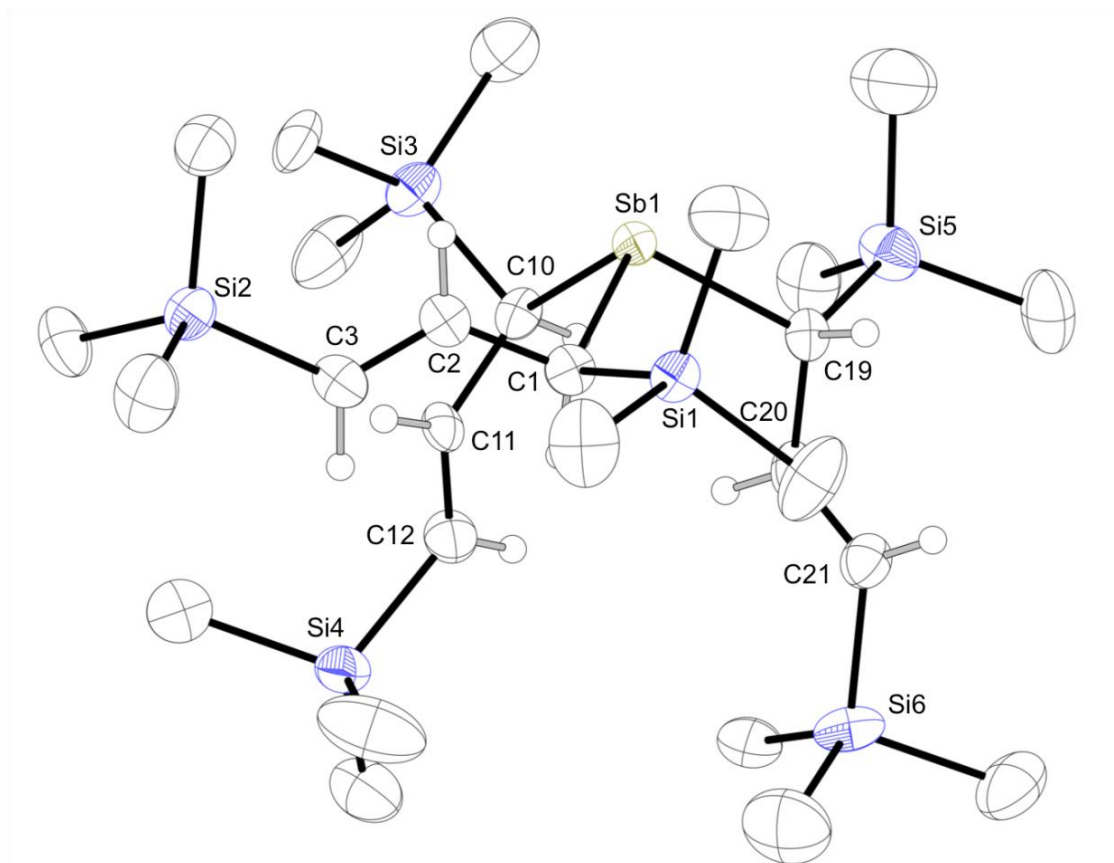
compound	As[1,3-(SiMe ₃) ₂ C ₃ H ₃] ₃	Sb[1,3-(SiMe ₃) ₂ C ₃ H ₃] ₃
formula	C ₂₇ H ₆₃ AsSi ₆	C ₂₇ H ₆₃ SbSi ₆
formula weight	631.23	678.07
color of cryst	colorless	colorless
cryst dimens, mm	0.24 x 0.14 x 0.08	0.26 x 0.16 x 0.12
space group	<i>P</i> 1	<i>P</i> 1
cell dimens	<i>a</i> , Å	
	10.539(2)	10.643(4)
	<i>b</i> , Å	
	10.791(2)	10.792(4)
	<i>c</i> , Å	
	19.921(4)	20.226(7)
	∠, deg	
	99.233(4)	81.289(7)
	∠, deg	
	90.021(4)	89.569(7)
	∠, deg	
	118.479(4)	61.724(6)
volume, Å ³	1957.9(7)	2017.0(12)
<i>Z</i>	2	2
calcd density, Mg/m ³	1.071	1.116
abs coeff, mm ⁻¹	1.065	0.876
<i>F</i> (000)	684	720
radiation type	Mo- <i>K</i> α(0.71073 Å)	Mo- <i>K</i> α(0.71073 Å)
temperature, K	100.0(5)	100.0(5)
limits of data collection	2.21 ≤ θ ≤ 28.21 °	1.02 ≤ θ ≤ 33.81 °
index ranges	-14 ≤ <i>h</i> ≤ 14, -14 ≤ <i>k</i> ≤ 14, -27 ≤ <i>l</i> ≤ 27	-16 ≤ <i>h</i> ≤ 16, -16 ≤ <i>k</i> ≤ 16, -31 ≤ <i>l</i> ≤ 31
total reflns collected	44 064	55 659
unique reflns	11 007 (<i>R</i> _{int} = 0.0925)	16 088 (<i>R</i> _{int} = 0.0432)
transmission factors	0.6653–0.7459	0.3741–0.4359
data/restraints/param	11 007 / 0 / 325	16088 / 177 / 463
<i>R</i> indices (<i>I</i> > 2σ(<i>I</i>))	<i>R</i> ₁ = 0.0493, <i>wR</i> ₂ = 0.0933	<i>R</i> ₁ = 0.0675, <i>wR</i> ₂ = 0.1557
<i>R</i> indices (all data)	<i>R</i> ₁ = 0.0915, <i>wR</i> ₂ = 0.1067	<i>R</i> ₁ = 0.0864, <i>wR</i> ₂ = 0.1657
goodness of fit on <i>F</i> ²	1.011	1.123
max/min peak in final diff map, e ⁻ /Å ³	0.596/-0.589	1.205/-1.089

Table 7. Atomic coordinates ($\times 10^4$) and equivalent isotropic displacement parameters ($\text{\AA}^2 \times 10^3$) for As[1,3-(SiMe₃)₂C₃H₃]₃. U_{eq} is defined as one third of the trace of the orthogonalized U_{ij} tensor.

	<i>x</i>	<i>y</i>	<i>z</i>	U_{eq}
As1	4493(1)	881(1)	3026(1)	16(1)
Si1	1419(1)	-8(1)	3736(1)	21(1)
Si2	-135(1)	-3233(1)	1295(1)	21(1)
Si3	7355(1)	3607(1)	3860(1)	21(1)
Si4	4369(1)	6172(1)	3517(1)	23(1)
Si5	5894(1)	526(1)	1602(1)	21(1)
Si6	2777(1)	2835(1)	913(1)	22(1)
C1	2378(3)	284(3)	2921(1)	18(1)
C2	1682(3)	-1108(3)	2422(1)	19(1)
C3	757(3)	-1471(3)	1880(1)	22(1)
C4	2013(4)	-990(4)	4232(2)	39(1)
C5	-571(3)	-1097(4)	3493(2)	40(1)
C6	1732(3)	1698(3)	4283(2)	35(1)
C7	460(3)	-4458(3)	1565(2)	28(1)
C8	339(3)	-2990(3)	406(2)	32(1)
C9	-2140(3)	-4004(3)	1319(2)	32(1)
C10	5326(3)	2788(3)	3649(1)	18(1)
C11	4995(3)	3872(3)	3425(1)	19(1)
C12	4671(3)	4780(3)	3820(1)	22(1)
C13	7884(3)	5069(3)	4616(2)	33(1)
C14	7807(3)	2234(3)	4070(2)	34(1)
C15	8402(3)	4447(3)	3153(2)	28(1)
C16	5186(3)	7850(3)	4180(2)	33(1)
C17	2388(3)	5511(4)	3366(2)	35(1)
C18	5211(4)	6565(3)	2703(2)	35(1)
C19	5130(3)	1588(3)	2140(1)	18(1)
C20	4030(3)	1685(3)	1715(1)	19(1)
C21	4161(3)	2839(3)	1495(1)	21(1)
C22	7339(3)	435(3)	2100(2)	32(1)
C23	4419(3)	-1327(3)	1274(2)	31(1)
C24	6688(4)	1462(3)	872(2)	35(1)
C25	3490(3)	4676(3)	721(2)	30(1)
C26	1043(3)	2284(3)	1326(2)	35(1)
C27	2440(4)	1522(4)	112(2)	43(1)

Section B3
Single Crystal Analysis of [Sb(1,3-(SiMe₃)₂C₃H₃)₃]

Figure B1. Diagram of [Sb(1,3-(SiMe₃)₂C₃H₃)₃]



Thermal ellipsoid plot of [SbA'₃] (**2**), illustrating the numbering scheme used in the text. Thermal ellipsoids are drawn at the 50% level, and for clarity, hydrogen atoms have been removed from the trimethylsilyl groups. Selected bond distances (Å) and angles (deg): Sb1–C1, 2.20(3); Sb1–C10, 2.214(3); Sb1–C19, 2.205(3); C1–C2, 1.508(5); C2–C3, 1.315(5); C10–C11, 1.510(5); C11–C12, 1.322(5); C19–C20, 1.515(7); C20–C21, 1.330(7); C1–Sb1–C10, 98.55(15); C1–Sb1–C19, 101.33(14); C10–Sb1–C19, 96.08(14).

Data Collection

A crystal (0.26 x 0.16 x 0.12 mm³) of [Sb(1,3-(SiMe₃)₂C₃H₃)₃] was placed onto the tip of a 0.1 mm diameter glass capillary tube or fiber and mounted on a Bruker SMART APEX II CCD platform diffractometer for a data collection at 100.0(5) K.^[1] A preliminary set of cell constants and an orientation matrix were calculated from reflections harvested from three orthogonal wedges of reciprocal space. The full data collection was carried out using MoK α radiation (graphite monochromator) with a frame time of 45 seconds and a detector distance of 4.01 cm. A randomly oriented region of reciprocal space was surveyed: six major sections of frames were collected with 0.50° steps in ω at six different ϕ settings and a detector position of -38° in 2θ . The intensity data were corrected for absorption.^[2] Final cell constants were calculated from the xyz centroids of 4096 strong reflections from the actual data collection after integration.³

Structure Solution and Refinement

The structure was solved using SIR2011^[4] and refined using SHELXL-2014.^[5] The space group $P-1$ was determined based on intensity statistics. For a test, the structure was also examined in chiral space group $P1$ as an inversion twin, which led to similar disorder ratios at the two independent sites and no significant improvement over the current model in centrosymmetric space group $P-1$. A direct-methods solution was calculated which provided most non-hydrogen atoms from the E-map. Full-matrix least squares / difference Fourier cycles were performed which located the remaining non-hydrogen atoms. All non-hydrogen atoms were refined with anisotropic displacement parameters. All hydrogen atoms were placed in ideal positions and refined as riding atoms with relative isotropic displacement parameters. The asymmetric unit contains one [Sb(1,3-(SiMe₃)₂C₃H₃)₃] molecule in a general position, modeled as disordered with its opposite enantiomer (75:25).

[1] APEX2, version 2013.10-0; Bruker AXS: Madison, WI, 2013.

[2] G. M. Sheldrick, SADABS, version 2012/1; University of Göttingen: Göttingen, Germany, 2012.

[3] SAINT, version 8.34A; Bruker AXS: Madison, WI, 2013.

[4] M. C. Burla, R. Caliendo, M. Camalli, B. Carrozzini, G. L. Casciaro, C. Giacovazzo, M. Mal-lamo, A. Mazzone, G. Polidori, R. Spagna, SIR2011: a new package for crystal structure determination and refinement, version 1.0; Istituto di Cristallografia: Bari, Italy, 2012.

[5] G. M. Sheldrick, SHELXL-2014/3; University of Göttingen: Göttingen, Germany, 2014.

Table 8. Atomic coordinates ($\times 10^4$) and equivalent isotropic displacement parameters ($\text{\AA}^2 \times 10^3$) for $\text{Sb}[1,3-(\text{SiMe}_3)_2\text{C}_3\text{H}_3]_3$. U_{eq} is defined as one third of the trace of the orthogonalized U_{ij} tensor.

	<i>x</i>	<i>y</i>	<i>z</i>	U_{eq}
Sb1	529(1)	745(1)	1957(1)	22(1)
C1	2786(4)	222(5)	2086(2)	29(1)
C2	3476(4)	-1149(5)	2584(2)	31(1)
C3	4288(5)	-1439(4)	3132(2)	33(1)
Si1	3752(2)	-58(2)	1288(1)	28(1)
C4	3274(8)	-1132(8)	801(3)	58(2)
C5	3391(7)	1643(6)	741(4)	61(2)
C6	5744(6)	-1076(8)	1522(3)	61(2)
Si2	5178(3)	-3212(2)	3704(1)	32(1)
C7	4675(7)	-4486(6)	3431(3)	46(1)
C8	4675(7)	-2969(7)	4583(3)	47(1)
C9	7163(6)	-3944(7)	3689(3)	57(2)
C10	-198(4)	1589(4)	2900(2)	27(1)
C11	917(6)	1700(5)	3308(2)	26(1)
C12	825(5)	2878(5)	3472(2)	35(1)
Si3	-900(2)	510(2)	3443(1)	32(1)
C13	-2366(8)	435(7)	2971(4)	50(2)
C14	-1624(8)	1371(6)	4200(3)	57(2)
C15	554(7)	-1351(6)	3735(3)	44(1)
Si4	2239(2)	2873(2)	4037(1)	38(1)
C16	3897(8)	2397(10)	3631(5)	83(3)
C17	1495(7)	4670(7)	4263(4)	56(1)
C18	2604(12)	1522(10)	4810(4)	99(3)
C19	-386(4)	2841(4)	1297(2)	28(1)
C20	-92(12)	3930(14)	1558(3)	31(1)
C21	362(5)	4754(4)	1194(2)	35(1)
Si5	-2385(2)	3676(2)	1089(1)	41(1)
C22	-2781(9)	2267(9)	851(5)	82(3)
C23	-3390(6)	4395(7)	1811(3)	53(1)
C24	-2915(7)	5134(7)	380(3)	58(2)
Si6	717(2)	6126(2)	1510(1)	42(1)
C25	2624(8)	5562(10)	1648(5)	80(2)
C26	-216(8)	6600(7)	2303(3)	50(1)
C27	-129(9)	7792(6)	840(3)	62(2)
Sb1'	2760(1)	2537(1)	2370(1)	41(1)
C1'	2948(13)	593(8)	2055(5)	29(1)
C2'	3890(13)	-505(12)	2642(6)	31(1)
C3'	3811(12)	-1628(11)	2960(6)	33(1)
Si1'	3965(8)	141(8)	1280(4)	28(1)
C4'	4690(20)	-1808(14)	1281(9)	59(5)
C5'	2700(19)	1100(20)	527(9)	66(5)
C6'	5400(20)	640(30)	1287(13)	83(7)
Si2'	5260(9)	-2938(8)	3627(4)	32(1)
C7'	6000(30)	-4688(18)	3323(11)	78(6)
C8'	4338(19)	-3130(20)	4405(8)	47(1)
C9'	6700(20)	-2550(30)	3822(10)	66(5)
C10'	1233(10)	2741(13)	3145(4)	35(1)
C11'	677(14)	1679(17)	3195(11)	26(1)
C12'	-662(11)	1940(10)	3182(6)	27(1)
Si3'	1857(7)	2839(8)	4002(4)	38(1)

C13'	3687(17)	1188(16)	4270(11)	56(1)
C14'	2220(30)	4410(20)	3907(14)	99(3)
C15'	610(20)	2960(30)	4646(12)	83(3)
Si4'	-1300(6)	584(8)	3438(4)	32(1)
C16'	-2660(20)	850(30)	2823(12)	50(2)
C17'	-2120(20)	931(19)	4248(8)	57(2)
C18'	290(20)	-1207(18)	3503(9)	44(1)
C19'	1148(11)	4155(7)	1584(5)	35(1)
C20'	-100(30)	3890(50)	1477(9)	31(1)
C21'	-742(10)	3790(13)	942(6)	28(1)
Si5'	248(6)	6173(6)	1581(3)	42(1)
C22'	1960(20)	6210(30)	1802(15)	80(2)
C23'	-920(20)	6680(20)	2280(8)	50(1)
C24'	-530(20)	7230(19)	806(8)	62(2)
Si6'	-2249(5)	3320(6)	871(3)	41(1)
C25'	-1880(30)	1628(19)	614(14)	82(3)
C26'	-3509(17)	3750(20)	1573(8)	53(1)
C27'	-3400(20)	4800(20)	110(8)	58(2)

Section B4

Single Crystal Analysis of $\text{K}[\text{Be}(\text{1,3-(SiMe}_3)_2\text{C}_3\text{H}_3)_3]$

Data collection

A crystal ($0.20 \times 0.20 \times 0.08 \text{ mm}^3$) was placed onto the tip of a thin glass optical fiber and mounted on a Bruker SMART APEX II CCD platform diffractometer for a data collection at $100.0(5) \text{ K}$.^[1] A preliminary set of cell constants and an orientation matrix were calculated from reflections harvested from three orthogonal wedges of reciprocal space. The full data collection was carried out using $\text{MoK}\alpha$ radiation (graphite monochromator) with a frame time of 60 seconds and a detector distance of 4.02 cm. A randomly oriented region of reciprocal space was surveyed: four major sections of frames were collected with 0.50° steps in ω at four different ϕ settings and a detector position of -38° in 2θ . The intensity data were corrected for absorption.^[2] Final cell constants were calculated from the xyz centroids of 2886 strong reflections from the actual data collection after integration.^[3]

Structure solution and refinement

The structure was solved using SIR2011^[4] and refined using SHELXL-2014/7.^[5] The space group $P-1$ was determined based on intensity statistics. A direct-methods solution was calculated which provided most non-hydrogen atoms from the E-map. Full-matrix least squares / difference Fourier cycles were performed which located the remaining non-hydrogen atoms. All non-hydrogen atoms were refined with anisotropic displacement parameters. The allylic hydrogen atoms were found from the difference Fourier map and refined freely. All other hydrogen atoms were placed in ideal positions and refined as riding atoms with relative isotropic displacement parameters. The final full matrix least squares refinement converged to $R1 = 0.0588$ (F^2 , $I > 2\sigma(I)$) and $wR2 = 0.1326$ (F^2 , all data).

Structure description

The structure is similar to the one suggested. The asymmetric unit contains one molecule in a general position. The structure is isotopic with the zinc analog (CSD refcode PICGUE).^[6]

[1] APEX2, version 2014.11-0; Bruker AXS: Madison, WI, 2014.

[2] Sheldrick, G. M. SADABS, version 2014/5; University of Göttingen: Göttingen, Germany, 2014.

[3] SAINT, version 8.32B; Bruker AXS: Madison, WI, 2014.

[4] Burla, M. C.; Caliandro, R.; Camalli, M.; Carrozzini, B.; Cascarano, G. L.; Giacovazzo, C.; Mal-lamo, M.; Mazzone, A.; Polidori, G.; Spagna, R. SIR2011: a new package for crystal structure determination and refinement, version 1.0; Istituto di Cristallografia: Bari, Italy, 2012.

[5] Sheldrick, G. M. SHELXL-2014/7; University of Göttingen: Göttingen, Germany, 2014.

[6] Gren, C. K.; Hanusa, T. P.; Rheingold, A. L. *Organometallics* **2007**, *26*, 1643-1649.

Table 9. Crystal Data and Summary for $\text{K}[\text{Be}(1,3\text{-(SiMe}_3)_2\text{C}_3\text{H}_3)_3]$.

Identification code	hannr05	
Empirical formula	C ₂₇ H ₆₃ Be K Si ₆	
Formula weight	604.42	
Temperature	100.0(5) K	
Wavelength	0.71073 Å	
Crystal system	triclinic	
Space group	<i>P</i> -1	
Unit cell dimensions	$a = 11.936(3)$ Å	$\alpha = 80.165(5)^\circ$
	$b = 13.097(3)$ Å	$\beta = 73.087(5)^\circ$
	$c = 13.758(3)$ Å	$\gamma = 89.739(5)^\circ$
Volume	2025.3(9) Å ³	
<i>Z</i>	2	
Density (calculated)	0.991 Mg/m ³	
Absorption coefficient	0.322 mm ⁻¹	
<i>F</i> (000)	664	
Crystal color, morphology	colorless, plate	
Crystal size	0.20 x 0.20 x 0.08 mm ³	
Theta range for data collection	2.001 to 25.741°	
Index ranges	$-14 \leq h \leq 14, -15 \leq k \leq 15, -16 \leq l \leq 16$	
Reflections collected	23415	
Independent reflections	7725 [<i>R</i> (int) = 0.1195]	
Observed reflections	4292	
Completeness to theta = 25.741°	99.7%	
Absorption correction	Multi-scan	
Max. and min. transmission	0.7453 and 0.6317	
Refinement method	Full-matrix least-squares on <i>F</i> ²	
Data / restraints / parameters	7725 / 0 / 370	
Goodness-of-fit on <i>F</i> ²	0.965	
Final <i>R</i> indices [<i>I</i> > 2σ(<i>I</i>)]	<i>R</i> 1 = 0.0588, <i>wR</i> 2 = 0.1071	
<i>R</i> indices (all data)	<i>R</i> 1 = 0.1280, <i>wR</i> 2 = 0.1326	
Largest diff. peak and hole	0.364 and -0.336 e.Å ⁻³	

Table 10. Atomic coordinates ($\times 10^4$) and equivalent isotropic displacement parameters ($\text{\AA}^2 \times 10^3$) for $\text{K}[\text{Be}(1,3\text{-(SiMe}_3)_2\text{C}_3\text{H}_3)_3]$. U_{eq} is defined as one third of the trace of the orthogonalized U_{ij} tensor.

	<i>x</i>	<i>y</i>	<i>z</i>	U_{eq}
K1	5696(1)	3014(1)	2347(1)	32(1)
Be1	8409(4)	2907(4)	2988(4)	23(1)
Si1	8118(1)	1815(1)	5254(1)	27(1)
Si2	3875(1)	2222(1)	4895(1)	27(1)
Si3	9703(1)	5076(1)	2732(1)	28(1)
Si4	5764(1)	5761(1)	1744(1)	29(1)
Si5	10257(1)	1691(1)	1555(1)	31(1)
Si6	6456(1)	1294(1)	494(1)	30(1)
C1	7597(3)	1978(3)	4081(3)	22(1)
C2	6369(3)	2277(3)	4389(3)	23(1)
C3	5374(3)	1775(3)	4411(3)	28(1)
C4	7347(4)	646(4)	6189(3)	49(1)
C5	7808(4)	2969(3)	5913(3)	40(1)
C6	9721(3)	1606(3)	4946(3)	40(1)
C7	3957(4)	3537(3)	5220(3)	37(1)
C8	3000(4)	1299(3)	6024(3)	41(1)
C9	3101(3)	2332(3)	3876(3)	39(1)
C10	8314(3)	4276(3)	3048(3)	25(1)
C11	7609(3)	4713(3)	2371(3)	24(1)
C12	6500(3)	5031(3)	2636(3)	25(1)
C13	9386(4)	6417(3)	3006(4)	43(1)
C14	10678(3)	4512(3)	3512(3)	38(1)
C15	10526(3)	5222(3)	1332(3)	40(1)
C16	5731(4)	7161(3)	1863(4)	47(1)
C17	4203(4)	5278(3)	2053(3)	42(1)
C18	6550(4)	5609(4)	396(3)	49(1)
C19	8948(3)	2507(3)	1744(3)	26(1)
C20	8020(3)	1925(3)	1524(3)	24(1)
C21	7487(3)	2159(3)	772(3)	28(1)
C22	9871(4)	347(3)	2311(3)	43(1)
C23	11471(3)	2246(3)	1939(3)	41(1)
C24	10852(4)	1590(4)	154(3)	51(1)
C25	4955(3)	1826(4)	731(3)	45(1)
C26	6284(4)	17(3)	1367(4)	50(1)
C27	6982(4)	1153(4)	-879(3)	55(1)

Section B5

Single Crystal Analysis of $\text{K}[\text{Ca}(\text{1,3-(SiMe}_3)_2\text{C}_3\text{H}_3)_3]$

Data collection

A crystal ($0.36 \times 0.24 \times 0.20 \text{ mm}^3$) was placed onto the tip of a thin glass optical fiber and mounted on a Bruker SMART APEX II CCD platform diffractometer for a data collection at $100.0(5) \text{ K}$.^[1] A preliminary set of cell constants and an orientation matrix were calculated from reflections harvested from three orthogonal wedges of reciprocal space. The full data collection was carried out using $\text{MoK}\alpha$ radiation (graphite monochromator) with a frame time of 60 seconds and a detector distance of 4.03 cm. A randomly oriented region of reciprocal space was surveyed: four major sections of frames were collected with 0.50° steps in ω at four different ϕ settings and a detector position of -38° in 2θ . The intensity data were corrected for absorption.^[2] Final cell constants were calculated from the xyz centroids of 3884 strong reflections from the actual data collection after integration.^[3]

Structure solution and refinement

The structure was solved using *SHELXT-2014/5*^[4] and refined using *SHELXL-2014/7*.^[5] The space group $P2_1/m$ was determined based on systematic absences and intensity statistics. A direct-methods solution was calculated which provided most non-hydrogen atoms from the E-map. Full-matrix least squares / difference Fourier cycles were performed which located the remaining non-hydrogen atoms. All non-hydrogen atoms were refined with anisotropic displacement parameters. All hydrogen atoms were placed in ideal positions and refined as riding atoms with relative isotropic displacement parameters. The final full matrix least squares refinement converged to $R1 = 0.0457$ (F^2 , $I > 2\sigma(I)$) and $wR2 = 0.1398$ (F^2 , all data).

Structure description

The structure is the one suggested. The asymmetric unit contains one calcium cation on a crystallographic mirror plane, one potassium cation near a crystallographic inversion center, and three allyl ligands whose occupancies are restricted to one half because they are disordered as a set over crystallographic symmetry. Because the silicon atoms are approximately evenly spaced from one another (about six Angstroms apart), the connecting allyls are able to connect in two directions, and thus the structure is a disorder of the two motifs, the ratio of which is exactly 0.50:0.50 due to the aforementioned crystallographic symmetry. SiMe_3 group containing Si5 is modeled as disordered over two additional positions (0.82:0.18).

[1] *APEX3*, version 2015.5-2; Bruker AXS: Madison, WI, 2015.

[2] Sheldrick, G. M. *SADABS*, version 2014/5; *J. Appl. Cryst.* **2015**, *48*, 3-10.

[3] *SAINT*, version 8.34A; Bruker AXS: Madison, WI, 2013.

[4] Sheldrick, G. M. *SHELXT-2014/5*; University of Göttingen: Göttingen, Germany, 2014.

[5] Sheldrick, G. M. *SHELXL-2014/7*; *Acta. Cryst.* **2015**, *C71*, 3-8.

Table 11. Crystal data and Summary for K[Ca(1,3-(SiMe₃)₂C₃H₃)₃].

Identification code	hannr07	
Empirical formula	C ₂₇ H ₆₃ Ca K Si ₆	
Formula weight	635.49	
Temperature	100.0(5) K	
Wavelength	0.71073 Å	
Crystal system	monoclinic	
Space group	<i>P</i> 2 ₁ / <i>m</i>	
Unit cell dimensions	<i>a</i> = 11.235(2) Å	$\alpha = 90^\circ$
	<i>b</i> = 17.338(3) Å	$\beta = 115.571(4)^\circ$
	<i>c</i> = 11.856(2) Å	$\gamma = 90^\circ$
Volume	2083.4(7) Å ³	
<i>Z</i>	2	
Density (calculated)	1.013 Mg/m ³	
Absorption coefficient	0.437 mm ⁻¹	
<i>F</i> (000)	696	
Crystal color, morphology	colorless, block	
Crystal size	0.36 x 0.24 x 0.20 mm ³	
Theta range for data collection	1.904 to 29.629°	
Index ranges	-15 ≤ <i>h</i> ≤ 15, -24 ≤ <i>k</i> ≤ 24, -16 ≤ <i>l</i> ≤ 16	
Reflections collected	30710	
Independent reflections	6049 [<i>R</i> (int) = 0.0445]	
Observed reflections	3947	
Completeness to theta = 26.373°	100.0%	
Absorption correction	Multi-scan	
Max. and min. transmission	0.7459 and 0.6422	
Refinement method	Full-matrix least-squares on <i>F</i> ²	
Data / restraints / parameters	6049 / 30 / 356	
Goodness-of-fit on <i>F</i> ²	1.032	
Final <i>R</i> indices [<i>I</i> > 2σ(<i>I</i>)]	<i>R</i> 1 = 0.0457, <i>wR</i> 2 = 0.1162	
<i>R</i> indices (all data)	<i>R</i> 1 = 0.0796, <i>wR</i> 2 = 0.1398	
Largest diff. peak and hole	0.455 and -0.184 e.Å ⁻³	

Table 12. Atomic coordinates ($\times 10^4$) and equivalent isotropic displacement parameters ($\text{\AA}^2 \times 10^3$) for $\text{K}[\text{Ca}(1,3\text{-(SiMe}_3)_2\text{C}_3\text{H}_3)_3]$. U_{eq} is defined as one third of the trace of the orthogonalized U_{ij} tensor.

	<i>x</i>	<i>y</i>	<i>z</i>	U_{eq}
Ca1	3112(1)	7500	5746(1)	36(1)
K1	4860(7)	4946(4)	5049(7)	61(1)
C6	1402(6)	8584(3)	8609(5)	66(1)
C5	1636(7)	6840(3)	8829(5)	82(2)
C4	-990(4)	7638(13)	7300(4)	81(5)
Si1	820(1)	7660(1)	7748(1)	43(1)
C1	1100(3)	7410(10)	6336(3)	47(3)
C2	903(3)	6792(2)	5509(3)	39(1)
C3	860(3)	6811(2)	4305(3)	43(1)
Si2	416(1)	6004(1)	3209(1)	45(1)
C7	-1393(4)	5775(3)	2574(4)	65(1)
C8	677(13)	6306(8)	1797(8)	90(4)
C9	1364(5)	5114(3)	3997(4)	68(1)
C15	1254(6)	10268(3)	3188(7)	100(2)
C14	675(11)	8803(7)	1791(9)	81(3)
C13	-304(5)	9073(3)	3811(6)	93(2)
Si3	1035(2)	9191(1)	3285(2)	63(1)
C10	2606(3)	8777(2)	4403(3)	44(1)
C11	3221(4)	8980(2)	5663(3)	49(1)
C12	4465(10)	8760(9)	6577(7)	45(2)
Si4	5801(4)	9049(2)	8294(3)	41(1)
C16	4976(5)	8929(3)	9323(4)	63(1)
C17	7396(4)	8540(3)	8927(4)	59(1)
C18	6123(10)	10127(4)	8289(8)	67(2)
C24	6524(14)	5187(7)	8407(13)	113(5)
C23	3769(7)	5251(3)	8330(5)	77(2)
C22	5733(10)	6587(5)	9449(6)	97(3)
Si5	5081(3)	5838(1)	8165(2)	54(1)
C24'	7470(20)	5860(30)	8660(30)	103(11)
C23'	5050(40)	4907(15)	8410(20)	97(11)
C22'	5300(50)	6620(20)	9160(40)	97(3)
Si5'	5640(30)	5874(13)	8160(20)	41(1)
C19	4773(11)	6258(8)	6677(8)	41(2)
C20	5212(3)	6658(2)	5897(3)	35(1)
C21	4551(3)	6845(2)	4616(3)	37(1)
Si6	5311(1)	7317(1)	3691(1)	43(1)
C25	4050(4)	7390(9)	2031(3)	62(3)
C26	6761(5)	6755(3)	3768(5)	78(1)
C27	5922(4)	8317(2)	4233(4)	52(1)

Section B6

Single Crystal Analysis for $[\text{K}_{0.5}\text{Cs}_{0.5}(1,3\text{-(SiMe}_3)_2\text{C}_3\text{H}_3)]$

Data collection

A crystal ($0.25 \times 0.16 \times 0.14 \text{ mm}^3$) was placed onto the tip of a thin glass optical fiber and mounted on a Bruker SMART APEX II CCD platform diffractometer for a data collection at 100.0(5) K.^[1] A preliminary set of cell constants and an orientation matrix were calculated from reflections harvested from three orthogonal wedges of reciprocal space. The full data collection was carried out using MoK α radiation (graphite monochromator) with a frame time of 60 seconds and a detector distance of 4.03 cm. A randomly oriented region of reciprocal space was surveyed: four major sections of frames were collected with 0.50° steps in ω at four different ϕ settings and a detector position of -38° in 2θ . The intensity data were corrected for absorption.^[2] Final cell constants were calculated from the xyz centroids of 4067 strong reflections from the actual data collection after integration.^[3]

Structure solution and refinement

The structure was solved using SHELXT-2014/5^[4] and refined using SHELXL-2014/7.^[5] The space group $P-1$ was determined based on intensity statistics. A direct-methods solution was calculated which provided most non-hydrogen atoms from the E-map. Full-matrix least squares / difference Fourier cycles were performed which located the remaining non-hydrogen atoms. All non-hydrogen atoms were refined with anisotropic displacement parameters. Hydrogen atoms on the allylic portions of the anions were found from the difference Fourier map and their positions were refined independently from those of their respective bonded carbon atoms. However, their isotropic displacement parameters were refined relative to the (equivalent) anisotropic displacement parameters of their respective bonded carbon atoms. All other hydrogen atoms were placed in ideal positions and refined as riding atoms with relative isotropic displacement parameters. The final full matrix least squares refinement converged to $R1 = 0.0445$ (F^2 , $I > 2\sigma(I)$) and $wR2 = 0.1234$ (F^2 , all data).

Structure description

The structure is the one suggested. The asymmetric unit contains three alkali metal cations and three substituted allyl anions, all in general positions. Each of the three metal sites is modeled as a site disorder of atoms types K and Cs. Because two distinct peaks were found in the difference Fourier map for the site containing atoms Cs1 and K1, their positions were refined freely, but their anisotropic displacement parameters were constrained to be equivalent. For the other two site disorders (atom pairs Cs2/K2 and Cs3/K3), the atoms were constrained to be isopositional and their anisotropic displacement parameters were constrained to be equivalent. The ratios of Cs to K in the three sites refined to 0.60:0.40, 0.29:0.71, and 0.61:0.39, respectively, for atom pairs Cs1/K1, Cs2/K2, and Cs3/K3. One SiMe₃ group is modeled as disordered over two positions (0.60:0.40). The structure is polymeric in two dimensions.

[1] APEX3, version 2015.5-2; Bruker AXS: Madison, WI, 2015.

[2] Sheldrick, G. M. SADABS, version 2014/5; *J. Appl. Cryst.* **2015**, *48*, 3-10.

[3] SAINT, version 8.34A; Bruker AXS: Madison, WI, 2013.

[4] Sheldrick, G. M. SHELXT-2014/5; University of Göttingen: Göttingen, Germany, 2014.

[5] Sheldrick, G. M. SHELXL-2014/7; *Acta. Cryst.* **2015**, *C71*, 3-8.

Table 13. Crystal Data and Summary for $[\text{K}_{0.5}\text{Cs}_{0.5}(1,3\text{-(SiMe}_3)_2\text{C}_3\text{H}_3)]$.

Identification code	hanmr06	
Empirical formula	C27 H63 Cs1.50 K1.50 Si6	
Formula weight	814.33	
Temperature	100.0(5) K	
Wavelength	0.71073 Å	
Crystal system	triclinic	
Space group	<i>P</i> -1	
Unit cell dimensions	$a = 11.1741(8)$ Å	$\alpha = 73.9101(15)^\circ$
	$b = 14.6733(11)$ Å	$\beta = 85.2391(16)^\circ$
	$c = 14.7968(11)$ Å	$\gamma = 71.6969(15)^\circ$
Volume	2213.1(3) Å ³	
Z	2	
Density (calculated)	1.222 Mg/m ³	
Absorption coefficient	1.559 mm ⁻¹	
<i>F</i> (000)	840	
Crystal color, morphology	colorless, block	
Crystal size	0.25 x 0.16 x 0.14 mm ³	
Theta range for data collection	1.788 to 27.500°	
Index ranges	$-14 \leq h \leq 14, -19 \leq k \leq 19, -19 \leq l \leq 19$	
Reflections collected	29788	
Independent reflections	10133 [<i>R</i> (int) = 0.0374]	
Observed reflections	6622	
Completeness to theta = 27.485°	99.9%	
Absorption correction	Multi-scan	
Max. and min. transmission	0.7456 and 0.6622	
Refinement method	Full-matrix least-squares on <i>F</i> ²	
Data / restraints / parameters	10133 / 43 / 404	
Goodness-of-fit on <i>F</i> ²	1.046	
Final <i>R</i> indices [<i>I</i> > 2σ(<i>I</i>)]	<i>R</i> 1 = 0.0445, <i>wR</i> 2 = 0.1080	
<i>R</i> indices (all data)	<i>R</i> 1 = 0.0746, <i>wR</i> 2 = 0.1234	
Largest diff. peak and hole	0.938 and -0.622 e.Å ⁻³	

Table 14. Atomic coordinates ($\times 10^4$) and equivalent isotropic displacement parameters ($\text{\AA}^2 \times 10^3$) for $[\text{K}_{0.5}\text{Cs}_{0.5}(1,3\text{-(SiMe}_3)_2\text{C}_3\text{H}_3)]$. U_{eq} is defined as one third of the trace of the orthogonalized U_{ij} tensor.

	<i>x</i>	<i>y</i>	<i>z</i>	U_{eq}
Cs1	1960(1)	1395(1)	3401(1)	53(1)
Cs2	5380(1)	3864(1)	2632(1)	61(1)
Cs3	4851(1)	7971(1)	2056(1)	58(1)
K1	2406(3)	1176(2)	3556(2)	53(1)
K2	5380(1)	3864(1)	2632(1)	61(1)
K3	4851(1)	7971(1)	2056(1)	58(1)
Si1	2702(1)	3465(1)	4657(1)	55(1)
Si2	6505(1)	747(1)	3042(1)	52(1)
Si4	8207(1)	5229(1)	2093(1)	55(1)
Si5	2222(1)	11129(1)	766(1)	88(1)
Si6	1990(1)	8116(1)	4118(1)	53(1)
C1	3337(4)	2945(3)	3674(3)	57(1)
C2	4404(3)	2130(3)	3682(3)	51(1)
C3	4999(4)	1726(3)	2953(3)	54(1)
C4	3498(4)	2639(3)	5792(3)	62(1)
C5	2899(5)	4715(3)	4501(4)	92(2)
C6	971(4)	3632(4)	4802(4)	91(2)
C7	7889(4)	1226(3)	2634(3)	72(1)
C8	6848(3)	9(3)	4304(3)	53(1)
C9	6524(4)	-121(3)	2319(3)	68(1)
C10	4289(3)	6103(3)	1695(3)	58(1)
C11	5583(3)	5877(3)	1616(3)	53(1)
C12	6516(3)	5580(3)	2290(3)	56(1)
Si3	3187(3)	6644(3)	702(2)	54(1)
C13	2508(8)	8035(5)	424(6)	88(3)
C14	1841(8)	6121(9)	1029(7)	113(4)
C15	3887(18)	6380(10)	-431(8)	65(1)
Si3'	3036(4)	6271(4)	888(4)	54(1)
C13'	1706(11)	7450(8)	806(9)	90(4)
C14'	2321(10)	5230(8)	1195(8)	69(3)
C15'	3730(30)	6351(15)	-319(12)	65(1)
C16	8983(4)	5966(5)	2540(5)	111(2)
C17	8538(4)	5391(4)	816(3)	80(1)
C18	9015(4)	3880(4)	2673(4)	96(2)
C19	2934(4)	10231(3)	1855(3)	67(1)
C20	2382(4)	9582(3)	2487(3)	63(1)
C21	2769(4)	8988(3)	3389(3)	58(1)
C22	3452(5)	11474(4)	-43(4)	106(2)
C23	1087(6)	12295(4)	981(5)	139(3)
C24	1301(7)	10628(6)	123(5)	161(3)
C25	679(4)	8660(3)	4873(3)	67(1)
C26	1274(4)	7585(3)	3369(3)	75(1)
C27	3142(4)	7097(3)	4972(3)	72(1)

Appendix C

Computational Details

Section C1

Mechanochemical Synthesis and Investigations as a Potential Allyl Transfer Agent of the Base-Free Tris(allyl)aluminum Complex [Al(1,3-(SiMe₃)₂C₃H₃)₃]

Density functional calculations were performed with the Gaussian 09W²¹⁰ suite of programs. Both Hartree-Fock and DFT methods were used; for the latter, the meta-GGA functional M06-L²²⁹ was employed; this provides an accounting for dispersion interactions. The triple- ζ polarized def2-TZVP basis set¹⁶⁵ and an ultrafine grid (Gaussian keyword: Int=Ultrafine) were used for all calculations. No symmetry was applied, and stationary points were characterized by the calculation of vibrational frequencies; the geometries were found to be minima ($N_{\text{imag}} = 0$).

References

1. **Gaussian 09**, Revision D.01, Frisch, M. J.; Trucks, G. W.; Schlegel, H. B.; Scuseria, G. E.; Robb, M. A.; Cheeseman, J. R.; Scalmani, G.; Barone, V.; Mennucci, B.; Petersson, G. A.; Nakatsuji, H.; Caricato, M.; Li, X.; Hratchian, H. P.; Izmaylov, A. F.; Bloino, J.; Zheng, G.; Sonnenberg, J. L.; Hada, M.; Ehara, M.; Toyota, K.; Fukuda, R.; Hasegawa, J.; Ishida, M.; Nakajima, T.; Honda, Y.; Kitao, O.; Nakai, H.; Vreven, T.; Montgomery, J. A., Jr.; Peralta, J. E.; Ogliaro, F.; Bearpark, M.; Heyd, J. J.; Brothers, E.; Kudin, K. N.; Staroverov, V. N.; Kobayashi, R.; Normand, J.; Raghavachari, K.; Rendell, A.; Burant, J. C.; Iyengar, S. S.; Tomasi, J.; Cossi, M.; Rega, N.; Millam, N. J.; Klene, M.; Knox, J. E.; Cross, J. B.; Bakken, V.; Adamo, C.; Jaramillo, J.; Gomperts, R.; Stratmann, R. E.; Yazyev, O.; Austin, A. J.; Cammi, R.; Pomelli, C.; Ochterski, J. W.; Martin, R. L.; Morokuma, K.; Zakrzewski, V. G.; Voth, G. A.; Salvador, P.; Dannenberg, J. J.; Dapprich, S.; Daniels, A. D.; Farkas, Ö.; Foresman, J. B.; Ortiz, J. V.; Cioslowski, J.; Fox, D. J. Gaussian, Inc., Wallingford CT, 2009.
2. Zhao, Y.; Truhlar, D. G., A new local density functional for main-group thermochemistry, transition metal bonding, thermochemical kinetics, and noncovalent interactions. *J. Chem. Phys.* **2006**, 125, 194101-194118.
3. Weigend, F.; Ahlrichs, R., Balanced basis sets of split valence, triple zeta valence and quadruple zeta valence quality for H to Rn: Design and assessment of accuracy. *Phys. Chem. Chem. Phys.* **2005**, 7, 3297-3305.

Table 15. Coordinates of Optimized Structures (Å)

25

 $(\eta^1\text{-C}_3\text{H}_5)_3\text{Al}$, HF/def2TZVP

Al	-0.118909	-0.143114	0.255511
C	-3.522690	-0.238897	-0.887585
C	-2.904725	0.036935	0.247416
C	-1.865209	-0.806058	0.924599
C	2.688504	-2.394183	0.254181
C	1.484496	-2.358582	-0.289638
C	0.889831	-1.221288	-1.065386
C	1.303159	3.362720	-0.646981
C	1.551501	2.280077	0.064030
C	0.590819	1.568946	0.963450
H	3.393380	-1.590504	0.126984
H	0.836706	-3.206325	-0.127234
H	1.666778	-0.618114	-1.523295
H	0.349329	3.860363	-0.609893
H	-3.360389	-1.164620	-1.412524
H	2.532312	1.837967	-0.018534
H	-0.257798	2.208613	1.196577
H	-3.124497	0.981455	0.720823
H	-1.988644	-1.851615	0.659158
H	3.016570	-3.240690	0.827973
H	0.249418	-1.597610	-1.856944
H	-1.956096	-0.722697	2.003137
H	1.072758	1.347451	1.916441
H	-4.227543	0.446582	-1.319630
H	2.049416	3.792193	-1.289196

25

 $(\eta^1\text{-C}_3\text{H}_5)(\eta^3\text{-C}_3\text{H}_5)_2\text{Al}$, M06-L/def2TZVP

Al	-0.121376	0.240692	0.275440
C	3.240550	-1.401075	0.120443
C	2.033295	-1.523682	-0.428813
C	0.737037	-1.533390	0.275482
C	1.004874	1.903248	0.975432
C	1.273642	1.713786	-0.393213
C	0.283711	1.573838	-1.373451
C	-3.397788	-1.394980	-0.202607
C	-2.863117	-0.179203	-0.288291
C	-2.028125	0.493494	0.729568
H	0.176109	2.542853	1.266193
H	2.246815	1.287439	-0.631066
H	-0.633580	2.151128	-1.296317
H	-3.298519	-1.998711	0.692830
H	3.373715	-1.347668	1.195636
H	-3.000950	0.370191	-1.218317
H	-2.198507	0.071344	1.722931
H	1.976843	-1.572315	-1.515360
H	0.857055	-1.841074	1.317476
H	1.827848	1.869359	1.674043
H	0.570716	1.291501	-2.375497
H	0.035368	-2.232088	-0.185961
H	-2.240770	1.563081	0.783844

H	4.139117	-1.366542	-0.479908
H	-3.957846	-1.829719	-1.018564

97

 $[1,3\text{-(SiMe}_3)_2\text{C}_3\text{H}_3]_3\text{Al}$, M06-L/def2TZVP

Al	0.417158	0.008164	-0.226477
C	-1.916929	2.793246	0.284062
C	-1.200241	2.105727	-0.621399
C	0.270598	1.912584	-0.657356
C	-4.493922	1.800920	-0.974019
C	-4.389174	2.459773	2.014227
C	-4.279741	4.711151	-0.025558
C	0.493552	1.477399	-3.709103
C	2.961887	2.160337	-1.979386
C	0.803136	4.261032	-2.549492
C	3.773308	-0.808767	1.101718
C	2.664302	-0.090049	1.348024
C	1.269651	-0.578127	1.435069
C	5.477723	1.706309	1.275295
C	6.092337	-0.430210	-0.832766
C	6.649753	-1.001041	2.098199
C	0.868101	-1.024138	4.440732
C	-1.516555	-0.337805	2.643812
C	0.595594	1.782887	3.280231
C	-2.821953	-1.823914	-0.820849
C	-1.496381	-1.957014	-0.648731
C	-0.408331	-1.308613	-1.416171
C	-3.290010	-4.024003	1.220788
C	-5.370427	-3.469175	-0.960366
C	-5.007725	-1.506436	1.329073
C	2.516231	-1.666997	-2.342774
C	0.248345	-3.170145	-3.751525
C	1.096156	-3.935283	-0.911658
H	3.633264	-1.886247	0.982306
H	2.778922	0.990772	1.466282
H	1.251156	-1.675125	1.403804
H	4.834451	2.249530	0.582792
H	6.478536	2.128867	1.183464
H	5.127769	1.919049	2.285957
H	5.491050	0.109049	-1.565393
H	6.044202	-1.488573	-1.092271
H	7.127900	-0.111904	-0.959407
H	7.675843	-0.651466	1.978267
H	6.653786	-2.078402	1.930444
H	6.365630	-0.836241	3.137314
H	0.354229	-0.715537	5.351661
H	1.938359	-0.899723	4.608383
H	0.682734	-2.089991	4.306112
H	-2.125888	-0.047911	3.501525
H	-1.722894	-1.390304	2.441393
H	-1.887549	0.233376	1.786206
H	0.309793	2.401671	2.429152
H	1.641520	1.993776	3.505348
H	0.007234	2.121084	4.133980
H	-3.141918	-1.175319	-1.638923
H	-1.349000	3.298763	1.068126

H	-1.155936	-2.609311	0.159488	C	-1.90167	0.06500	0.27944
H	-0.834852	-0.738904	-2.250141	C	-2.39471	-1.30391	0.09988
H	-2.738826	-4.731464	0.600098	C	-1.87230	-2.31973	0.89826
H	-4.029365	-4.592818	1.785353	C	-3.29689	-1.62406	-0.91468
H	-2.587605	-3.610356	1.945444	C	-2.24881	-3.62973	0.69141
H	-5.841115	-2.716766	-1.594314	C	-3.65618	-2.93937	-1.13168
H	-6.166030	-3.967079	-0.405073	C	-3.13530	-3.94117	-0.32850
H	-4.915745	-4.208906	-1.618981	C	-2.73353	1.22931	-0.04288
H	-4.322859	-1.058708	2.049651	C	-4.12260	1.20844	0.08536
H	-5.788844	-2.017640	1.893847	C	-2.09541	2.40594	-0.43834
H	-5.484480	-0.692128	0.782450	C	-4.85832	2.34702	-0.17838
H	2.908498	-1.273364	-1.399060	C	-2.83803	3.53319	-0.72200
H	2.478743	-0.839516	-3.052744	C	-4.21799	3.50568	-0.58908
H	3.266043	-2.366985	-2.715652	C	1.22515	0.17060	-1.52418
H	0.926423	-3.911403	-4.175397	C	0.07592	-1.82942	-2.51008
H	0.142047	-2.367892	-4.482611	C	0.11030	-0.54552	-2.15905
H	-0.729363	-3.640542	-3.642241	H	2.16786	3.67320	-0.45801
H	0.173091	-4.494044	-0.754146	H	0.65651	4.58925	0.08724
H	1.443271	-3.594310	0.064833	H	0.95093	-2.46518	-2.40607
H	1.841150	-4.637175	-1.287842	H	-3.67241	-0.84560	-1.56825
H	-1.750273	1.598150	-1.419569	H	-5.93474	2.33385	-0.05843
H	0.743139	2.471344	0.160370	H	-4.62046	0.30833	0.42588
H	-4.165300	0.773572	-0.808568	H	-1.84417	-4.41332	1.32020
H	-4.201100	2.081266	-1.986413	H	-4.33561	-3.18680	-1.93811
H	-5.583847	1.805496	-0.939401	H	-3.41939	-4.97276	-0.50049
H	-4.187724	1.411481	2.232582	H	-2.33644	4.43889	-1.04158
H	-5.465782	2.610431	2.104031	H	-1.01369	2.42581	-0.52433
H	-3.912473	3.053495	2.795492	H	-4.79927	4.39530	-0.80229
H	-5.363376	4.826489	0.019856	H	-1.16985	-2.06646	1.68292
H	-3.954863	5.040122	-1.012545	H	2.18522	-0.29857	-1.77043
H	-3.850299	5.399255	0.702954	H	1.26960	1.22170	-1.82406
H	0.712356	0.411313	-3.648818	H	-0.80449	0.03580	-2.30597
H	0.942732	1.844893	-4.632562	H	-0.81740	-2.28763	-2.91787
H	-0.587139	1.580800	-3.817523	H	2.72677	-1.80509	0.94872
H	3.367105	2.894300	-1.281113	H	1.13293	-2.50545	0.64428
H	3.535455	2.243447	-2.903062	H	0.44902	-2.08823	2.97641
H	3.167445	1.173193	-1.556815	H	3.35989	-1.25717	3.35827
H	-0.263515	4.449922	-2.675087	H	2.08118	-1.58317	4.65271
H	1.307738	4.617103	-3.448158	H	2.92150	1.71841	1.03433
H	1.143079	4.876608	-1.716318	H	1.96685	1.38204	2.48920
Si	-3.766095	2.942418	0.315505	H	0.24462	2.97156	1.81411
Si	1.128153	2.446801	-2.236779	O	-0.75736	0.26391	0.70873
Si	5.487860	-0.129541	0.916407				
Si	0.305989	-0.035833	2.956756				
Si	-4.111713	-2.693883	0.188606				
Si	0.859699	-2.518289	-2.110143				

49

Al(C3H5)(OPPh2), M06/def2TZVP

Al	1.12417	0.05658	0.46972
C	1.66068	-1.71764	1.19290
C	1.45355	-1.81191	2.64853
C	2.33892	-1.53821	3.60205
C	1.11727	2.83517	1.17290
C	1.31813	3.73993	0.21602
C	1.90105	1.61721	1.42326

62

Al(C3H5)(OPPh2)(THF), M06/def2TZVP

Al	0.46715	-0.78851	0.54029
C	-1.22065	-1.30664	1.47534
C	-2.05905	-2.14350	0.59875
C	-3.23274	-1.82024	0.06114
C	1.20454	-2.07551	-0.78608
C	2.65091	-1.88862	-0.98193
C	3.25717	-1.36663	-2.04564
C	1.07058	1.42278	2.25793
C	1.08337	2.70542	1.89690
C	1.75797	0.30971	1.59077
C	0.62519	1.13647	-1.71081

C	-1.38037	2.36383	-1.63285
C	0.10936	2.54338	-1.88234
C	-1.39288	1.39136	-0.47842
C	0.94640	-3.59537	2.96947
C	0.14673	-4.64463	2.28256
C	0.70962	-5.28922	1.18401
C	-1.16993	-4.92489	2.63578
C	-0.02402	-6.21156	0.46443
C	-1.91091	-5.83326	1.90098
C	-1.33675	-6.48207	0.82109
C	0.72915	-3.32818	4.41621
C	0.37025	-4.32879	5.31391
C	0.95868	-2.03890	4.88891
C	0.24388	-4.04370	6.66176
C	0.80860	-1.75025	6.23051
C	0.45387	-2.75398	7.11912
H	-1.62985	-4.39933	3.46510
H	0.51479	0.53867	-2.62117
H	1.66106	1.06147	-1.37245
H	-1.86488	1.92606	-2.50988
H	-1.89378	3.29310	-1.38833
H	0.34144	2.95079	-2.86577
H	0.54273	3.19901	-1.12237
H	-0.01893	-4.83145	7.35780
H	0.21318	-5.34070	4.95831
H	0.42441	-6.71707	-0.38250
H	-1.26791	1.89705	0.48386
H	-2.26235	0.73369	-0.44432
H	-2.94292	-6.02740	2.16730
H	-1.91628	-7.19772	0.24945
H	0.97405	-0.74102	6.58851
H	1.25410	-1.27030	4.18268
H	0.34450	-2.52950	8.17387
H	1.72994	-5.04893	0.90664
H	-1.76685	-0.42746	1.83624
H	-0.90196	-1.86691	2.36343
H	-1.63445	-3.11445	0.33258
H	-3.73031	-0.88494	0.30606
H	-3.75112	-2.48199	-0.62172
H	0.65025	-1.98903	-1.72864
H	0.99053	-3.06316	-0.36336
H	3.27129	-2.16781	-0.12878
H	2.69755	-1.08383	-2.93417
H	4.33016	-1.22310	-2.07981
H	2.54952	0.66916	0.92277
H	2.21750	-0.38324	2.30346
H	0.43984	1.15000	3.10754
H	1.70971	3.05016	1.07705
H	0.50666	3.45730	2.42188
O	-0.22737	0.56207	-0.69627
O	1.76228	-2.94678	2.34558

Section C2

Mechanochemical Influence on Stereoisomer Formation in the Syntheses of Group 15 Bis(1,3-trimethylsilyl)allyl Complexes (As–Bi)

All calculations were performed with the Gaussian 09W suite of programs.^[1] Each conformation of the complexes (C_1 , C_3 , 1U2D) was studied with four different metals (Al, As, Sb, Bi) and with three separate density functionals: M06-L,^[2] APF-D,^[3] wB97X-D,^[4] each of which includes some accounting for dispersion interactions. M06-L is a *meta*-GGA functional, APF-D is a global hybrid with 23% exact exchange; wB97X-D is a range-separated hybrid, with 22.2–100% exact exchange. The def2TZVP basis set was used on the metal atoms; for Sb and Bi, an effective core potential is used to account for relativistic effects. The def2SVP basis was used on all other atoms.^[5] An ultrafine grid was used for all calculations (Gaussian Keyword: Int=Ultrafine). The C_3 conformations were studied with imposed C_3 symmetry; the C_1 and 1U2D conformations had no symmetry. The nature of the stationary points was determined with analytical frequency calculations; all optimized geometries were found to be minima ($N_{\text{imag}} = 0$).

A total of 36 optimizations was completed for the $[\text{EA}'_3]$ species. The conformation with the lowest ΔG° value for each metal/functional combination was assigned a relative energy of 0.0 kJ mol⁻¹, and the others adjusted appropriately. The differences were then averaged across the functionals. All functionals produced the same relative ordering of the conformational energies, although the absolute values varied. For example, the C_3 conformation was found to be lowest in energy for $[\text{SbA}'_3]$ with all three functionals, but C_1 was 8.01, 9.44, and 10.07 kJ mol⁻¹ higher for the M06-L, APF-D, and wB97X-D functionals, respectively, averaging to 9.17 kJ mol⁻¹. A summary of the energy differences is given in the table below; individual values of the energies can be found in the listing of fractional coordinates (Table S2).

Table 16. Summary of Average Energy Differences in $[\text{EA}'_3]$ Conformations (ΔG° , kJ mol⁻¹)

Element	C_3	C_1	1U2D
Al	27.84	6.34	0.00
As	5.14	0.00	18.91
Sb	0.00	9.17	24.94
Bi	0.00	15.85	16.63

Table 17. Coordinates of Optimized Structures (Å)

97

[AlA'3], C3; M06-L/ def2TZVP(Al);

def2SVP(C,H,Si); $\Delta G^\circ = -3044.226073$ au

C	0.959990	-1.699927	0.610415
C	-1.952175	0.018588	0.610415
C	0.992186	1.681339	0.610415
C	0.000000	-2.631198	-0.035981
C	-2.278684	1.315599	-0.035981
C	2.278684	1.315599	-0.035981
C	-0.063188	-2.969775	-1.342242
C	-2.540306	1.539610	-1.342242
C	2.603495	1.430165	-1.342242
C	3.319103	-1.295876	2.550746
C	-2.781813	-2.226490	2.550746
C	-0.537290	3.522366	2.550746
C	2.694534	-4.077313	1.431101
C	-4.878323	-0.294879	1.431101
C	2.183789	4.372191	1.431101
C	0.859948	-2.815072	3.526074
C	-2.867898	0.662799	3.526074
C	2.007950	2.152273	3.526074
C	5.146202	-0.190587	-0.858562
C	-2.408048	4.552035	-0.858562
C	-2.738154	-4.361448	-0.858562
C	5.248284	2.291691	-2.674579
C	-4.608804	3.399301	-2.674579
C	-0.639479	-5.690992	-2.674579
C	-2.095970	-3.168063	-3.606459
C	-1.695639	3.399195	-3.606459
C	3.791608	-0.231131	-3.606459
H	1.731085	-1.401107	-0.131196
H	-2.078936	-0.798610	-0.131196
H	0.347851	2.199717	-0.131196
H	-0.767061	-3.049593	0.639228
H	-2.257494	2.189091	0.639228
H	3.024555	0.860502	0.639228
H	0.709401	-2.533895	-1.997463
H	-2.549118	0.652588	-1.997463
H	1.839717	1.881307	-1.997463
H	4.021796	-1.088737	1.730157
H	-2.953772	-2.938609	1.730157
H	-1.068024	4.027346	1.730157
H	3.904481	-1.730385	3.375284
H	-3.450798	-2.516187	3.375284
H	-0.453683	4.246572	3.375284
H	2.932096	-0.330421	2.906861
H	-1.752201	-2.374060	2.906861
H	-1.179896	2.704480	2.906861
H	3.341619	-3.913090	0.555810
H	-5.059645	-0.937382	0.555810
H	1.718026	4.850472	0.555810

H	1.916243	-4.791863	1.123616
H	-5.107997	0.736416	1.123616
H	3.191754	4.055447	1.123616
H	3.305203	-4.563893	2.206370
H	-5.605049	-0.580443	2.206370
H	2.299846	5.144336	2.206370
H	1.462518	-3.225042	4.350967
H	-3.524227	0.345943	4.350967
H	2.061709	2.879099	4.350967
H	0.076122	-3.555638	3.307150
H	-3.117334	1.711895	3.307150
H	3.041212	1.843743	3.307150
H	0.364836	-1.909527	3.913115
H	-1.836117	0.638806	3.913115
H	1.471281	1.270721	3.913115
H	5.371756	0.370612	0.061199
H	-3.006837	4.466771	0.061199
H	-2.364919	-4.837383	0.061199
H	6.107027	-0.533313	-1.270964
H	-2.591651	5.555497	-1.270964
H	-3.515376	-5.022184	-1.270964
H	-3.233188	-3.420581	-0.570511
H	-1.345716	4.510313	-0.570511
H	4.578904	-1.089732	-0.570511
H	4.712353	2.921353	-3.400247
H	-4.886142	2.620341	-3.400247
H	0.173790	-5.541694	-3.400247
H	6.178191	1.955656	-3.158022
H	-4.782743	4.372642	-3.158022
H	-1.395448	-6.328298	-3.158022
H	5.528414	2.937767	-1.829551
H	-5.308388	3.318863	-1.829551
H	-0.220026	-6.256630	-1.829551
H	-1.322176	-2.930985	-4.351933
H	-1.877220	2.610530	-4.351933
H	3.199395	0.320455	-4.351933
H	-2.573034	-2.218853	-3.319583
H	-0.635066	3.337739	-3.319583
H	3.208100	-1.118886	-3.319583
H	-2.858220	-3.780212	-4.111851
H	-1.844650	4.365397	-4.111851
H	4.702870	-0.585185	-4.111851
Si	1.944951	-2.463495	2.030104
Si	-3.105925	-0.452629	2.030104
Si	1.160974	2.916125	2.030104
Si	-1.371500	-4.052278	-2.112559
Si	-2.823626	3.213893	-2.112559
Si	4.195126	0.838385	-2.112559
Al	0.000000	0.000000	0.812969

97

[AlA'3], C1; M06-L/def2TZVP(Al);

def2SVP(C,H,Si); $\Delta G^\circ = -3044.240014$ au

C	-0.255355	-1.469149	1.194756	H	-1.887494	-1.542796	-3.067249
C	0.944949	-2.079382	0.568601	H	2.350670	-1.558533	-3.564596
C	2.234912	-1.944722	0.945922	H	2.758505	0.011123	-2.838327
C	-2.249155	-3.702275	0.417061	H	2.306468	-1.348417	-1.798052
C	-0.278675	-4.136821	2.704817	H	0.406007	0.100369	-5.335652
C	-2.601962	-2.225435	3.117191	H	-0.934741	1.017552	-4.623899
C	2.973640	-4.199796	-0.977689	H	0.732285	1.577128	-4.409723
C	5.014051	-1.937182	-0.457514	H	3.529301	4.898424	-2.347349
C	4.366705	-3.947782	1.736897	H	5.043910	4.530880	-1.504658
C	-3.154863	-0.021373	-0.003719	H	4.303113	3.321278	-2.571696
C	-2.688335	1.197662	0.648305	H	2.214835	5.614794	0.405595
C	-1.930246	1.249591	1.800230	H	2.284917	4.462604	1.749354
C	-5.936036	0.928321	-0.894185	H	3.766645	5.259502	1.184227
C	-4.777914	-1.669312	-2.007488	H	4.244386	1.191955	-0.280889
C	-3.601804	1.071068	-2.840051	H	5.076729	2.368177	0.750662
C	-1.892299	3.220483	4.137705	H	3.578720	1.604964	1.309513
C	0.717786	2.207872	2.900321	H	-2.919778	-4.500685	0.768998
C	-1.100610	4.151244	1.308832	H	-2.857810	-3.002994	-0.176661
C	-0.131486	0.798161	-1.385868	H	-1.529150	-4.173562	-0.270437
C	1.105407	1.440171	-0.878018	H	-0.873325	-4.942555	3.161082
C	1.480011	2.733876	-0.987551	H	0.425399	-4.602274	1.998327
C	-0.834945	-1.824429	-2.909249	H	0.327433	-3.678963	3.501751
C	2.087243	-0.858421	-2.757017	H	-3.137144	-3.073624	3.571234
C	0.097137	0.678635	-4.451593	H	-2.092635	-1.696524	3.937922
C	4.083225	4.101929	-1.828116	H	-3.367484	-1.545419	2.716630
C	2.818338	4.809812	0.852447	H	3.778103	-4.839341	-1.371040
C	4.084306	2.021815	0.425057	H	2.219719	-4.866778	-0.531197
H	0.073714	-0.888748	2.077793	H	2.504298	-3.704297	-1.840842
H	0.737276	-2.769349	-0.269300	H	5.859750	-2.565836	-0.775885
H	2.430805	-1.260700	1.788953	H	4.675608	-1.370213	-1.336942
H	-3.385234	-0.816950	0.724195	H	5.405142	-1.210763	0.270791
H	-2.714891	2.116073	0.036338	H	5.201869	-4.590536	1.419399
H	-1.945784	0.335693	2.416566	H	4.752124	-3.275509	2.518109
H	-0.812517	1.572873	-1.789050	H	3.610604	-4.594008	2.207593
H	1.805097	0.748354	-0.376728	Si	-1.363412	-2.862505	1.848496
H	0.783595	3.407642	-1.514282	Si	3.642268	-2.982614	0.292245
H	-6.664092	1.005466	-1.716056	Si	-4.352897	0.068551	-1.437480
H	-6.428073	0.391490	-0.069470	Si	-1.047910	2.733071	2.531249
H	-5.735172	1.950990	-0.539962	Si	0.295458	-0.314412	-2.868273
H	-5.501967	-1.646561	-2.835798	Si	3.103814	3.411647	-0.376049
H	-3.902466	-2.236824	-2.355230	Al	-1.126760	-0.141041	0.018249
H	-5.239624	-2.250486	-1.194529				
H	-4.309531	1.182082	-3.675345				
H	-3.328586	2.087770	-2.516602	97			
H	-2.691467	0.603975	-3.243832	[AlA ³], 1U2D; M06-L/def2TZVP(Al);			
H	-2.936203	3.525160	3.973844	def2SVP(C,H,Si); ΔG° = -3044.242640 au			
H	-1.903323	2.389626	4.858697	Al	0.419499	-0.022854	-0.262133
H	-1.374411	4.063108	4.620341	C	-1.736285	2.874327	0.271260
H	1.258266	1.970177	1.970351	C	-1.064774	2.138455	-0.644694
H	1.282891	2.993972	3.423838	C	0.396144	1.878238	-0.711459
H	0.743415	1.312302	3.540493	C	-4.381320	1.900127	-0.878660
H	-2.132246	4.463995	1.087072	C	-4.175698	2.664746	2.094803
H	-0.572018	5.032953	1.700752	C	-4.073828	4.849904	-0.033877
H	-0.614036	3.877370	0.360076	C	0.562358	1.355473	-3.768418
H	-0.565381	-2.519550	-3.718995	C	3.089131	2.017506	-2.082139
H	-0.793784	-2.403167	-1.970599	C	0.971748	4.167945	-2.682574
				C	3.766193	-0.884922	1.142546

C	2.645022	-0.158013	1.354579	H	-0.837846	-3.578802	-3.734711
C	1.243482	-0.637561	1.397704	H	-0.083407	-4.545877	-0.849201
C	5.446747	1.657467	1.329106	H	1.186019	-3.715859	0.069411
C	6.169078	-0.522888	-0.721707	H	1.617791	-4.741327	-1.306281
C	6.623548	-1.029974	2.251173	H	-1.663600	1.631619	-1.423396
C	0.776631	-1.109589	4.402142	H	0.920092	2.425486	0.095227
C	-1.578772	-0.355277	2.572095	H	-4.071059	0.862158	-0.680669
C	0.571036	1.726331	3.260082	H	-4.102030	2.137215	-1.916582
C	-2.934620	-1.748185	-0.835397	H	-5.479810	1.932924	-0.822043
C	-1.604340	-1.912103	-0.658839	H	-3.997519	1.609669	2.347892
C	-0.496583	-1.296223	-1.426855	H	-5.254076	2.851864	2.212786
C	-3.457557	-3.927337	1.237945	H	-3.655089	3.275801	2.848254
C	-5.551825	-3.318258	-0.928928	H	-5.162491	4.995880	0.036027
C	-5.095990	-1.340579	1.349533	H	-3.765192	5.141317	-1.048569
C	2.449401	-1.754543	-2.262525	H	-3.604827	5.558574	0.664861
C	0.169234	-3.140275	-3.800639	H	0.735035	0.272809	-3.680381
C	0.875642	-4.014420	-0.943498	H	1.020105	1.678465	-4.715731
H	3.627515	-1.972628	1.021496	H	-0.523824	1.503633	-3.872017
H	2.762767	0.933628	1.471205	H	3.535548	2.793825	-1.441694
H	1.212754	-1.743484	1.363215	H	3.650398	2.018885	-3.028672
H	4.810990	2.185477	0.602898	H	3.279243	1.049599	-1.589555
H	6.452229	2.098715	1.260269	H	-0.100497	4.387087	-2.797290
H	5.059665	1.884935	2.333961	H	1.475843	4.491675	-3.605591
H	5.580384	-0.012537	-1.498770	H	1.344645	4.800893	-1.863569
H	6.157696	-1.597956	-0.958067	Si	-3.590462	3.073867	0.354323
H	7.210580	-0.180154	-0.819616	Si	1.252005	2.346446	-2.324342
H	7.658087	-0.663745	2.168152	Si	5.491848	-0.192605	1.004190
H	6.651603	-2.119713	2.101652	Si	0.252490	-0.091539	2.914848
H	6.291538	-0.852229	3.284543	Si	-4.248823	-2.570158	0.201982
H	0.258956	-0.794326	5.320521	Si	0.746349	-2.551624	-2.115069
H	1.857973	-1.011891	4.580896				
H	0.565868	-2.179484	4.256824	97			
H	-2.195546	-0.052607	3.432622	[AlA '3], C3; APF-D/def2TZVP(Al);			
H	-1.810069	-1.411133	2.361861	def2SVP(C,H,Si); $\Delta G^\circ = -3042.975353$ au			
H	-1.932809	0.231135	1.705661	C	0.128815	2.755124	-1.334137
H	0.347405	2.357939	2.387333	C	0.000000	2.582892	-0.001069
H	1.616882	1.913404	3.546829	C	-0.973815	1.694986	0.690413
H	-0.061787	2.084214	4.086377	C	-0.980993	-1.690841	0.690413
H	-3.241728	-1.095949	-1.669070	C	-2.450415	-1.266005	-1.334137
H	-1.124194	3.385810	1.032106	C	2.321600	-1.489119	-1.334137
H	-1.279841	-2.570533	0.165925	C	2.236851	-1.291446	-0.001069
H	-0.904230	-0.711774	-2.272059	C	2.236851	-1.291446	-0.001069
H	-2.936388	-4.665180	0.609089	C	1.954808	-0.004144	0.690413
H	-4.215377	-4.471528	1.821390	H	-0.300726	-2.181300	-0.035472
H	-2.723654	-3.535057	1.958251	H	-1.628101	-1.617427	-1.977912
H	-6.015121	-2.550245	-1.566640	H	2.214783	-0.601264	-1.977912
H	-6.360938	-3.796139	-0.356168	H	-0.586682	2.218690	-1.977912
H	-5.123756	-4.080277	-1.596665	H	2.327584	-2.169027	0.657325
H	-4.377074	-0.879785	2.043492	H	2.039425	0.830214	-0.035472
H	-5.870446	-1.834309	1.956806	H	0.714641	3.100261	0.657325
H	-5.587315	-0.525851	0.796528	H	-1.738699	1.351087	-0.035472
H	2.817289	-1.369711	-1.293855	Si	1.475905	3.746520	-2.165701
H	2.475692	-0.920149	-2.980241	Si	-1.950180	2.524657	2.076074
H	3.202257	-2.482914	-2.601666	Si	2.506629	-3.151431	-2.165701
H	0.837746	-3.905159	-4.223466	Si	3.161507	0.426577	2.076074
H	0.116956	-2.312865	-4.523993				

Si	-3.982534	-0.595089	-2.165701
H	-3.042225	-0.931233	0.657325
Si	-1.211328	-2.951234	2.076074
Al	0.000000	0.000000	0.927790
C	-2.236851	-1.291446	-0.001069
C	3.012841	-0.761478	3.534052
H	3.755084	-0.504331	4.306858
H	2.016959	-0.711835	4.003103
H	3.198400	-1.803492	3.231084
C	-0.846961	2.989936	3.534052
H	-1.440779	3.504163	4.306858
H	-0.392012	2.102656	4.003103
H	-0.037330	3.671641	3.231084
C	-2.165880	-2.228458	3.534052
H	-2.314305	-2.999833	4.306858
H	-1.624947	-1.390820	4.003103
H	-3.161070	-1.868149	3.231084
C	0.467140	-3.548707	2.687982
H	1.058264	-3.995194	1.873946
H	1.057070	-2.731596	3.127291
H	0.334252	-4.318899	3.464541
C	-3.306841	1.369798	2.687982
H	-3.989071	1.081113	1.873946
H	-2.894166	0.450348	3.127291
H	-3.907403	1.869979	3.464541
C	2.839701	2.178909	2.687982
H	2.930807	2.914081	1.873946
H	1.837096	2.281247	3.127291
H	3.573151	2.448920	3.464541
C	4.910972	0.324270	1.383298
H	5.666371	0.555734	2.151116
H	5.116634	-0.683869	0.990216
H	5.039868	1.035930	0.552021
C	-2.736312	4.090891	1.383298
H	-3.314465	4.629354	2.151116
H	-1.966068	4.773069	0.990216
H	-3.417076	3.846689	0.552021
C	-2.174660	-4.415161	1.383298
H	-2.351906	-5.185088	2.151116
H	-3.150565	-4.089200	0.990216
H	-1.622792	-4.882619	0.552021
C	2.412373	2.611361	-3.349710
H	2.896209	1.787194	-2.801520
H	1.730643	2.167430	-4.092820
H	3.194902	3.161444	-3.896845
C	-3.467691	0.783496	-3.349710
H	-2.995860	1.614593	-2.801520
H	-2.742371	0.415066	-4.092820
H	-4.335342	1.186144	-3.896845
C	1.055318	-3.394856	-3.349710
H	0.099651	-3.401787	-2.801520

H	1.011728	-2.582496	-4.092820
H	1.140440	-4.347588	-3.896845
C	0.732423	5.175763	-3.146315
H	1.513153	5.743380	-3.677894
H	0.014681	4.805573	-3.895721
H	0.195130	5.870592	-2.481840
C	-4.848554	-1.953585	-3.146315
H	-5.730489	-1.561261	-3.677894
H	-4.169089	-2.390073	-3.895721
H	-5.181647	-2.766309	-2.481840
C	4.116131	-3.222178	-3.146315
H	4.217336	-4.182119	-3.677894
H	4.154408	-2.415501	-3.895721
H	4.986517	-3.104283	-2.481840
C	2.677504	4.409601	-0.871858
H	2.167381	5.022478	-0.112107
H	3.195271	3.584379	-0.358078
H	3.445643	5.038858	-1.348870
C	-5.157578	0.113986	-0.871858
H	-5.433284	-0.634232	-0.112107
H	-4.701799	0.974996	-0.358078
H	-6.086601	0.464585	-1.348870
C	2.480074	-4.523587	-0.871858
H	3.265903	-4.388246	-0.112107
H	1.506528	-4.559375	-0.358078
H	2.640958	-5.503443	-1.348870

97

[AlA³], C1; APF-D/def2TZVP(Al);

def2SVP(C,H,Si); $\Delta G^\circ = -3042.979779$ au

C	0.265519	-1.509895	-1.183790
C	-0.946612	-2.100623	-0.552079
C	-2.229607	-1.907524	-0.923557
C	2.252204	-3.755899	-0.372329
C	0.289505	-4.192023	-2.685982
C	2.635953	-2.292046	-3.073873
C	-3.116248	-4.195001	0.935768
C	-5.004756	-1.784466	0.475238
C	-4.466018	-3.766174	-1.789737
C	3.164033	0.013998	-0.036324
C	2.657353	1.225034	-0.681979
C	1.912607	1.251878	-1.837858
C	5.965310	0.981646	0.767527
C	4.828142	-1.601745	1.959168
C	3.683936	1.157254	2.791288
C	1.823811	3.214818	-4.182631
C	-0.769062	2.146614	-2.919617
C	1.008926	4.146005	-1.348670
C	0.148163	0.749043	1.411866
C	-1.099546	1.375710	0.899756
C	-1.469728	2.668927	1.015615
C	0.900072	-1.836363	3.016403
C	-2.036710	-0.937530	2.831986

C	-0.061957	0.703463	4.476221	H	2.135024	-1.768329	-3.904051
C	-4.074593	4.038285	1.864928	H	3.389821	-1.612467	-2.650372
C	-2.768774	4.791675	-0.798413	H	-3.970968	-4.808207	1.263424
C	-4.086623	2.014430	-0.452480	H	-2.375257	-4.870769	0.479798
H	-0.049170	-0.930146	-2.070857	H	-2.665064	-3.746559	1.833557
H	-0.756489	-2.809575	0.269701	H	-5.879410	-2.377426	0.788126
H	-2.406199	-1.197184	-1.747043	H	-4.615862	-1.257285	1.359065
H	3.426985	-0.771396	-0.762313	H	-5.351214	-1.028623	-0.247054
H	2.668563	2.145426	-0.077263	H	-5.343493	-4.361143	-1.488991
H	1.939676	0.340838	-2.453789	H	-4.797199	-3.036080	-2.545546
H	0.829608	1.527978	1.801538	H	-3.740268	-4.441794	-2.269194
H	-1.790751	0.682194	0.396973	Si	1.372378	-2.917138	-1.815396
H	-0.778306	3.342510	1.546868	Si	-3.693288	-2.894564	-0.303552
H	6.715229	1.060098	1.571256	Si	4.389932	0.134260	1.372264
H	6.418149	0.421716	-0.066201	Si	0.991511	2.715957	-2.566317
H	5.749393	2.000369	0.407115	Si	-0.255362	-0.342656	2.919313
H	5.571530	-1.559918	2.771160	Si	-3.088616	3.367685	0.400346
H	3.950886	-2.151216	2.331809	Al	1.141992	-0.185730	0.000681
H	5.267286	-2.188686	1.136527				
H	4.439618	1.289496	3.581882	97			
H	3.381189	2.161417	2.453569	[AlA '3], 1U/2D; APF-D/def2TZVP(Al);			
H	2.804564	0.675565	3.241829	def2SVP(C,H,Si); $\Delta G^\circ = -3042.982264$ au			
H	2.861445	3.540906	-4.010154	Al	0.424678	0.024097	-0.188216
H	1.847334	2.373177	-4.893036	C	-1.991128	2.735242	0.322650
H	1.280023	4.044904	-4.661895	C	-1.229628	2.085066	-0.585023
H	-1.276274	1.895223	-1.976277	C	0.252579	1.933815	-0.585287
H	-1.353732	2.927889	-3.430270	C	-4.513871	1.711103	-1.084808
H	-0.770816	1.252421	-3.563393	C	-4.580096	2.372439	1.930158
H	2.036322	4.467087	-1.114282	C	-4.359632	4.639086	-0.119849
H	0.473792	5.012916	-1.766898	C	0.455746	1.621754	-3.684193
H	0.501898	3.859784	-0.415015	C	2.945781	2.337334	-1.983539
H	0.641367	-2.470966	3.879030	C	0.676786	4.380144	-2.383683
H	0.837524	-2.467860	2.115097	C	3.690998	-0.795604	1.078575
H	1.948916	-1.526699	3.135972	C	2.586804	-0.080449	1.394678
H	-2.258488	-1.638805	3.651834	C	1.191328	-0.576113	1.509689
H	-2.726160	-0.082909	2.912845	C	5.394848	1.748170	1.322604
H	-2.234790	-1.439091	1.876146	C	6.039240	-0.337898	-0.856918
H	-0.364106	0.140389	5.373910	C	6.576495	-0.995821	2.086913
H	0.973448	1.047341	4.622885	C	0.738781	-1.062355	4.511284
H	-0.705795	1.594597	4.401133	C	-1.621009	-0.245258	2.703331
H	-3.505896	4.815735	2.399921	C	0.574994	1.798301	3.409559
H	-5.026392	4.484607	1.534147	C	-2.700132	-1.898806	-0.884586
H	-4.304130	3.235462	2.583256	C	-1.367438	-1.994023	-0.686020
H	-2.158278	5.574479	-0.320391	C	-0.286003	-1.302893	-1.438513
H	-2.228601	4.442440	-1.690782	C	-3.132393	-4.047446	1.267353
H	-3.713690	5.253680	-1.127063	C	-5.134915	-3.743087	-1.054943
H	-4.289965	1.181308	0.237528	C	-5.012169	-1.615815	1.151058
H	-5.055311	2.411776	-0.795315	C	2.652044	-1.579982	-2.446386
H	-3.561454	1.606787	-1.329956	C	0.382986	-3.218723	-3.736553
H	2.893882	-4.575849	-0.732447	C	1.356019	-3.879712	-0.897045
H	2.885997	-3.054184	0.190741	H	3.559259	-1.879125	0.930851
H	1.524651	-4.192858	0.330292	H	2.709758	1.003004	1.549050
H	0.894926	-5.015372	-3.097582	H	1.160840	-1.680552	1.478640
H	-0.449928	-4.620756	-1.992040	H	4.743124	2.307390	0.634095
H	-0.268244	-3.728090	-3.515249	H	6.409048	2.170076	1.239513
H	3.173185	-3.152332	-3.504972	H	5.040971	1.923264	2.350835

H	5.433487	0.231299	-1.578695
H	5.995695	-1.400259	-1.145267
H	7.085337	-0.004823	-0.953468
H	7.608515	-0.621197	1.992424
H	6.590097	-2.076744	1.873747
H	6.258080	-0.863373	3.132849
H	0.222426	-0.744164	5.431206
H	1.824022	-0.979388	4.680914
H	0.504945	-2.125559	4.342028
H	-2.216905	-0.006334	3.598505
H	-1.844192	-1.283562	2.414691
H	-1.965467	0.412277	1.888491
H	0.316460	2.449710	2.561561
H	1.636028	1.959158	3.656818
H	-0.023045	2.125539	4.275084
H	-3.037242	-1.256458	-1.712842
H	-1.465824	3.242435	1.146647
H	-1.020245	-2.641876	0.133474
H	-0.708586	-0.738838	-2.289187
H	-2.514671	-4.761385	0.700007
H	-3.884133	-4.624423	1.829267
H	-2.484537	-3.546217	2.003418
H	-5.629153	-3.045974	-1.750540
H	-5.921894	-4.278833	-0.500085
H	-4.577257	-4.478801	-1.655574
H	-4.371965	-1.072957	1.862703
H	-5.784251	-2.153334	1.725054
H	-5.519589	-0.872192	0.517193
H	3.077125	-1.172727	-1.514111
H	2.535864	-0.751943	-3.162116
H	3.397611	-2.274520	-2.865897
H	1.080306	-3.964286	-4.150970
H	0.235996	-2.432839	-4.494532
H	-0.588164	-3.710932	-3.569273
H	0.454515	-4.489063	-0.728669
H	1.697915	-3.498360	0.077340
H	2.142192	-4.545270	-1.288092
H	-1.749298	1.583347	-1.416948
H	0.703077	2.496881	0.252234
H	-4.185463	0.676784	-0.902213
H	-4.164825	2.012598	-2.085127
H	-5.615320	1.722196	-1.097871
H	-4.362008	1.320880	2.168467
H	-5.674265	2.502464	1.937640
H	-4.161261	2.997472	2.735109
H	-5.456319	4.745354	-0.143014
H	-3.963215	4.960171	-1.095959
H	-3.970004	5.329756	0.644977
H	0.729321	0.556775	-3.670565
H	0.884728	2.064939	-4.597188
H	-0.640513	1.688949	-3.768451
H	3.325643	2.985671	-1.178171
H	3.473258	2.612721	-2.910435
H	3.217611	1.300417	-1.734512
H	-0.413339	4.528472	-2.437885
H	1.125940	4.788774	-3.303004

H	1.050877	4.968443	-1.530715
Si	-3.857377	2.859069	0.257191
Si	1.081938	2.553179	-2.166647
Si	5.414387	-0.090408	0.907834
Si	0.220657	-0.014368	3.033031
Si	-3.984532	-2.815952	0.118738
Si	1.027782	-2.486876	-2.125127

97

[AlA'3], C3; □B97X-D/def2TZVP(Al);

def2SVP(C,H,Si); ΔG° = -3044.121073 au

C	-1.205283	2.687075	-1.348925
C	-1.130725	2.382349	-0.039310
C	-1.600315	1.122451	0.611937
C	-0.171914	-1.947139	0.611937
C	-1.724434	-2.387343	-1.348925
C	2.929716	-0.299732	-1.348925
C	2.628537	-0.211938	-0.039310
C	1.772229	0.824688	0.611937
H	0.631637	-2.159903	-0.122286
H	-0.838045	-2.447860	-1.999953
H	2.538932	0.498162	-1.999953
H	-1.700887	1.949698	-1.999953
H	2.999534	-1.002251	0.630217
H	1.554712	1.626965	-0.122286
H	-0.631792	3.098798	0.630217
H	-2.186349	0.532938	-0.122286
Si	-0.482954	4.215923	-2.142870
Si	-2.779090	1.386427	2.061628
Si	3.892573	-1.689711	-2.142870
Si	2.590225	1.713549	2.061628
Si	-3.409619	-2.526211	-2.142870
H	-2.367742	-2.096547	0.630217
Si	0.188864	-3.099975	2.061628
Al	0.000000	0.000000	0.797235
C	-1.497812	-2.170411	-0.039310
C	2.716316	0.613549	3.589381
H	3.110869	1.190870	4.440849
H	1.737832	0.205555	3.892822
H	3.400480	-0.233055	3.423133
C	-1.889507	2.045624	3.589381
H	-2.586759	2.098657	4.440849
H	-1.046932	1.402229	3.892822
H	-1.498408	3.061429	3.423133
C	-0.826809	-2.659174	3.589381
H	-0.524111	-3.289527	4.440849
H	-0.690900	-1.607785	3.892822
H	-1.902071	-2.828374	3.423133
C	2.014613	-2.994341	2.503923
H	2.652595	-3.265610	1.649001
H	2.294095	-1.981696	2.828116
H	2.249317	-3.684496	3.329839

C	-3.600482	-0.247535	2.503923
H	-4.154399	-0.664409	1.649001
H	-2.863246	-0.995897	2.828116
H	-4.315525	-0.105718	3.329839
C	1.585869	3.241876	2.503923
H	1.501804	3.930020	1.649001
H	0.569151	2.977593	2.828116
H	2.066208	3.790213	3.329839
C	4.323919	2.237675	1.549988
H	4.842153	2.771702	2.362354
H	4.933607	1.363816	1.270836
H	4.284406	2.905010	0.674190
C	-4.099842	2.625786	1.549988
H	-4.821440	2.807577	2.362354
H	-3.647903	3.590721	1.270836
H	-4.658015	2.257900	0.674190
C	-0.224076	-4.863461	1.549988
H	-0.020712	-5.579278	2.362354
H	-1.285704	-4.954537	1.270836
H	0.373609	-5.162909	0.674190
C	0.599490	3.686452	-3.593376
H	1.425425	3.041987	-3.252177
H	0.016158	3.118821	-4.335996
H	1.037924	4.557671	-4.106042
C	-3.492306	-1.324052	-3.593376
H	-3.347150	-0.286540	-3.252177
H	-2.709058	-1.545417	-4.335996
H	-4.466021	-1.379967	-4.106042
C	2.892816	-2.362400	-3.593376
H	1.921726	-2.755447	-3.252177
H	2.692899	-1.573404	-4.335996
H	3.428097	-3.177704	-4.106042
C	-1.856282	5.338956	-2.778641
H	-1.445137	6.229453	-3.280831
H	-2.495158	4.808996	-3.502986
H	-2.499644	5.679131	-1.951902
C	-3.695530	-4.277065	-2.778641
H	-4.672296	-4.366252	-3.280831
H	-2.917133	-4.565368	-3.502986
H	-3.668450	-5.004321	-1.951902
C	5.551812	-1.061891	-2.778641
H	6.117433	-1.863201	-3.280831
H	5.412291	-0.243628	-3.502986
H	6.168094	-0.674810	-1.951902
C	0.573995	5.146245	-0.890186
H	0.000000	5.422989	0.008490
H	1.432832	4.533448	-0.572426
H	0.971074	6.074219	-1.331288
C	-4.743776	-2.076028	-0.890186
H	-4.696446	-2.711494	0.008490
H	-4.642497	-1.025855	-0.572426

H	-5.745964	-2.196135	-1.331288
C	4.169781	-3.070217	-0.890186
H	4.696446	-2.711494	0.008490
H	3.209665	-3.507593	-0.572426
H	4.774891	-3.878084	-1.331288

97

[AlA'3], C₁; □B97X-D/def2TZVP(Al);

def2SVP(C,H,Si); ΔG° = -3044.127275 au

C	0.228411	-1.509638	-1.185977
C	-1.017033	-2.070656	-0.580424
C	-2.285558	-1.818209	-0.954388
C	2.193724	-3.790182	-0.444327
C	0.163180	-4.182731	-2.706439
C	2.523012	-2.310628	-3.141627
C	-3.268286	-4.099837	0.854417
C	-5.033407	-1.590153	0.474470
C	-4.622229	-3.539853	-1.843828
C	3.138516	-0.041738	-0.059446
C	2.649724	1.201150	-0.691693
C	1.950383	1.266625	-1.862825
C	5.942041	0.919715	0.758277
C	4.817327	-1.708758	1.862992
C	3.671223	1.007161	2.799349
C	1.820933	3.254257	-4.186471
C	-0.740875	2.178488	-2.868770
C	1.084411	4.160177	-1.325034
C	0.184616	0.672830	1.465872
C	-1.044887	1.353209	0.964856
C	-1.358770	2.658055	1.081255
C	0.879743	-1.972976	2.954334
C	-2.028622	-0.978516	2.871290
C	0.030135	0.532228	4.537413
C	-3.916653	4.110983	1.933066
C	-2.574884	4.840113	-0.716995
C	-3.985659	2.108156	-0.397876
H	-0.061572	-0.893895	-2.057407
H	-0.861436	-2.803923	0.227083
H	-2.423491	-1.083360	-1.763035
H	3.430351	-0.790016	-0.812639
H	2.662879	2.106979	-0.066619
H	1.962796	0.361803	-2.488084
H	0.888131	1.427639	1.863196
H	-1.766215	0.690321	0.463860
H	-0.633756	3.299740	1.606230
H	6.696139	0.973808	1.559957
H	6.393958	0.392199	-0.096829
H	5.721545	1.949808	0.434650
H	5.562538	-1.700652	2.674244
H	3.939158	-2.269648	2.218107
H	5.251178	-2.268596	1.018711
H	4.430890	1.129750	3.587458
H	3.340249	2.014745	2.499528
H	2.807345	0.490556	3.242654
H	2.864241	3.573697	-4.037457

H	1.823359	2.419289	-4.905080	C	-2.028270	2.715241	0.250077
H	1.271440	4.091219	-4.646582	C	-1.257867	2.055313	-0.637538
H	-1.221038	1.908825	-1.915347	C	0.229073	1.903777	-0.613372
H	-1.346954	2.962279	-3.350173	C	-4.532360	1.642846	-1.146044
H	-0.758190	1.292945	-3.524653	C	-4.601943	2.332264	1.862394
H	2.121264	4.459968	-1.103850	C	-4.425542	4.579161	-0.211774
H	0.557796	5.042451	-1.721460	C	0.486017	1.540738	-3.694458
H	0.590764	3.872537	-0.384105	C	2.944475	2.253809	-1.954915
H	0.653008	-2.624346	3.812973	C	0.714741	4.321140	-2.441885
H	0.747340	-2.579683	2.042406	C	3.678397	-0.733612	1.096764
H	1.943986	-1.698122	3.020470	C	2.575286	-0.032036	1.431936
H	-2.265183	-1.695883	3.673000	C	1.177948	-0.540773	1.541535
H	-2.692944	-0.107022	2.982534	C	5.362122	1.820601	1.324530
H	-2.254081	-1.448008	1.904544	C	5.999269	-0.260389	-0.860245
H	-0.265085	-0.058003	5.419696	C	6.574784	-0.909979	2.075999
H	1.078148	0.841525	4.671098	C	0.729255	-0.941637	4.559484
H	-0.588529	1.443927	4.516949	C	-1.641590	-0.281167	2.706170
H	-3.326652	4.866317	2.476586	C	0.465278	1.867728	3.352161
H	-4.853447	4.589314	1.604465	C	-2.655790	-1.886562	-0.862733
H	-4.173760	3.310768	2.645022	C	-1.329131	-2.021733	-0.667742
H	-1.943138	5.601056	-0.231069	C	-0.226667	-1.348427	-1.416893
H	-2.039357	4.479743	-1.608117	C	-3.147526	-4.028714	1.275172
H	-3.501289	5.334540	-1.050913	C	-5.141271	-3.654516	-1.044034
H	-4.217113	1.277132	0.286459	C	-4.959143	-1.549745	1.175298
H	-4.940726	2.534068	-0.744341	C	2.689582	-1.617761	-2.450242
H	-3.467497	1.687921	-1.274026	C	0.444816	-3.365183	-3.629000
H	2.802516	-4.628798	-0.817853	C	1.460827	-3.860988	-0.771661
H	2.864655	-3.101981	0.093366	H	3.547542	-1.814566	0.933064
H	1.479938	-4.203316	0.286849	H	2.691224	1.050025	1.597642
H	0.745260	-5.002663	-3.156630	H	1.168909	-1.646088	1.531011
H	-0.552546	-4.621830	-1.994050	H	4.693196	2.372657	0.646478
H	-0.423686	-3.700708	-3.504857	H	6.369145	2.256211	1.227272
H	3.041553	-3.167925	-3.600121	H	5.020359	1.992477	2.357533
H	2.006014	-1.768317	-3.950019	H	5.375095	0.295549	-1.577103
H	3.293641	-1.643393	-2.728233	H	5.969844	-1.324442	-1.144728
H	-4.146995	-4.676161	1.185245	H	7.038168	0.089023	-0.974101
H	-2.568331	-4.802978	0.375319	H	7.602507	-0.525727	1.974416
H	-2.780671	-3.692873	1.753370	H	6.598263	-1.990632	1.862453
H	-5.930257	-2.143516	0.796654	H	6.264827	-0.782440	3.125096
H	-4.601365	-1.098357	1.359318	H	0.191784	-0.613926	5.463701
H	-5.357253	-0.804152	-0.226116	H	1.808451	-0.810182	4.737363
H	-5.523686	-4.100875	-1.549092	H	0.540861	-2.018855	4.426036
H	-4.927253	-2.776396	-2.577370	H	-2.258073	-0.040054	3.586767
H	-3.935866	-4.236786	-2.350210	H	-1.821716	-1.336107	2.446160
Si	1.286764	-2.931497	-1.857499	H	-2.005394	0.336072	1.867486
Si	-3.792663	-2.745780	-0.348119	H	0.181817	2.473438	2.478156
Si	4.375102	0.045153	1.339149	H	1.518614	2.083382	3.591359
Si	1.027048	2.745319	-2.556993	H	-0.145934	2.206492	4.203790
Si	-0.229847	-0.442303	2.947039	H	-2.970746	-1.229196	-1.687479
Si	-2.949052	3.420880	0.468207	H	-1.508931	3.235264	1.069306
Al	1.148560	-0.262702	0.038503	H	-0.998906	-2.680159	0.149856
				H	-0.641870	-0.800911	-2.282103
97				H	-2.553191	-4.758651	0.703004
[AlA'3], 1U/2D; □B97X-D/def2TZVP(Al);				H	-3.910010	-4.585989	1.842254
def2SVP(C,H,Si); ΔG° = -3044.129407 au				H	-2.479630	-3.547493	2.007163
Al	0.432338	0.009436	-0.177696	H	-5.619237	-2.938178	-1.731444

H	-5.941212	-4.176568	-0.494849	H	-2.755605	-1.555714	0.637616
H	-4.604467	-4.397813	-1.654264	H	0.204379	-1.842779	-0.157228
H	-4.304624	-1.032816	1.893673	H	2.725091	-1.608567	0.637616
H	-5.747972	-2.067989	1.744088	H	1.493704	1.098387	-0.157228
H	-5.443987	-0.784196	0.549511	Si	3.021626	-2.607557	-2.174696
H	3.130528	-1.183021	-1.537711	Si	2.979419	1.200897	1.816446
H	2.539375	-0.803794	-3.176541	Si	-3.769023	-1.313026	-2.174696
H	3.438361	-2.304615	-2.876155	Si	-0.449702	-3.180701	1.816446
H	1.152773	-4.115225	-4.016139	Si	0.747398	3.920583	-2.174696
H	0.271651	-2.621281	-4.422984	H	0.030514	3.164281	0.637616
H	-0.513633	-3.869818	-3.428351	Si	-2.529717	1.979804	1.816446
H	0.576334	-4.483386	-0.563892	As	0.000000	0.000000	1.595726
H	1.795287	-3.418639	0.179716	C	-0.452662	2.435598	-0.034856
H	2.261954	-4.527973	-1.128010	C	-1.753668	-3.013473	3.157772
H	-1.765765	1.536368	-1.465660	H	-1.759617	-3.898019	3.812467
H	0.657076	2.489239	0.220894	H	-1.558820	-2.139434	3.797893
H	-4.189031	0.614886	-0.952358	H	-2.769874	-2.906975	2.748992
H	-4.182650	1.937170	-2.148487	C	3.486578	-0.011985	3.157772
H	-5.633785	1.635755	-1.165334	H	4.255593	0.425136	3.812467
H	-4.349326	1.292166	2.117631	H	2.632215	-0.280261	3.797893
H	-5.699811	2.425346	1.872101	H	3.902452	-0.945294	2.748992
H	-4.202607	2.982428	2.657413	C	-1.732910	3.025458	3.157772
H	-5.523538	4.669368	-0.236625	H	-2.495975	3.472883	3.812467
H	-4.034576	4.897388	-1.191058	H	-1.073394	2.419695	3.797893
H	-4.047563	5.284814	0.545169	H	-1.132577	3.852269	2.748992
H	0.753563	0.474425	-3.652202	C	-3.425323	0.541441	2.628056
H	0.930673	1.959742	-4.611147	H	-3.992628	-0.069189	1.909951
H	-0.608862	1.608583	-3.797303	H	-2.728097	-0.127627	3.155592
H	3.316624	2.904101	-1.147195	H	-4.144685	0.908147	3.376079
H	3.503501	2.505128	-2.869998	C	2.181563	2.695697	2.628056
H	3.191519	1.214989	-1.684787	H	1.936395	3.492311	1.909951
H	-0.371366	4.483804	-2.528286	H	1.253520	2.426415	3.155592
H	1.192678	4.709646	-3.355318	H	2.858821	3.135329	3.376079
H	1.073242	4.919968	-1.589569	C	1.243760	-3.237137	2.628056
Si	-3.895023	2.813707	0.183544	H	2.056233	-3.423123	1.909951
Si	1.089788	2.495187	-2.183964	H	1.474577	-2.298788	3.155592
Si	5.394745	-0.016017	0.909559	H	1.285864	-4.043476	3.376079
Si	0.186445	0.031007	3.041641	C	-0.744285	-4.747051	0.824899
Si	-3.967429	-2.770003	0.135666	H	-0.692400	-5.647194	1.455561
Si	1.090307	-2.541325	-2.065037	H	-1.734875	-4.734565	0.346183
				H	0.000000	-4.865723	0.022902
				C	4.483209	1.728956	0.824899
97				H	5.236813	2.223961	1.455561
[AsA'3], C3; M06-L/def2TZVP(As);				H	4.967691	0.864837	0.346183
def2SVP(C,H,Si); $\Delta G^\circ = -5037.582725$ au				H	4.213840	2.432862	0.022902
C	2.397074	-1.045517	-1.364812	C	-3.738925	3.018095	0.824899
C	2.335621	-0.825782	-0.034856	H	-4.544413	3.423233	1.455561
C	1.755594	0.364910	0.623684	H	-3.232816	3.869728	0.346183
C	-1.193818	1.337934	0.623684	H	-4.213840	2.432862	0.022902
C	-0.293093	2.598685	-1.364812	C	1.604550	-3.376198	-3.146119
C	-2.103981	-1.553168	-1.364812	H	0.762911	-3.640068	-2.487254
C	-1.882959	-1.609816	-0.034856	H	1.214334	-2.684792	-3.908369
C	-0.561776	-1.702844	0.623684	H	1.915964	-4.293823	-3.667966
H	-1.698083	0.744392	-0.157228	C	2.121598	3.077680	-3.146119
H	-0.765846	1.837229	-2.008198	H	2.770936	2.480735	-2.487254
H	-1.208164	-1.581857	-2.008198	H	1.717931	2.394040	-3.908369
H	1.974011	-0.255372	-2.008198				

H	2.760578	3.806185	-3.667966
C	-3.726148	0.298518	-3.146119
H	-3.533847	1.159334	-2.487254
H	-2.932265	0.290752	-3.908369
H	-4.676542	0.487638	-3.667966
C	4.434706	-2.221827	-3.351675
H	4.783488	-3.124993	-3.874799
H	4.130447	-1.496269	-4.120675
H	5.297709	-1.791675	-2.822737
C	-0.293194	4.951481	-3.351675
H	0.314580	5.705119	-3.874799
H	-0.769417	4.325207	-4.120675
H	-1.097218	5.483788	-2.822737
C	-4.141511	-2.729654	-3.351675
H	-5.098067	-2.580125	-3.874799
H	-3.361030	-2.828938	-4.120675
H	-4.200490	-3.692113	-2.822737
C	3.588449	-3.810014	-0.847431
H	4.363497	-3.378039	-0.196225
H	2.750529	-4.119720	-0.204337
H	4.008832	-4.725328	-1.290030
C	1.505345	5.012695	-0.847431
H	0.743719	5.467918	-0.196225
H	2.192518	4.441888	-0.204337
H	2.087838	5.834414	-1.290030
C	-5.093794	-1.202680	-0.847431
H	-5.107216	-2.089880	-0.196225
H	-4.943047	-0.322168	-0.204337
H	-6.096670	-1.109086	-1.290030

97

[AsA'3], C1; M06-L/def2TZVP(As);

def2SVP(C,H,Si); $\Delta G^\circ = -5037.585831$ au

As	-0.181112	-1.787391	-0.090967
C	0.683038	-0.655766	1.316530
C	2.158327	-0.693891	1.135397
C	3.009558	0.351667	1.107542
C	0.128186	-3.183508	3.043613
C	1.737285	-0.853162	4.196514
C	-1.262166	-0.543954	3.790484
C	5.340892	-1.611803	0.973618
C	5.594722	1.120894	-0.418496
C	5.580567	0.968937	2.624099
C	-2.100774	-1.383146	0.293305
C	-2.466895	0.055403	0.322697
C	-3.268319	0.665690	1.219038
C	-4.993464	-2.253125	-0.028287
C	-2.748904	-4.129173	-0.973328
C	-3.422113	-1.557356	-2.546631
C	-5.629112	2.584747	1.422356
C	-2.911383	3.392011	2.570883
C	-3.289222	3.196819	-0.483718
C	0.045339	-0.604854	-1.718074
C	0.532068	0.768885	-1.458164
C	-0.061243	1.932145	-1.796071
C	0.468954	-3.155981	-3.413242

C	2.885059	-1.691556	-2.214090
C	1.288061	-0.396131	-4.507991
C	0.103759	4.832551	-2.743375
C	0.353684	4.229384	0.251168
C	2.601824	3.376310	-1.615645
H	0.304972	0.380831	1.242067
H	2.585922	-1.710478	1.072671
H	2.555042	1.353754	1.187976
H	-2.289729	-1.843315	1.283004
H	-2.072654	0.653102	-0.513122
H	-3.665880	0.039962	2.034994
H	-0.958385	-0.563155	-2.175750
H	1.520949	0.817956	-0.978306
H	-1.045636	1.869120	-2.288855
H	-5.751899	-2.785568	-0.621640
H	-4.987820	-2.703377	0.975898
H	-5.330442	-1.211220	0.080836
H	-3.492998	-4.741573	-1.504552
H	-1.795254	-4.227968	-1.512529
H	-2.605274	-4.578434	0.021474
H	-4.287808	-1.962700	-3.092408
H	-3.564900	-0.467173	-2.481517
H	-2.537116	-1.741524	-3.172996
H	-6.178092	2.063722	0.623732
H	-5.939197	2.135356	2.377784
H	-5.972076	3.630449	1.428975
H	-1.816816	3.311959	2.493641
H	-3.165752	4.463041	2.568361
H	-3.199477	2.990459	3.554314
H	-3.823188	2.703793	-1.310972
H	-3.515919	4.272585	-0.537402
H	-2.212364	3.077318	-0.673676
H	1.080004	-3.655619	-4.180090
H	0.441914	-3.820271	-2.536165
H	-0.554651	-3.087467	-3.812263
H	3.608491	-2.090995	-2.941050
H	3.284908	-0.737197	-1.836353
H	2.852808	-2.392804	-1.365544
H	1.891268	-0.864724	-5.299852
H	0.289867	-0.197470	-4.927599
H	1.740649	0.579940	-4.277848
H	-0.989957	4.936824	-2.672245
H	0.536926	5.832671	-2.593362
H	0.336040	4.523362	-3.773145
H	-0.696944	4.534124	0.366348
H	0.555076	3.457914	1.010527
H	0.974106	5.104279	0.500417
H	2.899952	2.992214	-2.603157
H	3.142497	4.319936	-1.446923
H	2.966470	2.656109	-0.866742
H	0.006745	-3.587613	4.060332
H	-0.738533	-3.520041	2.453643
H	1.017764	-3.660940	2.605275
H	1.526281	-1.123537	5.242336
H	2.664984	-1.364965	3.899930
H	1.945441	0.227477	4.167057

H	-1.314511	-0.746303	4.871383	H	-1.862241	1.358847	5.046067
H	-1.285057	0.547735	3.656661	H	-0.268112	0.597876	4.947420
H	-2.179277	-0.946533	3.339510	H	-1.650980	-0.114895	4.084490
H	6.433987	-1.737272	0.969749	H	-3.003474	3.002402	2.661867
H	4.953875	-2.172825	1.838113	H	-2.944962	1.552744	1.645102
H	4.954879	-2.096177	0.064201	H	-2.141852	3.048853	1.117339
H	6.688426	1.000583	-0.453533	H	4.857547	2.685928	-1.530841
H	5.194906	0.757997	-1.377045	H	4.142539	3.973341	-2.512854
H	5.390501	2.200836	-0.368971	H	3.434370	2.345916	-2.534085
H	6.680566	0.930214	2.631048	H	4.641596	4.246536	1.100523
H	5.292139	2.026271	2.722868	H	3.157760	5.125711	1.505225
H	5.226009	0.448966	3.526369	H	4.145721	5.637403	0.122296
Si	0.296115	-1.311473	3.082851	H	0.634749	4.869841	-0.298273
Si	4.872412	0.204843	1.057406	H	0.676530	3.941528	-1.807227
Si	-3.305112	-2.342108	-0.841969	H	1.602700	5.439495	-1.669163
Si	-3.768682	2.464090	1.176721	H	-0.019222	-2.755855	-0.070486
Si	1.183884	-1.474771	-2.976935	H	2.219563	-0.687110	0.393827
Si	0.739496	3.595853	-1.481983	H	2.063108	-3.244823	-1.294712
				H	2.896928	-4.181280	1.303055
97				H	1.453861	-5.132635	0.911869
[AsA'3], 1U2D; M06-L/def2TZVP(As);				H	2.110538	-5.161913	2.557602
def2SVP(C,H,Si); $\Delta G^\circ = -5037.578408$ au				H	2.602028	-1.521630	3.050047
C	0.290330	0.871998	1.645409	H	2.044719	-2.642211	4.303064
C	0.901308	1.794605	0.662318	H	1.053573	-1.240784	3.881272
C	2.193164	2.174892	0.584872	H	-0.615093	-4.399598	3.692133
C	0.194755	3.410992	3.385394	H	-1.368811	-4.249052	2.095945
C	-1.172628	0.835011	4.367164	H	-1.434775	-2.893265	3.232824
C	-2.354800	2.416025	1.993732	H	3.531000	-0.586799	-3.616875
C	3.902731	3.101002	-1.885335	H	3.743710	-2.314645	-3.950374
C	3.769142	4.758578	0.667337	H	5.161343	-1.264415	-3.783464
C	1.291826	4.539321	-1.117790	H	5.482652	-3.458346	-0.152667
C	0.498334	-2.030015	0.586800	H	6.403696	-3.003840	-1.598763
C	1.790816	-1.618040	-0.010401	H	5.064712	-4.156112	-1.726531
C	2.506403	-2.305448	-0.924121	H	4.832986	-0.481209	0.477403
C	1.921909	-4.511201	1.690349	H	4.009816	0.532514	-0.722427
C	1.709101	-2.018228	3.460998	H	5.712676	0.093395	-0.954103
C	-0.792541	-3.703422	2.858391	H	-1.532080	1.212048	-0.577231
C	4.154062	-1.463088	-3.386700	H	-3.066857	-1.430310	-0.934269
C	5.393960	-3.233080	-1.225900	H	-3.858351	1.531638	-0.916112
C	4.740504	-0.282542	-0.601797	H	-0.189441	-1.980625	-3.976147
C	-1.519477	0.120837	-0.752696	H	-1.505794	-2.398614	-2.870607
C	-2.934043	-0.336309	-0.886229	H	0.186351	-2.466398	-2.318353
C	-4.029344	0.443053	-0.964817	H	-1.278122	0.791347	-4.686792
C	-0.526838	-1.899038	-2.931228	H	-1.936266	1.825394	-3.405630
C	-1.747093	0.778568	-3.690831	H	-2.727169	0.289471	-3.790210
C	1.031007	0.752210	-2.531696	H	1.431264	0.624202	-3.550399
C	-6.496197	0.510683	-2.769310	H	1.774043	0.361242	-1.823758
C	-5.773484	-2.049857	-1.225442	H	0.939383	1.834596	-2.357589
C	-6.829575	0.427763	0.270372	H	-6.483430	1.610843	-2.779493
As	-0.876187	-0.635909	0.998922	H	-7.540774	0.195841	-2.914238
H	1.079627	0.384390	2.244723	H	-5.924404	0.171005	-3.645666
H	0.184747	2.298489	-0.006871	H	-5.358952	-2.483985	-0.303280
H	2.898887	1.680212	1.273005	H	-5.174890	-2.429585	-2.067350
H	-0.329593	3.981476	4.166536	H	-6.791261	-2.450091	-1.344841
H	0.361758	4.088274	2.534405	H	-6.824245	1.525829	0.340774
H	1.186211	3.141595	3.780735	H	-6.458310	0.038451	1.229801

H	-7.879159	0.112855	0.168714	H	0.573745	-2.748217	-3.871842
Si	-0.776564	1.891312	2.867412	H	0.932884	-4.480690	-3.673041
Si	2.789577	3.610602	-0.456259	H	3.148808	1.784678	-2.441923
Si	0.830826	-3.062232	2.169291	H	2.093153	1.870986	-3.871842
Si	4.198757	-1.814581	-1.539681	H	3.413949	3.048246	-3.673041
Si	-0.641908	-0.091385	-2.439090	H	-5.367513	-1.496268	-3.957970
Si	-5.780681	-0.172866	-1.169806	H	-3.696635	-2.081429	-4.154265
97							
[AsA'3], C3; APF-D/def2TZVP(As);							
def2SVP(C,H,Si); $\Delta G^\circ = -5036.320622$ au							
As	0.000000	0.000000	1.627724	H	1.648369	0.820162	-0.119484
C	0.185496	2.552044	-1.351614	H	1.832533	-0.578695	-1.980595
C	-2.269378	-2.644988	3.187911	H	-0.415102	1.876368	-1.980595
C	0.000000	2.463306	-0.019413	H	-1.417431	-1.297673	-1.980595
C	-1.596219	-4.513606	0.818632	H	0.599452	3.109268	0.637873
C	-0.926869	1.518630	0.651408	H	-1.534465	1.017449	-0.119484
C	-2.133286	-1.231653	-0.019413	H	-2.992431	-1.035493	0.637873
C	3.425316	-0.642846	3.187911	H	-0.113904	-1.837610	-0.119484
C	4.707007	0.874437	0.818632	H	2.392979	-2.073775	0.637873
C	-2.302883	-1.115378	-1.351614	H	-1.838706	3.861579	3.834849
C	2.440893	4.595365	-0.908166	H	-0.621680	2.563000	3.821718
C	2.759257	-4.411558	-0.908166	H	-0.417540	3.990903	2.772693
C	-3.466041	1.049372	-3.132966	H	-2.424872	-3.523156	3.834849
C	2.651542	2.272704	2.636718	H	-1.908783	-1.819891	3.821718
C	-5.200149	-0.183807	-0.908166	H	-3.247454	-2.357052	2.772693
C	0.640437	4.798494	-3.412328	H	4.263579	-0.338423	3.834849
C	0.824237	-3.526366	-3.132966	H	2.530463	-0.743109	3.821718
C	-0.851738	-1.562007	0.651408	H	3.664994	-1.633852	2.772693
C	0.642449	-3.432655	2.636718	H	2.574368	3.082518	1.895958
C	3.835399	-2.953882	-3.412328	H	1.687169	2.193919	3.160957
C	2.641804	2.476993	-3.132966	H	3.411616	2.569973	3.377000
C	2.133286	-1.231653	-0.019413	H	1.382355	-3.770727	1.895958
C	-3.293991	1.159951	2.636718	H	1.056405	-2.558091	3.160957
C	-4.475836	-1.844612	-3.412328	H	0.519854	-4.239532	3.377000
C	-1.155937	3.287833	3.187911	H	-3.956723	0.688209	1.895958
C	1.778607	0.043377	0.651408	H	-2.743574	0.364172	3.160957
C	-3.110788	3.639170	0.818632	H	-3.931469	1.669559	3.377000
C	2.117387	-1.436666	-1.351614	H	-6.142984	0.103581	-1.400058
H	-3.824698	4.199434	1.443070	H	3.624044	-4.148820	-0.278758
H	-2.439789	4.361296	0.327869	H	1.890207	-4.568224	-0.250397
H	-3.681070	3.124469	0.028553	H	2.981788	-5.371771	-1.400058
H	-1.724467	-5.412003	1.443070	H	1.780962	5.212924	-0.278758
H	-2.557099	-4.293567	0.327869	H	3.011094	3.921079	-0.250397
H	-0.865335	-4.750135	0.028553	H	3.979562	-3.900268	-3.957970
H	5.549165	1.212569	1.443070	H	3.650887	-2.160665	-4.154265
H	4.996887	-0.067729	0.327869	H	4.774696	-2.713171	-2.890072
H	4.546405	1.625665	0.028553	H	1.387950	5.396536	-3.957970
H	-3.119980	1.834608	-2.441923	H	0.045747	4.242094	-4.154265
H	-2.666898	0.877231	-3.871842	H	-0.037673	5.491594	-2.890072
H	-4.346833	1.432444	-3.673041	H	-5.405006	-1.064104	-0.278758
H	-0.028827	-3.619287	-2.441923	H	-4.901301	0.647144	-0.250397
				Si	3.140528	0.638430	1.837199

Si	-3.869836	-0.539240	-2.194927	H	-2.694664	-4.567832	0.203660
Si	-1.017367	-3.038992	1.837199	H	-4.264764	-2.095548	-3.050262
Si	-2.123160	2.400562	1.837199	H	-3.559463	-0.560346	-2.494298
Si	2.401914	-3.081756	-2.194927	H	-2.505233	-1.867369	-3.099117
Si	1.467922	3.620997	-2.194927	H	-6.136500	2.312055	0.642352
				H	-5.806266	2.430769	2.388171
97				H	-5.787769	3.897235	1.379282
				H	-1.612064	3.332039	2.242059
[AsA'3], C1; APF-D/def2TZVP(As);				H	-2.890548	4.569002	2.371730
def2SVP(C,H,Si); $\Delta G^\circ = -5036.321639$ au				H	-2.949224	3.113775	3.396802
As	-0.226920	-1.789578	0.051867	H	-3.862301	2.752658	-1.415729
C	0.625752	-0.554662	1.361142	H	-3.406149	4.318748	-0.696236
C	2.104210	-0.611491	1.182251	H	-2.189421	3.032035	-0.878877
C	2.951061	0.432202	1.093371	H	1.074056	-3.995522	-3.879383
C	0.465558	-2.928685	3.363467	H	0.375322	-4.034280	-2.241988
C	1.576107	-0.200036	4.259802	H	-0.559508	-3.349530	-3.599440
C	-1.407690	-0.515081	3.786579	H	3.603431	-2.431136	-2.706315
C	5.307532	-1.538632	1.091175	H	3.302591	-1.013878	-1.663672
C	5.516625	1.095751	-0.499389	H	2.814309	-2.637073	-1.122700
C	5.520302	1.162242	2.564075	H	2.037988	-1.307937	-5.128238
C	-2.142545	-1.356203	0.354332	H	0.409954	-0.620950	-4.889359
C	-2.487471	0.091013	0.305147	H	1.827383	0.213126	-4.215430
C	-3.288124	0.747945	1.166181	H	-1.151404	4.737673	-2.742890
C	-5.034707	-2.214440	0.017771	H	0.363889	5.665352	-2.868747
C	-2.798705	-4.160749	-0.814539	H	0.032290	4.340759	-4.013770
C	-3.411043	-1.651341	-2.513687	H	-0.471966	4.243300	0.239073
C	-5.524621	2.827445	1.399552	H	0.959928	3.289311	0.688357
C	-2.692120	3.485185	2.391777	H	1.147930	4.975380	0.140956
C	-3.243962	3.230651	-0.639681	H	2.751839	2.963575	-3.230205
C	0.048237	-0.762253	-1.660598	H	3.114362	4.252710	-2.050623
C	0.536188	0.632856	-1.517689	H	3.075354	2.550589	-1.531233
C	-0.040479	1.750479	-2.000689	H	0.366410	-3.224050	4.420372
C	0.448322	-3.437789	-3.164265	H	-0.302826	-3.466063	2.785919
C	2.890631	-1.976731	-1.999919	H	1.449379	-3.271918	3.007126
C	1.390343	-0.778014	-4.411800	H	1.359996	-0.374287	5.326108
C	-0.075175	4.659655	-2.964866	H	2.592033	-0.563148	4.046023
C	0.579208	4.044735	-0.017144	H	1.569710	0.887321	4.082452
C	2.595740	3.290695	-2.190228	H	-1.447928	-0.621166	4.882842
H	0.243087	0.471165	1.219358	H	-1.600452	0.538357	3.535092
H	2.529376	-1.626777	1.175219	H	-2.221784	-1.118426	3.361863
H	2.510032	1.440975	1.114019	H	6.404905	-1.635802	1.089644
H	-2.365192	-1.770802	1.354385	H	4.928987	-2.037372	1.997358
H	-2.055914	0.644574	-0.538264	H	4.920834	-2.078656	0.213499
H	-3.712883	0.172432	2.001740	H	6.614293	1.000977	-0.524268
H	-0.935138	-0.766674	-2.158589	H	5.117164	0.634847	-1.416008
H	1.496146	0.727984	-0.994356	H	5.273213	2.169407	-0.528196
H	-0.995687	1.646832	-2.537299	H	6.621097	1.113709	2.577114
H	-5.790563	-2.735792	-0.591051	H	5.229462	2.224899	2.570399
H	-5.046455	-2.658893	1.025708	H	5.145773	0.706289	3.494046
H	-5.332642	-1.158541	0.108342	Si	0.289753	-1.061359	3.185744
H	-3.549515	-4.766590	-1.346956	Si	4.817169	0.279927	1.051503
H	-1.833629	-4.286785	-1.326870				

Si	-3.329462	-2.356048	-0.766962	H	-0.866572	-1.826932	2.550653
Si	-3.685180	2.573770	1.069335	H	-1.644683	-0.413299	1.790444
Si	1.208016	-1.750372	-2.810788	H	-0.255767	2.420420	2.468759
Si	0.757462	3.438429	-1.797767	H	1.508833	2.464560	2.754805
97				H	0.399632	2.013355	4.068393
[AsA'3], 1U/2D; APF-D/def2TZVP(As);				H	-2.842170	-1.709538	-1.458958
def2SVP(C,H,Si); $\Delta G^\circ = -5036.314892$ au				H	-2.233509	2.998334	1.508077
C	-2.652092	2.133666	0.970036	H	-0.215805	-2.236092	0.030301
C	-1.882769	1.559153	0.024700	H	-1.008691	-0.320207	-2.264744
C	-0.540624	2.022226	-0.413370	H	-0.693377	-4.902031	0.261430
C	-4.960015	0.316613	0.121228	H	-1.742915	-5.436947	1.597114
C	-4.521208	0.926072	3.114105	H	-0.794959	-3.945556	1.760983
C	-5.517567	3.140739	1.239728	H	-4.645114	-4.202750	-1.296675
C	-1.389956	2.243917	-3.411881	H	-4.207666	-5.603066	-0.288153
C	0.923578	3.977769	-2.328075	H	-3.159105	-5.118521	-1.647590
C	-1.964219	4.544333	-1.452592	H	-3.453396	-2.312548	2.364427
C	4.030907	-0.527270	0.959407	H	-4.286319	-3.888293	2.314967
C	2.961038	0.286583	0.901499	H	-4.873389	-2.539711	1.313896
C	1.529444	-0.133184	0.807909	H	1.843863	0.271677	-3.904849
C	5.849814	1.940219	1.123039	H	0.480039	-0.367675	-4.866232
C	6.776699	-0.581234	-0.396258	H	2.069201	-1.163084	-4.938321
C	6.573206	-0.629884	2.669907	H	0.497974	-3.802081	-4.248286
C	1.831500	-0.749570	3.763494	H	-1.028062	-2.922032	-3.970370
C	-0.978733	-0.734041	2.600737	H	-0.352136	-3.943837	-2.684057
C	0.577230	1.924182	2.984566	H	2.155120	-3.041601	-1.097339
C	-2.176262	-2.175115	-0.716010	H	3.009488	-1.537283	-1.533963
C	-0.893977	-1.762994	-0.692773	H	3.063487	-2.945720	-2.622019
C	-0.249528	-0.807630	-1.628982	H	-2.290172	0.706782	-0.534023
C	-1.377279	-4.552726	1.051001	H	-0.076422	2.672963	0.349475
C	-3.799641	-4.738565	-0.836051	H	-4.285945	-0.552041	0.144124
C	-3.967695	-3.027434	1.704984	H	-4.963424	0.721223	-0.903192
C	1.361701	-0.648409	-4.268587	H	-5.977629	-0.036619	0.351335
C	-0.088901	-3.250060	-3.496882	H	-3.934889	0.000027	3.207737
C	2.418043	-2.375645	-1.934627	H	-5.565897	0.697368	3.379743
H	3.837869	-1.610816	0.926980	H	-4.134958	1.648601	3.850553
H	3.126753	1.374120	0.933138	H	-6.564425	2.888456	1.473616
H	1.493562	-1.222586	0.634757	H	-5.488277	3.568924	0.225251
H	5.406632	2.367402	0.209654	H	-5.194789	3.923466	1.944829
H	6.889294	2.298472	1.191728	H	-0.650476	1.517505	-3.780781
H	5.299876	2.339415	1.989962	H	-1.612490	2.939874	-4.236481
H	6.358368	-0.186095	-1.335367	H	-2.319329	1.705181	-3.168751
H	6.739706	-1.681152	-0.447728	H	1.330799	4.511652	-1.454472
H	7.835483	-0.281295	-0.339134	H	0.811101	4.707487	-3.146034
H	7.627942	-0.325106	2.764474	H	1.660296	3.221464	-2.637225
H	6.538395	-1.731014	2.679110	H	-2.951589	4.121181	-1.215315
H	6.031817	-0.269203	3.558746	H	-2.081642	5.261705	-2.280608
H	1.374716	-0.735694	4.766450	H	-1.616826	5.101907	-0.568187
H	2.813145	-0.256088	3.821112	Si	-4.407851	1.619126	1.363596
H	2.004262	-1.801385	3.484134	Si	-0.739367	3.194692	-1.921022
H	-1.458970	-0.488817	3.561784	Si	5.804654	0.056578	1.089353
				Si	0.700089	0.103788	2.517425

Si	-2.829775	-3.599824	0.313737	H	1.989106	2.118761	-3.956581
Si	0.879941	-1.775923	-2.839955	H	3.342959	3.245022	-3.698721
As	0.858191	0.684388	-0.892408	H	-5.593500	-1.641286	-3.748074
				H	-3.952149	-2.278744	-4.010431
97				H	-4.927020	-2.875172	-2.647267
				H	3.200801	5.282228	-1.251166
[AsA'3], C3; □B97X-D/def2TZVP(As);				H	1.658849	0.810161	-0.176560
def2SVP(C,H,Si); ΔG° = -5037.59901997 au				H	2.008221	-0.601381	-2.003186
As	0.000000	0.000000	1.571674	H	-0.483299	2.039861	-2.003186
C	0.151838	2.654011	-1.346243	H	-1.524922	-1.438479	-2.003186
C	-2.261709	-2.689919	3.124856	H	0.633534	3.056693	0.660870
C	0.000000	2.474344	-0.022463	H	-1.531045	1.031525	-0.176560
C	-1.527423	-4.533504	0.757940	H	-2.963941	-0.979690	0.660870
C	-0.936641	1.509059	0.617108	H	-0.127804	-1.841686	-0.176560
C	-2.142845	-1.237172	-0.022463	H	2.330407	-2.077003	0.660870
C	3.460393	-0.613738	3.124856	H	-1.888015	3.867949	3.772981
C	4.689842	0.943965	0.757940	H	-0.640235	2.599900	3.762262
C	-2.374360	-1.195510	-1.346243	H	-0.480367	4.020129	2.696527
C	2.470486	4.591002	-0.801609	H	-2.405735	-3.569043	3.772981
C	2.740682	-4.435004	-0.801609	H	-1.931462	-1.854410	3.762262
C	-3.582312	0.895292	-3.186178	H	-3.241350	-2.426074	2.696527
C	2.638462	2.293310	2.610136	H	4.293749	-0.298906	3.772981
C	-5.211167	-0.155998	-0.801609	H	2.571697	-0.745490	3.762262
C	0.624711	5.040540	-3.237325	H	3.721717	-1.594055	2.696527
C	1.015810	-3.550019	-3.186178	H	2.550051	3.113280	1.881212
C	-0.838563	-1.565684	0.617108	H	1.677751	2.202854	3.140450
C	0.666834	-3.431630	2.610136	H	3.400029	2.589304	3.349316
C	4.052880	-3.061286	-3.237325	H	1.421154	-3.765049	1.881212
C	2.566502	2.654727	-3.186178	H	1.068852	-2.554402	3.140450
C	2.142845	-1.237172	-0.022463	H	0.542389	-4.239163	3.349316
C	-3.305296	1.138320	2.610136	H	-3.971205	0.651769	1.881212
C	-4.677591	-1.979255	-3.237325	H	-2.746603	0.351548	3.140450
C	-1.198683	3.303657	3.124856	H	-3.942418	1.649859	3.349316
C	1.775204	0.056625	0.617108	H	-6.174944	0.130861	-1.251166
C	-3.162418	3.589540	0.757940	H	3.557519	-4.181513	-0.107272
C	2.222522	-1.458501	-1.346243	H	1.816652	-4.551936	-0.213427
H	-3.886388	4.142921	1.376855	H	2.974143	-5.413088	-1.251166
H	-2.507072	4.320385	0.258877	H	1.842537	5.171659	-0.107272
H	-3.725009	3.058003	-0.026632	H	3.033767	3.849235	-0.213427
H	-1.644681	-5.437171	1.376855	H	4.218145	-4.023470	-3.748074
H	-2.488027	-4.331381	0.258877	H	3.949524	-2.283289	-4.010431
H	-0.785804	-4.754954	-0.026632	H	4.953482	-2.829338	-2.647267
H	5.531069	1.294250	1.376855	H	1.375355	5.664756	-3.748074
H	4.995099	0.010995	0.258877	H	0.002624	4.562033	-4.010431
H	4.510813	1.696951	-0.026632	H	-0.026462	5.704510	-2.647267
H	-3.181207	1.708982	-2.560381	H	-5.400056	-0.990145	-0.107272
H	-2.829454	0.663235	-3.956581	H	-4.850418	0.702702	-0.213427
H	-4.481751	1.272577	-3.698721	Si	3.139346	0.673615	1.789095
H	0.110582	-3.609497	-2.560381	Si	-3.969533	-0.624253	-2.138052
H	0.840348	-2.781996	-3.956581	Si	-0.986305	-3.055561	1.789095
H	1.138792	-4.517599	-3.698721	Si	-2.153041	2.381946	1.789095
H	3.070625	1.900515	-2.560381				

Si	2.525386	-3.125590	-2.138052	H	-2.431366	-2.269727	-2.906080
Si	1.444147	3.749843	-2.138052	H	-6.211529	2.211863	0.292297
				H	-5.935391	2.508906	2.025424
97				H	-5.940335	3.871435	0.881130
[AsA'3], C1; □B97X-D/def2TZVP(As);				H	-1.772372	3.539492	1.900466
def2SVP(C,H,Si); ΔG° = -3041.986616 au				H	-3.089369	4.740732	1.874577
As	-0.196494	-1.754846	0.216425	H	-3.136060	3.390670	3.034207
C	0.637430	-0.392307	1.398890	H	-3.885590	2.530920	-1.743190
C	2.123947	-0.476139	1.240642	H	-3.537118	4.182088	-1.168723
C	2.975289	0.543356	1.035745	H	-2.249987	2.953779	-1.187113
C	0.387315	-2.490974	3.682610	H	1.091185	-4.352875	-3.496165
C	1.568991	0.291944	4.241603	H	0.408769	-4.237784	-1.856390
C	-1.415717	0.003717	3.772308	H	-0.539410	-3.684320	-3.261979
C	5.308804	-1.436645	1.219265	H	3.629855	-2.685765	-2.488208
C	5.525174	1.006190	-0.645151	H	3.338188	-1.161127	-1.609275
C	5.569379	1.403232	2.390938	H	2.854163	-2.711908	-0.885247
C	-2.118615	-1.334873	0.456920	H	2.034585	-1.808471	-5.008093
C	-2.500184	0.095842	0.256087	H	0.414162	-1.090929	-4.818528
C	-3.331927	0.811903	1.031680	H	1.844926	-0.204155	-4.249438
C	-4.999135	-2.273539	0.195434	H	-1.078850	4.471370	-3.170218
C	-2.728015	-4.266038	-0.372352	H	0.436753	5.400097	-3.266875
C	-3.348281	-1.992741	-2.364440	H	0.192816	3.980591	-4.315840
C	-5.638880	2.819613	1.010758	H	-0.618276	4.218468	-0.111715
C	-2.861006	3.670565	2.004532	H	0.802592	3.348848	0.510155
C	-3.321487	3.115150	-0.998971	H	0.985570	4.986719	-0.169257
C	0.087198	-0.918534	-1.589843	H	2.860290	2.689511	-3.217153
C	0.584774	0.485835	-1.575746	H	3.125769	4.086079	-2.139078
C	-0.016109	1.571740	-2.091537	H	3.055307	2.440085	-1.468249
C	0.473396	-3.728904	-2.830765	H	0.275920	-2.645907	4.767746
C	2.920966	-2.155049	-1.833047	H	-0.395308	-3.077110	3.175319
C	1.399249	-1.207018	-4.338703	H	1.360984	-2.907878	3.380611
C	0.010964	4.384962	-3.307536	H	1.332759	0.266522	5.317505
C	0.452219	4.029116	-0.283013	H	2.575444	-0.128821	4.098746
C	2.622361	3.110136	-2.227556	H	1.605419	1.346948	3.925460
H	0.274529	0.614257	1.127953	H	-1.466836	0.047457	4.872291
H	2.542506	-1.488002	1.350183	H	-1.585402	1.017944	3.380365
H	2.535169	1.547785	0.936934	H	-2.242188	-0.632240	3.425428
H	-2.336170	-1.637332	1.497454	H	6.404255	-1.552444	1.213909
H	-2.072362	0.573310	-0.633582	H	4.935652	-1.832184	2.177335
H	-3.752421	0.307878	1.914138	H	4.901085	-2.060707	0.408896
H	-0.900320	-0.949842	-2.076951	H	6.619419	0.881197	-0.681399
H	1.569812	0.614328	-1.112071	H	5.096010	0.464270	-1.502475
H	-0.999649	1.435902	-2.565338	H	5.307268	2.077022	-0.782878
H	-5.732920	-2.893915	-0.343503	H	6.669820	1.347337	2.396453
H	-5.015275	-2.576046	1.254700	H	5.287481	2.463313	2.287655
H	-5.328824	-1.224680	0.138298	H	5.204970	1.054006	3.369872
H	-3.468428	-4.942353	-0.828888	Si	0.269696	-0.658397	3.265175
H	-1.759725	-4.441911	-0.864548	Si	4.839613	0.372097	0.992274
H	-2.621076	-4.547898	0.687214	Si	-3.281642	-2.476852	-0.544447
H	-4.189085	-2.508405	-2.855308	Si	-3.784876	2.605177	0.752447
H	-3.505437	-0.909157	-2.484859	Si	1.230996	-2.014761	-2.648606

Si	0.761882	3.275555	-1.986032	H	1.475951	-2.443864	-2.784391
				H	0.374662	-1.960452	-4.092564
97				H	-2.838543	1.656526	1.467620
[AsA'3], 1U/2D; □B97X-D/def2TZVP(As);				H	-2.200763	-2.996880	-1.499489
def2SVP(C,H,Si); ΔG° = -5037.593336 au				H	-0.232660	2.240582	-0.025461
C	-2.628139	-2.134105	-0.965908	H	-0.986246	0.310347	2.268786
C	-1.866771	-1.560053	-0.018092	H	-0.798597	4.926280	-0.220550
C	-0.521999	-2.022064	0.431033	H	-1.835059	5.412044	-1.584821
C	-4.964617	-0.366535	-0.102269	H	-0.828759	3.955782	-1.712831
C	-4.462113	-0.869419	-3.104278	H	-4.744146	4.062853	1.265790
C	-5.478031	-3.150944	-1.326966	H	-4.340501	5.485868	0.276688
C	-1.346218	-2.240394	3.432517	H	-3.300717	5.029996	1.651404
C	0.923378	-4.011751	2.323771	H	-3.407349	2.258323	-2.391135
C	-1.977266	-4.525868	1.477616	H	-4.326394	3.783618	-2.325433
C	4.039106	0.526730	-0.955355	H	-4.850444	2.386722	-1.356729
C	2.971828	-0.287061	-0.916414	H	1.888438	-0.217795	3.935953
C	1.534743	0.133540	-0.810493	H	0.485928	0.376158	4.867660
C	5.864028	-1.927083	-1.184072	H	2.044855	1.224463	4.969972
C	6.775886	0.549363	0.412327	H	0.447345	3.810154	4.262155
C	6.586004	0.688173	-2.649844	H	-1.063155	2.912904	3.960850
C	1.829872	0.778885	-3.758489	H	-0.384830	3.951310	2.689842
C	-0.970806	0.781466	-2.593588	H	2.126893	3.070141	1.098819
C	0.552198	-1.887044	-3.007614	H	3.014898	1.593395	1.558260
C	-2.186286	2.138608	0.723441	H	3.033413	3.017153	2.626663
C	-0.898746	1.753636	0.699282	H	-2.279507	-0.708834	0.537622
C	-0.230271	0.807230	1.636909	H	-0.058351	-2.668269	-0.335484
C	-1.451272	4.546093	-1.022332	H	-4.296409	0.507446	-0.080639
C	-3.910318	4.632298	0.824619	H	-4.981443	-0.806765	0.907449
C	-3.967943	2.931646	-1.725285	H	-5.980608	-0.010279	-0.335287
C	1.368583	0.687138	4.286036	H	-3.875339	0.059805	-3.156839
C	-0.122153	3.254301	3.500300	H	-5.501174	-0.631462	-3.383287
C	2.402108	2.422630	1.947210	H	-4.060903	-1.565888	-3.857758
H	3.841151	1.607982	-0.896690	H	-6.522417	-2.899781	-1.572478
H	3.136984	-1.373155	-0.973252	H	-5.466116	-3.614176	-0.327643
H	1.514838	1.220903	-0.624933	H	-5.136488	-3.907564	-2.051475
H	5.417651	-2.381713	-0.285451	H	-0.593338	-1.522460	3.792993
H	6.903190	-2.284549	-1.260120	H	-1.569446	-2.931078	4.261152
H	5.316172	-2.301401	-2.063502	H	-2.270307	-1.686767	3.201021
H	6.353248	0.127415	1.337806	H	1.315501	-4.549126	1.445338
H	6.736910	1.647269	0.495888	H	0.804388	-4.743960	3.138481
H	7.835843	0.253896	0.355001	H	1.678139	-3.273269	2.632907
H	7.641788	0.389673	-2.751603	H	-2.968207	-4.092491	1.275632
H	6.549130	1.789035	-2.626711	H	-2.078635	-5.255844	2.296672
H	6.049167	0.354081	-3.551772	H	-1.662151	-5.073259	0.574822
H	1.362097	0.793554	-4.756325	Si	-4.379626	-1.619731	-1.378174
H	2.801806	0.269366	-3.840616	Si	-0.726731	-3.197294	1.932865
H	2.027220	1.822044	-3.462736	Si	5.815136	-0.046959	-1.095053
H	-1.441617	0.573630	-3.568426	Si	0.697833	-0.075650	-2.515951
H	-0.850059	1.871867	-2.506400	Si	-2.879075	3.539670	-0.312761
H	-1.654307	0.445195	-1.803412	Si	0.873248	1.796800	2.849791
H	-0.287501	-2.381427	-2.500270	As	0.869551	-0.677803	0.889663

97
 [SbA'3], C3; M06-L/def2TZVP(Sb);
 def2SVP(C,H,Si); $\Delta G^\circ = -3042.199584$ au

C	-2.213466	1.036706	-1.454660
C	-2.354986	0.812044	-0.129605
C	-1.891746	-0.378933	0.606727
C	1.274039	-1.448834	0.606727
C	0.208919	-2.435271	-1.454660
C	2.004547	1.398565	-1.454660
C	1.880744	1.633455	-0.129605
C	0.617708	1.827767	0.606727
H	1.774388	-0.784852	-0.120392
H	0.654024	-1.606143	-2.030305
H	1.063948	1.369473	-2.030305
H	-1.717972	0.236670	-2.030305
H	2.801417	1.641308	0.479592
H	-0.207493	1.929091	-0.120392
H	-2.822123	1.605444	0.479592
H	-1.566896	-1.144239	-0.120392
Si	-2.671104	2.611313	-2.343977
Si	-3.179106	-1.163041	1.751136
Si	3.597016	1.007588	-2.343977
Si	0.582330	3.334708	1.751136
Si	-0.925911	-3.618901	-2.343977
H	0.020706	-3.246752	0.479592
Si	2.596776	-2.171666	1.751136
Sb	0.000000	0.000000	1.750013
C	0.474242	-2.445499	-0.129605
C	1.958573	3.200450	3.023825
H	1.970777	4.073237	3.693797
H	1.841313	2.308230	3.658475
H	2.952232	3.141302	2.554261
C	-3.750958	0.095949	3.023825
H	-4.512915	-0.329875	3.693797
H	-2.919643	0.440509	3.658475
H	-4.196563	0.986057	2.554261
C	1.792385	-3.296399	3.023825
H	2.542138	-3.743361	3.693797
H	1.078330	-2.748739	3.658475
H	1.244331	-4.127359	2.554261
C	3.484436	-0.763874	2.629127
H	3.926090	-0.047002	1.919639
H	2.813761	-0.197317	3.294548
H	4.306075	-1.142547	3.255716
C	-2.403753	-2.635673	2.629127
H	-2.003750	-3.376593	1.919639
H	-1.577762	-2.338130	3.294548
H	-3.142512	-3.157897	3.255716
C	-1.080683	3.399547	2.629127
H	-1.922340	3.423595	1.919639
H	-1.235999	2.535447	3.294548
H	-1.163563	4.300444	3.255716
C	0.814728	4.883969	0.716755
H	0.841751	5.792624	1.336805
H	1.755191	4.843888	0.146857

H	0.000000	5.009164	-0.012349
C	-4.637005	-1.736409	0.716755
H	-5.437435	-2.167334	1.336805
H	-5.072525	-0.901904	0.146857
H	-4.338064	-2.504582	-0.012349
C	3.822277	-3.147560	0.716755
H	4.595684	-3.625289	1.336805
H	3.317335	-3.941984	0.146857
H	4.338064	-2.504582	-0.012349
C	-1.134171	3.292159	-3.192101
H	-0.338965	3.529792	-2.468368
H	-0.713541	2.568780	-3.907622
H	-1.355267	4.212484	-3.754073
C	-2.284008	-2.628301	-3.192101
H	-2.887407	-2.058449	-2.468368
H	-1.867858	-1.902335	-3.907622
H	-2.970485	-3.279937	-3.754073
C	3.418179	-0.663858	-3.192101
H	3.226372	-1.471343	-2.468368
H	2.581399	-0.666445	-3.907622
H	4.325752	-0.932547	-3.754073
C	-3.983528	2.275281	-3.647082
H	-4.228349	3.180481	-4.223038
H	-3.646703	1.512183	-4.364880
H	-4.916379	1.906130	-3.196423
C	0.021313	-4.587477	-3.647082
H	-0.640203	-5.252099	-4.223038
H	0.513763	-3.914229	-4.364880
H	0.807432	-5.210774	-3.196423
C	3.962215	2.312196	-3.647082
H	4.868552	2.071617	-4.223038
H	3.132940	2.402046	-4.364880
H	4.108947	3.304644	-3.196423
C	-3.298471	3.865447	-1.092822
H	-4.177820	3.499766	-0.541227
H	-2.523048	4.113173	-0.351502
H	-3.590661	4.807170	-1.580951
C	-1.698340	-4.789284	-1.092822
H	-0.941976	-5.367981	-0.541227
H	-2.300588	-4.241611	-0.351502
H	-2.367801	-5.513189	-1.580951
C	4.996811	0.923836	-1.092822
H	5.119796	1.868215	-0.541227
H	4.823637	0.128437	-0.351502
H	5.958462	0.706019	-1.580951

97
 [SbA'3], C1; M06-L/def2TZVP(Sb);
 def2SVP(C,H,Si); $\Delta G^\circ = -3042.196532$ au

C	0.678422	0.086853	1.449228
C	2.146172	-0.052688	1.276775
C	3.009462	0.824490	0.721736
C	1.693745	-0.302622	4.331472
C	-1.293625	0.077216	3.946266
C	0.613291	2.418731	3.387491
C	5.284862	-1.036479	1.545262

C	5.638489	0.741640	-0.932243	H	-1.246197	4.197553	0.782876
C	5.574695	2.005385	1.848499	H	-2.488789	5.416725	0.444787
C	0.009144	-1.459736	-1.377623	H	-2.523414	4.516099	1.970098
C	0.557298	-0.132715	-1.723118	H	-2.010106	2.607933	-1.918887
C	-0.011452	0.843266	-2.463604	H	-3.722278	2.285937	-2.239770
C	0.291997	-4.498284	-1.769032	H	-3.115375	3.955029	-2.248540
C	1.420196	-2.554070	-3.874591	H	-5.426047	4.572231	-0.087975
C	2.767111	-2.769332	-1.120888	H	-5.882449	2.858183	-0.108230
C	0.690189	3.741526	-1.558795	H	-5.455015	3.645036	1.420494
C	0.230228	3.099317	-4.516044	H	1.679904	-1.395106	4.192566
C	2.725200	2.022854	-3.034748	H	2.709762	0.046874	4.093031
C	-2.394091	-0.988735	0.792129	H	1.522496	-0.110310	5.401348
C	-2.522250	0.388933	0.268965	H	-2.113707	0.570317	3.405445
C	-3.114481	1.439043	0.878698	H	-1.466204	-1.010088	3.914002
C	-3.286439	-3.931199	0.439653	H	-1.371008	0.378919	5.002255
C	-3.651196	-1.989814	-1.917387	H	0.584148	2.779517	4.426542
C	-5.341237	-1.642402	0.593736	H	1.579108	2.726264	2.957474
C	-2.316177	4.425966	0.892908	H	-0.179851	2.942093	2.832648
C	-3.029389	2.981796	-1.741543	H	4.882844	-1.874457	0.956014
C	-5.200222	3.588843	0.351424	H	6.374590	-1.176066	1.606434
H	0.279763	0.910157	0.826644	H	4.889516	-1.131530	2.568146
H	2.573777	-0.966475	1.724272	H	5.236487	-0.015615	-1.622091
H	2.573575	1.742908	0.294138	H	5.471011	1.725414	-1.395195
H	-0.997283	-1.580512	-1.814769	H	6.727620	0.590503	-0.878910
H	1.579986	0.045436	-1.355552	H	5.327630	2.998484	1.444187
H	-1.031044	0.661480	-2.841496	H	6.671292	1.946100	1.921292
H	-2.699747	-1.016169	1.854580	H	5.172080	1.962146	2.871970
H	-2.121891	0.538562	-0.746611	Sb	-0.328631	-1.759401	0.809519
H	-3.525360	1.256804	1.885975	Si	0.395050	0.560301	3.280454
H	0.154464	-4.720510	-0.699302	Si	4.867386	0.627741	0.779454
H	-0.700174	-4.534217	-2.245558	Si	1.130583	-2.838679	-2.043323
H	0.883495	-5.322658	-2.194688	Si	0.894258	2.424786	-2.893726
H	2.041607	-3.343783	-4.322498	Si	-3.650947	-2.152469	-0.043397
H	0.471717	-2.523173	-4.431921	Si	-3.398877	3.110701	0.095427
H	1.926855	-1.592840	-4.047734				
H	3.498181	-3.485822	-1.524829				
H	3.218765	-1.765880	-1.184607				
H	2.643035	-3.002893	-0.050841				
H	-0.322991	4.168654	-1.540331				
H	0.892646	3.336119	-0.554620				
H	1.389460	4.576700	-1.720981				
H	0.731655	4.035399	-4.803933				
H	0.366873	2.385114	-5.341416				
H	-0.846801	3.315348	-4.445760				
H	3.109373	1.596448	-2.095178				
H	2.921478	1.285758	-3.828161				
H	3.327768	2.917251	-3.254716				
H	-4.071649	-4.611259	0.076360				
H	-2.332706	-4.289187	0.021301				
H	-3.228738	-4.054769	1.531888				
H	-3.620313	-0.937886	-2.241226				
H	-2.813453	-2.512922	-2.401494				
H	-4.574871	-2.424780	-2.328823				
H	-6.144397	-2.250388	0.150972				
H	-5.414153	-1.745177	1.686814				
H	-5.550759	-0.589588	0.350426				
				97			
				[SbA'3], 1U/2D; M06-L/def2TZVP(Sb);			
				def2SVP(C,H,Si); $\Delta G^\circ = -3042.190005$ au			
				C	0.243333	0.589291	1.821582
				C	0.775786	1.685680	0.985627
				C	2.043039	2.149729	0.947985
				C	-0.029524	2.795097	3.945294
				C	-1.252659	0.022312	4.465380
				C	-2.493433	1.894006	2.349648
				C	3.593556	3.557552	-1.404676
				C	3.527181	4.737786	1.408689
				C	0.979113	4.717429	-0.302719
				C	0.892249	-2.187913	0.103406
				C	2.107494	-1.453247	-0.310196
				C	2.874430	-1.718100	-1.389572
				C	2.882148	-4.370306	0.951986
				C	1.644008	-2.575914	3.104488
				C	-0.094835	-4.655835	1.663951
				C	4.489778	0.052483	-3.352433

C	5.798841	-2.312769	-1.935034	H	5.075239	-0.389394	0.624279
C	4.988469	0.179481	-0.314666	H	4.223026	0.954935	-0.159584
C	-1.596730	0.177024	-0.917029	H	5.948150	0.691445	-0.481314
C	-3.021274	-0.208662	-1.095428	H	-1.561440	1.208817	-0.520356
C	-4.104860	0.562280	-0.872128	H	-3.186045	-1.234254	-1.469554
C	-0.375257	-1.494081	-3.259629	H	-3.909858	1.583713	-0.505378
C	-1.880875	1.096922	-3.787406	H	-0.113619	-1.452282	-4.327887
C	0.866823	1.243207	-2.488608	H	-1.259756	-2.143679	-3.170545
C	-6.656039	1.210308	-2.423116	H	0.460833	-1.983571	-2.741689
C	-5.907656	-1.710801	-1.823385	H	-1.406532	1.269335	-4.765664
C	-6.838389	0.156276	0.444330	H	-2.203036	2.075098	-3.398205
Sb	-0.869827	-1.035255	0.796220	H	-2.793237	0.505934	-3.960148
H	1.070818	0.071492	2.340112	H	1.359187	1.282462	-3.473268
H	0.018782	2.241919	0.407905	H	1.592162	0.839650	-1.767537
H	2.785495	1.603975	1.553674	H	0.643592	2.280697	-2.195457
H	-0.614040	3.220017	4.774921	H	-6.635687	2.253950	-2.075286
H	0.139673	3.596996	3.210964	H	-7.708061	0.952055	-2.617540
H	0.956754	2.513216	4.344659	H	-6.123962	1.178406	-3.385676
H	-1.948390	0.407175	5.226178	H	-5.461449	-2.422092	-1.112205
H	-0.335754	-0.283283	4.991783	H	-5.355362	-1.800662	-2.771269
H	-1.710235	-0.883546	4.038780	H	-6.937670	-2.046234	-2.015527
H	-3.180715	2.339822	3.084465	H	-6.799010	1.171189	0.867918
H	-3.037909	1.067031	1.863429	H	-6.431387	-0.528566	1.202966
H	-2.305578	2.660149	1.580406	H	-7.900014	-0.097663	0.304111
H	4.556987	3.069266	-1.196605	Si	-0.895864	1.326473	3.162018
H	3.818025	4.541476	-1.845059	Si	2.538944	3.761878	0.139900
H	3.079930	2.962625	-2.173876	Si	1.331737	-3.450121	1.469283
H	4.436469	4.194769	1.708353	Si	4.529078	-0.935576	-1.753004
H	2.942230	4.921995	2.322416	Si	-0.706544	0.231355	-2.598261
H	3.846238	5.715062	1.016083	Si	-5.874667	0.048736	-1.167117
H	0.343537	4.880388	0.581474				
H	0.362623	4.205366	-1.057112	97			
H	1.227343	5.707566	-0.713685	[SbA'3], C3; APF-D/def2TZVP(Sb);			
H	0.523744	-2.819925	-0.727171	def2SVP(C,H,Si); $\Delta G^\circ = -3040.910588$ au			
H	2.443608	-0.664679	0.384150	Sb	0.000000	0.000000	1.742837
H	2.525955	-2.526639	-2.054081	C	2.024263	1.374612	-1.437144
H	3.752150	-3.698313	0.909275	C	-3.731678	0.068298	3.023319
H	2.773910	-4.818356	-0.047495	C	1.893897	1.617007	-0.115697
H	3.119698	-5.182387	1.655535	C	-4.604040	-1.724326	0.663555
H	2.446375	-1.825920	3.023549	C	0.611604	1.798989	0.598854
H	1.951048	-3.293636	3.880237	C	-2.347318	0.831659	-0.115697
H	0.743856	-2.065004	3.481992	C	1.806691	-3.265878	3.023319
H	0.147903	-5.437113	2.399861	C	3.795330	-3.125052	0.663555
H	-0.327289	-5.164055	0.715959	C	-2.202580	1.065757	-1.437144
H	-1.016647	-4.162287	2.006331	C	5.046092	0.951663	-1.072639
H	3.817362	0.918906	-3.278882	C	-1.698882	-4.845875	-1.072639
H	4.143790	-0.561261	-4.197949	C	-1.118398	3.350045	-3.128234
H	5.489580	0.432737	-3.612672	C	3.512539	-0.737699	2.587910
H	5.876763	-2.915988	-1.018158	C	-3.347210	3.894212	-1.072639
H	6.801349	-1.915944	-2.155891	C	3.971050	2.280497	-3.646199
H	5.533783	-2.998742	-2.753765	C	-2.342025	-2.643583	-3.128234

C	-1.863772	-0.369830	0.598854	H	3.973860	-0.055922	1.857045
C	-2.395136	-2.673098	2.587910	H	2.846354	-0.143053	3.233062
C	-0.010557	-4.579279	-3.646199	H	4.317239	-1.140395	3.223570
C	3.460423	-0.706462	-3.128234	H	-2.035360	-3.413503	1.857045
C	0.453421	-2.448666	-0.115697	H	-1.547064	-2.393488	3.233062
C	-1.117403	3.410797	2.587910	H	-3.146230	-3.168641	3.223570
C	-3.960494	2.298782	-3.646199	H	-1.938500	3.469425	1.857045
C	1.924987	3.197579	3.023319	H	-1.299290	2.536541	3.233062
C	1.252168	-1.429159	0.598854	H	-1.171009	4.309036	3.223570
C	0.808710	4.849378	0.663555	H	-3.655491	4.819162	-1.585423
C	0.178317	-2.440369	-1.437144	H	-0.918818	-5.409233	-0.536650
H	0.821240	5.768834	1.270245	H	-2.315441	-4.319671	-0.327300
H	1.760570	4.786445	0.113184	H	-2.345771	-5.575329	-1.585423
H	0.000000	4.942636	-0.078775	H	5.143942	1.908897	-0.536650
H	-5.406577	-2.173203	1.270245	H	4.898666	0.154605	-0.327300
H	-5.025468	-0.868524	0.113184	H	-0.677454	-5.250270	-4.211195
H	-4.280448	-2.471318	-0.078775	H	0.454786	-3.883196	-4.362230
H	4.585337	-3.595632	1.270245	H	0.791942	-5.188157	-3.201034
H	3.264898	-3.917920	0.113184	H	4.885595	2.038443	-4.211195
H	4.280448	-2.471318	-0.078775	H	3.135554	2.335454	-4.362230
H	-0.342916	3.570179	-2.377666	H	4.097105	3.279920	-3.201034
H	-0.692366	2.631567	-3.846972	H	-4.225124	3.500336	-0.536650
H	-1.340302	4.280326	-3.675667	H	-2.583224	4.165067	-0.327300
H	-2.920408	-2.082063	-2.377666	Si	2.592396	-2.143229	1.729439
H	-1.932821	-1.915391	-3.846972	Si	-2.671459	2.647843	-2.315223
H	-3.036720	-3.300899	-3.675667	Si	-3.152289	-1.173466	1.729439
H	3.263324	-1.488116	-2.377666	Si	0.559893	3.316695	1.729439
H	2.625187	-0.716177	-3.846972	Si	-0.957370	-3.637472	-2.315223
H	4.377022	-0.979427	-3.675667	Si	3.628828	0.989630	-2.315223
H	-4.208140	3.211828	-4.211195				
H	-3.590340	1.547742	-4.362230				
H	-4.889046	1.908237	-3.201034				
H	6.001262	0.756167	-1.585423				
H	1.739829	-0.765852	-0.135605				
H	0.607718	-1.613922	-2.024360				
H	1.093838	1.333260	-2.024360				
H	-1.701556	0.280661	-2.024360				
H	2.804250	1.643760	0.501848				
H	-0.206667	1.889663	-0.135605				
H	-2.825662	1.606672	0.501848				
H	-1.533162	-1.123811	-0.135605				
H	0.021413	-3.250431	0.501848				
H	1.919636	4.083200	3.678512				
H	1.789672	2.308135	3.659155				
H	2.920433	3.133028	2.556649				
H	-4.495973	-0.379146	3.678512				
H	-2.893739	0.395834	3.659155				
H	-4.173499	0.962655	2.556649				
H	2.576337	-3.704054	3.678512				
H	1.104068	-2.703968	3.659155				
H	1.253066	-4.095683	2.556649				
				97			
				[SbA'3], C1; APF-D/def2TZVP(Sb);			
				def2SVP(C,H,Si); $\Delta G^\circ = -3040.906993$ au			
				C	-0.535589	0.585106	1.553242
				C	0.025794	-3.243009	3.596039
				C	-1.627983	-0.766272	4.364128
				C	-2.452781	-2.453394	1.932145
				C	-2.040025	3.480584	0.278267
				C	-0.482521	4.794204	2.617488
				C	-2.913450	3.009609	3.169256
				C	2.685786	-0.646945	-0.197803
				C	2.336468	0.749883	-0.548269
				C	-0.274189	-0.979481	-1.466886
				C	2.576803	1.381063	-1.716273
				C	3.832420	-2.345550	2.170563
				C	3.657677	0.724092	2.432673
				C	5.645218	-0.524317	0.471305
				C	0.412377	3.116319	-3.037203
				C	1.757500	4.014926	-0.410228
				C	3.342753	4.034377	-3.063541
				C	-1.743159	-1.056508	-1.256397

C	-2.619739	-0.039044	-1.377775	H	0.488021	1.771084	2.948209
C	-0.796287	-3.495660	-3.181793	H	3.186576	-1.144737	-1.046151
C	1.941295	-2.149398	-3.394875	H	1.811068	1.300394	0.244374
C	-0.543071	-0.708877	-4.491037	H	3.097045	0.815830	-2.504323
C	-4.957609	-2.015451	-1.114898	H	0.455041	-3.851996	2.785026
C	-5.018460	0.652993	0.430194	H	0.852936	-2.880598	4.227209
C	-5.322827	0.653978	-2.621553	H	-0.602388	-3.902599	4.215950
C	0.132486	-0.710441	1.844817	H	-2.222232	-1.379719	5.060111
C	-0.309696	1.753745	2.189239	H	-0.790754	-0.324121	4.927431
H	-3.574862	3.891193	3.159474	H	-2.257795	0.061005	4.004212
H	4.630066	-2.401423	2.928788	H	-3.173323	-2.966318	2.588688
H	2.869922	-2.470047	2.691275	H	-2.974287	-1.625433	1.430228
H	3.955928	-3.202025	1.488803	H	-2.130918	-3.171530	1.161765
H	3.764951	1.689167	1.913809	H	-1.220589	3.684602	-0.425830
H	2.660287	0.703094	2.895213	H	-2.564977	2.575934	-0.061794
H	4.405578	0.688643	3.240962	H	-2.751855	4.320139	0.226858
H	6.429292	-0.459919	1.242550	H	-1.134245	5.682020	2.586212
H	5.881324	-1.378191	-0.183392	H	-0.136151	4.670105	3.656244
H	5.687744	0.392495	-0.137995	H	0.397285	4.994742	1.988127
H	-0.363152	2.545350	-2.503478	H	-3.501765	2.139882	2.836876
H	0.030980	4.136297	-3.206296	H	-2.600980	2.829751	4.210030
H	0.557621	2.644276	-4.021827	Sb	0.898535	-1.875226	0.145881
H	1.071530	3.442134	0.231548	Si	0.100519	-1.838013	-3.131997
H	2.709058	4.127572	0.132696	Si	-4.473050	-0.194631	-1.168145
H	1.326395	5.017433	-0.558865	Si	-1.416966	3.261483	2.043397
H	3.033170	5.067161	-3.290562	Si	3.936178	-0.708097	1.240796
H	4.297898	4.077537	-2.516733	Si	2.026262	3.137943	-2.054957
H	3.524639	3.520388	-4.021111	Si	-0.994060	-1.804624	2.928875
H	-1.889113	-3.363346	-3.173416				
H	-0.530618	-4.046780	-4.097955				
H	2.517211	-1.212978	-3.370683				
H	2.359445	-2.837250	-2.642867				
H	2.091073	-2.612324	-4.383675				
H	-0.453710	-1.181604	-5.482010				
H	-1.603041	-0.467405	-4.316542				
H	0.020890	0.236602	-4.508781				
H	-4.513193	-2.533209	-0.251157				
H	-6.051953	-2.117007	-1.038201				
H	-4.633755	-2.536576	-2.029753				
H	-4.518135	0.213567	1.307162				
H	-4.781551	1.728125	0.412450				
H	-6.106171	0.551665	0.575460				
H	-5.027837	1.713776	-2.682388				
H	-6.419300	0.614233	-2.520651				
H	-5.049313	0.172902	-3.573854				
H	-0.520807	-4.124813	-2.319959				
H	0.060425	0.068089	-1.556020				
H	-2.139539	-2.055690	-1.026681				
H	-2.201803	0.948061	-1.627103				
H	1.023292	-0.545498	2.477624				
H	-1.341354	0.538369	0.808225				
				97			
				[SbA'3], 1U2D; APF-D/def2TZVP(Sb);			
				def2SVP(C,H,Si); $\Delta G^\circ = -3040.899779$ au			
				C	5.042776	0.226924	-0.168537
				C	-2.991341	-0.226646	-1.117223968
				C	-4.058393	0.572796	-0.931490
				C	-0.376332	-1.622363	-3.273241
				C	-1.832062	0.997221	-3.880247
				C	0.923926	1.111001	-2.570267
				C	-6.667092	1.116618	-2.450026
				C	-5.908784	-1.767399	-1.659399
				C	-6.746955	0.269960	0.502058
				C	0.217901	0.605117	1.785909
				C	0.729319	1.726412	0.961830
				C	1.979065	2.232286	0.965470
				C	-0.101922	2.731488	3.989180
				C	-1.347548	-0.053758	4.376572
				C	-2.543223	1.905706	2.302755
				C	3.604024	3.590217	-1.345394
				C	3.319006	4.921649	1.400650
				C	0.880204	4.712642	-0.463958
				C	0.904539	-2.153949	0.093149
				C	2.147088	-1.424352	-0.261766
				C	2.952103	-1.696085	-1.308859

C	2.771031	-4.461401	0.897652	H	-6.298546	-0.359104	1.287116
C	1.716940	-2.571090	3.082016	H	-7.811264	-0.000859	0.411407
C	-0.189899	-4.566682	1.705621	H	-0.129027	-1.608113	-4.346809
C	4.637608	0.057509	-3.225137	H	-1.270310	-2.253171	-3.145732
C	5.906340	-2.293381	-1.725314	H	0.463489	-2.091588	-2.743158
C	-1.558618	0.154790	-0.974075	H	-1.349065	1.105927	-4.864889
H	3.007381	-5.241655	1.638768	H	-2.101915	2.002474	-3.518924
H	2.539552	-1.850495	2.951193	H	-2.767460	0.432581	-4.013870
H	2.037693	-3.311537	3.832167	H	1.470022	1.026998	-3.523335
H	0.848751	-2.035773	3.496633	H	1.578666	0.751036	-1.766009
H	0.051762	-5.358806	2.432431	H	0.709549	2.175977	-2.396572
H	-0.472918	-5.054650	0.759123	H	-6.622694	2.181899	-2.172418
H	-1.067686	-4.018040	2.079804	H	-7.727608	0.845279	-2.576540
H	3.954391	0.917756	-3.174598	Sb	-0.849750	-1.012882	0.748360
H	4.322767	-0.578068	-4.068079	Si	-0.958830	1.297289	3.122147
H	5.648300	0.436786	-3.446366	Si	2.447328	3.840112	0.123205
H	5.940625	-2.880766	-0.794118	Si	4.624112	-0.912383	-1.607797
H	6.913239	-1.885025	-1.909070	Si	-0.676347	0.134034	-2.663802
H	5.668124	-2.984236	-2.549960	Si	-5.840770	0.042356	-1.137348
H	5.109761	-0.335237	0.776269	Si	1.297109	-3.435650	1.459718
H	4.272944	1.003197	-0.051798				
H	6.009362	0.728121	-0.335302	97			
H	-1.499731	1.201274	-0.627540	[SbA'3], C3; wB97x-D/def2TZVP(Sb);			
H	-3.171093	-1.269373	-1.429778	def2SVP(C,H,Si); $\Delta G^\circ = -3041.990452$ au			
H	-3.855769	1.611720	-0.628364	Sb	0.000000	0.000000	1.713052
H	1.045049	0.105590	2.319102	C	1.490418	2.016237	-1.424175
H	-0.026638	2.242548	0.353395	C	-3.622046	-1.229486	2.948140
H	2.724886	1.726559	1.597776	C	1.273978	2.154671	-0.102818
H	-0.735598	3.144853	4.789981	C	-3.723483	-3.193635	0.569970
H	0.128969	3.538594	3.277269	C	-0.014343	1.900933	0.592692
H	0.848544	2.404192	4.440036	C	-2.502989	0.025962	-0.102818
H	-2.045626	0.325445	5.140063	C	2.875789	-2.522041	2.948140
H	-0.433281	-0.384255	4.894751	C	4.627511	-1.627814	0.569970
H	-1.811895	-0.931887	3.901685	C	-2.491322	0.282621	-1.424175
H	-3.230153	2.321170	3.057274	C	4.485805	2.510233	-0.980311
H	-3.075127	1.096733	1.776265	C	-0.068977	-5.139938	-0.980311
H	-2.330467	2.702526	1.572296	C	-2.169576	2.809156	-3.074165
H	4.562100	3.144484	-1.038139	C	3.577110	0.452208	2.577044
H	3.822369	4.557834	-1.825753	C	-4.416828	2.629704	-0.980311
H	3.146888	2.930496	-2.097461	C	3.134251	3.481930	-3.581428
H	4.229528	4.427479	1.775978	C	-1.348013	-3.283486	-3.074165
H	2.663559	5.119906	2.263386	C	-1.639085	-0.962888	0.592692
H	3.616414	5.889555	0.966103	C	-1.396932	-3.323972	2.577044
H	0.189168	4.891757	0.374841	C	1.448315	-4.455306	-3.581428
H	0.342094	4.133636	-1.230286	C	3.517588	0.474330	-3.074165
H	1.134005	5.689135	-0.906412	C	1.229011	-2.180633	-0.102818
H	0.554929	-2.772175	-0.753594	C	-2.180178	2.871764	2.577044
H	2.453977	-0.640129	0.443863	C	-4.582566	0.973376	-3.581428
H	2.632580	-2.495609	-1.995463	C	0.746257	3.751527	2.948140
H	3.661394	-3.830327	0.758059	C	1.653428	-0.938046	0.592692
H	2.560210	-4.956900	-0.063452	C	-0.904027	4.821449	0.569970
H	-6.165453	1.001973	-3.423856	C	1.000903	-2.298858	-1.424175
H	-5.437350	-2.419622	-0.907372	H	-1.201599	5.709389	1.150082
H	-5.396692	-1.927427	-2.621431				
H	-6.954360	-2.093398	-1.778305				
H	-6.692685	1.317702	0.838531				

H	0.000000	5.074822	-0.005963
H	-1.707672	4.604322	-0.151970
H	-4.343676	-3.895309	1.150082
H	-4.394925	-2.537411	-0.005963
H	-3.133624	-3.781048	-0.151970
H	5.545275	-1.814079	1.150082
H	4.394925	-2.537411	-0.005963
H	4.841296	-0.823274	-0.151970
H	-1.475616	3.227053	-2.326974
H	-1.566791	2.265623	-3.819744
H	-2.661309	3.649478	-3.590149
H	-2.056902	-2.891448	-2.326974
H	-1.178692	-2.489692	-3.819744
H	-1.829887	-4.129500	-3.590149
H	3.532518	-0.335605	-2.326974
H	2.745482	0.224069	-3.819744
H	4.491195	0.480022	-3.590149
H	-5.105901	1.780525	-4.118671
H	-4.021009	0.383691	-4.323517
H	-5.341720	0.312345	-3.134569
H	5.470841	2.613981	-1.462256
H	1.897771	-0.177277	-0.165644
H	1.172846	-1.398104	-2.033403
H	0.624371	1.714766	-2.033403
H	-1.797216	-0.316662	-2.033403
H	2.123675	2.433829	0.537796
H	-0.795358	1.732156	-0.165644
H	-3.169595	0.622242	0.537796
H	-1.102412	-1.554879	-0.165644
H	1.045920	-3.056071	0.537796
H	0.427461	4.584299	3.594911
H	0.962074	2.887430	3.596971
H	1.686858	4.050575	2.459183
H	-4.183850	-1.921958	3.594911
H	-2.981625	-0.610535	3.596971
H	-4.351329	-0.564426	2.459183
H	3.756389	-2.662342	3.594911
H	2.019551	-2.276895	3.596971
H	2.664472	-3.486149	2.459183
H	3.717990	1.282573	1.867372
H	2.779441	0.740281	3.280508
H	4.507968	0.350686	3.157425
H	-0.748254	-3.861161	1.867372
H	-0.748619	-2.777207	3.280508
H	-1.950281	-4.079358	3.157425
H	-2.969736	2.578587	1.867372
H	-2.030823	2.036926	3.280508
H	-2.557687	3.728672	3.157425
H	-4.999194	3.430897	-1.462256
H	0.845077	-5.428475	-0.437338
H	-0.810956	-4.799151	-0.240912

H	-0.471647	-6.044877	-1.462256
H	4.278659	3.446096	-0.437338
H	4.561665	1.697268	-0.240912
H	1.010971	-5.312102	-4.118671
H	1.678218	-3.674141	-4.323517
H	2.400361	-4.782238	-3.134569
H	4.094930	3.531577	-4.118671
H	2.342790	3.290450	-4.323517
H	2.941359	4.469892	-3.134569
H	-5.123736	1.982379	-0.437338
H	-3.750709	3.101884	-0.240912
Si	3.184029	-1.161043	1.683174
Si	-3.430165	1.664436	-2.262083
Si	-2.597507	-2.176928	1.683174
Si	-0.586522	3.337971	1.683174
Si	0.273639	-3.802828	-2.262083
Si	3.156526	2.138393	-2.262083

97

[SbA'3], C1; wB97x-D/def2TZVP(Sb);

def2SVP(C,H,Si); $\Delta G^\circ = -3041.986616$ au

C	-0.577025	-0.400510	1.667417
C	-0.953872	-4.728273	1.055463
C	-1.941564	-2.907736	3.331999
C	-3.148289	-2.625060	0.524085
C	-0.347653	3.363229	2.031307
C	0.416225	2.348548	4.829774
C	-2.363059	1.714679	3.618626
C	2.296460	-1.069655	-0.879151
C	2.523620	0.275070	-0.277629
C	-0.627687	0.315505	-1.464969
C	3.328255	1.241648	-0.756383
C	2.791108	-4.094855	-0.240419
C	3.533572	-1.961887	1.861502
C	5.125755	-2.148278	-0.731205
C	2.402963	4.164810	-0.553591
C	3.386743	2.641842	1.960872
C	5.372880	3.456053	-0.246654
C	-2.111027	0.298912	-1.288534
C	-2.861199	1.177697	-0.599022
C	-1.556925	0.207390	-4.410508
C	1.419599	0.585268	-3.876536
C	-0.543990	2.837366	-3.159472
C	-5.370139	-0.239844	-1.648651
C	-5.372020	0.946159	1.193074
C	-5.356343	2.813617	-1.232601
C	-0.232374	-1.724922	1.081850
C	0.134137	0.329826	2.546115
H	-2.811903	2.643746	4.004857
H	3.505336	-4.816908	0.186651
H	1.817050	-4.268895	0.243172
H	2.679248	-4.328007	-1.311459
H	3.860954	-0.923390	2.026442
H	2.584746	-2.105562	2.399404

H	4.280351	-2.627304	2.323656	H	-2.527615	0.918759	4.361798
H	5.860792	-2.786059	-0.214982	Sb	0.207962	-1.653643	-1.072549
H	5.128062	-2.422775	-1.797993	Si	-0.303600	0.974974	-3.230338
H	5.463957	-1.103072	-0.648788	Si	-4.733240	1.164129	-0.567461
H	1.363436	3.838879	-0.395304	Si	-0.528084	1.936984	3.254551
H	2.532339	5.140647	-0.058343	Si	3.410624	-2.335106	0.018888
H	2.547943	4.313141	-1.635874	Si	3.614593	2.879108	0.104701
H	2.430717	2.146818	2.189455	Si	-1.576823	-3.005009	1.489185
H	4.193197	2.011698	2.368311				
H	3.403338	3.604586	2.496259				
H	5.580128	4.421395	0.242259	97			
H	6.110885	2.725327	0.120523	[SbA ⁻³], 1U2D; wB97x-D/def2TZVP(Sb);			
H	5.537566	3.586790	-1.328255	def2SVP(C,H,Si); $\Delta G^\circ = -3041.982348$ au			
H	-2.584021	0.524985	-4.173383	C	5.034797	0.204952	-0.177423
H	-1.340415	0.512395	-5.446747	C	-3.001548	-0.218185	-1.147629
H	2.196325	0.979376	-3.205891	C	-4.065258	0.570521	-0.916749
H	1.580693	-0.497414	-4.003073	C	-0.342583	-1.544637	-3.312846
H	1.550898	1.054713	-4.864776	C	-1.834135	1.062100	-3.865352
H	-0.484600	3.287923	-4.162974	C	0.907197	1.192045	-2.540844
H	-1.529471	3.081851	-2.732515	C	-6.676643	1.192618	-2.394037
H	0.227136	3.307424	-2.529225	C	-5.922720	-1.725538	-1.746035
H	-5.037017	-1.220664	-1.275369	C	-6.744404	0.206854	0.513217
H	-6.471676	-0.242699	-1.661551	C	0.192639	0.574875	1.799550
H	-5.023668	-0.134890	-2.689140	C	0.722408	1.706241	0.989488
H	-4.996105	0.017661	1.651083	C	1.977454	2.190150	0.993709
H	-5.064943	1.785713	1.836471	C	-0.069138	2.675276	4.032999
H	-6.473158	0.904156	1.203425	C	-1.343838	-0.092849	4.403707
H	-4.973455	3.652252	-0.629234	C	-2.540358	1.906333	2.368784
H	-6.456987	2.862100	-1.214772	C	3.601196	3.538549	-1.323933
H	-5.025060	2.969097	-2.271530	C	3.393035	4.834490	1.442554
H	-1.524032	-0.893758	-4.372967	C	0.921997	4.711032	-0.386583
H	-0.159339	1.022724	-0.759049	C	0.891217	-2.159858	0.086327
H	-2.634397	-0.501186	-1.832502	C	2.131575	-1.420937	-0.281759
H	-2.328468	1.978527	-0.064632	C	2.930382	-1.687263	-1.331084
H	0.704703	-2.099334	1.525578	C	2.789191	-4.455960	0.856279
H	-1.551090	-0.006614	1.347720	C	1.744380	-2.586275	3.057988
H	1.110268	-0.062539	2.867538	C	-0.153845	-4.598249	1.698826
H	2.675970	-1.079205	-1.916028	C	4.565061	0.133526	-3.227902
H	2.006504	0.448497	0.675057	C	5.875103	-2.255681	-1.832649
H	3.847335	1.039524	-1.705562	C	-1.562753	0.158066	-0.979067
H	-0.697634	-4.814909	-0.012474	H	3.024118	-5.252423	1.580407
H	-0.058827	-4.986286	1.644138	H	2.552268	-1.850212	2.918182
H	-1.725039	-5.483566	1.275694	H	2.089340	-3.322867	3.800898
H	-2.688110	-3.659799	3.633140	H	0.875336	-2.064874	3.489985
H	-1.027683	-3.078168	3.923295	H	0.115233	-5.401126	2.403752
H	-2.328722	-1.912452	3.600687	H	-0.456289	-5.073028	0.751567
H	-3.972107	-3.282768	0.843646	H	-1.029949	-4.071065	2.106461
H	-3.461626	-1.582111	0.685163	H	3.875345	0.985505	-3.137028
H	-3.005861	-2.768675	-0.559134	H	4.238648	-0.476774	-4.085112
H	0.705210	3.643361	1.883579	H	5.566800	0.530664	-3.458066
H	-0.762967	3.093561	1.047271	H	5.931867	-2.873929	-0.922762
H	-0.884776	4.255636	2.391393	H	6.876958	-1.838326	-2.023180
H	0.050651	3.284997	5.280256	H	5.623950	-2.920709	-2.674532
H	0.308710	1.547496	5.578159	H	5.122736	-0.388900	0.746321
H	1.490654	2.473481	4.620273	H	4.262652	0.971808	-0.016218
H	-2.907850	1.434857	2.703254	H	5.994490	0.719629	-0.343416
				H	-1.520256	1.197812	-0.611409

H	-3.181854	-1.245525	-1.499940
H	-3.856528	1.592843	-0.565861
H	1.021854	0.063959	2.318616
H	-0.026387	2.244797	0.392400
H	2.715734	1.659120	1.613653
H	-0.678017	3.072052	4.860938
H	0.145340	3.500325	3.336461
H	0.892592	2.335697	4.449884
H	-2.006056	0.292701	5.195302
H	-0.423686	-0.457102	4.888432
H	-1.847530	-0.952394	3.934629
H	-3.207988	2.336318	3.132237
H	-3.097999	1.109051	1.850101
H	-2.323441	2.698465	1.633779
H	4.546876	3.050002	-1.043703
H	3.848850	4.507785	-1.786323
H	3.109503	2.914348	-2.084898
H	4.298144	4.313627	1.794242
H	2.758556	5.034377	2.320493
H	3.706568	5.802612	1.020180
H	0.250349	4.901444	0.465554
H	0.354879	4.147800	-1.144314
H	1.187882	5.683654	-0.830210
H	0.544290	-2.774660	-0.763843
H	2.438521	-0.633892	0.420291
H	2.608923	-2.490271	-2.012265
H	3.681702	-3.824088	0.734276
H	2.583650	-4.931452	-0.116131
H	-6.177647	1.125968	-3.373733
H	-5.449987	-2.413654	-1.027350
H	-5.411523	-1.840445	-2.715134
H	-6.968032	-2.046514	-1.879356
H	-6.686830	1.237224	0.899284
H	-6.292381	-0.458712	1.265534
H	-7.809846	-0.057868	0.418918
H	-0.087868	-1.501287	-4.383821
H	-1.227482	-2.192572	-3.207681
H	0.500517	-2.016357	-2.789494
H	-1.344935	1.208719	-4.841932
H	-2.129428	2.051476	-3.480368
H	-2.756963	0.483743	-4.027175
H	1.446424	1.163778	-3.501484
H	1.579658	0.813161	-1.759200
H	0.675618	2.244456	-2.315593
H	-6.630987	2.243294	-2.065662
H	-7.737772	0.930171	-2.532914
Sb	-0.859197	-1.021280	0.729042
Si	-0.954427	1.264895	3.158623
Si	2.475616	3.795732	0.164906
Si	4.591809	-0.886697	-1.644590
Si	-0.674695	0.189745	-2.661511
Si	-5.849940	0.055526	-1.138852
Si	1.312927	-3.446720	1.437065

97

[BiA ³], C3; M06-L/def2TZVP(Bi); def2SVP(C,H,Si); $\Delta G^\circ = -3016.539878$ au			
Bi	0.000000	0.000000	1.708270
C	1.350198	1.928759	-1.611165
C	-3.639270	-1.200766	2.876727
C	1.174067	2.206041	-0.298536
C	-3.844904	-3.250068	0.594642
C	-0.060099	2.005286	0.473711
C	-2.497521	-0.086249	-0.298536
C	2.859529	-2.551317	2.876727
C	4.737094	-1.704750	0.594642
C	-2.345454	0.204926	-1.611165
C	4.316189	2.595459	-1.366820
C	0.089639	-5.035659	-1.366820
C	-2.038644	2.727558	-3.302107
C	3.595443	0.409021	2.516839
C	-4.405828	2.440200	-1.366820
C	2.781577	3.329820	-3.941347
C	-1.342813	-3.129296	-3.302107
C	-1.706579	-1.054690	0.473711
C	-1.443499	-3.318256	2.516839
C	1.492920	-4.073826	-3.941347
C	3.381456	0.401738	-3.302107
C	1.323454	-2.119792	-0.298536
C	-2.151944	2.909235	2.516839
C	-4.274497	0.744006	-3.941347
C	0.779741	3.752083	2.876727
C	1.766678	-0.950595	0.473711
C	-0.892190	4.954818	0.594642
C	0.995255	-2.133686	-1.611165
H	-1.162261	5.818447	1.220861
H	0.000000	5.232782	0.013460
H	-1.710664	4.801672	-0.124683
H	-4.457792	-3.915772	1.220861
H	-4.531722	-2.616391	0.013460
H	-3.303038	-3.882315	-0.124683
H	5.620054	-1.902676	1.220861
H	4.531722	-2.616391	0.013460
H	5.013702	-0.919357	-0.124683
H	-1.426246	3.221833	-2.531813
H	-1.343384	2.220386	-3.989098
H	-2.545594	3.516171	-3.879204
H	-2.077066	-2.846082	-2.531813
H	-1.251218	-2.273598	-3.989098
H	-1.772296	-3.962634	-3.879204
H	3.503312	-0.375751	-2.531813
H	2.594603	0.053212	-3.989098
H	4.317890	0.446464	-3.879204
H	-4.791957	1.503295	-4.547056
H	-3.629532	0.167361	-4.621585
H	-5.036390	0.051738	-3.554134

H	5.283303	2.688381	-1.883049
H	1.987457	-0.116738	-0.216744
H	1.089124	-1.169739	-2.139286
H	0.468461	1.528079	-2.139286
H	-1.557586	-0.358340	-2.139286
H	2.043877	2.585250	0.266568
H	-0.892630	1.779557	-0.216744
H	-3.260830	0.477424	0.266568
H	-1.094827	-1.662819	-0.216744
H	1.216953	-3.062674	0.266568
H	0.513431	4.590564	3.537686
H	0.966498	2.880365	3.523404
H	1.734818	4.012849	2.395868
H	-4.232261	-1.850637	3.537686
H	-2.977718	-0.603170	3.523404
H	-4.342638	-0.504028	2.395868
H	3.718830	-2.739927	3.537686
H	2.011220	-2.277195	3.523404
H	2.607820	-3.508821	2.395868
H	3.707112	1.251969	1.816978
H	2.797105	0.677142	3.227386
H	4.527141	0.349809	3.099463
H	-0.769319	-3.836438	1.816978
H	-0.812131	-2.760935	3.227386
H	-1.960627	-4.095524	3.099463
H	-2.937793	2.584469	1.816978
H	-1.984974	2.083793	3.227386
H	-2.566514	3.745715	3.099463
H	-4.969858	3.231284	-1.883049
H	1.035966	-5.339417	-0.894296
H	-0.615453	-4.782945	-0.559783
H	-0.313445	-5.919665	-1.883049
H	4.106088	3.566881	-0.894296
H	4.449878	1.858475	-0.559783
H	1.094087	-4.901604	-4.547056
H	1.669827	-3.226947	-4.621585
H	2.473389	-4.387510	-3.554134
H	3.697870	3.398309	-4.547056
H	1.959705	3.059587	-4.621585
H	2.563001	4.335772	-3.554134
H	-5.142054	1.772536	-0.894296
H	-3.834426	2.924470	-0.559783
Si	3.243102	-1.207707	1.617842
Si	-3.273345	1.520030	-2.551753
Si	-2.667456	-2.204755	1.617842
Si	-0.575646	3.412463	1.617842
Si	0.320288	-3.594815	-2.551753
Si	2.953057	2.074785	-2.551753

[BiA³], C1; M06-L/def2TZVP(Bi);
def2SVP(C,H,Si); $\Delta G^\circ = -3016.536688$ au

C	0.687129	0.319673	1.471546
C	2.143907	0.102728	1.319313
C	3.049928	0.900352	0.711474
C	1.086372	-0.599779	4.378358
C	-1.491656	0.893037	3.661796
C	1.180953	2.379610	3.663121
C	5.246446	-1.014919	1.615908
C	5.554488	0.457021	-1.065813
C	5.768831	2.011769	1.545255
C	0.129369	-1.231706	-1.532325
C	0.700004	0.102015	-1.781206
C	0.121942	1.149867	-2.411128
C	0.331912	-4.255890	-2.044985
C	1.777344	-2.264515	-3.913333
C	2.781374	-2.689480	-1.046459
C	0.809890	3.996255	-1.331977
C	0.282631	3.534163	-4.307883
C	2.834476	2.419398	-2.964605
C	-2.534335	-0.904044	0.567213
C	-2.654422	0.488726	0.093723
C	-3.326572	1.490149	0.702523
C	-3.232699	-3.874424	0.069575
C	-3.475462	-1.892209	-2.270033
C	-5.411391	-1.707225	0.077459
C	-2.221666	4.293066	1.132076
C	-2.920122	3.312872	-1.708950
C	-5.151843	3.922617	0.324876
H	0.329748	1.143756	0.824614
H	2.528141	-0.809766	1.809783
H	2.655921	1.817081	0.242088
H	-0.870009	-1.313032	-1.992557
H	1.738870	0.230185	-1.435424
H	-0.911559	1.006952	-2.767945
H	-2.912249	-0.980381	1.605255
H	-2.156186	0.703034	-0.866346
H	-3.821397	1.235742	1.654426
H	0.097957	-4.530585	-1.004046
H	-0.617477	-4.230433	-2.601897
H	0.928711	-5.080685	-2.462498
H	2.407390	-3.064289	-4.330268
H	0.907467	-2.145851	-4.576520
H	2.352204	-1.327210	-3.966315
H	3.556622	-3.355177	-1.455498
H	3.232530	-1.691137	-0.929472
H	2.544320	-3.056277	-0.034345
H	-0.225087	4.348626	-1.215064
H	1.118125	3.561032	-0.368270
H	1.437044	4.885464	-1.502189
H	0.760895	4.496108	-4.545807

97

H	0.410057	2.877565	-5.181188
H	-0.795695	3.724852	-4.196993
H	3.258790	1.964835	-2.056754
H	3.026134	1.723253	-3.795011
H	3.403553	3.340374	-3.162583
H	-3.948605	-4.581855	-0.375582
H	-2.231109	-4.180689	-0.271123
H	-3.267913	-4.023006	1.159886
H	-3.460897	-0.831782	-2.565924
H	-2.573535	-2.365981	-2.684123
H	-4.336708	-2.354503	-2.776081
H	-6.132500	-2.345742	-0.454808
H	-5.579627	-1.847454	1.155754
H	-5.658558	-0.660999	-0.157304
H	-1.201686	3.881860	1.087624
H	-2.172851	5.338373	0.789850
H	-2.520191	4.309803	2.191673
H	-1.923093	2.874821	-1.864988
H	-3.627239	2.745925	-2.333978
H	-2.888616	4.343523	-2.094312
H	-5.224343	4.977203	0.019094
H	-5.883484	3.356522	-0.270317
H	-5.473032	3.866641	1.375841
H	0.694716	-1.601637	4.141279
H	2.181646	-0.644956	4.281001
H	0.865231	-0.413248	5.440118
H	-1.961312	1.675534	3.048713
H	-2.043664	-0.042436	3.484010
H	-1.643123	1.162167	4.718346
H	1.051917	2.672091	4.716186
H	2.261515	2.326236	3.462278
H	0.773709	3.194290	3.045241
H	4.767764	-1.885187	1.142364
H	6.327620	-1.216949	1.646917
H	4.895516	-0.970363	2.658353
H	4.993831	-0.262238	-1.682366
H	5.520827	1.425333	-1.586662
H	6.606380	0.131979	-1.059926
H	5.549960	2.969692	1.050010
H	6.861701	1.881989	1.535085
H	5.456992	2.109566	2.595726
Bi	-0.336911	-1.629858	0.735657
Si	0.339496	0.742911	3.290853
Si	4.891371	0.583193	0.692809
Si	1.256457	-2.621060	-2.146621
Si	0.999889	2.767480	-2.749922
Si	-3.640880	-2.101469	-0.408065
Si	-3.409146	3.254299	0.103114

97

[BiA³], 1U2D; M06-L/def2TZVP(Sb);
def2SVP(C,H,Si); $\Delta G^\circ = -3016.539252$ au

C	3.094011	-1.424326	1.459193
C	2.233315	-1.899072	0.530870
C	0.781439	-2.085703	0.680074
C	5.372563	-1.522628	-0.574478
C	5.076561	0.860749	1.344193
C	5.990930	-1.853975	2.425202
C	0.788847	-4.493975	-1.224131
C	-1.725442	-3.854489	0.425086
C	0.788382	-4.929592	1.827347
C	-4.112951	0.516684	-0.238678
C	-3.076375	-0.066379	0.403236
C	-1.714905	0.471660	0.607277
C	-5.791079	-1.949112	0.392657
C	-6.238813	-0.429304	-2.243215
C	-7.095921	0.836537	0.400331
C	-2.278967	1.991785	3.153236
C	0.579904	0.955842	2.708936
C	-1.739363	-0.988885	3.340868
C	1.278245	3.114821	0.225052
C	0.806539	2.244440	-0.694180
C	1.334933	0.904931	-1.015856
C	-1.151696	4.918597	-0.196943
C	1.664274	6.140725	-0.160589
C	0.464088	5.073271	2.429609
C	2.370976	-0.936687	-3.310796
C	3.708267	1.785509	-2.741105
C	0.896341	1.655312	-3.961820
H	-3.930393	1.518763	-0.660859
H	-3.245603	-1.068004	0.833478
H	-1.641691	1.488496	0.178162
H	-5.059219	-2.624107	-0.076535
H	-6.775659	-2.434246	0.316637
H	-5.542065	-1.887643	1.463331
H	-5.526728	-1.081809	-2.769625
H	-6.228818	0.544155	-2.755922
H	-7.243330	-0.858093	-2.379089
H	-8.107587	0.416905	0.291786
H	-7.112717	1.844617	-0.040103
H	-6.900517	0.955200	1.476282
H	-2.042494	2.187032	4.210549
H	-3.353589	1.763676	3.088665
H	-2.114748	2.929479	2.600493
H	0.930042	0.523291	3.659426
H	0.764462	2.038775	2.754021
H	1.222077	0.554258	1.909301
H	-1.192721	-1.885311	3.012494
H	-2.814103	-1.199802	3.227887
H	-1.548647	-0.877900	4.419523
H	2.153785	2.784232	0.807208
H	2.663488	-1.182701	2.443957
H	-0.061216	2.563922	-1.298101
H	2.108688	0.601096	-0.285727
H	-1.119727	4.803929	-1.291217
H	-1.616009	5.894711	0.008813

H	-1.830908	4.145496	0.194623	C	4.698218	-1.671787	0.470545
H	2.682942	6.093667	0.252336	C	-2.383992	0.291506	-1.585868
H	1.273653	7.148602	0.047156	C	4.436157	2.524347	-1.241632
H	1.751544	6.037663	-1.252427	C	-0.031930	-5.103998	-1.241632
H	-0.218984	4.367022	2.923930	C	-2.068958	2.832489	-3.235974
H	0.114472	6.088713	2.670298	C	3.608938	0.422641	2.450809
H	1.452388	4.951866	2.899195	C	-4.404227	2.579652	-1.241632
H	1.426190	-1.484775	-3.456418	C	2.983546	3.345418	-3.840172
H	2.984118	-1.520031	-2.607218	C	-1.418529	-3.208014	-3.235974
H	2.894878	-0.955785	-4.278946	C	-1.686266	-1.011828	0.446178
H	4.146402	1.863759	-3.747548	C	-1.438451	-3.336752	2.450809
H	4.459667	1.310842	-2.092740	C	1.405444	-4.256535	-3.840172
H	3.555258	2.808993	-2.365834	C	3.487486	0.375525	-3.235974
H	0.763951	2.725379	-3.742295	C	1.270344	-2.158379	-0.276656
H	-0.101402	1.189356	-3.938868	C	-2.170487	2.914111	2.450809
H	1.262707	1.579204	-4.996516	C	-4.388990	0.911118	-3.840172
H	2.643754	-2.151839	-0.462720	C	0.765272	3.780674	2.814444
H	0.459256	-1.731667	1.674301	C	1.719402	-0.954435	0.446178
H	4.788249	-0.983073	-1.335091	C	-0.901299	4.904670	0.470545
H	5.218040	-2.599304	-0.743279	C	0.939545	-2.210351	-1.585868
H	6.433520	-1.310596	-0.774522	H	-1.185741	5.783258	1.071340
H	4.484637	1.398927	0.587631	H	0.000000	5.160156	-0.108568
H	6.123147	1.184771	1.237387	H	-1.713186	4.705318	-0.246715
H	4.726804	1.204334	2.330164	H	-4.415578	-3.918510	1.071340
H	7.046139	-1.570992	2.292941	H	-4.468826	-2.580078	-0.108568
H	5.930316	-2.949344	2.347280	H	-3.218332	-3.836322	-0.246715
H	5.708587	-1.584875	3.453915	H	5.601319	-1.864748	1.071340
H	0.461314	-3.862448	-2.065245	H	4.468826	-2.580078	-0.108568
H	0.424183	-5.511974	-1.426960	H	4.931518	-0.868997	-0.246715
H	1.888348	-4.532503	-1.253030	H	-1.421708	3.280484	-2.465804
H	-2.141661	-3.425990	1.350359	H	-1.417691	2.307120	-3.952993
H	-2.119093	-4.879011	0.342151	H	-2.574310	3.648141	-3.777975
H	-2.148894	-3.286377	-0.419506	H	-2.130128	-2.871477	-2.465804
H	1.886974	-4.906071	1.879778	H	-1.289179	-2.381316	-3.952993
H	0.482343	-5.980318	1.713758	H	-1.872228	-4.053488	-3.777975
H	0.409327	-4.580279	2.799714	H	3.551836	-0.409007	-2.465804
Si	4.885707	-1.004334	1.164890	H	2.706870	0.074197	-3.952993
Si	0.158140	-3.852809	0.426357	H	4.446538	0.405347	-3.777975
Si	-5.803076	-0.254836	-0.421477	H	-4.909746	1.699797	-4.406793
Si	-1.246059	0.591431	2.439032	H	-3.773492	0.335006	-4.549450
Si	0.561076	4.802772	0.570217	H	-5.147208	0.229148	-3.424312
Si	2.086048	0.841285	-2.755335	H	5.404543	2.627434	-1.756538
Bi	-0.346957	-0.705468	-0.856174	H	1.925285	-0.140517	-0.269757
97				H	1.040249	-1.273694	-2.155322
[BiA'3], C3; APF-D/def2TZVP(Bi);				H	0.582927	1.537729	-2.155322
def2SVP(C,H,Si); ΔG° = -3015.292840 au				H	-1.623176	-0.264035	-2.155322
Bi	0.000000	0.000000	1.684087	H	2.082058	2.543986	0.323098
C	1.444448	1.918845	-1.585868	H	-0.840951	1.737604	-0.269757
C	-3.656796	-1.227592	2.814444	H	-3.244185	0.531122	0.323098
C	1.234039	2.179340	-0.276656	H	-1.084334	-1.597087	-0.269757
C	-3.796919	-3.232883	0.470545	H	1.162127	-3.075108	0.323098
C	-0.033136	1.966263	0.446178				
C	-2.504383	-0.020961	-0.276656				
C	2.891524	-2.553082	2.814444				

H	0.459399	4.606320	3.476546	C	0.580637	0.002418	-1.777458
H	0.979253	2.904561	3.447703	C	-0.076030	0.906277	-2.536335
H	1.704491	4.078272	2.322202	C	0.781774	-4.372741	-1.917450
H	-4.218890	-1.905309	3.476546	C	1.918184	-2.241558	-3.838417
H	-3.005050	-0.604223	3.447703	C	3.025771	-2.475900	-0.979088
H	-4.384133	-0.563003	2.322202	C	0.610128	3.824650	-1.623332
H	3.759491	-2.701012	3.476546	C	-0.239826	3.227649	-4.514967
H	2.025797	-2.300339	3.447703	C	2.500469	2.264189	-3.445283
H	2.679641	-3.515269	2.322202	C	-2.437014	-0.942774	0.627815
H	3.742926	1.251414	1.738423	C	-2.540271	0.484533	0.247053
H	2.803410	0.704621	3.148030	C	-3.258540	1.435016	0.881501
H	4.536716	0.332472	3.037979	C	-2.993981	-3.790756	-0.540012
H	-0.787706	-3.867176	1.738423	C	-3.594142	-1.301090	-2.265831
H	-0.791485	-2.780134	3.148030	C	-5.289706	-1.872053	0.207687
H	-1.980429	-4.095147	3.037979	C	-2.072868	4.260442	1.139263
H	-2.955219	2.615762	1.738423	C	-3.163337	3.248197	-1.581327
H	-2.011924	2.075514	3.148030	C	-5.093251	3.879698	0.737272
H	-2.556287	3.762676	3.037979	H	0.201834	1.047498	0.892636
H	-4.977696	3.366754	-1.756538	H	2.635310	-0.681333	1.741419
H	0.906867	-5.394592	-0.744211	H	2.429119	1.995908	0.264478
H	-0.757605	-4.818535	-0.464169	H	-0.783132	-1.633219	-1.954770
H	-0.426846	-5.994188	-1.756538	H	1.559919	0.290122	-1.369533
H	4.218421	3.482666	-0.744211	H	-1.054251	0.616071	-2.948304
H	4.551776	1.753162	-0.464169	H	-2.845539	-1.100691	1.641955
H	0.982806	-5.101864	-4.406793	H	-2.002572	0.758935	-0.670847
H	1.596622	-3.435443	-4.549450	H	-3.803038	1.135424	1.790335
H	2.375156	-4.572187	-3.424312	H	0.495379	-4.620582	-0.882868
H	3.926941	3.402067	-4.406793	H	-0.106728	-4.494352	-2.557200
H	2.176869	3.100437	-4.549450	H	1.530128	-5.113583	-2.241535
H	2.772052	4.343039	-3.424312	H	2.659825	-2.953679	-4.234028
H	-5.125287	1.911927	-0.744211	H	1.022887	-2.287019	-4.478663
H	-3.794171	3.065373	-0.464169	H	2.334726	-1.225638	-3.921382
Si	3.232250	-1.194275	1.552155	H	3.845314	-3.090056	-1.384818
Si	-3.321040	1.644703	-2.469715	H	3.367561	-1.431208	-0.934687
Si	-2.650397	-2.202074	1.552155	H	2.837367	-2.809669	0.053912
Si	-0.581853	3.396348	1.552155	H	-0.420202	4.152058	-1.425764
Si	0.236165	-3.698456	-2.469715	H	1.016917	3.413036	-0.686983
Si	3.084875	2.053753	-2.469715	H	1.202693	4.716150	-1.885988
				H	0.185997	4.188352	-4.845578
				H	-0.189660	2.524214	-5.361189
				H	-1.301953	3.394193	-4.274650
				H	3.035087	1.824195	-2.589681
				H	2.598209	1.569834	-4.294538
				H	3.006319	3.206381	-3.710479
				H	-3.710763	-4.406538	-1.106729
				H	-2.008304	-3.909439	-1.016408
				H	-2.929442	-4.206123	0.478572
				H	-3.888434	-0.240123	-2.256826
				H	-2.627116	-1.379212	-2.783470
				H	-4.337921	-1.853745	-2.862029
				H	-6.027915	-2.374525	-0.437574
				H	-5.339694	-2.333654	1.206587
				H	-5.583588	-0.814902	0.306230
				H	-1.066623	3.865768	0.933225
				H	-2.105949	5.307675	0.797871
				H	-2.221341	4.254841	2.230997
97							
[BiA'3], C1; APF-D/def2TZVP(Bi);							
def2SVP(C,H,Si); $\Delta G^\circ = -3015.283188$ au							
C	0.667922	0.240754	1.484081				
C	2.138527	0.192475	1.293122				
C	2.924840	1.115671	0.700042				
C	1.508319	-0.502283	4.361659				
C	-1.419428	0.207606	3.851838				
C	0.737059	2.395891	3.636817				
C	5.369612	-0.528730	1.564463				
C	5.460100	1.042238	-1.084333				
C	5.472044	2.552468	1.577582				
C	0.171521	-1.382836	-1.463711				

H	-2.239135	2.735365	-1.885405	C	-0.729311	-4.797472	-0.139834
H	-4.006290	2.742380	-2.078253	C	-3.079265	-4.894275	-2.121451
H	-3.116128	4.282490	-1.957461	C	-3.553496	-3.951112	0.751756
H	-5.204065	4.926212	0.410906	C	1.318743	0.794805	-4.251315
H	-5.890158	3.288378	0.259093	C	0.180340	-2.058131	-4.434566
H	-5.256630	3.848819	1.826558	C	2.568978	-1.479940	-2.578107
H	1.398402	-1.568256	4.103300	H	3.757536	-1.742988	0.357211
H	2.562818	-0.222935	4.214319	H	3.099223	0.822633	1.904946
H	1.277424	-0.394037	5.433502	H	1.391406	-1.390918	0.585288
H	-2.134150	0.756930	3.223102	H	5.360778	2.082032	1.638076
H	-1.650140	-0.867715	3.788227	H	6.896428	1.542558	2.356469
H	-1.571368	0.516492	4.898632	H	5.358728	1.160060	3.165054
H	0.690225	2.643066	4.709441	H	6.154321	0.668029	-1.037549
H	1.748056	2.635315	3.271480	H	6.547942	-1.067618	-1.054294
H	0.020193	3.040854	3.105365	H	7.687331	0.093213	-0.328520
H	5.005464	-1.436215	1.058684	H	7.683629	-1.494592	2.335957
H	6.470359	-0.571675	1.579869	H	6.564044	-2.686165	1.630573
H	5.019456	-0.552947	2.608604	H	6.146166	-1.873655	3.157956
H	5.062141	0.201926	-1.673944	H	1.101414	-1.842126	4.856778
H	5.195691	1.975400	-1.605642	H	2.555923	-1.094187	4.141867
H	6.559275	0.961747	-1.081218	H	1.896882	-2.589284	3.445619
H	5.126597	3.480432	1.094382	H	-1.662908	-1.604254	3.381218
H	6.573976	2.559643	1.572575	H	-0.842415	-2.596414	2.151827
H	5.133843	2.572825	2.625578	H	-1.681750	-1.096040	1.673426
Bi	-0.285799	-1.719158	0.778482	H	-0.604950	1.595335	3.033297
Si	0.351473	0.579734	3.335523	H	1.098794	1.684397	3.564223
Si	4.795335	1.035400	0.682285	H	-0.122464	0.914495	4.602262
Si	1.481593	-2.626970	-2.048552	H	-2.711457	-1.626970	-1.777912
Si	0.685975	2.553200	-3.018670	H	-2.859597	1.982047	2.370561
Si	-3.553258	-1.989456	-0.512236	H	0.105805	-2.265349	-0.758259
Si	-3.389407	3.206486	0.290700	H	-1.100339	0.142546	-2.284016
				H	-0.008274	-4.852257	-0.970723
				H	-0.945188	-5.827646	0.185479
				H	-0.240964	-4.280392	0.700529
				H	-4.002056	-4.405387	-2.472902
				H	-3.335582	-5.924842	-1.827287
				H	-2.380174	-4.943669	-2.971167
				H	-3.173477	-3.370091	1.604717
				H	-3.732993	-4.983736	1.092543
				H	-4.522997	-3.523750	0.453589
				H	1.749496	1.582297	-3.612911
				H	0.399217	1.190206	-4.711304
				H	2.037218	0.594311	-5.062261
				H	0.847510	-2.304093	-5.276013
				H	-0.766807	-1.677240	-4.848642
				H	-0.045931	-2.986298	-3.887526
				H	2.383321	-2.403587	-2.007284
				H	3.070417	-0.764404	-1.906447
				H	3.274059	-1.725825	-3.388188
				H	-2.580189	0.621236	-0.367169
				H	-0.811613	2.600519	1.227500
				H	-4.322593	-1.226053	-0.138985
				H	-5.173986	0.195566	-0.796892
				H	-6.074996	-1.041054	0.116194
				H	-4.101019	-1.598007	2.958353
				H	-5.813593	-1.203423	3.250773

97

[BiA'3], 1U/2D; APF-D/def2TZVP(Bi);

def2SVP(C,H,Si); $\Delta G^\circ = -3015.279727$ au

C	-3.139835	1.311624	1.542968
C	-2.314298	1.274398	0.476095
C	-1.107657	2.109294	0.283144
C	-5.119806	-0.495476	0.059086
C	-4.808679	-0.771396	3.117231
C	-6.125513	1.730796	1.942607
C	-1.877061	2.888684	-2.637606
C	-0.032428	4.721292	-0.986564
C	-3.005515	4.462944	-0.246306
C	3.970153	-0.819408	0.917402
C	2.907321	-0.103467	1.339376
C	1.475643	-0.429213	1.119185
C	5.846799	1.256895	2.182315
C	6.619007	-0.144502	-0.456962
C	6.619212	-1.729290	2.173873
C	1.621659	-1.628382	3.909016
C	-1.068062	-1.563326	2.455125
C	0.195129	1.054129	3.556582
C	-1.926677	-2.209796	-1.271992
C	-0.688483	-1.674899	-1.237043
C	-0.243573	-0.414265	-1.868480

H	-4.532411	-0.262067	4.054213	H	0.000000	5.141986	-0.175601
H	-7.119191	1.262866	2.032502	H	-1.711041	4.677455	-0.296327
H	-6.159597	2.447682	1.106980	H	-4.415825	-3.914256	0.997956
H	-5.937199	2.300514	2.866735	H	-4.453090	-2.570993	-0.175601
H	-0.989580	2.430639	-3.100731	H	-3.195274	-3.820532	-0.296327
H	-2.204370	3.711609	-3.292947	H	5.597758	-1.867089	0.997956
H	-2.682175	2.137572	-2.616824	H	4.453090	-2.570993	-0.175601
H	0.244406	5.072960	0.020308	H	4.906315	-0.856923	-0.296327
H	-0.284459	5.606163	-1.592823	H	-1.344390	3.269129	-2.401304
H	0.855472	4.249927	-1.436214	H	-1.409894	2.344190	-3.917213
H	-3.873364	3.790088	-0.174283	H	-2.493098	3.736009	-3.683669
H	-3.271219	5.308885	-0.900215	H	-2.158954	-2.798841	-2.401304
H	-2.807432	4.859821	0.762098	H	-1.325181	-2.393099	-3.917213
Si	-4.784601	0.430356	1.663823	H	-1.988929	-4.027091	-3.683669
Si	-1.503785	3.543323	-0.909043	H	3.503344	-0.470288	-2.401304
Si	5.758026	-0.355348	1.209494	H	2.735075	0.048909	-3.917213
Si	0.524821	-0.616974	2.752090	H	4.482027	0.291082	-3.683669
Si	-2.323008	-3.941384	-0.677854	H	-4.930533	1.897160	-4.335460
Si	0.965390	-0.788037	-3.288784	H	-3.854168	0.491532	-4.525757
Bi	0.810555	1.098482	-0.484991	H	-5.215733	0.415688	-3.384442
97				H	5.482815	2.483915	-1.646387
[BiA'3], C3; w-B97x-D/def2TZVP(Bi);				H	1.927773	-0.188429	-0.297248
def2SVP(C,H,Si); $\Delta G^\circ = -3016.370449$ au				H	1.067104	-1.343767	-2.163795
Bi	0.000000	0.000000	1.649659	H	0.630185	1.596023	-2.163795
C	1.496129	1.939318	-1.577110	H	-1.697288	-0.252255	-2.163795
C	-3.703827	-1.241434	2.775587	H	2.126068	2.495150	0.351704
C	1.276225	2.171097	-0.267992	H	-0.800703	1.763715	-0.297248
C	-3.788445	-3.222327	0.413756	H	-3.223897	0.593654	0.351704
C	-0.007907	1.965132	0.440721	H	-1.127071	-1.575286	-0.297248
C	-2.518337	0.019695	-0.267992	H	1.097830	-3.088804	0.351704
C	2.927027	-2.586891	2.775587	H	0.462610	4.662052	3.423375
C	4.684839	-1.669726	0.413756	H	1.004062	2.967824	3.425739
C	-2.427564	0.326027	-1.577110	H	1.711783	4.128665	2.276629
C	4.496212	2.420269	-1.160653	H	-4.268760	-1.930394	3.423375
C	-0.152092	-5.103968	-1.160653	H	-3.072242	-0.614369	3.425739
C	-2.025010	2.878065	-3.174661	H	-4.431421	-0.581885	2.276629
C	3.620474	0.394137	2.430644	H	3.806150	-2.731658	3.423375
C	-4.344120	2.683699	-1.160653	H	2.068180	-2.353455	3.425739
C	3.148860	3.302869	-3.793912	H	2.719638	-3.546780	2.276629
C	-1.479972	-3.192742	-3.174661	H	3.697211	1.240951	1.730251
C	-1.697901	-0.989414	0.440721	H	2.851345	0.645422	3.179096
C	-1.468904	-3.332491	2.430644	H	4.581577	0.315342	2.963156
C	1.285938	-4.378427	-3.793912	H	-0.773911	-3.822354	1.730251
C	3.504982	0.314677	-3.174661	H	-0.866720	-2.792048	3.179096
C	1.242112	-2.190792	-0.267992	H	-2.017694	-4.125433	2.963156
C	-2.151570	2.938354	2.430644	H	-2.923300	2.581404	1.730251
C	-4.434798	1.075558	-3.793912	H	-1.984625	2.146626	3.179096
C	0.776800	3.828326	2.775587	H	-2.563883	3.810091	2.963156
C	1.705808	-0.975718	0.440721	H	-4.892541	3.506299	-1.646387
C	-0.896394	4.892053	0.413756	H	0.778478	-5.421025	-0.663527
C	0.931434	-2.265345	-1.577110	H	-0.856127	-4.768647	-0.382664
H	-1.181933	5.781345	0.997956				

H	-0.590274	-5.990214	-1.646387
H	4.305507	3.384694	-0.663527
H	4.557833	1.642896	-0.382664
H	0.822277	-5.218547	-4.335460
H	1.501405	-3.583574	-4.525757
H	2.247870	-4.724802	-3.384442
H	4.108255	3.321387	-4.335460
H	2.352764	3.092041	-4.525757
H	2.967863	4.309114	-3.384442
H	-5.083985	2.036331	-0.663527
H	-3.701706	3.125751	-0.382664
Si	3.233398	-1.213848	1.521462
Si	-3.320931	1.731165	-2.423846
Si	-2.667922	-2.193281	1.521462
Si	-0.565476	3.407129	1.521462
Si	0.161232	-3.741593	-2.423846
Si	3.159698	2.010428	-2.423846

97

[BiA'3], C1; w-B97x-D/def2TZVP(Bi);

def2SVP(C,H,Si); $\Delta G^\circ = -3016.364740$ au

C	0.654066	0.389311	1.434627
C	2.134410	0.361005	1.267192
C	2.906002	1.241879	0.602163
C	1.493611	0.015670	4.379745
C	-1.459840	0.489230	3.783838
C	0.562390	2.762254	3.339241
C	5.369827	-0.270722	1.620643
C	5.443331	1.026805	-1.167457
C	5.430426	2.796387	1.328217
C	0.272850	-1.502589	-1.365891
C	0.641300	-0.126778	-1.782633
C	-0.068101	0.733348	-2.538614
C	0.964168	-4.501738	-1.600673
C	2.066292	-2.487088	-3.651591
C	3.147645	-2.484988	-0.779364
C	0.391715	3.708152	-1.709537
C	-0.274475	2.969882	-4.613394
C	2.462116	2.216268	-3.377758
C	-2.384895	-0.995948	0.662619
C	-2.573038	0.401371	0.189472
C	-3.367256	1.335728	0.745620
C	-2.795263	-3.935573	-0.330117
C	-3.522854	-1.587310	-2.191935
C	-5.186242	-2.107703	0.311104
C	-2.401077	4.249410	0.863031
C	-3.331994	3.001084	-1.818671
C	-5.368390	3.621242	0.404917
H	0.190809	1.128557	0.758907
H	2.645115	-0.458013	1.795933
H	2.392301	2.065712	0.084971
H	-0.670165	-1.810789	-1.845311
H	1.631322	0.199324	-1.436244
H	-1.060221	0.409573	-2.886607

H	-2.788901	-1.100162	1.685383
H	-2.036919	0.654172	-0.734880
H	-3.907117	1.053556	1.662290
H	0.675675	-4.694354	-0.554716
H	0.084055	-4.689834	-2.236381
H	1.734231	-5.241170	-1.872591
H	2.825474	-3.211069	-3.987914
H	1.180290	-2.595967	-4.297191
H	2.466396	-1.472823	-3.807110
H	3.986804	-3.102551	-1.136832
H	3.463020	-1.430692	-0.808332
H	2.966073	-2.748751	0.275411
H	-0.665809	3.975401	-1.572341
H	0.774595	3.351349	-0.740181
H	0.938465	4.629103	-1.969616
H	0.105344	3.945557	-4.956049
H	-0.140242	2.246257	-5.432918
H	-1.355706	3.076059	-4.430044
H	2.978238	1.852595	-2.475705
H	2.654121	1.493735	-4.186394
H	2.918573	3.178425	-3.659994
H	-3.482180	-4.616773	-0.857317
H	-1.806812	-4.034725	-0.806262
H	-2.706697	-4.292306	0.708909
H	-3.894701	-0.552123	-2.246659
H	-2.548178	-1.621016	-2.700834
H	-4.217718	-2.225618	-2.760836
H	-5.891308	-2.695646	-0.297880
H	-5.211696	-2.504747	1.338312
H	-5.547207	-1.067204	0.341127
H	-1.361689	3.926107	0.699165
H	-2.505163	5.272600	0.467410
H	-2.574147	4.287862	1.950690
H	-2.376187	2.517340	-2.070753
H	-4.134616	2.427264	-2.308523
H	-3.321945	4.012857	-2.254571
H	-5.548645	4.633584	0.009207
H	-6.105219	2.942440	-0.053042
H	-5.562137	3.646647	1.489310
H	1.445438	-1.078077	4.249529
H	2.532938	0.332297	4.201575
H	1.250718	0.235513	5.431606
H	-2.203866	0.938059	3.110380
H	-1.636636	-0.597986	3.822944
H	-1.630484	0.886031	4.797495
H	0.484429	3.122076	4.377551
H	1.562567	3.024912	2.959691
H	-0.183507	3.302254	2.735339
H	5.017097	-1.227764	1.205533
H	6.470811	-0.300849	1.642657
H	5.016507	-0.198812	2.661651
H	5.041953	0.136249	-1.676203
H	5.185586	1.906231	-1.778142
H	6.541931	0.940587	-1.155449
H	5.074443	3.666963	0.754341
H	6.532046	2.819660	1.325136

H	5.089287	2.918164	2.368414	H	-1.195789	0.512996	-2.145058
Bi	-0.210210	-1.643150	0.880960	H	1.047164	-1.933148	-3.033220
Si	0.289884	0.905701	3.232145	H	2.738079	-1.399140	-3.188588
Si	4.777460	1.190209	0.589532	H	1.552742	-0.980208	-4.442246
Si	1.615720	-2.750465	-1.844225	H	-2.086619	2.867876	-0.817535
Si	0.615501	2.402224	-3.054530	H	-2.686422	-1.114480	-2.353086
Si	-3.445572	-2.167057	-0.401559	H	0.131750	2.582085	1.271046
Si	-3.608260	3.054009	0.045389	H	-2.049049	0.659472	0.204513
97							
[BiA'3], 1U/2D; w-B97x-D/def2TZVP(Bi);							
def2SVP(C,H,Si); $\Delta G^\circ = -3016.370449$ au							
C	-3.113685	-1.384046	-1.375678	H	1.921032	4.122717	-0.088884
C	-2.259250	-1.874353	-0.457201	H	-2.532700	6.176120	-0.393322
C	-0.795178	-2.045530	-0.619335	H	-1.106589	7.210353	-0.134938
C	-5.442433	-1.550898	0.631236	H	-1.674851	6.128832	1.164193
C	-5.174973	0.843624	-1.287568	H	0.471080	4.305583	-2.854104
C	-5.970536	-1.913816	-2.383079	H	0.177346	6.052363	-2.677103
C	-0.766894	-4.474286	1.282142	H	-1.186255	4.943601	-2.954643
C	1.689566	-3.871376	-0.482801	H	-1.532458	-1.418858	3.418377
C	-0.916362	-4.880402	-1.770847	H	-3.087388	-1.415124	2.550321
C	4.089255	0.435440	0.243726	H	-2.997083	-0.819202	4.219245
C	3.062732	-0.142418	-0.408055	H	-4.220996	1.976278	3.526260
C	1.705696	0.426573	-0.640868	H	-4.456145	1.344552	1.877985
C	5.739625	-2.089583	-0.288703	H	-3.563792	2.863898	2.124780
C	6.089283	-0.543199	2.353906	H	-0.833123	2.808647	3.667935
C	7.106259	0.673393	-0.272486	H	0.001366	1.259928	3.950905
C	2.439002	1.847433	-3.205985	H	-1.419287	1.696224	4.926753
C	-0.488435	1.023169	-2.814996	H	-2.665070	-2.157195	0.525408
C	1.690878	-1.101145	-3.355658	H	-0.497241	-1.712263	-1.624330
C	-1.205443	3.172249	-0.233270	H	-4.926996	-0.961470	1.404984
C	-0.740091	2.287282	0.667032	H	-5.223222	-2.615502	0.810875
C	-1.293626	0.938610	0.958309	H	-6.525262	-1.403976	0.770383
C	1.255534	4.925345	0.268068	H	-4.571189	1.398073	-0.551291
C	-1.536387	6.217676	0.075071	H	-6.230090	1.128069	-1.146351
C	-0.220356	5.053594	-2.435726	H	-4.866965	1.179977	-2.290683
C	-2.461878	-0.848927	3.256473	H	-7.038894	-1.670024	-2.267929
C	-3.742907	1.859717	2.540687	H	-5.858301	-3.005621	-2.291109
C	-0.987151	1.746590	3.914750	H	-5.669801	-1.630797	-3.404451
H	3.921688	1.448113	0.641810	H	-0.376087	-3.862363	2.111237
H	3.216528	-1.154896	-0.809955	H	-0.419034	-5.507575	1.439293
H	1.665253	1.460395	-0.254306	H	-1.865996	-4.477969	1.354272
H	4.958025	-2.732432	0.146745	H	2.055044	-3.423730	-1.420666
H	6.708418	-2.592206	-0.139315	H	2.051249	-4.911316	-0.447179
H	5.559870	-2.026182	-1.373832	H	2.160892	-3.332129	0.355283
H	5.323283	-1.168022	2.839775	H	-2.015720	-4.813716	-1.772421
H	6.079566	0.442597	2.845821	H	-0.635886	-5.940061	-1.661160
H	7.073402	-1.002146	2.541318	H	-0.559606	-4.535633	-2.754551
H	8.100745	0.225541	-0.115643	Si	-4.924398	-1.016578	-1.098902
H	7.120735	1.684453	0.164993	Si	-0.194984	-3.824963	-0.391515
H	6.947494	0.779952	-1.357192	Si	5.752031	-0.381254	0.506242
H	2.262212	1.994946	-4.283524	Si	1.297048	0.530657	-2.489102
H	3.494721	1.567091	-3.065162	Si	-0.428175	4.838203	-0.574091
H	2.282300	2.814486	-2.701585	Si	-2.123438	0.911485	2.664780
H	-0.767230	0.785634	-3.854327	Bi	0.339959	-0.659255	0.836925
H	-0.618719	2.104304	-2.666284				

Section C3

Organometallic Mechanochemistry of s-Block Metal Complexes

All calculations were performed with the Gaussian 09W suite of programs.^[1] Each complex was studied with the wB97X-D functional,^[2] which is a range-separated hybrid, with 22.2–100% exact exchange. The def2TZVP basis set was used on the metal atoms; the def2SVP basis was used on all other atoms.^[3] An ultrafine grid was used for all calculations (Gaussian Keyword: Int=Ultrafine). The C₃ conformations were studied with imposed C₃ symmetry; otherwise, no symmetry was used. The nature of the stationary points was determined with analytical frequency calculations; all optimized geometries were found to be minima ($N_{\text{imag}} = 0$).

References

1. **Gaussian 09**, Revision D.01, Frisch, M. J.; Trucks, G. W.; Schlegel, H. B.; Scuseria, G. E.; Robb, M. A.; Cheeseman, J. R.; Scalmani, G.; Barone, V.; Mennucci, B.; Petersson, G. A.; Nakatsuji, H.; Caricato, M.; Li, X.; Hratchian, H. P.; Izmaylov, A. F.; Bloino, J.; Zheng, G.; Sonnenberg, J. L.; Hada, M.; Ehara, M.; Toyota, K.; Fukuda, R.; Hasegawa, J.; Ishida, M.; Nakajima, T.; Honda, Y.; Kitao, O.; Nakai, H.; Vreven, T.; Montgomery, J. A., Jr.; Peralta, J. E.; Ogliaro, F.; Bearpark, M.; Heyd, J. J.; Brothers, E.; Kudin, K. N.; Staroverov, V. N.; Kobayashi, R.; Normand, J.; Raghavachari, K.; Rendell, A.; Burant, J. C.; Iyengar, S. S.; Tomasi, J.; Cossi, M.; Rega, N.; Millam, N. J.; Klene, M.; Knox, J. E.; Cross, J. B.; Bakken, V.; Adamo, C.; Jaramillo, J.; Gomperts, R.; Stratmann, R. E.; Yazyev, O.; Austin, A. J.; Cammi, R.; Pomelli, C.; Ochterski, J. W.; Martin, R. L.; Morokuma, K.; Zakrzewski, V. G.; Voth, G. A.; Salvador, P.; Dannenberg, J. J.; Dapprich, S.; Daniels, A. D.; Farkas, Ö.; Foresman, J. B.; Ortiz, J. V.; Cioslowski, J.; Fox, D. J. Gaussian, Inc., Wallingford CT, 2009.
2. Chai, J.-D.; Head-Gordon, M., Long-range corrected hybrid density functionals with damped atom-atom dispersion corrections. *Phys Chem Chem Phys* **2008**, *10*, 6615-6620.
3. Weigend, F.; Ahlrichs, R., Balanced basis sets of split valence, triple zeta valence and quadruple zeta valence quality for H to Rn: Design and assessment of accuracy. *Phys. Chem. Chem. Phys.* **2005**, *7*, 3297-3305.

Table 18. Coordinates of Optimized Structures (Å)

98

K[MgA₃] (C₃); w-B97x-D/def2TZVP(Mg,K);
def2SVP(C,H,Si)

C	3.38653	-1.95522	2.52508
C	-1.22286	-2.19711	-0.04748
C	-0.76134	-2.71096	1.13458
C	-3.25187	-1.80066	-2.79911
C	-0.67240	-2.20551	-4.40186
C	-1.83517	-4.51457	-2.76288
C	-0.85076	-2.34619	4.20175
C	-3.38653	-1.95522	2.52508
C	-2.19052	-4.77365	2.93378
C	-1.53450	1.51824	-1.32876
C	-1.29133	2.15758	-0.04748
C	-1.96709	2.01481	1.13458
C	-2.99214	3.84659	-2.76288
C	0.06652	3.71653	-2.79911
C	-1.57382	1.68507	-4.40186
C	0.00000	3.91043	2.52508
C	-3.03884	4.28387	2.93378
C	-1.60648	1.90988	4.20175
C	2.08208	0.56980	-1.32876
C	2.51418	0.03953	-0.04748
C	2.72843	0.69614	1.13458
C	4.82731	0.66798	-2.76288
C	2.24623	0.52043	-4.40186
C	3.18535	-1.91587	-2.79911
C	5.22936	0.48978	2.93378
C	2.45724	0.43631	4.20175
C	-0.54758	-2.08803	-1.32876
H	2.35908	-2.32035	2.35719
H	-3.15761	-0.70350	-2.81560
H	-3.82977	-2.10133	-3.68768
H	-3.84636	-2.07156	-1.91202
H	-0.67136	-1.11815	-4.58044
H	0.37401	-2.55050	-4.39579
H	-1.17099	-2.66977	-5.26746
H	-2.33808	-4.81317	-1.82897
H	-2.45339	-4.85556	-3.60911
H	-0.87352	-5.05071	-2.80670
H	0.20989	-2.64777	4.17635
H	-0.89532	-1.25188	4.34321
H	-1.28904	-2.78101	5.11416
H	-4.01356	-2.30777	1.69117
H	-3.98026	-2.04281	3.44879
H	-3.18902	-0.88284	2.35719
H	-2.74977	-5.17723	2.07536
H	-1.26737	-5.36592	3.03697
H	-2.79483	-4.92536	3.84252
H	-2.97834	4.55248	-3.60911
H	-2.47860	0.94109	-1.31065
H	-0.42831	2.84581	-0.03187
H	-2.85681	1.36371	1.11016

H	2.05431	1.67599	-1.31065
H	2.67870	-1.05198	-0.03187
H	2.60941	1.79222	1.11016
H	0.42429	-2.61708	-1.31065
H	-2.25039	-1.79383	-0.03187
H	0.24740	-3.15593	1.11016
H	4.81081	1.76887	-2.80670
H	5.33737	0.38174	-1.82897
H	5.43174	0.30308	-3.60911
H	2.02179	1.59915	-4.39579
H	2.89759	0.32078	-5.26746
H	1.30403	-0.02234	-4.58044
H	2.18805	-2.38282	-2.81560
H	3.73468	-2.26601	-3.68768
H	3.71720	-2.29526	-1.91202
H	5.85850	0.20724	2.07536
H	5.28071	1.58538	3.03697
H	5.66290	0.04228	3.84252
H	1.53182	-0.14943	4.34321
H	3.05294	0.27416	5.11416
H	2.18809	1.50566	4.17635
H	4.00536	-2.32196	1.69117
H	3.75926	-2.42560	3.44879
H	0.82994	3.20319	2.35719
H	0.00819	4.62973	1.69117
H	-4.01334	3.78053	3.03697
H	-2.86807	4.88308	3.84252
H	-3.10873	4.96999	2.07536
H	-2.39798	1.14211	4.17635
H	-0.63650	1.40131	4.34321
H	-1.76390	2.50684	5.11416
H	-3.93729	3.28185	-2.80670
H	-2.99928	4.43143	-1.82897
H	0.96956	3.08632	-2.81560
H	0.09508	4.36734	-3.68768
H	0.12916	4.36682	-1.91202
H	-0.63267	1.14049	-4.58044
H	-2.39580	0.95135	-4.39579
H	-1.72660	2.34900	-5.26746
H	0.22100	4.46841	3.44879
K	0.00000	0.00000	2.00339
Mg	0.00000	0.00000	-1.62646
Si	-1.56295	-2.64703	-2.79430
Si	-1.79143	-2.95465	2.66127
Si	3.45452	-0.07410	2.66127
Si	-1.51092	2.67707	-2.79430
Si	-1.66308	3.02875	2.66127
Si	3.07387	-0.03004	-2.79430

98

K[CaA₃] (C₃); w-B97x-D/def2TZVP(Ca,K);
def2SVP(C,H,Si)

C	-1.08272	-5.11051	-3.07625
C	2.34906	0.38099	1.35205
C	2.49178	1.02119	0.06929
C	2.83277	0.47777	-1.14474

C	4.83551	1.33034	3.02095	H	-1.71727	-1.93696	-4.16607
C	2.25851	0.45575	4.39924	H	-0.00749	-1.42354	-4.22830
C	2.31655	3.07950	2.82827	H	-0.53213	-2.84109	-5.13030
C	4.96719	1.61759	-3.07625	H	-0.94445	-5.40967	3.91609
C	2.33006	0.56457	-4.18136	H	-1.93190	-2.00736	1.33554
C	2.35000	3.15935	-2.54964	H	0.68435	-3.02273	0.06695
C	-0.67610	-2.30017	-4.18136	H	-2.06399	-2.39134	-1.13919
C	-1.50448	1.84385	1.35205	H	2.70437	-0.66940	1.33554
C	-2.13026	1.64735	0.06929	H	2.27558	2.10402	0.06695
C	-1.83014	2.21436	-1.14474	H	3.10296	-0.59180	-1.13919
C	-3.82520	0.46644	2.82827	H	-0.77247	2.67675	1.33554
C	-1.52395	1.72806	4.39924	H	-2.95993	0.91870	0.06695
C	-3.56986	3.52250	3.02095	H	-1.03897	2.98314	-1.13919
C	-1.65396	1.73560	-4.18136	H	5.23676	0.30673	3.09121
C	-3.91108	0.45549	-2.54964	H	5.29318	1.80426	2.13809
C	-3.88447	3.49291	-3.07625	H	5.15714	1.88692	3.91609
C	-0.84458	-2.22484	1.35205	H	2.40285	-0.63787	4.37326
C	-0.36152	-2.66853	0.06929	H	2.77259	0.82624	5.30028
C	-1.00262	-2.69213	-1.14474	H	1.18742	0.66163	4.58136
C	-1.26564	-4.85284	3.02095	H	1.21986	3.12246	2.71978
C	1.50865	-3.54594	2.82827	H	2.58217	3.59907	3.76282
C	-0.73457	-2.18381	4.39924	H	2.74867	3.65592	1.99489
C	1.56108	-3.61484	-2.54964	H	5.48239	2.14107	-2.25566
Ca	0.00000	0.00000	2.13340	H	5.43805	0.62755	-3.18562
H	-3.31406	-0.50480	2.71978	H	5.14024	2.18057	-4.00766
H	-4.40797	0.43669	3.76282	H	1.23657	0.70529	-4.22830
H	-4.54046	0.55245	1.99489	H	2.72652	0.95970	-5.13030
H	-1.16670	0.69752	4.58136	H	2.53609	-0.51872	-4.16607
H	-0.64901	2.39986	4.37326	H	2.81701	3.74869	-1.74470
H	-2.10184	1.98801	5.30028	H	2.47104	3.72407	-3.48777
H	-4.20912	3.68190	2.13809	H	1.26993	3.10107	-2.33307
H	-4.21269	3.52275	3.91609	K	0.00000	0.00000	-1.71464
H	-2.88402	4.38180	3.09121	Si	-0.35242	-3.21413	2.83879
H	-0.81882	2.45567	-4.16607	Si	-0.31282	-3.43227	-2.69796
H	-1.22908	0.71826	-4.22830	Si	3.12884	1.44523	-2.69796
H	-2.19439	1.88138	-5.13030	Si	-2.60731	1.91227	2.83879
H	-4.65496	0.56526	-1.74470	Si	-2.81602	1.98704	-2.69796
H	-4.46066	0.27795	-3.48777	Si	2.95973	1.30186	2.83879
H	-3.32057	-0.45075	-2.33307				
H	-4.59542	3.67736	-2.25566				
H	-3.26250	4.39572	-3.18562				
H	-4.45855	3.36129	-4.00766				
H	-2.35274	-4.68854	3.09121				
H	-1.08406	-5.48616	2.13809				
H	2.09420	-2.61766	2.71978				
H	1.82580	-4.03576	3.76282				
H	1.79179	-4.20838	1.99489				
H	-0.02072	-1.35915	4.58136				
H	-1.75383	-1.76199	4.37326				
H	-0.67075	-2.81425	5.30028				
H	1.98962	-4.00202	-3.48777				
H	2.05064	-2.65032	-2.33307				
H	1.83795	-4.31394	-1.74470				
H	-2.17555	-5.02327	-3.18562				
H	-0.68169	-5.54186	-4.00766				
H	-0.88698	-5.81842	-2.25566				
				98			
				K[CaA ₃](C ₁); w-B97x-D/def2TZVP(Ca,K);			
				def2SVP(C,H,Si)			
				C	-1.37246	-4.21982	1.54231
				C	-3.48535	-1.99246	-1.75472
				C	-3.13702	-0.72796	-4.45368
				C	-3.78016	1.08788	-2.11952
				C	-0.99125	-0.20798	-2.23486
				C	-0.33859	1.03735	-2.30163
				C	1.02922	1.29718	-2.17807
				C	4.56333	0.18259	3.62733
				C	3.18379	2.39285	2.07229
				C	5.29632	0.61855	0.67818
				C	2.56079	-0.54766	1.39873
				C	2.62309	-1.37952	0.27017
				C	1.65267	-2.28631	-0.17761
				C	2.49604	-2.37283	-3.13745

C	0.10765	-4.04401	-2.14991	H	-3.45842	1.55998	-1.17591
C	2.95045	-4.83605	-1.38784	H	-4.86298	0.87361	-2.07681
C	-3.19261	2.91842	3.29020	H	5.32008	0.90740	3.96943
C	-2.49473	4.18875	0.58915	H	5.02833	-0.81579	3.60713
C	-1.61847	1.35269	1.19241	H	3.75749	0.15882	4.37921
C	-1.48917	0.16205	1.92807	H	-0.52539	4.73313	3.19829
C	-1.47939	-1.16235	1.47207	H	0.48821	3.88650	2.00215
C	-3.05097	-2.68892	3.59421	H	0.05922	3.08332	3.52591
C	0.00139	-2.60428	3.78642	H	2.71358	2.72392	1.13156
C	-0.31986	3.75353	2.73758	H	3.96221	3.12758	2.33530
C	3.60091	2.93843	-1.91938	H	2.41232	2.43186	2.85825
C	0.86037	4.27464	-1.42624	H	4.95009	0.83122	-0.34477
C	1.70405	3.49848	-4.24520	H	2.14384	4.49705	-4.40252
Ca	0.45203	0.01525	0.01593	H	2.24548	2.78313	-4.88477
H	5.79069	-0.36603	0.66927	H	-0.18101	4.36487	-1.77606
H	6.05479	1.37468	0.93658	H	0.83694	4.01934	-0.35468
H	1.78648	-1.59958	-3.47314	H	1.32745	5.26716	-1.52973
H	2.70603	-3.03273	-3.99466	H	3.72049	2.75207	-0.84193
H	3.43900	-1.86779	-2.87075	H	4.14365	2.14528	-2.45900
H	-0.60076	-3.23876	-2.39862	H	-1.35756	0.28882	3.01588
H	-0.32715	-4.63042	-1.32480	H	0.65900	3.52782	-4.59399
H	0.18482	-4.70760	-3.02630	K	-4.16159	-0.12823	0.87459
H	3.02811	-5.47931	-2.27979	Si	-1.44259	-2.65055	2.57979
H	2.58409	-5.45379	-0.55202	Si	1.80744	-3.35674	-1.67722
H	3.96439	-4.49395	-1.12466	Si	1.78820	2.96928	-2.43161
H	-4.17241	2.62880	2.87016	Si	-2.76716	-0.45197	-2.62386
H	-3.33552	3.88245	3.80431	Si	-1.86316	3.03288	1.93713
H	-2.92069	2.17411	4.05707	Si	3.87960	0.63641	1.92440
H	-3.45004	3.83607	0.16618				
H	-1.76864	4.26179	-0.23433				
H	-2.65877	5.20512	0.98071				
H	-3.18116	-1.75138	4.16148				
H	-3.06705	-3.51766	4.32022				
H	-3.92986	-2.81990	2.93742				
H	0.02194	-1.65911	4.35295				
H	0.95826	-2.69035	3.24758				
H	-0.05579	-3.42995	4.51365				
H	-1.51494	-5.11120	2.17362				
H	-0.39897	-4.31875	1.03843				
H	-2.15355	-4.22924	0.76476				
H	4.09266	3.89654	-2.15173				
H	-1.78294	1.25372	0.10595				
H	-1.62773	-1.32658	0.38959				
H	-0.33846	-1.08930	-2.34903				
H	-0.99351	1.92569	-2.31909				
H	1.69485	0.42350	-2.30080				
H	1.80567	-0.82672	2.15744				
H	3.45550	-1.17965	-0.42369				
H	0.90020	-2.58033	0.57264				
H	-4.58612	-2.03101	-1.83558				
H	-3.18930	-2.12444	-0.70120				
H	-3.10582	-2.89091	-2.26792				
H	-2.79766	0.13528	-5.04775				
H	-4.21184	-0.87892	-4.64751				
H	-2.59723	-1.61442	-4.82331				
H	-3.65440	1.86710	-2.88808				

Section C4

Balancing Adduct Formation and Ligand Coupling with the Bulky Allyl Complexes [1,3-(SiMe₃)₂C₃H₃]₂M (M = Fe, Co, Ni)

Geometry optimization calculations were performed using the *Gaussian* 03 and 09 suites of programs.¹ The PW91PW91 functional, which employs the 1991 gradient-corrected functional of Perdew and Wang for both correlation and exchange,² was used. The triple- ζ polarized def2-TZVP basis set³ and an ultrafine grid were used for all calculations. Stationary points were characterized by the calculation of vibrational frequencies, and unless otherwise noted, all geometries were found to be minima ($N_{\text{imag}} = 0$).

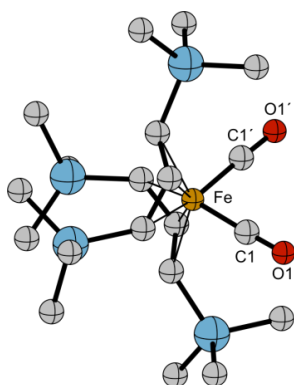
References

1. a) Frisch, M. J.; Trucks, G. W.; Schlegel, H. B.; Scuseria, G. E.; Robb, M. A.; Cheeseman, J. R.; Montgomery, Jr., J. A.; Vreven, T.; Kudin, K. N.; Burant, J. C.; Millam, J. M.; Iyengar, S. S.; Tomasi, J.; Barone, V.; Mennucci, B.; Cossi, M.; Scalmani, G.; Rega, N.; Petersson, G. A.; Nakatsuji, H.; Hada, M.; Ehara, M.; Toyota, K.; Fukuda, R.; Hasegawa, J.; Ishida, M.; Nakajima, T.; Honda, Y.; Kitao, O.; Nakai, H.; Klene, M.; Li, X.; Knox, J. E.; Hratchian, H. P.; Cross, J. B.; Bakken, V.; Adamo, C.; Jaramillo, J.; Gomperts, R.; Stratmann, R. E.; Yazyev, O.; Austin, A. J.; Cammi, R.; Pomelli, C.; Ochterski, J. W.; Ayala, P. Y.; Morokuma, K.; Voth, G. A.; Salvador, P.; Dannenberg, J. J.; Zakrzewski, V. G.; Dapprich, S.; Daniels, A. D.; Strain, M. C.; Farkas, O.; Malick, D. K.; Rabuck, A. D.; Raghavachari, K.; Foresman, J. B.; Ortiz, J. V.; Cui, Q.; Baboul, A. G.; Clifford, S.; Cioslowski, J.; Stefanov, B. B.; Liu, G.; Liashenko, A.; Piskorz, P.; Komaromi, I.; Martin, R. L.; Fox, D. J.; Keith, T.; Al-Laham, M. A.; Peng, C. Y.; Nanayakkara, A.; Challacombe, M.; Gill, P. M. W.; Johnson, B.; Chen, W.; Wong, M. W.; Gonzalez, C.; and Pople, J. A. *Gaussian 03*, Revision E.01; Gaussian, Inc., Wallingford CT, **2004**.
b) Frisch, M. J.; Trucks, G. W.; Schlegel, H. B.; Scuseria, G. E.; Robb, M. A.; Cheeseman, J. R.; Scalmani, G.; Barone, V.; Mennucci, B.; Petersson, G. A.; Nakatsuji, H.; Caricato, M.; Li, X.; Hratchian, H. P.; Izmaylov, A. F.; Bloino, J.; Zheng, G.; Sonnenberg, J. L.; Hada, M.; Ehara, M.; Toyota, K.; Fukuda, R.; Hasegawa, J.; Ishida, M.; Nakajima, T.; Honda, Y.; Kitao, O.; Nakai, H.; Vreven, T.; Montgomery, J. A., Jr.; Peralta, J. E.; Ogliaro, F.; Bearpark, M.; Heyd, J. J.; Brothers, E.; Kudin, K. N.; Staroverov, V. N.; Kobayashi, R.; Normand, J.; Raghavachari, K.; Rendell, A.; Burant, J. C.; Iyengar, S. S.; Tomasi, J.; Cossi, M.; Rega, N.; Millam, N. J.; Klene, M.; Knox, J. E.; Cross, J. B.; Bakken, V.; Adamo, C.; Jaramillo, J.; Gomperts, R.; Stratmann, R. E.; Yazyev, O.; Austin, A. J.; Cammi, R.; Pomelli, C.; Ochterski, J. W.; Martin, R. L.; Morokuma, K.; Zakrzewski, V. G.; Voth, G. A.; Salvador, P.; Dannenberg, J. J.; Dapprich, S.; Daniels, A. D.; Farkas, Ö.; Foresman, J. B.; Ortiz, J. V.; Cioslowski, J.; Fox, D. J. *Gaussian 09*, Revision D.01; Gaussian, Inc., Wallingford CT, **2009**.
2. Becke, A. D., *J. Chem. Phys.* 1993, 98, 5648-5652.
3. Weigend, F.; Ahlrichs, R., *Phys. Chem. Chem. Phys.* 2005, 7, 3297-3305.

Table 19. Cartesian coordinates of optimized structures (PW91PW91/def2-TZVP)

(a) eclipsed $(C_3H_5)_2Fe(CO)_2$ (C_2); (b) eclipsed-front $A'_2Fe(CO)_2$ (C_2); (c) eclipsed-back $A'_2Fe(CO)_2$ (C_2); (d) staggered $A'_2Fe(CO)_2$ (C_1); (e) distal $(C_3H_5)Co(CO)_3$ (C_s); (f) *syn, syn* $A'Co(CO)_3$ (C_1); (g) *syn, anti* $A'Co(CO)_3$ (C_1); (h) eclipsed-front $(C_3H_5)_2NiCO$ (C_{2v}); (i) eclipsed-back $(C_3H_5)_2NiCO$ (C_2); (j) staggered $(C_3H_5)_2NiCO$ (C_s); (k) $[\eta^6-2,3,5\text{-tris(methylene)-1,6-hexanediyl}]$ -nickel carbonyl; (l) eclipsed-front A'_2NiCO (C_2); (m) eclipsed-back A'_2NiCO (C_2); (n) staggered A'_2NiCO (C_1).

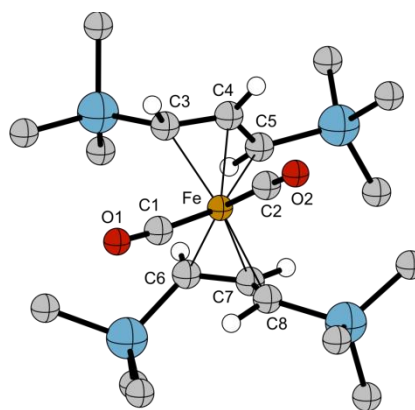
a) eclipsed $(C_3H_5)_2Fe(CO)_2$ (C_2)				H5	-2.709702	-0.004705	0.071633
C1	-0.652468	-1.119825	-1.156574	H6	2.709702	0.004705	0.071633
C1'	0.652468	1.119825	-1.156574	H7	-0.188609	-1.747734	-4.131680
C2	0.000000	-1.727659	1.372858	H8	1.472393	-2.181913	-4.565976
C2'	0.000000	1.727659	1.372858	H9	1.140890	-0.615640	-3.812455
C3	1.215032	-1.011256	1.354570	H10	-1.140890	0.615640	-3.812455
C3'	-1.215032	1.011256	1.354570	H11	0.188609	1.747734	-4.131680
C4	1.945265	-0.871844	0.154499	H12	-1.472393	2.181913	-4.565976
C4'	-1.945265	0.871844	0.154499	H13	1.351852	-4.816693	-3.088251
H1	-0.609828	-1.714340	2.275861	H14	-0.331906	-4.492056	-2.625035
H1'	0.609828	1.714340	2.275861	H15	0.870669	-4.888655	-1.381602
H2	-0.123343	-2.615601	0.754990	H16	-1.351852	4.816693	-3.088251
H2'	0.123343	2.615601	0.754990	H17	0.331906	4.492056	-2.625035
H3	1.489883	-0.403218	2.216603	H18	-0.870669	4.888655	-1.381602
H3'	-1.489883	0.403218	2.216603	H19	3.117061	-2.776305	-0.640582
H4	2.809592	-0.209210	0.140183	H20	3.291315	-1.324621	-1.647765
H4'	-2.809592	0.209210	0.140183	H21	3.575662	-2.927823	-2.348417
H5	1.968364	-1.677457	-0.577762	H22	-3.575662	2.927823	-2.348417
H5'	-1.968364	1.677457	-0.577762	H23	-3.291315	1.324621	-1.647765
Fe1	0.000000	0.000000	0.035360	H24	-3.117061	2.776305	-0.640582
O1	-1.134434	-1.811617	-1.952709	H25	-3.328039	-1.922723	3.914533
O1'	1.134434	1.811617	-1.952709	H26	-1.758973	-1.131373	3.668492
				H27	-3.254750	-0.284928	3.233151
				H28	3.328039	1.922723	3.914533
b) eclipsed-front $A'_2Fe(CO)_2$ (C_2)				H29	1.758973	1.131373	3.668492
C1	0.681615	-1.087286	1.695455	H30	3.254750	0.284928	3.233151
C2	-0.681615	1.087286	1.695455	H31	-1.754353	-4.181366	0.627552
C3	0.000000	-1.884774	-0.771534	H32	-2.380285	-4.345725	2.276149
C4	-1.145573	-1.066991	-0.864291	H33	-0.790667	-3.615486	2.016606
C5	-1.979197	-0.801540	0.261714	H34	2.380285	4.345725	2.276149
C6	0.000000	1.884774	-0.771534	H35	1.754353	4.181366	0.627552
C7	1.145573	1.066991	-0.864291	H36	0.790667	3.615486	2.016606
C8	1.979197	0.801540	0.261714	H37	-4.479514	-2.800367	-0.063800
C9	0.714960	-4.347264	-2.325016	H38	-5.043317	-1.411417	0.886764
C10	2.944369	-2.366355	-1.645076	H39	-4.984115	-3.024044	1.624214
C11	0.858301	-1.675587	-3.807129	H40	4.984115	3.024044	1.624214
C12	-4.463460	-2.343618	0.935392	H41	5.043317	1.411417	0.886764
C13	-2.760680	-1.265559	3.240045	H42	4.479514	2.800367	-0.063800
C14	-1.806131	-3.687553	1.607067	Fe1	0.000000	0.000000	0.500611
C15	-0.714960	4.347264	-2.325016	O2	-1.199671	1.748123	2.498899
C16	-2.944369	2.366355	-1.645076	O1	1.199671	-1.748123	2.498899
C17	-0.858301	1.675587	-3.807129	Si1	1.130932	-2.513122	-2.140610
C18	4.463460	2.343618	0.935392	b) eclipsed-front $A'_2Fe(CO)_2$ (C_2) (cont.)			
C19	2.760680	1.265559	3.240045	Si3	-1.130932	2.513122	-2.140610
C20	1.806131	3.687553	1.607067	Si2	-2.691697	-2.023160	1.517475
H1	-0.035402	-2.618991	0.039002	Si4	2.691697	2.023160	1.517475
H2	0.035402	2.618991	0.039002				
H3	-1.310377	-0.504400	-1.787529	c) eclipsed-back $A'_2Fe(CO)_2$ (C_2)			
H4	1.310377	0.504400	-1.787529				



C1	1.068407	0.558113	2.225245
C2	-1.068407	-0.558113	2.225245
C3	-1.563634	1.284719	0.447686
C4	-1.860212	0.120037	-0.327251
C5	-0.394018	2.041014	0.232014
C6	1.563634	-1.284719	0.447686
C7	1.860212	-0.120037	-0.327251
C8	0.394018	-2.041014	0.232014
C9	1.859324	3.966656	1.108428
C10	-0.822806	5.028266	0.074316
C11	-0.697112	3.705584	2.846884
C12	-4.153840	0.621246	-2.155228
C13	-1.435849	1.259002	-3.298555
C14	-2.319666	-1.703899	-2.782752
C15	-1.859324	-3.966656	1.108428
C16	0.822806	-5.028266	0.074316
C17	0.697112	-3.705584	2.846884
C18	4.153840	-0.621246	-2.155228
C19	1.435849	-1.259002	-3.298555
C20	2.319666	1.703899	-2.782752
Fe1	0.000000	0.000000	0.941506
H1	0.071277	1.909250	-0.749019
H2	-2.188621	1.535443	1.311265
H3	-2.631143	-0.495596	0.163536
H4	-0.071277	-1.909250	-0.749019
H5	2.188621	-1.535443	1.311265
H6	2.631143	0.495596	0.163536
H7	-2.083582	-4.968392	1.501298
H8	-2.271291	-3.910062	0.091193
H9	-2.389576	-3.236043	1.732076
H10	0.616003	-6.018640	0.504422
H11	1.913027	-4.897435	0.039657
H12	0.451991	-5.029966	-0.960062
H13	0.511679	-4.690128	3.299392
H14	0.232832	-2.951027	3.494350
H15	1.783487	-3.542052	2.856686
H16	4.257598	-1.657879	-1.806396
H17	4.771140	0.014651	-1.506056
H18	4.569546	-0.565112	-3.171994
H19	1.326688	2.168601	-2.782426
H20	2.705920	1.744204	-3.811222
H21	2.979153	2.325813	-2.160470

H22	1.508910	-2.289021	-2.922738
H23	1.921919	-1.234409	-4.284825
H24	0.377662	-1.024774	-3.446673
H25	-1.913027	4.897435	0.039657
H26	-0.451991	5.029966	-0.960062
H27	-0.616003	6.018640	0.504422
H28	-0.232832	2.951027	3.494350
H29	-1.783487	3.542052	2.856686
H30	-0.511679	4.690128	3.299392
H31	2.389576	3.236043	1.732076
H32	2.083582	4.968392	1.501298
H33	2.271291	3.910062	0.091193
H34	-2.705920	-1.744204	-3.811222
H35	-2.979153	-2.325813	-2.160470
H36	-1.326688	-2.168601	-2.782426
H37	-4.771140	-0.014651	-1.506056
H38	-4.569546	0.565112	-3.171994
H39	-4.257598	1.657879	-1.806396
H40	-1.921919	1.234409	-4.284825
H41	-0.377662	1.024774	-3.446673
H42	-1.508910	2.289021	-2.922738
O1	1.737780	0.916901	3.103752
O2	-1.737780	-0.916901	3.103752
Si1	0.000000	3.667429	1.097312
Si2	-2.339122	0.074118	-2.146334
Si3	0.000000	-3.667429	1.097312
Si4	2.339122	-0.074118	-2.146334

d) staggered $A_2Fe(CO)_2 (C_1)$



C1	0.613795	-1.342858	-1.707394
C2	-0.999228	0.600904	-2.051136
C3	1.913040	0.889995	-1.214612
C4	0.945299	1.867573	-0.829406
C5	0.378647	1.904235	0.456041
C6	0.408931	-1.198443	1.082241
C7	-0.919595	-0.682522	0.982151
C8	-1.782464	-1.101403	-0.052786
C9	4.540113	2.239647	-0.783543
C10	3.665561	0.389968	1.459857
C11	4.489580	-0.769796	-1.292033

d) staggered $A_2Fe(CO)_2 (C_1)$ (cont.)

C12	-1.761929	2.791554	2.525000	Si3	0.808233	-3.044538	1.218160
C13	-1.702183	4.093293	-0.305075	Si4	-3.632424	-0.780891	-0.257745
C14	0.523961	4.636400	1.731965				
C15	-0.382268	-4.204395	0.322423	e) distal (C₃H₅)Co(CO)₃ (C_s)			
C16	0.684496	-3.417675	3.070095	C1	0.470178	-1.076041	1.315667
C17	2.556192	-3.473072	0.659690	C1'	0.470178	-1.076041	-1.315667
C18	-4.163690	-1.612533	-1.861789	C2	-1.795025	0.123855	0.000000
C19	-4.162637	1.024265	-0.294159	C3	0.470178	1.696004	1.203118
C20	-4.480331	-1.635576	1.200320	C3'	0.470178	1.696004	-1.203118
H1	2.078032	0.886098	-2.302261	C4	1.214396	1.642063	0.000000
H2	0.548294	2.545880	-1.591590	H3A	0.969667	1.532683	2.156570
H3	0.952050	1.387077	1.232167	H3A'	0.969667	1.532683	-2.156570
H4	1.030041	-0.643911	1.797039	H3B	-0.443805	2.286175	1.249156
H5	-1.234129	0.132068	1.637699	H3B'	-0.443805	2.286175	-1.249156
H6	-1.525859	-2.069842	-0.491863	H4	2.275561	1.396743	0.000000
H7	5.582896	2.169719	-0.441837	Co1	0.012448	0.017191	0.000000
H8	4.555593	2.454025	-1.860936	O1	0.757359	-1.781340	2.182979
H9	4.076220	3.097557	-0.277419	O1'	0.757359	-1.781340	-2.182979
H10	4.719768	0.391110	1.774177	O2	-2.947699	0.120968	0.000000
H11	3.225275	-0.560152	1.781985				
H12	3.165158	1.205043	1.999549	f) syn, syn A'Co(CO)₃ (C₁)			
H13	5.523749	-0.858494	-0.930234	C1	1.389527	-1.922029	0.498769
H14	3.996629	-1.736928	-1.141285	C2	-0.422998	-1.941689	-1.580937
H15	4.532248	-0.580171	-2.373658	C3	-1.025629	-1.521212	1.299239
H16	-1.152449	2.354678	3.328904	C4	1.244629	0.651812	-0.691542
H17	-2.286382	3.660234	2.947628	C5	0.029657	1.001118	-0.057812
H18	-2.522347	2.053187	2.241540	C6	-1.205289	0.650739	-0.678480
H19	-2.399688	3.375673	-0.753188	C7	4.257013	-0.014071	-0.806170
H20	-2.292051	4.934849	0.084937	C8	3.278195	2.885721	-0.609657
H21	-1.061387	4.488059	-1.105530	C9	3.013516	1.042252	1.838692
H22	1.153271	4.234184	2.537954	C10	-4.105895	-0.358462	-0.326053
H23	1.189814	4.997585	0.936299	C12	-3.510844	2.569233	-1.028446
H24	-0.021184	5.502311	2.134518	C13	-2.865757	1.542377	1.795976
H25	-0.077417	-5.238845	0.540727	H1	1.178777	0.510875	-1.776405
H26	-1.417647	-4.088438	0.668292	H2	0.034723	1.406017	0.956548
H27	-0.361626	-4.083712	-0.768350	H3	-1.154929	0.572627	-1.770633
H28	0.917541	-4.472959	3.272533	H4	5.265493	0.326824	-0.532761
H29	1.386796	-2.803943	3.651312	H5	4.152942	-1.053812	-0.472111
H30	-0.326968	-3.216708	3.449131	H6	4.190639	-0.002417	-1.903068
H31	3.317858	-2.838181	1.130433	H7	4.276147	3.219244	-0.291163
H32	2.777238	-4.513701	0.938319	H8	3.231155	2.970635	-1.703912
H33	2.665459	-3.391562	-0.428881	H9	2.539741	3.580551	-0.187244
H34	-3.893958	-2.677821	-1.867744	H10	3.990580	1.396333	2.196754
H35	-5.252785	-1.545117	-1.992263	H11	2.246901	1.684985	2.292887
H36	-3.692334	-1.139399	-2.733440	H12	2.869261	0.022924	2.218387
H37	-3.771640	1.538623	-1.180700	H13	-5.135981	-0.068685	-0.075101
H38	-5.260339	1.073075	-0.338751	H14	-4.093363	-0.665378	-1.381025
H39	-3.846265	1.581145	0.596182	H15	-3.844530	-1.234230	0.281334
H40	-4.212623	-2.699860	1.251099	H16	-2.841828	3.430059	-0.894536
H41	-4.193583	-1.173299	2.155011	H17	-3.552280	2.339549	-2.102074
H42	-5.573864	-1.568736	1.109035	f) syn, syn A'Co(CO)₃ (C₁) (cont.)			
Fe	0.013401	-0.004241	-0.746763	H18	-4.518990	2.874763	-0.714317
O1	1.056780	-2.173151	-2.386998	H19	-2.204557	2.402555	1.969934
O2	-1.680474	0.920320	-2.937461	H20	-3.871048	1.830202	2.135188
Si1	3.604015	0.636777	-0.408614	H21	-2.528066	0.716048	2.433634
Si2	-0.677540	3.329733	1.077332	Co1	-0.017072	-1.036761	-0.078856

O1	2.292467	-2.542290	0.867654
O2	-0.722828	-2.589136	-2.488365
O3	-1.652927	-1.922517	2.184275
Si1	2.957753	1.112178	-0.041834
Si2	-2.926346	1.077085	-0.028252

g) syn, anti A'Co(CO)₃ (C_i)

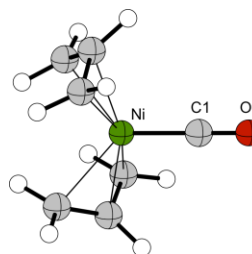
C1	0.468426	1.040054	1.733180
C2	-1.356533	2.113427	-0.274070
C3	1.207889	2.341356	-0.629014
C4	-0.891345	-0.802022	-0.069533
C5	-0.118775	-0.512861	-1.227765
C6	1.283369	-0.313177	-1.114178
C7	-3.512765	-0.305853	1.486498
C8	-3.565772	-0.438921	-1.615381
C9	-2.995947	-2.965133	0.043209
C10	1.977607	-2.212168	1.367442
C11	3.904027	0.017048	0.447985
C12	3.398582	-2.432174	-1.327736
H1	-0.352967	-1.308682	0.735136
H2	-0.622588	-0.286377	-2.170382
H3	1.731699	0.101261	-2.027856
H4	-4.572425	-0.582815	1.578299
H5	-2.999685	-0.643877	2.397448
H6	-3.452635	0.789458	1.454325
H7	-4.642428	-0.659892	-1.593416
H8	-3.455686	0.647037	-1.726820
H9	-3.152801	-0.919053	-2.513270
H10	-4.065377	-3.217589	0.074080
H11	-2.557167	-3.468321	-0.829086
H12	-2.528842	-3.385654	0.944475
H13	1.523151	-1.587482	2.146471
H14	1.256003	-2.985089	1.071241
H15	2.836479	-2.726419	1.823708
H16	3.512840	0.698091	1.214802
H17	4.772909	-0.505469	0.872333
H18	4.260693	0.627762	-0.392829
H19	2.671993	-3.172774	-1.688832
H20	3.808465	-1.909600	-2.202960
H21	4.224309	-2.977347	-0.848636
Co1	0.093771	1.116859	-0.028158
O1	0.637438	1.107417	2.874071
O2	-2.259625	2.824525	-0.398742
O3	1.949156	3.139820	-1.012372
Si1	-2.755759	-1.093244	-0.045930
Si2	2.603182	-1.223464	-0.110172

h) eclipsed-front (C₃H₅)₂NiCO (C_{2v})

C1	0.000000	0.000000	1.821704
C2	-1.217986	1.618594	-0.537817
C2'	1.217986	1.618594	-0.537817
C2'A	1.217986	-1.618594	-0.537817
C3	0.000000	1.564909	-1.251700
C3A	0.000000	-1.564909	-1.251700
C3'A	-1.217986	-1.618594	-0.537817
H1	2.156034	-1.425014	-1.055471

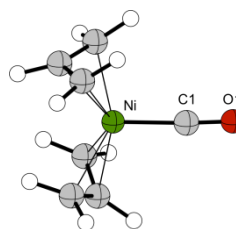
H1'	-1.295956	-2.212680	0.371731
H1A	1.295956	2.212680	0.371731
H1'A	-1.295956	2.212680	0.371731
H2	0.000000	1.272116	-2.303092
H2'	-2.156034	1.425013	-1.055471
H2A	-2.156034	-1.425013	-1.055471
H2'A	2.156034	1.425013	-1.055471
H3	0.000000	-1.272116	-2.303092
H3A	1.295956	-2.212680	0.371731
Ni	0.000000	0.000000	0.027209
O1	0.000000	0.000000	2.976308

i) eclipsed-back (C₃H₅)₂NiCO (C_{2v})



C1	1.831599	0.000000	0.000000
C2	-0.408920	0.941164	1.789695
C2'	-0.408920	-0.941164	-1.789695
C3	-0.458914	1.845760	0.688247
C3'	-0.458914	-1.845760	-0.688247
C4	-1.369006	1.646416	-0.350364
C4'	-1.369006	-1.646416	0.350364
H1	-1.327867	0.484649	2.154076
H1'	-1.327867	-0.484649	-2.154076
H2	0.381569	1.050291	2.529569
H2'	0.381569	-1.050291	-2.529569
H3	0.348305	2.568370	0.555901
H3'	0.348305	-2.568370	-0.555901
H4	-2.315035	1.136851	-0.170652
H4'	-2.315035	-1.136851	0.170652
H5	-1.303697	2.243021	-1.257697
H5'	-1.303697	-2.243021	1.257697
Ni1	0.037532	0.000000	0.000000
O1	2.987468	0.000000	0.000000

j) staggered (C₃H₅)₂NiCO (C_s)



C1	-1.765745	-0.500732	-0.000080
C2	0.062475	1.693401	-1.214631
C2'	0.062349	1.693367	1.214655

C3	0.778509	1.827661	0.000052	C12	2.660774	3.941864	-1.806048
C4	1.280220	-1.155061	-1.220901	C13	-2.660774	-3.941864	-1.806048
C4'	1.280108	-1.155100	1.220964	C14	2.683731	-2.450546	2.256885
C5	0.980431	-1.787859	0.000007	C15	-2.683731	2.450546	2.256885
H1	0.601396	1.651680	-2.159309	C16	4.754548	-1.557056	0.191090
H1'	0.601172	1.651619	2.159388	C17	-4.754548	1.557056	0.191090
H2	-0.970781	2.032893	-1.278653	C18	3.554672	0.502568	2.094083
H2'	-0.970911	2.032865	1.278579	C19	-3.554672	-0.502568	2.094083
H3	1.870033	1.835167	0.000113	H1	1.844800	1.722521	0.525557
H4	2.144381	-0.494686	-1.297298	H2	-1.844800	-1.722521	0.525557
H4'	2.144268	-0.494735	1.297463	H3	1.273614	0.162106	-2.083910
H5	0.917388	-1.577519	-2.155551	H4	-1.273614	-0.162106	-2.083910
H5'	0.917187	-1.577588	2.155566	H5	1.755237	-1.792908	-0.804737
H6	0.313837	-2.651873	-0.000038	H6	-1.755237	1.792908	-0.804737
Ni1	-0.018064	-0.001434	-0.000015	H7	-0.040145	3.694880	-3.594516
O1	-2.891533	-0.757716	-0.000029	H8	-0.883602	2.314965	-2.870210

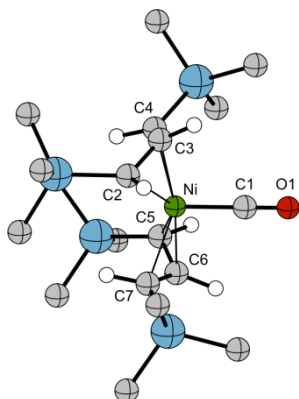
k) [η^6 -2,3,5-tris(methylene)-1,6-hexanediyl]-nickel carbonyl

C1	1.736184	0.025001	-0.004818	H9	0.690248	2.084315	-3.660427
C2	-0.633945	1.182764	1.650013	H10	0.040145	-3.694880	-3.594516
C3	-1.513817	1.284205	0.538879	H11	0.883602	-2.314965	-2.870210
C4	-0.961962	1.805970	-0.659084	H12	-0.690248	-2.084315	-3.660427
C5	-0.931045	-1.818641	0.645281	H13	-0.095131	5.315386	-0.876652
C6	-1.502236	-1.290459	-0.533927	H14	-1.010173	3.978434	-0.147988
C7	-0.639670	-1.137666	-1.650563	H15	0.495004	4.533740	0.602775
C8	-2.851110	-0.575866	-0.496798	H16	0.095131	-5.315386	-0.876652
C9	-2.801776	0.520211	0.544818	H17	1.010173	-3.978434	-0.147988
C10	-3.750393	0.728226	1.464952	H18	-0.495004	-4.533740	0.602775
H1	-1.503315	-1.821677	1.572132	H19	2.518614	4.883617	-2.355456
H2	-0.108673	-2.529028	0.584121	H20	3.222582	4.171208	-0.890014
H3	-0.998573	-0.629065	-2.543967	H21	3.283832	3.280733	-2.423545
H4	0.187345	-1.830451	-1.800885	H22	-2.518614	-4.883617	-2.355456
H5	-0.964011	0.662573	2.546717	H23	-3.222582	-4.171208	-0.890014
H6	0.168078	1.908878	1.780004	H24	-3.283832	-3.280733	-2.423545
H7	-1.544213	1.802234	-1.578774	H25	1.788739	-2.208280	2.843211
H8	-0.167803	2.548564	-0.604132	H26	2.482194	-3.378063	1.703753
H9	-4.656529	0.123072	1.491755	H27	3.502270	-2.656668	2.961297
H10	-3.655424	1.518503	2.208761	H28	-1.788739	2.208280	2.843211
H11	-3.668875	-1.279163	-0.286423	H29	-2.482194	3.378063	1.703753
H12	-3.047438	-0.149009	-1.492413	H30	-3.502270	2.656668	2.961297
Ni1	-0.045752	0.016052	-0.002926	H31	5.088350	-0.769264	-0.498056
O1	2.891781	0.035743	-0.004973	H32	4.606180	-2.474241	-0.395574

l) eclipsed-front A_2NiCO (C_2)

C1	0.000000	0.000000	2.054406	H33	5.567847	-1.746415	0.906364
C2	-1.361227	-1.566941	-0.443119	H34	-5.088350	0.769264	-0.498056
C3	-1.543490	-0.297863	-1.031936	H35	-4.606180	2.474241	-0.395574
C4	-1.860243	0.852282	-0.248976	H36	-5.567847	1.746415	0.906364
C5	1.361227	1.566941	-0.443119	H37	3.935711	1.313154	1.458695
C6	1.543490	0.297863	-1.031936	H38	2.691698	0.877882	2.658039
C7	1.860243	-0.852282	-0.248976	H39	4.342289	0.260931	2.823043
C8	0.105673	2.765202	-3.026321	H40	-3.935711	-1.313154	1.458695
C9	-0.105673	-2.765202	-3.026321	H41	-2.691698	-0.877882	2.658039
C10	0.000000	4.349483	-0.360869	H42	-4.342289	-0.260931	2.823043
C11	0.000000	-4.349483	-0.360869	Ni1	0.000000	0.000000	0.265081
				O1	0.000000	0.000000	3.211610
				Si1	-0.996532	-3.137759	-1.404446
				Si2	-3.169313	1.049705	1.093647
				Si3	3.169313	-1.049705	1.093647
				Si4	0.996532	3.137759	-1.404446

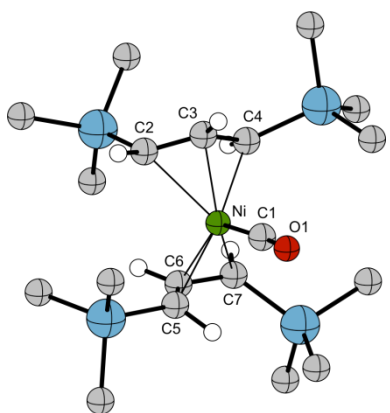
m) eclipsed-back A'_2NiCO (C_2)



C1	0.000000	0.000000	2.701845
C2	-2.023438	-0.038601	0.012550
C3	-1.637419	1.163861	0.661010
C4	-0.555105	1.959376	0.204953
C5	2.023438	0.038601	0.012550
C6	1.637419	-1.163861	0.661010
C7	0.555105	-1.959376	0.204953
C8	-4.277330	-0.913771	-1.725843
C9	-1.504790	-1.450269	-2.834925
C10	-2.576558	1.428044	-2.693406
C11	-0.597884	4.988912	-0.044640
C12	1.878089	3.646194	1.160456
C13	-0.761166	3.707919	2.749184
C14	2.576558	-1.428044	-2.693406
C15	4.277330	0.913771	-1.725843
C16	1.504790	1.450269	-2.834925
C17	0.597884	-4.988912	-0.044640
C18	-1.878089	-3.646194	1.160456
C19	0.761166	-3.707919	2.749184
H1	0.438521	-4.650341	3.214106
H2	-0.438521	4.650341	3.214106
H3	0.454969	-2.890308	3.414843
H4	-0.454969	2.890308	3.414843
H5	-2.354618	-3.523958	0.178155
H6	4.309992	1.887083	-1.216244
H7	-4.309992	-1.887083	-1.216244
H8	4.686563	1.051911	-2.736690
H9	-4.686563	-1.051911	-2.736690
H10	4.944729	0.230576	-1.182979
H11	-4.944729	-0.230576	-1.182979
H12	0.473297	1.113771	-2.995327
H13	-0.473297	-1.113771	-2.995327
H14	-2.670599	-0.666103	0.637370
H15	2.075794	-1.399464	1.635433
H16	-2.075794	1.399464	1.635433
H17	0.291001	-1.843469	-0.849774
H18	-0.291001	1.843469	-0.849774
H19	1.692479	-4.988334	-0.137372
H20	-1.692479	4.988334	-0.137372

H21	0.177892	-4.929615	-1.058474
H22	-0.177892	4.929615	-1.058474
H23	0.296032	-5.954565	0.385449
H24	-0.296032	5.954565	0.385449
H25	-2.189092	-4.620757	1.562834
H26	2.189092	4.620757	1.562834
H27	2.354618	3.523958	0.178155
H28	-2.268592	-2.864176	1.824690
H29	2.268592	2.864176	1.824690
H30	1.859024	-3.722093	2.709557
H31	-1.859024	3.722093	2.709557
H32	-3.026467	1.293380	-3.687791
H33	1.591782	-1.889057	-2.837118
H34	-1.591782	1.889057	-2.837118
H35	3.199066	-2.141507	-2.136754
H36	-3.199066	2.141507	-2.136754
H37	2.670599	0.666103	0.637370
H38	1.973565	1.556386	-3.824171
H39	-1.973565	-1.556386	-3.824171
H40	1.471966	2.448136	-2.377151
H41	-1.471966	-2.448136	-2.377151
H42	3.026467	-1.293380	-3.687791
Ni1	0.000000	0.000000	0.842523
O1	0.000000	0.000000	3.857600
Si1	-2.513312	-0.235253	-1.802167
Si2	0.000000	3.553288	1.031462
Si3	2.513312	0.235253	-1.802167
Si4	0.000000	-3.553288	1.031462

n) staggered A₂NiCO (C₁)



C1	-0.190575	0.971951	2.054752
C2	0.334054	-2.172353	0.418435
C3	-0.868866	-1.647316	0.918012
C4	-1.776960	-0.914903	0.096171
C5	1.924580	1.001375	0.211622
C6	1.258140	0.706486	-1.014794
C7	0.031347	1.326227	-1.349077
C8	1.770710	-4.503407	-0.846105
C9	0.922539	-2.300897	-2.789160
C10	-1.182335	-4.063066	-1.481518
C11	-3.634166	0.774587	2.010091
C12	-4.498971	0.087569	-0.883218
C13	-4.330063	-2.101599	1.250735
C14	3.370430	-0.374129	2.583165
C15	4.824735	1.645387	0.795907
C16	4.121047	-1.127713	-0.322358
C17	-2.316727	3.328058	-1.233663
C18	0.251494	4.108405	0.246094
C19	0.228575	3.948340	-2.800182
H1	-1.066384	-1.700811	1.993873
H2	-0.480262	0.854825	-2.199837
H3	1.613042	-0.133210	-1.611827
H4	1.736088	2.001789	0.612792
H5	3.001473	0.417052	3.250212
H6	4.339946	-0.716444	2.972044
H7	2.663784	-1.212396	2.639693
H8	4.962119	2.049055	-0.216561
H9	5.800740	1.282934	1.148659
H10	4.522549	2.475343	1.449797
H11	5.063951	-1.553651	0.048593
H12	4.301734	-0.761029	-1.342156
H13	3.388160	-1.941962	-0.377460
H14	1.324610	3.885555	-2.840254
H15	-0.051645	5.010539	-2.848745
H16	-0.167277	3.456068	-3.699126
H17	1.348039	4.163667	0.228474
H18	-0.060454	3.697893	1.214291
H19	-0.125276	5.140514	0.188951
H20	-2.762452	2.810863	-2.094462
H21	-2.592110	4.389709	-1.307747

H22	-2.773972	2.925381	-0.321225
H23	-1.653760	-1.076183	-0.981533
H24	1.030595	-2.519501	1.191097
H25	2.764560	-4.072831	-0.663921
H26	1.856976	-5.181871	-1.706639
H27	1.502754	-5.108980	0.030644
H28	-1.499542	-4.620035	-0.589673
H29	-1.078804	-4.778951	-2.309681
H30	-1.988326	-3.364993	-1.742147
H31	1.951326	-1.917692	-2.782702
H32	0.245561	-1.469696	-3.026773
H33	0.851256	-3.028037	-3.611633
H34	-3.206758	1.740543	1.712619
H35	-3.102418	0.439257	2.910755
H36	-4.684400	0.940853	2.290009
H37	-5.378962	-1.932542	1.533580
H38	-3.805500	-2.492189	2.133745
H39	-4.310410	-2.882988	0.478742
H40	-4.083477	1.012461	-1.301863
H41	-5.548824	0.280728	-0.621893
H42	-4.490423	-0.676246	-1.673609
Ni1	0.021922	0.139689	0.479022
O1	-0.222233	1.499684	3.083274
Si2	-3.536736	-0.500754	0.626505
Si1	0.463254	-3.181324	-1.181000
Si3	3.542159	0.256716	0.816209
Si4	-0.442083	3.146821	-1.220669

References

1. Evans, W. J., *Inorg. Chem.* **2007**, *46* (9), 3435-3449.
2. MacDonald, M. R.; Bates, J. E.; Fieser, M. E.; Ziller, J. W.; Furche, F.; Evans, W. J., *J. Am. Chem. Soc.* **2012**, *134* (20), 8420-8423.
3. MacDonald, M. R.; Bates, J. E.; Ziller, J. W.; Furche, F.; Evans, W. J., *J. Am. Chem. Soc.* **2013**, *135* (26), 9857-9868.
4. Liebman, J. F.; Deakyne, C. A., *J. Fluor. Chem.* **2003**, *121* (1), 1-8.
5. Grochala, W., *Chem. Soc. Rev.* **2007**, *36* (10), 1632-1655.
6. It has been suggested that this phrase, although ultimately derived from Aristotle's *De Generatione et Corruptione*, is a misinterpretation of the original Greek, which could be rendered as "liquids are the type of bodies most liable to mixing". Such a reading is of course much less problematic than the traditional phrasing, although from the modern perspective it is still incomplete, as gases (which were not clearly distinguished from 'air' in the ancient world) are not included. For a discussion of this point, see: C. Reichardt and T. Welton, *Solvents and Solvent Effects in Organic Chemistry*, Wiley-VCH, Weinheim, 2011, pp. 1-5.
7. Tanaka, K.; Kaupp, G., *Solvent-free Organic Synthesis*. 2 ed.; Wiley-VCH: Mörtenbach, 2009; p 442.
8. Boldyreva, E., *Chem. Soc. Rev.* **2013**, *42* (18), 7719-7738.
9. Friščić, T.; Julien, P. A.; Mottillo, C., Environmentally-Friendly Designs and Syntheses of Metal-Organic Frameworks (MOFs). In *Green Technologies for the Environment*, American Chemical Society: 2014; Vol. 1186, pp 161-183.
10. Themed Issue on Mechanochemistry, *Chem. Soc. Rev.*, 2013, 7487-7740.
11. Tanaka, K.; Toda, F., *Chem. Rev.* **2000**, *100* (3), 1025-1074.
12. James, S. L.; Adams, C. J.; Bolm, C.; Braga, D.; Collier, P.; Friščić, T.; Grepioni, F.; Harris, K. D. M.; Hyett, G.; Jones, W.; Krebs, A.; Mack, J.; Maini, L.; Orpen, A. G.; Parkin, I. P.; Shearouse, W. C.; Steed, J. W.; Waddell, D. C., *Chem. Soc. Rev.* **2012**, *41* (1), 413-447.
13. Hernández, J. G.; Friščić, T., *Tetrahedron Lett.* **2015**, *56* (29), 4253-4265.
14. Wang, G.-W., *Chem. Soc. Rev.* **2013**, *42* (18), 7668-7700.
15. Jobbágy, C.; Tunyogi, T.; Pálinkás, G.; Deák, A., *Inorg. Chem.* **2011**, *50* (15), 7301-7308.
16. Jobbágy, C.; Molnar, M.; Baranyai, P.; Deák, A., *Dalton Trans.* **2014**, *43* (31), 11807-11810.
17. Bowmaker, G. A.; Hanna, J. V.; Hart, R. D.; Healy, P. C.; King, S. P.; Marchetti, F.; Pettinari, C.; Skelton, B. W.; Tabacaru, A.; White, A. H., *Dalton Trans.* **2012**, *41* (25), 7513-7525.
18. Garay, A. L.; Pichon, A.; James, S. L., *Chem. Soc. Rev.* **2007**, *36* (6), 846-855.

19. Singh, N. K.; Hardi, M.; Balema, V. P., *Chem. Commun.* **2013**, 49 (10), 972-974.
20. Bisht, K. K.; Chaudhari, J.; Suresh, E., *Polyhedron* **2015**, 87 (0), 71-78.
21. Takacs, L., *Chem. Soc. Rev.* **2013**, 42 (18), 7649-7659.
22. Caley, E. R.; Richards, J. F. C., *Theophrastus on Stones*, Ohio State University Press: Columbus, OH, 1956; pp 204-205.
23. Faraday, M., *Quarterly Journal of Science, Literature and the Arts* **1820**, 8, 374-375.
24. Takacs, L., *J. Therm. Anal. Calorim.* **2007**, 90 (1), 81-84.
25. "Den man kann nicht annehmen, dass durch den mechanischen Eingriff selbst chemische Veränderungen zu Stande kommen." From *Graham-Otto's ausführliches Lehrbuch der Chemie, Physikalischen und Theoretische Chemie*, A. Horstman, 5th ed. Friedrich Vieweg und Sohn, Braunschweig, 1885, pp 350-351.
26. Lea, M. C., *Amer J. Sci.* **1892**, 43 (3), 527-31.
27. Lea, M. C., *Amer. J. Sci.* **1893**, 46 (3), 241-244.
28. Ostwald, W., *Handbuch der Allgemeinen Chemie, Band I*. Akademische Verlagsgesellschaft mbH: Leipzig, 1919; Vol. 70.
29. Takacs, L., *Bull. Hist. Chem.* **2003**, 28 (1), 26-34.
30. Vaska, L., *J. Am. Chem. Soc.* **1966**, 88 (22), 5325-5327.
31. Coville, N. J.; Cheng, L., *J. Organomet. Chem.* **1998**, 571 (2), 149-169.
32. Borisov, A. P.; Makhaev, V. D.; Usyatinskii, A. Y.; Bregadze, V. I., *Izv. Akad. Nauk, Ser. Khim.* **1993**, (10), 1715-1717.
33. Egbert, J. D.; Slawin, A. M. Z.; Nolan, S. P., *Organometallics* **2013**, 32 (7), 2271-2274.
34. Hernández, J. G.; Bolm, C., *Chem. Commun.* **2015**, 51 (63), 12582-12584.
35. Hernández, J. G.; Macdonald, N. A. J.; Mottillo, C.; Butler, I. S.; Friščić, T., *Green Chem.* **2014**, 16 (3), 1087-1092.
36. Makhaev, V. D.; Borisov, A. P.; Petrova, L. A., *J. Organomet. Chem.* **1999**, 590 (2), 222-226.
37. Rightmire, N. R.; Bruns, D. L.; Hanusa, T. P.; Brennessel, W. W., submitted for publication.
38. Rightmire, N. R.; Hanusa, T. P.; Rheingold, A. L., *Organometallics* **2014**, 33 (21), 5952-5955.
39. Wong, C.-H.; Zimmerman, S. C., *Chem. Commun.* **2013**, 49 (17), 1679-1695.
40. Lewiński, J.; Dutkiewicz, M.; Lesiuk, M.; Śliwiński, W.; Zelga, K.; Justyniak, I.; Lipkowski, J., *Angew. Chem. Int. Ed.* **2010**, 49 (44), 8266-8269.
41. Borisov, A. P.; Makhaev, V. D., Mechanosynthesis of cyclopentadienyl metal complexes. In *Mechanochemical Synthesis in Inorganic Chemistry*, Nauka, Siberian Branch: Novosibirsk, 1991; pp 165-168.

42. Borisov, A.; Petrova, L.; Makhaev, V. In *Mechanochemical synthesis of organometallic compounds*, 1st Int. Conf. Mechanochem., Košice (Slovakia), Cambridge Intersci. Publ.: Košice (Slovakia), 1993; pp 60-62.
43. Paneque, A.; Fernandez-Bertran, J.; Reguera, E.; Yee-Madeira, H., *Transition Met. Chem. (Dordrecht, Neth.)* **2001**, 26 (1-2), 76-80.
44. Mostafa, M. M.; Gomaa, E. A. H.; Mostafa, M. A.; El-Dossouki, F. I., *Spectrochim. Acta A* **1999**, 55 (14), 2869-2875.
45. Nichols, P. J.; Raston, C. L.; Steed, J. W., *Chem. Commun.* **2001**, (12), 1062-1063.
46. Orsa, D.; Ho, D. M.; Takacs, L.; Mandal, S. K. In *Mechanochemical synthesis of organometallic compounds*, American Chemical Society: 2000; pp INOR-234.
47. Borisov, A. P.; Petrova, L. A.; Karpova, T. P.; Makhaev, V. D., *Zh. Neorg. Khim.* **1996**, 41 (3), 411-416.
48. Bala, M. D.; Budhai, A.; Coville, N. J., *Organometallics* **2004**, 23 (9), 2048-2052.
49. Bala, M. D.; Coville, N. J., *J. Organomet. Chem.* **2007**, 692 (4), 709-730.
50. Balema, V. P.; Wiench, J. W.; Pruski, M.; Pecharsky, V. K., *Chem. Commun.* **2002**, (15), 1606-1607.
51. McNaught, A. A.; Wilkinson, A., *IUPAC Compendium of Chemical Technology (the Gold Book)*. 2nd ed.; Blackwell Scientific: Oxford, 1997.
52. Cravotto, G.; Gaudino, E. C.; Cintas, P., *Chem. Soc. Rev.* **2013**, 42 (18), 7521-7534.
53. Zink, J., *Naturwissenschaften* **1981**, 68 (10), 507-512.
54. Takacs, L., *Acta Phys. Pol. A* **2014**, 126 (4), 1040-1043.
55. Cinčić, D.; Juribašić, M.; Babić, D.; Molčanov, K.; Šket, P.; Plavec, J.; Čurić, M., *Chem. Commun.* **2011**, 47 (41), 11543-11545.
56. Katsenis, A. D.; Puškarić, A.; Štrukil, V.; Mottillo, C.; Julien, P. A.; Užarević, K.; Pham, M.-H.; Do, T.-O.; Kimber, S. A. J.; Lazić, P.; Magdysyuk, O.; Dinnebier, R. E.; Halasz, I.; Friščić, T., *Nature Commun.* **2015**, 6.
57. Nagarathinam, M.; Chanthapally, A.; Lapidus, S. H.; Stephens, P. W.; Vittal, J. J., *Chem. Commun.* **2012**, 48 (20), 2585-2587.
58. Friščić, T., Metal-Organic Frameworks: Mechanochemical Synthesis Strategies. In *Encyclopedia of Inorganic and Bioinorganic Chemistry*, Wiley: Chichester, 2014; pp 1-19.
59. Use of flasks that have been cleaned in alcoholic base baths should be avoided. Their surfaces have been compromised by exposure to the alkaline environment, and the flasks are much more likely to crack if subsequently used for mechanochemical synthesis with ball bearings.
60. Lu, S.-Y.; Mao, Q.-J.; Peng, Z.; Li, X.-D.; Yan, J.-H., *Chinese Physics B* **2012**, 21 (7), 078201.
61. Hernández, J. G.; Friščić, T., *Tetrahedron Lett.* **2015**, 56 (29), 4253-4265.

62. Rak, M. J.; Saade, N. K.; Friščić, T.; Moores, A., *Green Chemistry* **2014**, *16* (1), 86-89.
63. Gomes, C. S. B.; Gomes, P. T.; Duarte, M. T., *J. Organomet. Chem.* **2014**, *760*, 101-107.
64. White, R. E.; Hanusa, T. P.; Kucera, B. E., *J. Am. Chem. Soc.* **2006**, *128* (30), 9622-9623.
65. White, R. E.; Hanusa, T. P.; Kucera, B. E., *J. Organomet. Chem.* **2007**, *692*, 3479-3485.
66. White, R. E.; Hanusa, T. P., *Organometallics* **2006**, *25*, 5621-5630.
67. Gren, C. K.; Hanusa, T. P.; Brennessel, W. W., *Polyhedron* **2006**, *25*, 286-292.
68. Rightmire, N. R.; Hanusa, T. P., unpublished results.
69. Blanco, M. C.; Cámara, J.; Gimeno, M. C.; Laguna, A.; James, S. L.; Lagunas, M. C.; Villacampa, M. D., *Angew. Chem. Int. Ed.* **2012**, *51* (39), 9777-9779.
70. Quisenberry, K. T.; Smith, J. D.; Voehler, M.; Stec, D. F.; Hanusa, T. P.; Brennessel, W. W., *J. Am. Chem. Soc.* **2005**, *127*, 4376-4387.
71. Henc, B.; Jolly, P. W.; Salz, R.; Stobbe, S.; Wilke, G.; Benn, R.; Mynott, R.; Seevogel, K.; Goddard, R.; Krueger, C., *J. Organomet. Chem.* **1980**, *191* (2), 449-75.
72. Carlson, C. N.; Smith, J. D.; Hanusa, T. P.; Brennessel, W. W.; Young Jr, V. G., *J. Organomet. Chem.* **2003**, *683* (1), 191-199.
73. Engerer, L. K.; Carlson, C. N.; Hanusa, T. P.; Brennessel, W. W.; Young, J. V. G., *Organometallics* **2012**, *31* (17), 6131-6138.
74. Smith, J. D.; Hanusa, T. P.; Young, V. G., Jr., *J. Am. Chem. Soc.* **2001**, *123*, 6455-6456.
75. Smith, J. D.; Quisenberry, K. T.; Hanusa, T. P.; Brennessel, W. W., *Acta Crystallogr., Sect. C.* **2004**, *60*, m507-m508.
76. Grignard, V.; Jenkins, R. L., *Bull. Soc. Chim. Fr.* **1925**, *37*, 1376-85.
77. Lichtenberg, C.; Spaniol, T. P.; Okuda, J., *Organometallics* **2011**, *30* (16), 4409-4417.
78. Lichtenberg, C.; Robert, D.; Spaniol, T. P.; Okuda, J., *Organometallics* **2010**, *29* (21), 5714-5721.
79. Peters, D. W.; Blair, R. G., *Faraday Discuss.* **2014**, *170* (0), 83-91.
80. Belenguer, A. M.; Friscic, T.; Day, G. M.; Sanders, J. K. M., *Chem. Sci.* **2011**, *2* (4), 696-700.
81. Strukil, V.; Margetic, D.; Igrc, M. D.; Eckert-Maksic, M.; Friščić, T., *Chem. Commun.* **2012**, *48* (78), 9705-9707.
82. Štrukil, V.; Igrc, M. D.; Eckert-Maksić, M.; Friščić, T., *Chem.—Eur. J* **2012**, *18* (27), 8464-8473.
83. Bowmaker, G. A.; Chaichit, N.; Pakawatchai, C.; Skelton, B. W.; White, A. H., *Dalton Trans.* **2008**, (22), 2926-2928.
84. Chmely, S. C.; Hanusa, T. P.; Brennessel, W. W., *Angew. Chem. Int. Ed.* **2010**, *49* (34), 5870-5874.

85. Layfield, R. A.; Garcia, F.; Hannauer, J.; Humphrey, S. M., *Chem. Commun.* **2007**, (47), 5081-5083.
86. Gren, C. K.; Hanusa, T. P.; Rheingold, A. L., *Organometallics* **2007**, *26*, 1643–1649.
87. Tanaka, K.; Asakura, A.; Muraoka, T.; Kalicki, P.; Urbanczyk-Lipkowska, Z., *New J. Chem.* **2013**, *37* (9), 2851-2855.
88. Tan, Y.-J.; Zhang, Z.; Wang, F.-J.; Wu, H.-H.; Li, Q.-H., *RSC Adv.* **2014**, *4* (67), 35635-35638.
89. Chow, E. H. H.; Strobridge, F. C.; Frišćić, T., *Chem. Commun.* **2010**, *46* (34), 6368-6370.
90. Yu, J.; Li, Z.; Jia, K.; Jiang, Z.; Liu, M.; Su, W., *Tetrahedron Lett.* **2013**, *54*, 2006.
91. Sharma, H.; Singh, N.; Jang, D. O., *Green Chem.* **2014**, *16*, 4922.
92. Tan, D.; Štrukil, V.; Mottillo, C.; Frišćić, T., *Chem. Commun.* **2014**, *50*, 5248.
93. Chen, L.; Lemma, B. E.; Rich, J. S.; Mack, J., *Green Chem.* **2014**, *16*, 1101.
94. Cook, T. L.; Walker, J. A.; Mack, J., *Green Chem.* **2013**, *15*, 617.
95. Fulmer, D. A.; Shearouse, W. C.; Medonza, S. T.; Mack, J., *Green Chem.* **2009**, *11*, 1821.
96. Schneider, F.; Stolle, A.; Ondruschka, B.; Hopf, H., *Org. Process Res. Dev.* **2009**, *13*, 44.
97. Do, J.-L.; Mottillo, C.; Tan, D.; Štrukil, V.; Frišćić, T., *J. Am. Chem. Soc.* **2015**, *137* (7), 2476-2479.
98. Oakley, G. W.; Wagener, K. B., *Macromol. Chem. Phys.* **2005**, *206* (1), 15-24.
99. Bala, M. D.; Coville, N. J., *J. Organomet. Chem.* **2007**, *692* (4), 709-730.
100. Murugavel, R.; Gogoi, N., *J. Organomet. Chem.* **2008**, *693* (19), 3111-3116.
101. Hernandez, J. G.; Butler, I. S.; Frišćić, T., *Chem. Sci.* **2014**, *5* (9), 3576-3582.
102. Rainier, J. D.; Cox, J. M., *Organic Letters* **2000**, *2* (17), 2707-2709.
103. Majumder, U.; Cox, J. M.; Johnson, H. W. B.; Rainier, J. D., *Chem.–Eur. J.* **2006**, *12* (6), 1736-1746.
104. Picotin, G.; Miginiac, P., *J. Org. Chem.* **1985**, *50* (8), 1299-1301.
105. Shen, K.-H.; Yao, C.-F., *J. Org. Chem.* **2006**, *71* (10), 3980-3983.
106. Shen, K. H.; Liu, J. T.; Wu, Y. R.; Yao, C. F., *Synth. Commun.* **2007**, *37* (20), 3677-3687.
107. Shen, K.-H.; Kuo, C.-W.; Yao, C.-F., *Tetrahedron Lett.* **2007**, *48* (36), 6348-6351.
108. Kulkarni, N. A.; Yao, C.-F.; Chen, K., *Tetrahedron* **2007**, *63* (33), 7816-7822.
109. Solomon, S. A.; Layfield, R. A., *Dalton Trans.* **2010**, *39* (10), 2469-2483.
110. Chmely, S. C.; Hanusa, T. P., *Eur. J. Inorg. Chem.* **2010**, 1321-1337.

111. Perrin, D. D.; Armarego, W. L. F., *Purification of Laboratory Chemicals*. 3rd ed.; Pergamon: Oxford, 1988.
112. Fraenkel, G.; Chow, A.; Winchester, W. R., *J. Am. Chem. Soc.* **1990**, *112* (4), 1382-1386.
113. Rightmire, N. R.; Quisenberry, K. T.; Hanusa, T. P., *Organometallics* **2014**, *33* (20), 5678-5685.
114. Kim, D. Y.; Yang, Y.; Abelson, J. R.; Girolami, G. S., *Inorg. Chem.* **2007**, *46* (22), 9060-9066.
115. IKA Ultra-Turrax Tube Drive, which provides a range of 300-4000 oscillations per minute.
116. Tang, J. A.; Masuda, J. D.; Boyle, T. J.; Schurko, R. W., *ChemPhysChem* **2006**, *7* (1), 117-130.
117. Cowley, A. R.; Downs, A. J.; Marchant, S.; Macrae, V. A.; Taylor, R. A.; Parsons, S., *Organometallics* **2005**, *24* (23), 5702-5709.
118. Rahman, A. F. M. M.; Siddiqui, K. F.; Oliver, J. P., *Organometallics* **1982**, *1* (6), 881-883.
119. Jochmann, P.; Spaniol, T. P.; Chmely, S. C.; Hanusa, T. P.; Okuda, J., *Organometallics* **2011**, *30* (19), 5291-5296.
120. Alberti, D.; Goddard, R.; Ruffínska, A.; Pörschke, K.-R., *Organometallics* **2003**, *22* (20), 4025-4029.
121. Layfield, R. A.; Buehl, M.; Rawson, J. M., *Organometallics* **2006**, *25* (15), 3570-3575.
122. Standfuss, S.; Abinet, E.; Spaniol, T. P.; Okuda, J., *Chem. Commun.* **2011**, *47* (41), 11441-11443.
123. Erker, G.; Berg, K.; Angermund, K.; Krueger, C., *Organometallics* **1987**, *6* (12), 2620-1.
124. John, K. D.; Salazar, K. V.; Scott, B. L.; Baker, R. T.; Sattelberger, A. P., *Organometallics* **2001**, *20* (2), 296-304.
125. Antonelli, D. M.; Leins, A.; Stryker, J. M., *Organometallics* **1997**, *16* (12), 2500-2502.
126. Yue, N.; Hollink, E.; Guérin, F.; Stephan, D. W., *Organometallics* **2001**, *20* (21), 4424-4433.
127. Wielstra, Y.; Duchateau, R.; Gambarotta, S.; Bensimon, C.; Gabe, E., *J. Organomet. Chem.* **1991**, *418* (2), 183-190.
128. John, K. D.; Salazar, K. V.; Scott, B. L.; Baker, R. T.; Sattelberger, A. P., *Chem. Commun.* **2000**, (7), 581-582.
129. Webster, C. L.; Ziller, J. W.; Evans, W. J., *Organometallics* **2012**, *31* (20), 7191-7197.
130. Langeslay, R. R.; Walensky, J. R.; Ziller, J. W.; Evans, W. J., *Inorg. Chem.* **2014**, *53* (16), 8455-8463.
131. Pu, M. P.; Li, Q.-s.; Xie, Y.; King, R. B.; Schaefer, H. F., *J. Phys. Chem. A* **2011**, *115* (17), 4491-4504.

132. Calculation of the complete A_3Al molecule at the M06-L/def2TZVP level leaves the allyl ligands σ -bonded (Al–C bond lengths average to 1.958 Å).
133. Lichtenberg, C.; Robert, D.; Spaniol, T. P.; Okuda, J., *Organometallics* **2010**, *29* (21), 5714-5721.
134. Amemiya, F.; Fuse, K.; Fuchigami, T.; Atobe, M., *Chem. Commun.* **2010**, *46* (16), 2730-2732.
135. Fischbach, A.; Anwander, R., Rare-Earth Metals and Aluminum Getting Close in Ziegler-Type Organometallics. In *Neodymium Based Ziegler Catalysts – Fundamental Chemistry*, Nuyken, O., Ed. Springer Berlin Heidelberg: 2006; Vol. 204, pp 155-281.
136. The 1H NMR spectrum displays a singlet for the $SiMe_3$ groups (δ 0.23 in C_6D_6), a triplet for the central hydrogen atom on the allyl ligands (δ 7.60, $J = 16$ Hz), and a doublet for the terminal hydrogens (δ 3.83, $J = 16$ Hz).
137. Shannon, R. D., *Acta Crystallogr., Sect A* **1976**, *32*, 751-767.
138. Quisenberry, K. T.; Smith, J. D.; Voehler, M.; Stec, D. F.; Hanusa, T. P.; Brennessel, W. W., *J. Am. Chem. Soc.* **2005**, *127* (12), 4376-4387.
139. Lichtenberg, C.; Okuda, J., *Angew. Chem. Int. Ed.* **2013**, *52* (20), 5228-5246.
140. Chmely, S. C.; Carlson, C. N.; Hanusa, T. P.; Rheingold, A. L., *J. Am. Chem. Soc.* **2009**, *131* (18), 6344-6345.
141. Lichtenberg, C.; Spaniol, T. P.; Peckermann, I.; Hanusa, T. P.; Okuda, J., *J. Am. Chem. Soc.* **2013**, *135* (2), 811-821.
142. Sulway, S. A.; Girshfeld, R.; Solomon, S. A.; Muryn, C. A.; Poater, J.; Sola, M.; Bickelhaupt, F. M.; Layfield, R. A., *Eur. J. Inorg. Chem.* **2009**, (27), 4157-4167.
143. Reich, H. J., *Chem. Rev.* **2013**, *113* (9), 7130-7178.
144. Waddell, D. C.; Thiel, I.; Clark, T. D.; Marcum, S. T.; Mack, J., *Green Chemistry* **2010**, *12* (2), 209-211.
145. Naimi-Jamal, M. R.; Mokhtari, J.; Dekamin, M. G.; Kaupp, G., *Eur. J. Org. Chem.* **2009**, *2009* (21), 3567-3572.
146. Szuppa, T.; Stolle, A.; Ondruschka, B.; Hopfe, W., *Green Chemistry* **2010**, *12* (7), 1288-1294.
147. Harvey, M. J.; Hanusa, T. P.; Young, V. G., Jr., *Angew. Chem. Int. Ed.* **1999**, *38*, 217-219.
148. Carlson, C. N.; Smith, J. D.; Hanusa, T. P.; Brennessel, W. W.; Young, V. G., Jr., *J. Organomet. Chem.* **2003**, *683*, 191-199.
149. Carlson, C. N.; Hanusa, T. P.; Brennessel, W. W., *J. Am. Chem. Soc.* **2004**, *126*, 10550-10551.
150. Simpson, C. K.; White, R. E.; Carlson, C. N.; Wroblewski, D. A.; Kuehl, C. J.; Croce, T. A.; Steele, I. M.; Scott, B. L.; Hanusa, T. P.; Sattelberger, A. P.; John, K. D., *Organometallics* **2005**, *24*, 3685-3691.

151. Chmely, S. C.; Hanusa, T. P.; Rheingold, A. L., *Organometallics* **2010**, 29 (21), 5551-5557.
152. Boyde, N. C.; Chmely, S. C.; Hanusa, T. P.; Rheingold, A. L.; Brennessel, W. W., *Inorg. Chem.* **2014**, 53 (18), 9703-9714.
153. CCDC 1410602 (1) and CCDC 1410601 (2) contain the supplementary crystallographic data for these compounds. These data can be obtained free of charge from The Cambridge Crystallographic Data Centre via www.ccdc.cam.ac.uk/data_request/cif.
154. Akiba, K.-y.; Fujishima, H.; Ohtani, A.; Kojima, S.; Yamamoto, Y., *Bull. Soc. Chim. Belg.* **1997**, 106 (9-10), 577-584.
155. Phadnis, P. P.; Jain, V. K.; Klein, A.; Schurr, T.; Kaim, W., *New J. Chem.* **2003**, 27 (11), 1584-1591.
156. Pazik, J. C.; George, C., *Organometallics* **1989**, 8 (2), 482-487.
157. Sasaki, S.; Sutoh, K.; Murakami, F.; Yoshifuji, M., *J. Am. Chem. Soc.* **2002**, 124 (50), 14830-14831.
158. Sobolev, A. N.; Belsky, V. K., *J. Organomet. Chem.* **1981**, 214 (1), 41-46.
159. Sobolev, A. N.; Romm, I. P.; Chernikova, N. Y.; Belsky, V. K.; Guryanova, E. N., *J. Organomet. Chem.* **1981**, 219 (1), 35-42.
160. Hendershot, D. G.; Pazik, J. C.; George, C.; Berry, A. D., *Organometallics* **1992**, 11 (6), 2163-2168.
161. Becker, G.; Mundt, O.; Sachs, M.; Breunig, H. J.; Lork, E.; Probst, J.; Silvestru, A., *Z. Anorg. Allg. Chem.* **2001**, 627 (4), 699-714.
162. Zhao, Y.; Truhlar, D. G., *J. Chem. Phys.* **2006**, 125 (19), 194101-194118.
163. Austin, A.; Petersson, G. A.; Frisch, M. J.; Dobek, F. J.; Scalmani, G.; Throssell, K., *J. Chem. Theory. Comp.* **2012**, 8 (12), 4989-5007.
164. Chai, J.-D.; Head-Gordon, M., *Phys. Chem. Chem. Phys.* **2008**, 10 (44), 6615-6620.
165. Weigend, F.; Ahlrichs, R., *Phys. Chem. Chem. Phys.* **2005**, 7 (18), 3297-3305.
166. Quisenberry, K. T.; White, R. E.; Hanusa, T. P.; Brennessel, W. W., *New J. Chem.* **2010**, 34, 1579-1584
167. Quisenberry, K. T.; Gren, C. K.; White, R. E.; Hanusa, T. P.; Brennessel, W. W., *Organometallics* **2007**, 26 (17), 4354-4356.
168. Arrowsmith, M.; Hill, M. S.; Kociok-Köhn, G.; MacDougall, D. J.; Mahon, M. F., *Angew. Chem. Int. Ed.* **2012**, 51 (9), 2098-2100.
169. Weiss, E.; Wolfrum, R., *J. Organomet. Chem.* **1968**, 12 (2), 257-262.
170. Rightmire, N. R.; Quisenberry, K. T.; Hanusa, T. P., *Organometallics* **2014**, 33 (20), 5678-5685.
171. Woodman, T. J.; Schormann, M.; Hughes, D. L.; Bochmann, M., *Organometallics* **2003**, 22 (15), 3028-3030.

172. Gren, C. K.; Hanusa, T. P.; Rheingold, A. L., *Main Group Chem.* **2009**, *8*, 225-235.
173. White, R. E.; Hanusa, T. P.; Kucera, B. E., *J. Organomet. Chem.* **2007**, *692* (16), 3479–3485.
174. White, R. E.; Hanusa, T. P., *Organometallics* **2006**, *25* (23), 5621-5630.
175. Hanusa, T. P.; Bierschenk, E. J., unpublished results.
176. Gren, C. K.; Hanusa, T. P.; Rheingold, A. L., *Organometallics* **2007**, *26* (7), 1643-1649.
177. Smidt, J.; Hafner, W., *Angew. Chem.* **1959**, *71*, 284.
178. Wilke, G.; Bogdanovic, B., *Angew. Chem.* **1961**, *73*, 756.
179. Chance, J. M.; Linebarrier, D. L.; Nile, T. A., *Transition Met. Chem. (London)* **1987**, *12* (3), 276-7.
180. Chance, J. M.; Nile, T. A., *J. Mol. Catal.* **1987**, *42* (1), 91-7.
181. Wilke, G., *Angew. Chem., Int. Edit. Engl.* **1988**, *27* (1), 185-206.
182. Franks, R. J.; Nicholas, K. M., *Organometallics* **2000**, *19*, 1458-1460.
183. Sneed, R. P. A.; Zeiss, H. H., *J. Organomet. Chem.* **1971**, *28* (2), 259-63.
184. Karol, F. J.; Johnson, R. N., *J. Polym. Sci., Polym. Chem. Ed.* **1975**, *13* (7), 1607-17.
185. Bade, O. M.; Blom, R.; Ystenes, M., *Organometallics* **1998**, *17* (12), 2524-2533.
186. Woodman, T. J.; Sarazin, Y.; Fink, G.; Hauschild, K.; Bochmann, M., *Macromolecules* **2005**, *38* (8), 3060-3067.
187. Woodman, T. J.; Sarazin, Y.; Garratt, S.; Fink, G.; Bochmann, M., *J. Mol. Catal. A: Chem.* **2005**, *235* (1-2), 88-97.
188. Schormann, M.; Garratt, S.; Bochmann, M., *Organometallics* **2005**, *24* (7), 1718-1724.
189. Wilke, G. (Studiengesellschaft Kohle m.b.H.) (1965) Patent 651596; *Chem. Abstr.* **64**:52894.
190. Trost, B. M.; Van Vranken, D. L., *Chem. Rev.* **1996**, *96* (1), 395-422.
191. Trost, B. M., *Acc. Chem. Res.* **1996**, *29* (8), 355-364.
192. Agrofoglio, L. A.; Gillaizeau, I.; Saito, Y., *Chem. Rev.* **2003**, *103* (5), 1875-1916.
193. Belda, O.; Moberg, C., *Acc. Chem. Res.* **2003**, *37* (3), 159-167.
194. Bruneau, C.; Renaud, J.-L.; Demerseman, B., *Chem.–Eur. J.* **2006**, *12* (20), 5178-5187.
195. Bruneau, C.; Achard, M., *Coord. Chem. Rev.* **2012**, *256* (5–8), 525-536.
196. Takeuchi, R.; Kezuka, S., *Synthesis* **2006**, (20), 3349-3366.
197. Helmchen, G.; Pfaltz, A., *Acc. Chem. Res.* **2000**, *33* (6), 336-345.
198. Hartwig, J. F.; Stanley, L. M., *Acc. Chem. Res.* **2010**, *43* (12), 1461-1475.
199. Wilke, G.; Bogdanovic, B.; Hardt, P.; Heimbach, P.; Keim, W.; Kroner, M.; Oberkirch, W.; Tanaka, K.; Walter, D., *Angew. Chem., Int. Ed. Engl.* **1966**, *5*, 151-164.

200. Nesmeyanov, A. N.; Ustynyuk, Y. A.; Kritskaya, I. I.; Shchembelov, G. A., *J. Organomet. Chem.* **1968**, *14* (2), 395-403.
201. Nesmeyanov, A. N.; Kritskaya, I. I., *J. Organomet. Chem.* **1968**, *14* (2), 387-394.
202. Heck, R. F.; Breslow, D. S., *J. Am. Chem. Soc.* **1960**, *82*, 750-751.
203. Baker, R.; Copeland, A. H., *Tetrahedron Lett.* **1976**, (49), 4535-4538.
204. Grosselin, J. M.; Dixneuf, P. H., *J. Organomet. Chem.* **1986**, *314* (3), C76-C80.
205. Gabor, B.; Holle, S.; Jolly, P. W.; Mynott, R., *J. Organomet. Chem.* **1994**, *466* (1-2), 201-9.
206. Schott, A.; Schott, H.; Wilke, G.; Brandt, J.; Hoberg, H.; Hoffmann, E. G., *Liebigs Ann. Chem.* **1973**, (3), 508-30.
207. Fraenkel, G.; Chow, A.; Winchester, W. R., *J. Am. Chem. Soc.* **1990**, *112*, 1382-1386.
208. Alper, H.; Des Abbayes, H.; Des Roches, D., *J. Organomet. Chem.* **1976**, *121* (2), C31-C34.
209. Gaussian 03, Revision C.02, Frisch, M. J.; Trucks, G. W.; Schlegel, H. B.; Scuseria, G. E.; Robb, M. A.; Cheeseman, J. R.; Montgomery, Jr., J. A.; Vreven, T.; Kudin, K. N.; Burant, J. C.; Millam, J. M.; Iyengar, S. S.; Tomasi, J.; Barone, V.; Mennucci, B.; Cossi, M.; Scalmani, G.; Rega, N.; Petersson, G. A.; Nakatsuji, H.; Hada, M.; Ehara, M.; Toyota, K.; Fukuda, R.; Hasegawa, J.; Ishida, M.; Nakajima, T.; Honda, Y.; Kitao, O.; Nakai, H.; Klene, M.; Li, X.; Knox, J. E.; Hratchian, H. P.; Cross, J. B.; Bakken, V.; Adamo, C.; Jaramillo, J.; Gomperts, R.; Stratmann, R. E.; Yazyev, O.; Austin, A. J.; Cammi, R.; Pomelli, C.; Ochterski, J. W.; Ayala, P. Y.; Morokuma, K.; Voth, G. A.; Salvador, P.; Dannenberg, J. J.; Zakrzewski, V. G.; Dapprich, S.; Daniels, A. D.; Strain, M. C.; Farkas, O.; Malick, D. K.; Rabuck, A. D.; Raghavachari, K.; Foresman, J. B.; Ortiz, J. V.; Cui, Q.; Baboul, A. G.; Clifford, S.; Cioslowski, J.; Stefanov, B. B.; Liu, G.; Liashenko, A.; Piskorz, P.; Komaromi, I.; Martin, R. L.; Fox, D. J.; Keith, T.; Al-Laham, M. A.; Peng, C. Y.; Nanayakkara, A.; Challacombe, M.; Gill, P. M. W.; Johnson, B.; Chen, W.; Wong, M. W.; Gonzalez, C.; and Pople, J. A.; Gaussian, Inc., Wallingford CT, 2004.
210. Gaussian 09, Revision D.01, Frisch, M. J.; Trucks, G. W.; Schlegel, H. B.; Scuseria, G. E.; Robb, M. A.; Cheeseman, J. R.; Scalmani, G.; Barone, V.; Mennucci, B.; Petersson, G. A.; Nakatsuji, H.; Caricato, M.; Li, X.; Hratchian, H. P.; Izmaylov, A. F.; Bloino, J.; Zheng, G.; Sonnenberg, J. L.; Hada, M.; Ehara, M.; Toyota, K.; Fukuda, R.; Hasegawa, J.; Ishida, M.; Nakajima, T.; Honda, Y.; Kitao, O.; Nakai, H.; Vreven, T.; Montgomery, J. A., Jr.; Peralta, J. E.; Ogliaro, F.; Bearpark, M.; Heyd, J. J.; Brothers, E.; Kudin, K. N.; Staroverov, V. N.; Kobayashi, R.; Normand, J.; Raghavachari, K.; Rendell, A.; Burant, J. C.; Iyengar, S. S.; Tomasi, J.; Cossi, M.; Rega, N.; Millam, N. J.; Klene, M.; Knox, J. E.; Cross, J. B.; Bakken, V.; Adamo, C.; Jaramillo, J.; Gomperts, R.; Stratmann, R. E.; Yazyev, O.; Austin, A. J.; Cammi, R.; Pomelli, C.; Ochterski, J. W.; Martin, R. L.; Morokuma, K.; Zakrzewski, V. G.; Voth, G. A.; Salvador, P.; Dannenberg, J. J.; Dapprich, S.; Daniels, A. D.; Farkas, Ö.; Foresman, J. B.; Ortiz, J. V.; Cioslowski, J.; Fox, D. J. Gaussian, Inc., Wallingford CT, 2009.
211. Becke, A. D., *J. Chem. Phys.* **1993**, *98*, 5648-5652.

212. Elschenbroich, C., *Organometallics*. 3rd. ed.; VCH Publishers: Weinheim, 2006; p 804.
213. McClellan, W. R.; Hoehn, H. H.; Cripps, H. N.; Muetterties, E. L.; Howk, B. W., *J. Am. Chem. Soc.* **1961**, *83* (7), 1601-1607.
214. Cobalt. In *Comprehensive Organometallic Chemistry: The Synthesis, Reactions and Structures of Organometallic Compounds*, 1 ed.; Wilkinson, G.; Stone, F. G. A.; Abel, E. W., Eds. Pergamon Press: New York, 1982; Vol. 5.
215. Bertrand, J. A.; Jonassen, H. B.; Moore, D. W., *Inorg. Chem.* **1963**, *2* (3), 601-604.
216. Bönnemann, H.; Grard, C.; Kopp, W.; Pump, W.; Tanaka, K.; Wilke, G., *Angew. Chem. Int. Ed. Engl.* **1973**, *12* (12), 964-975.
217. Andrews, D. C.; Davidson, G., *J. Chem. Soc., Dalton Trans.* **1972**, *0* (13), 1381-1384.
218. A C_s -symmetric *syn, syn* conformation was found to be 1.8 kcal mol⁻¹ higher in energy (ΔG°) than the C_1 form. It is technically a rotational transition structure, with a small imaginary frequency ($\nu = -8 \text{ cm}^{-1}$) that persists even with the use of more stringent calculation limits (using keywords opt=tight and int=superfinegrid in Gaussian 09). It was not investigated further..
219. Hedberg, L.; Iijima, T.; Hedberg, K., *J. Chem. Phys.* **1979**, *70* (7), 3224-3229.
220. Suresh, C. H.; Koga, N., *J. Am. Chem. Soc.* **2002**, *124* (8), 1790-1797.
221. Moran, M. D.; Jones, J.-P.; Wilson, A. A.; Houle, S.; Surya Prakash, G. K.; Olah, G. A.; Vasdev, N., *Chem. Educ.* **2011**, *16*, 164-167.
222. Ryan, M. F.; Siedle, A. R.; Burk, M. J.; Richardson, D. E., *Organometallics* **1992**, *11* (12), 4231-7.
223. Gassman, P. G.; Deck, P. A.; Winter, C. H.; Dobbs, D. A.; Cao, D. H., *Organometallics* **1992**, *11* (2), 959-960.
224. Lappert, M. F.; Pickett, C. J.; Riley, P. I.; Yarrow, P. I. W., *J. Chem. Soc., Dalton Trans.* **1981**, (3), 805-813.
225. Antiñolo, A.; Bristow, G. S.; Campbell, G. K.; Duff, A. W.; Hitchcock, P. B.; Kamarudin, R. A.; Lappert, M. F.; Norton, R. J.; Sarjudeen, N.; Winterborn, D. J. W.; Atwood, J. L.; Hunter, W. E.; Zhang, H., *Polyhedron* **1989**, *8* (13-14), 1601-1606.
226. Langmaier, J.; Samec, Z.; Varga, V.; Horáček, M.; Choukroun, R.; Mach, K., *J. Organomet. Chem.* **1999**, *584* (2), 323-328.
227. Amiet, R. G.; Reeves, P. C.; Pettit, R., *Chem. Commun.* **1967**, (23), 1208-1208.
228. Takanashi, K.; Lee, V. Y.; Sekiguchi, A., *Organometallics* **2009**, *28* (4), 1248-1251.
229. Zhao, Y.; Truhlar, D. G., *J. Chem. Phys.* **2006**, *125* (19), 194101-194118.